A study of the regulation and function of Fab1p, a phosphatidylinositol 3-phosphate 5 kinase in *Saccharomyces cerevisiae*

John P. Phelan

A thesis submitted to University College London for the degree of Doctor of Philosophy

Department of Biochemistry and Molecular Biology,
University College London,
Gower Street,
London.
WC1E 6BT

April 2005

ProQuest LLC
789 East Eisenhower Parkway
P.O. Box 1346
Ann Arbor, MI 48106-1346

ABSTRACT

The *Saccharomyces cerevisiae* protein Fab1p is the archetypal type III phosphatidylinositol phosphate kinase. This family of enzymes is universal to all eukaryotes and is responsible for the synthesis of phosphatidylinositol 3,5-bisphosphate from phosphatidylinositol 3-phosphate. In *S. cerevisiae*, Fab1p regulates a number of cellular processes via the production of phosphatidylinositol 3,5-bisphosphate including: vacuole acidification, protein trafficking to the vacuole lumen, vacuole membrane recycling and apical bud formation. It is now clear that these processes are regulated independently; however the molecular details of Fab1p regulation have yet to be identified.

Using yeast two-hybrid analysis in a systematic screen with Fab1p and its domains, we have identified over 300 potential interactors. Phenotypic analyses on 17 corresponding deletion mutants of these proteins have identified 8 that display phenotypes consistent with loss of Fab1p. We have focused on Apl2p, which appears to be a *bona fide* activator of Fab1p. Apl2p, and Apl4p, which interacts with the Fab1p regulator Vac14p, are part of the heterotetrameric complex AP-1 involved in clathrin mediated trafficking from the trans-Golgi network.

We show that AP-1 regulates phosphatidylinositol 3,5-bisphosphate production *in vivo* and is required for the trafficking of the ubiquitinated cargoes CPS and Phm5p to the vacuole lumen, a process that requires Fab1p. Over-expression of Fab1p in AP-1 mutants reverts these trafficking defects. Using point mutants of AP-1 we show that these trafficking events are clathrin-dependant. AP-1 is not required for Fab1p-dependant vacuole morphology and vacuole acidity. Thus, we speculate that Fab1p is regulated by AP-1 for the maintenance of a pool of phosphatidylinositol 3,5-bisphosphate required for trafficking of cargoes to the vacuole. AP-1 is responsible for the retention of proteins at the trans-Golgi network; therefore we speculate that retention to this compartment might also be a Fab1p-dependent mechanism.

ACKNOWLEDGEMENTS

I am extremely grateful to my supervisor Dr. Frank Cooke for his help and supervision over the past 3 years. His professionalism, integrity and attitude to research have been inspirational and have made my time working with him enjoyable and rewarding. Notwithstanding these attributes, I am also a tad more cynical and jaundiced about life than when I started, but that's life!

I would also like to acknowledge the Wellcome Trust for supporting us in this work. I would like to thank Professor Peter Piper and Dr. John Ward for their help and also acknowledge the people in their laboratories who made working at UCL fun and interesting. Thanks also to Dr. Stephen Dove for prompt e-mail replies to queries and Dr. David Gems for the use of his microscope.

Thanks to my parents and family and in particular Caroline. Finally, thanks to my friends who have put up with my self imposed will to finish this thesis, in particular Ian, Amanda and Dave.

ABBREVIATIONS

Abbreviations used in this work:

[^{3}H]	Tritium/triated
3-AT	3-amino-1, 2, 4-triazole
AAA	ATPases associated with diverse cellular activities
ALP	Alkaline phosphatase
AP-1	Adaptor Complex 1
AP-2	Adaptor Complex 2
AP-3	Adaptor Complex 3
AP-4	Adaptor Complex 4
ATP	Adenosine triphosphate
bp	Base pair
cDNA	Complimentary DNA
chc	Clathrin heavy chain
clc	Clathrin light chain
cpm	Counts per minute
CPS	Carboxypeptidase S
CPY	Carboxypeptidase Y
Da	Daltons
dH_2O	Distilled water
DNA	Deoxyribonucleic acid
dNTPs	Deoxynucleotides
dNTPs	Deoxynucleotide triphosphate
EEA1	Early Endosome Antigen 1
Ent	Epsin N-terminal
ER	Endoplasmic reticulum
FAB	Formation of Aploid Binucleates
FM4-64	*N*-(3-triethylammoniumpropyl)-4-(6-(4-(diethylamino)phenyl)hexatrienyl)pyridium dibromide
FYVE	Fab1p, YOTB, Vac1p and EEA1
GFP	Green fluorescent protein
GST	Glutathione S-transferase
HOG1	High Osmolarity Glycerol response 1
HPLC	High performance liquid chromatography
MAPK	Mitogen Activated Protein Kinase
MVB	Multivesicular Body
NaCl	Sodium Chloride
OD	Optical density
ORF	Open reading frame
PBS	Phosphate buffered saline
PCR	Polymerase chain reaction
PDK1	Phosphoinositide-dependant kinase 1
PtdIns	Phosphatidylinositol
PtdIns(3,4)P_2	Phosphatidylinositol (3,4)-bisphosphate

PtdIns(3,4,5)P_2	Phosphatidylinositol (3,4,5)-trisphosphate
PtdIns(3,5)P_2	Phosphatidylinositol (3,5)-bisphosphate
PtdIns(4,5)P_2	Phosphatidylinositol (4,5)-bisphosphate
PtdIns3*P*	Phosphatidylinositol 3-phosphate
PtdIns4*P*	Phosphatidylinositol 4-phosphate
PtdIns5*P*	Phosphatidylinositol 5-phosphate
PVC	Prevacuolar Compartment
rpm	Revolutions per minute
SD	Synthetic Drop-out
SNARE	Soluble N-ethylmaleimide sensitive factor-attachment protein receptor
TGN	Trans-Golgi network
TMD	Transmembrane Domain
UIM	Ubiquitin interacting motif
UV	Ultraviolet

TABLE OF CONTENTS

LIST OF FIGURES

CHAPTER 5: Apl2p AND THE AP-1 COMPLEX

CHAPTER 6: DISCUSSION

LIST OF TABLES

1 INTRODUCTION

In eukaryotic cells, the phospholipid phosphatidylinositol (PtdIns) is the precursor molecule for the formation of a distinct class of second-messengers known as phosphoinositides (Simonsen et al., 2001). The diversity of this class of messengers is mediated at the D-*myo*-inositol headgroup of PtdIns (Figure 1), which can be reversibly phosphorylated at one or a combination of the D-3, D-4 and D-5 positions to yield several molecules involved in a wide range of biological functions, such as signal transduction, membrane trafficking, cytoskeletal regulation and apoptosis (Leevers et al., 1999; Rameh and Cantley, 1999). Synthesis of phosphoinositides occurs at the cytosolic face of cellular membranes to allow recruitment and activation of effector proteins. Instant alterations in phosphoinositide levels are dynamically mediated via the actions of lipid kinases, lipid phosphatases and phospholipases in precise membrane vicinities, providing a mechanism for the temporal and spatial regulation of a wide spectrum of cellular processes (Odorizzi et al., 2000; Simonsen et al., 2001).

In eukaryotes, seven phosphorylated derivatives of PtdIns are known to exist, each one functioning in distinctive roles within the cell (Figure 1.1).

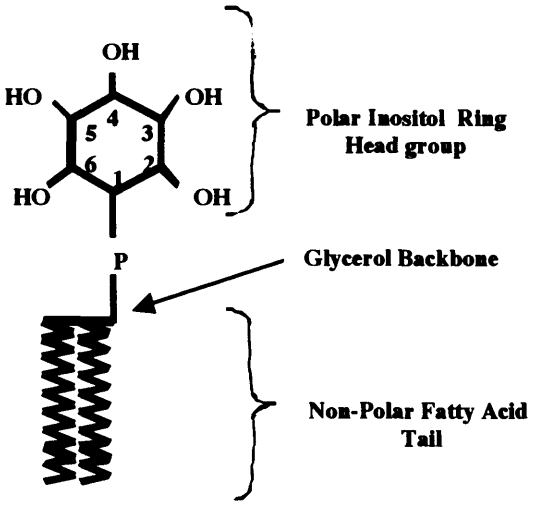

Figure 1. Basic structure of phosphatidylinositol (PtdIns). The molecule consists of an inositol headgroup that can be phosphorylated at the D-3, D-4 and D-5 positions. A phospodiester bond links the inositol headgroup via the –1,2-diacylglycerol (DG) backbone to a long fatty acid chain embedded in cell membranes, anchoring the molecule.

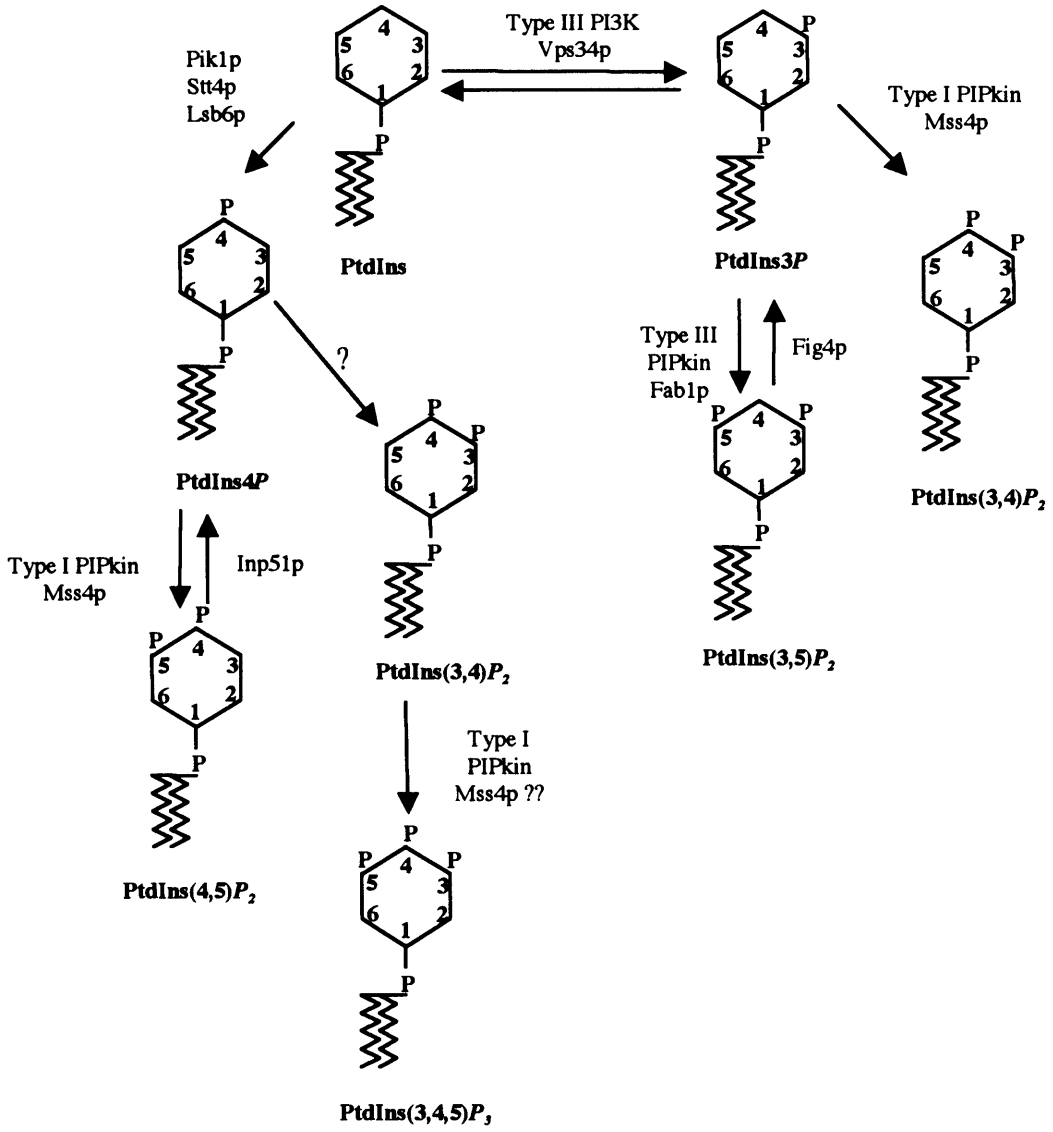

Figure 1.1. The phosphorylated derivatives of PtdIns and the enzymes responsible for their synthesis in *Saccharomyces cerevisiae*. The reversible production of these molecules is catalysed through the combined activities of a number of specific phosphatases and phosphoinositide kinases. PtdIns(3,4,5)P_3 production has not been detected in *S. cerevisiae* (Desrivières et al., 1998) but its presence is speculated (Cooke, 2004) PtdIns(3,4,5)P_3 has been detected in *Schizosaccharomyces pombe* (Mitra et al., 2004) and mammalian cells (Cantley, 2002). PtdIns5*P* (not shown) has not been detected in *S. cerevisiae* (McEwen et al., 1999) but is present in mammalian cells (Rameh et al., 1997).

1.1 Phosphatidylinositol metabolism in *S. cerevisiae*

In *S. cerevisiae*, the phosphorylation of PtdIns at the D-4 position of the inositol ring by the phosphatidylinositol 4 kinases (PtdIns4-kinase), Pik1p, Stt4p and Lsb6p produces phosphatidylinositol 4-phosphate (PtdIns4*P*), at certain locations leading to distinct functions (Audhya and Emr, 2002; Garcia-Bustos et al., 1994; Han et al., 2002). The phosphorylation of PtdIns4*P* at the trans-Golgi Network (TGN) by Pik1p is required for protein secretion and cytokinesis (Garcia-Bustos et al., 1994). Production of PtdIns4*P* by Stt4p occurs at the plasma membrane and is required for actin cytoskeleton organisation probably via the subsequent phosphorylation of phosphatidylinositol 4,5-bisphosphate, (PtdIns(4,5)P_2) by Mss4p, a phosphatidylinositol 4-phosphate 5-kinase (PtdIns4*P* 5-kinase) (Audhya and Emr, 2002). Finally, PtdIns4*P* is synthesised by Lsb6p at the plasma membrane and may have roles in endocytic or exocytic pathways (Han et al., 2002).

PtdIns4*P* can be further phosphorylated *in vivo* and i*n vitro* by the type I PIPkin (Section 1.5.1), Mss4p to produce the second messenger PtdIns(4,5)P_2 (Desrivières et al., 1998; Homma et al., 1998). To a lesser extent Mss4p can also phosphorylate phosphatidylinositol 3-phosphate (PtdIns3*P*) to produce phosphatidylinositol 3,4-bisphosphate (PtdIns(3,4)P_2) *in vitro* and over-expression of Mss4p slightly augments levels of yeast PtdIns(3,4) P_2 *in vivo* (Desrivières et al., 1998). It was thought that PtdIns(3,4)P_2 production in *S. cerevisiae* was not physiologically relevant (Desrivières et al., 1998); however, with the discovery of phosphatidylinositol 3,4,5- trisphosphate (PtdIns (3,4,5)P_3) in *S. pombe*, the relevance of PtdIns(3,4)P_2 production in *S. cerevisiae* may change (Cooke, 2004). Mss4p is essential for growth, and temperature sensitive mutants have reduced levels of PtdIns(4,5)P_2 (10% of wild-type) upon shifting to the restrictive temperature, concomitant with a defect in actin cytoskeleton organisation *in vivo* (Desrivières et al., 1998; Homma et al., 1998). Thus Mss4p appears to be the sole PtdIns 4*P* 5-kinase responsible for all PtdIns(4,5)P_2 production in *S. cerevisiae* (Desrivières et al., 1998; Homma et al., 1998).

The identification of PtdIns(3,4,5)P_3 in *S. cerevisiae* remains elusive (Cooke, 2004); however speculation of its existence in budding yeast stems from identification of

PtdIns(3,4,5)P_3 in the fission yeast *S. pombe* (Mitra et al., 2004). PtdIns(3,4,5)P_3 is barely detectable in *S. pombe* but disruption of *ptn1* (a PTEN homologue) reveals *in vivo* PtdIns(3,4,5)P_3 and PtdIns(3,4)P_2 to be 6-8 times those observed in wild-type cells and these levels are restored by re-introducing *PTN1* (Mitra et al., 2004). This implicates Ptn1p in the maintenance of both *in vivo* PtdIns(3,4,5)P_3 and PtdIns(3,4)P_2 levels. To infer a biosynthetic pathway for PtdIns(3,4,5)P_3 synthesis, *in vivo* PtdIns(3,4,5)P_3 was assayed in *vps34Δ/ptn1Δ* and *its3-1/ptn1Δ* strains and was greatly compromised. Vps34p is the only PtdIns 3-kinase in *S. pombe* (Takegawa et al., 1995) and *its3-1* is a mutant allele of Its3p (Zhang et al., 2000) that has approximately 10% of wild-type PtdIns4*P* 5-kinase activity. The reduced levels of PtdIns(3,4,5)P_3 observed in these cells suggests that PtdIns(3,4,5)P_3 production stems initially from synthesis of PtdIns3*P* by Vps34p, followed by the conversion of PtdIns3*P* to PtdIns(3,4)P_2 and subsequent conversion of PtdIns(3,4)P_2 to PtdIns(3,4,5)P_3, the latter steps being carried out by Its3p (Cooke, 2004; Mitra et al., 2004). However the detection of trace PtdIns(3,4)P_2 levels in *S. cerevisiae* (Cooke, 2002; Desrivières et al., 1998) has prompted speculation that PtdIns(3,4,5)P_3 may exist in this organism (Cooke, 2004). Homologues of phosphoinositide-dependant kinase 1 (PDK1), an archetypal PtdIns(3,4,5)P_3 effector, exist in *S. cerevisiae* and *S. pombe* (Vanhaesebroeck and Alessi, 2000) and *S. pombe* PDK1 appears to have PtdIns(3,4,5)P_3 binding specificity (Mitra et al., 2004). The precise role of PtdIns(3,4,5)P_3 in fission yeast is not known however *ptn1Δ* cells display enlarged vacuoles suggesting this lipid may be involved in some aspect of vacuole homeostasis (Mitra et al., 2004).

Phosphatidylinositol 5-phosphate (PtdIns5*P*) is undetectable in *S. cerevisiae* (McEwen et al., 1999) but is present in mammalian fibroblasts (Rameh et al., 1997). The precise role of PtdIns5*P* is not known and remains to be identified.

The membrane lipid PtdIns3*P* is constitutively produced by yeast and higher eukaryotes via the phosphorylation of PtdIns by PtdIns 3-kinase (Toker and Cantley, 1997). In yeast, the TGN/vacuole associated lipid kinase Vps34p is the sole PtdIns 3-kinase (Herman and Emr, 1990; Schu et al., 1993). Cells expressing a temperature sensitive allele of *vps34* reveal defects in both PtdIns 3-kinase activity and protein trafficking of the type II integral

membrane carboxypeptidase Y (CPY) to the vacuole implicating Vps34p and hence PtdIns3*P* in vesicular transport from the TGN to the vacuole (Stack et al., 1995). Vps34p is also responsible for providing PtdIns3*P* as a substrate for the synthesis of PtdIns(3,5)P_2 in *S. cerevisiae* (Dove et al., 1997). PtdIns(3,5)P_2, originally described in yeast and fibroblasts (Dove et al., 1997; Whiteford et al., 1997) is believed to be ubiquitous in all eukaryotes (Cooke et al., 1998) and in *S. cerevisiae* is required for several distinct biological functions, which will be discussed later.

Thus as a precursor molecule, the relevance of PtdIns in intracellular dynamics cannot be understated, as it provides the structural backbone for seven different phosphoinositides. However, the generation of second messenger molecules, while present only transiently and in low abundance in cells (Odorizzi et al., 2000) are key regulators in intracellular dynamics, membrane trafficking and downstream signalling (Corvera et al., 1999; Leevers et al., 1999).

1.2 The identification of *FAB1*

FAB1 was originally identified in a screen for abnormal nuclear segregation ; mutations in which led to the aberrant segregation and inheritance of chromosomes during mitosis in budding yeast (Yamamoto et al., 1995). When orientation of the yeast mitotic spindle is compromised, both sets of chromosomes are inherited by either the mother or the bud (Palmer et al., 1990). This defect leads to the formation of aploid and binucleate cells hence the acronym *fab* for this mutant phenotype (Yamamoto et al., 1995). However, abnormal nuclear segregation is not the only phenotype observed in these cells. Isolation of *fab1-2* temperature sensitive mutants and construction of a *fab1-Δ1* deletion allele (2236 residues out of 2279 removed) reveal temperature sensitivity at 37 °C, the accumulation of large vacuoles, vacuolar acidification defects, abnormal chromosome transmission and spindle morphology, and defects in processing the soluble vacuolar hydrolase CPY (Yamamoto et al., 1995). Sequencing of the *FAB1* gene identify a 6.8 kb open reading frame (ORF) predicting a protein of 2279 amino acids with a predicted size of 257 kDa (Yamamoto et al., 1995). Fab1p was originally speculated to have PtdIns4*P* 5-kinase activity based on its

homology with a human type II PIPkinase (Boronenkov and Anderson, 1995; Yamamoto et al., 1995); however, subsequent studies revealed that Fab1p displayed PtdIns*3P* 5-kinase activity (Cooke et al., 1998).

1.3 Discovery of PtdIns(3,5)P_2 and route of synthesis

Prior to 1997 positive identification of PtdIns(3,5)P_2 remained elusive although its existence was postulated in 1989 (Auger et al., 1989). PtdIns(3,5)P_2 was simultaneously identified by structural analyses of a novel [^{3}H]-inositol containing peak in zymolase treated yeast cells and mouse fibroblasts (Figure 1.3) (Dove et al., 1997; Whiteford et al., 1997). Zymolase is used to digest yeast cell walls and aid lysis. Non-equilibrium [^{32}P] labelling studies demonstrate that in both cases PtdIns(3,5)P_2 is synthesised predominantly by the actions of a PtdIns3*P* 5-kinase (Cooke et al., 1998; Whiteford et al., 1997). The discovery of a chromatographically identical PtdInsP_2 in *S. pombe*, Cos-7 cells and *Daucas carata* suggested that PtdIns(3,5)P_2 could be ubiquitous to all eukaryotic cells (Dove et al., 1997).

The concentration of PtdIns(3,5)P_2 rises rapidly to 7-20 times that of wild-type cells, 5-15 minutes after the application of hyperosmotic stress with either 1.1 M sorbitol or 0.9 M NaCl (Dove et al., 1997). Levels of PtdIns(3,5)P_2 remain static for between 30-60 minutes post stress after which time levels return to normal indicating that PtdIns(3,5) P_2 production is a regulated transient biological response to osmotic stress (Dove et al., 1997).

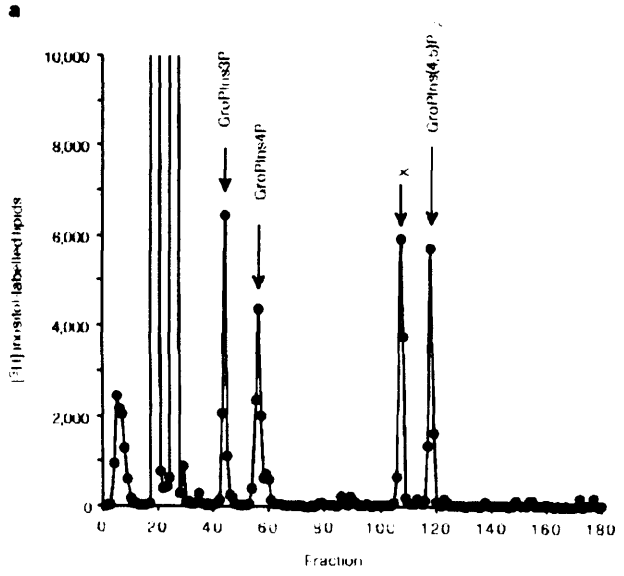

Figure 1.3. HPLC analysis of deacylated [^{3}H] inositol-labelled lipids of "stressed" zymolase treated *S. cerevisiae* cells. The unknown novel [^{3}H]-inositol containing peak labelled as "lipid x" was found to be PtdIns(3,5)P_2. Diagram taken from Dove *et al.* (Dove et al., 1997).

The stimulation of PtdIns(3,5)P_2 by hyperosmotic shock suggests that this molecule is part of an intracellular signalling cascade involved in controlling responses to various stresses (Dove et al., 1997). In *S. cerevisiae*, the *HOG1* (High Osmolarity Glycerol Response) pathway activates in response to hyperosmotic stress and is the most studied hyperosmotic stress pathway (Schuller et al., 1994; Wurgler-Murphy et al., 1997). The *HOG1* gene product encodes a mitogen activated protein kinase (MAPK), and the pathway is stimulated by the activation of plasma membrane bound receptor proteins which act as osmosensors to enable yeast to sense external osmolarity (Ruiss *et al* 1995). Thus in response to an increase in extracellular osmolarity, the *HOG1* cascade activates, prompting the transcriptional activation of several genes along its pathway. Deletion mutants of components involved in this pathway were assayed for PtdIns(3,5)P_2 accumulation in response to hyperosmotic stress: *SHO1*, the SH3-domain-containing osmosensor; *SSK1*, the response regulator element of the *SLN1* two-component osmosensor; and the *HOG1* protein kinase. Deletion mutants of these genes show normal PtdIns(3,5)P_2 accumulation responses suggesting that the *HOG1* pathway is not responsible for inducing hyperosomtic synthesis of PtdIns(3,5)P_2 (Dove et al., 1997). Therefore, an unknown osmoregulatory route is responsible for the synthesis of PtdIns(3,5)P_2 and to date the factors mediating this response have yet to be identified.

1.4 Identification of Fab1p as a phosphatidylinositol 3 phosphate 5-kinase

Based on searches of *S. cerevisiae* genome databases, Fab1p was speculated to have potential phosphatidylinositol 3-phosphate 5-kinase activity due to its homology with other PIPkinases (Dove et al., 1997). In a *fab1*Δ strain, production of PtdIns(3,5)P_2 is not detected *in vivo* either in the presence or absence of hyperosmotic stress (Cooke et al., 1998; Gary et al., 1998) (Figure 1.4a).

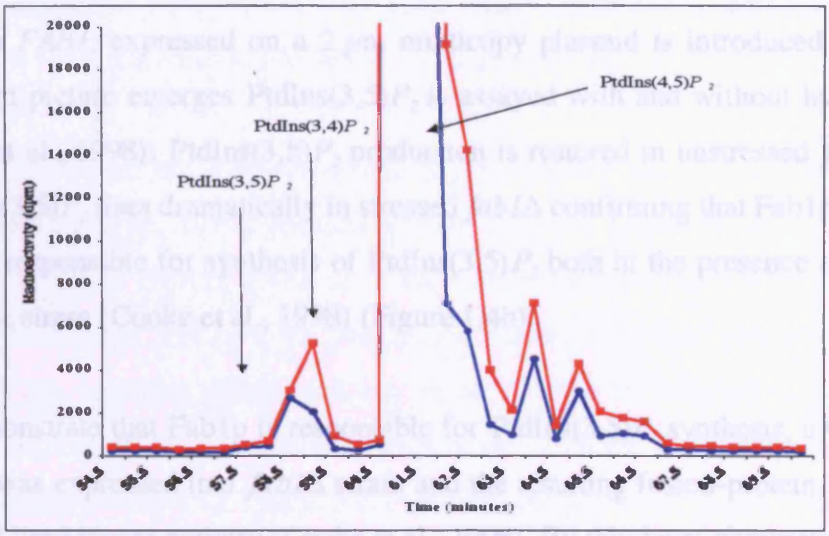

Figure 1.4a. HPLC chromatogram of deacylated [^{3}H]-inositol-labelled lipids in *fab1*Δ cells. The blue trace denotes unstressed *fab1*Δ cells. The red trace refers to stressed *fab1*Δ cells having undergone hyperosmotic shock with 1.1 M NaCl for 10 minutes. Assay levels of PtdIns(3,4)P_2 and PtdIns(4,5)P_2 are typical. However in both assays PtdIns(3,5)P_2 is undetected (Cooke et al., 1998).

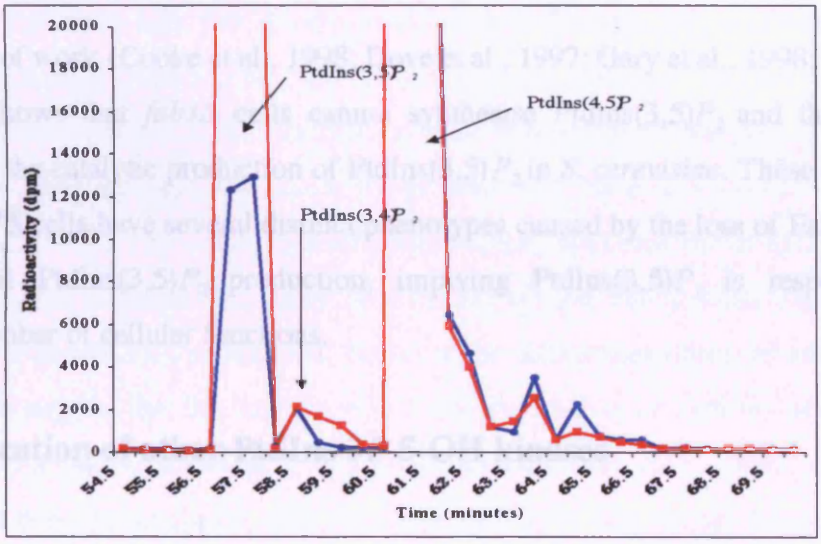

Figure 1.4b. HPLC chromatogram of deacylated [^{3}H]-inositol-labelled lipids in *fab1*Δ cells expressing *FAB1* on a 2 μm multicopy plasmid. The blue trace denotes the production of PtdIns(3,5)P_2 in unstressed *fab1*Δ cells expressing *FAB1* on a 2 μm muticopy plasmid. The red trace refers to the production of PtdIns(3,5)P_2 in stressed *fab1*Δ cells expressing *FAB1* on a 2 μm multicopy plasmid. Cells were stressed by incubation with 1.1 M NaCl for 10 minutes. In both cases levels of PtdIns(3,5)P_2 were augmented, significantly in unstressed cells but dramatically in stressed cells (Cooke et al., 1998).

However when *FAB1*, expressed on a 2 μm multicopy plasmid is introduced into *fab1*Δ cells, a different picture emerges PtdIns(3,5)P_2 is assayed with and without hyperosmotic stress (Cooke et al., 1998). PtdIns(3,5)P_2 production is restored in unstressed *fab1*Δ cells, whereas PtdIns(3,5)P_2 rises dramatically in stressed *fab1*Δ confirming that Fab1p is likely to be the enzyme responsible for synthesis of PtdIns(3,5)P_2 both in the presence and absence of hyperosmotic stress (Cooke et al., 1998) (Figure 1.4b).

To further demonstrate that Fab1p is responsible for PtdIns(3,5)P_2 synthesis, a GST-Fab1p fusion protein was expressed in a *fab1*Δ strain and the resulting fusion-protein assayed for *in vitro* inositol lipid kinase activity (Cooke et al., 1998). By thin layer chromatography and HPLC analysis the resulting lipid product of this enzyme was identified as PtdIns(3,5)P_2 confirming Fab1p as having phosphatidylinositol 3-phosphate 5-kinase activity (Cooke et al., 1998).

Thus this body of work (Cooke et al., 1998; Dove et al., 1997; Gary et al., 1998; Yamamoto et al., 1995) shows that *fab1*Δ cells cannot synthesise PtdIns(3,5)P_2 and that *FAB1* is responsible for the catalytic production of PtdIns(3,5)P_2 in *S. cerevisiae*. These studies also reveal that *fab1*Δ cells have several distinct phenotypes caused by the loss of Fab1p activity and subsequent PtdIns(3,5)P_2 production, implying PtdIns(3,5)P_2 is responsible for regulating a number of cellular functions.

1.5 Identification of other PtdIns 3*P* 5-OH kinases

PtdIns(3,5)P_2 is present in *S. pombe*, *Daucus carota*, monkey Cos-7 cells (Dove et al., 1997), mammalian cells (Shisheva et al., 1999) resting mouse fibroblasts (Whiteford et al., 1997), *Chlamydomonas moewusii* (Meijer et al., 1999), alfalfa, pea and tomato (Meijer et al., 2001; Meijer et al., 1999) and in both mouse T- and B-lymphocytes (Jones et al., 1999) suggesting that PtdIns(3,5)P_2 is ubiquitous to all eukaryotes and cell types (Cooke et al., 1998; Dove et al., 1997). This therefore suggests that Fab1p homologues exist in these

eukaryotic cells and other organisms (Cooke et al., 1998). Indeed, Fab1p homologues have been found in several eukaryotes and all model organisms (Figure 1.5).

Complementation analysis on *S. pombe* Fab1p (SpFab1p, later called *ste12*$^{+}$ (Morishita et al., 2002)) (McEwen et al., 1999) and mammalian PIKfyve (Shisheva et al., 1999) (see below) identified these two proteins as Fab1p homologues (McEwen et al., 1999). Expression of full-length PIKfyve in *fab1*Δ cells rescues several phenotypic defects originally observed in these cells (McEwen et al., 1999). In contrast to *fab1*Δ cells, *fab1*Δ/PIKfyve cells grow at the restrictive temperature, vacuolar morphology is similar to wild-type cells and synthesis of PtdIns(3,5)P_2 is restored; however when these cells are hyperosmotically challenged with 0.9 M NaCl, levels of PtdIns(3,5)P_2 remain approximately the same as resting cells (McEwen et al., 1999). This appears to suggest that PIKfyve is not able to couple to the hyperosmotic response in *S. cerevisiae*.

Introduction of SpFab1p into *fab1*Δ cells also restores PtdIns(3,5)P_2 production, and an hyperosmotic challenge with 0.9 M NaCl cause levels to increase two fold to those of resting cells (McEwen et al., 1999). Interestingly, the expression of SpFab1p in *fab1*Δ cells neither restores growth at the restrictive temperature nor corrects vacuolar morphology (McEwen et al., 1999). The restoration of PtdIns(3,5)P_2 synthesis in *fab1*Δ/PIKfyve and *fab1*Δ/SpFab1p cells indicate that these proteins are indeed Fab1p homologues and are responsible for PtdIns(3,5)P_2 production, however the differences observed in phenotypes between the two suggest that interactions with other factors may be instrumental for spatial and/or temporal regulation of PtdIns(3,5)P_2 production (McEwen et al., 1999). Additionally, PtdIns5*P* is not detected in *fab1*Δ cells expressing PIKfyve suggesting that PtdIns(3,5)P_2 and not PtdIns5*P* is the functional output of this class of enzyme as has been suggested (Cooke, 2002) (see below).

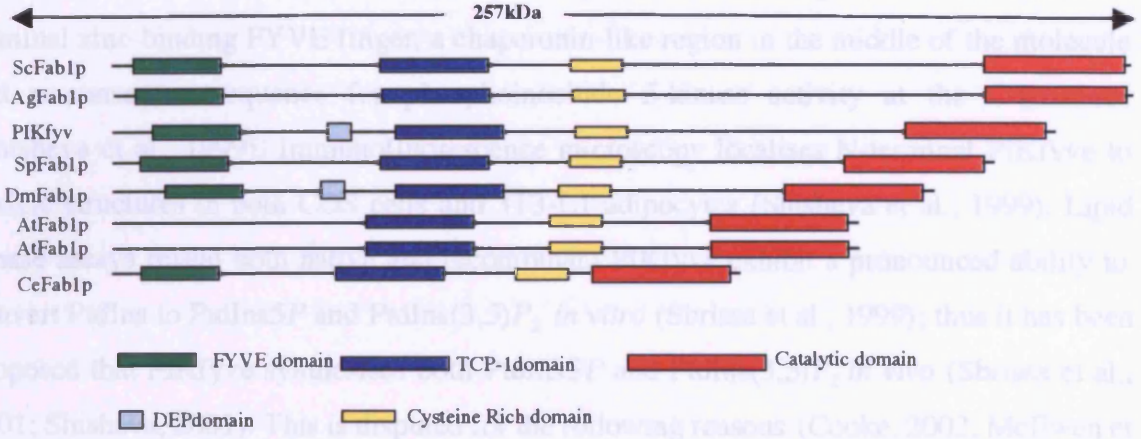

Figure 1.5. The domain structure of potential Type III PIP kinases (Section 1.5.1). This list is not exhaustive but is representative of model organisms. The basic domain structure is roughly equivalent in ScFab1p (*S. cerevisiae*) (Accession No. P34756), AgFab1p (*Anopheles gambiae*) (Accession No. EAA09386), SpFab1p (*S. pombe*) (Accession No. O59722) and CeFab1p (*Caenorhabditis elegans*) (Accession No. T18961), even though some of these homologues are considerably smaller than Fab1p. Mammalian PIKfyve (Accession No. NP-055855) and DmFab1p (*Drosophila melanogaster*) (Accession No. AAF57789) contain a signalling motif called a DEP domain not found in other homologues (Shisheva, 2001) (Section 1.6.5). Two out of the four AtFab1p homologues (*Arabadopsis thaliana*) (Accession Nos. NP-174686 and AAD55502/NP-177257) lack a FYVE domain; this could be due to incomplete sequence data or a genuine lack of a FYVE domain (Cooke, 2002; McEwen et al., 1999). All sequences were taken from the NCBI database and were aligned using the Pileup program in the GCG Wisconsin software package and Pfam (http://www-biocomp.doit.wisc.edu/gcg and http://www.sanger.ac.uk/Software/Pfam).

PIKfyve, the putative mammalian homologue of Fab1p, was identified from a mouse adipocyte cDNA library resulting from a differential display screen for fat and muscle-specific transcripts (Shisheva et al., 1999). Analysis of the full-length cDNA reveals an N-terminal zinc-binding FYVE finger, a chaperonin-like region in the middle of the molecule and a consensus sequence for phosphoinositide 5-kinase activity at the C-terminus (Shisheva et al., 1999). Immunofluorescence microscopy localises N-terminal PIKfyve to vesicle structures in both COS cells and 3T3-L1 adipocytes (Shisheva et al., 1999). Lipid kinase assays reveal both native and recombinant PIKfyve exhibit a pronounced ability to convert PtdIns to PtdIns5*P* and PtdIns(3,5)P_2 *in vitro* (Sbrissa et al., 1999); thus it has been proposed that PIKfyve synthesises both PtdIns5*P* and PtdIns(3,5)P_2 *in vivo* (Sbrissa et al., 2001; Shisheva, 2001). This is disputed for the following reasons (Cooke, 2002; McEwen et al., 1999): a) expression of PIKfyve in *fab1*Δ cells restores PtdIns(3,5)P_2 synthesis but does not yield detectable levels of PtdIns5*P* (McEwen et al., 1999); b) although PtdIns5*P* production has been observed in *in vitro* kinase assays, this should be interpreted with caution as these assays are not truly reflective of physiological lipid substrate environments (Sbrissa et al., 1999) and c) all functional studies implicate PtdIns(3,5)P_2 only and not PtdIns5*P* as the correct *in vivo* output of Fab1p, PIKfyve and SpFab1p (Cooke et al., 1998; McEwen et al., 1999; Morishita et al., 2002).

The *S. pombe* Fab1p homologue, *ste12*$^+$ was identified based on the fact that mutant cells exhibit enlarged vacuoles similar to *fab1*Δ cells (Morishita et al., 2002). The *ste12*$^+$ mutant is sterile and shows deficiencies in response to nitrogen starvation (Morishita et al., 2002). Sequencing of the cloned gene predicts it to be a 1932 amino acid PtdIns3*P*-5 kinase, (marginally smaller than Fab1p, 2278 amino acids) and when deleted and analysed in a *ste12-2* mutant for stress related PtdIns(3,5)P_2 production, none is detected confirming *ste12*$^+$ as the *S. pombe* PtdIns 3*P* 5-kinase (Morishita et al., 2002). Phenotypic analyses of the *ste12*$^+$ mutant reveal these cells are defective in sexual reproduction and in responding to mating pheromones and they also exhibit slightly flawed processing of certain pheromone receptors (Morishita et al., 2002). Thus it appears that PtdIns(3,5)P_2 production is important in maintaining cellular responses to stresses and mating pheromone signalling

in *S. pombe* (Morishita et al., 2002). As described above, *ste12*$^+$ cells display PtdIns(3,5)P_2 activity both *in vivo* and *in vitro* (McEwen et al., 1999).

Identification and sequencing of the Fab1p *Candida albicans* homologue (CaFab1p) reveal an ORF of 2,369 amino acids predicting a calculated molecular mass of 268kDa, (larger than Fab1p; 257kDa) (Augsten et al., 2002). Extensive homology to Fab1p is observed in the putative kinase domain and in the FYVE domain (Augsten et al., 2002). The authors of this study did not carry out biochemical analysis on the functional output of CaFab1p but based on phenotypic data (Section 1.10.2) and domain architecture it is likely this molecule is responsible for the synthesis of PtdIns(3,5)P_2 in *Candida albicans* (Augsten et al., 2002).

1.5.1 The type III PIPkins

To date, several Fab1p homologues, from mammalian cells (PIKfyve), *S. pombe* (*Ste12*$^+$) and *Candida albicans* (CaFab1p) have been determined and appear to be members of a large family of proteins called the type III PIPkins (Cooke et al., 1998; McEwen et al., 1999). This class of PIPkin differentiates these enzymes from the type I PIPkins, which are PtdIns4*P* 5-OH kinases and phosphorylate the 5-OH position of PtdIns4*P* to produce PtdIns(4,5)P_2 (Rameh et al., 1997), and the type II PIPkins, which are PtdIns5*P* 4-OH kinases and phosphorylate the 4-OH position of PtdIns5*P* producing PtdIns(4,5)P_2 (Hinchliffe et al., 1998). Thus the type III PIPkin classification is dedicated to those enzymes whose sole functional output is PtdIns(3,5)P_2 production (Cooke, 2002). The identification of these proteins in these cell types does not mean that no other homologues exist. Merely, these proteins have not been identified/characterised to the same extent as those just mentioned. By studying the NCBI database (http://www.ncbi.nlm.nih.gov/entrez) several potential homologues do exist in a wide variety of cell types: rice (*Oryza sativa*), honeybee (*Apis mellifera*), mosquito (*Anopheles gambiae*), Norwegian rat (*Rattus norvegicus*) *Candida glabrata*, *Kluveromyces lactis*, *Yarrowia lipolytica* and *Ashbya gossypii*. Whether or not these proteins perform similar functions to Fab1p remains to be established.

1.6 *S. cerevisiae* Fab1p contains 4 distinct domains

The *S. cerevisiae FAB1* gene encodes for Fab1p, a protein of predicted size 257 kDa (Yamamoto et al., 1995). Database searches reveal that there are 4 distinct domains within the Fab1p protein (Figure 1.6). These are the FYVE domain at the N-terminus, the TCP-1 domain, a cysteine-rich domain and the catalytic domain at the C-terminus. Some homologues contain a DEP domain, but Fab1p does not.

1.6.1 The FYVE domain

Initial studies on the FYVE domain identified it as a 60-70 amino acid cysteine-rich motif at the C-terminal end of the human early endosome antigen 1 (EEA1) (Mu et al., 1995). This region displays homology with *S. cerevisiae* Fab1p, *Caenorhabditis elegans* YOTB/ZK632 and limited conservation with *S. cerevisiae* proteins, Vac1p, Vps11p and Vps18p, proteins implicated in transport to the vacuole (Mu et al., 1995). Subsequent investigation with EEA1 redefined the motif as a zinc-binding FYVE domain (Stenmark et al., 1996). The acronym FYVE was assigned to the first four proteins identified containing this motif, Fab1p, YOTB, Vac1p and EEA1 (Stenmark et al., 1996). The FYVE domain is a conserved sequence in eukaryotes (Stenmark et al., 1996) and FYVE domain containing proteins are implicated in a variety of cellular functions such as endocytic membrane trafficking, cytoskeletal regulation, and signal transduction (Gillooly et al., 2001).

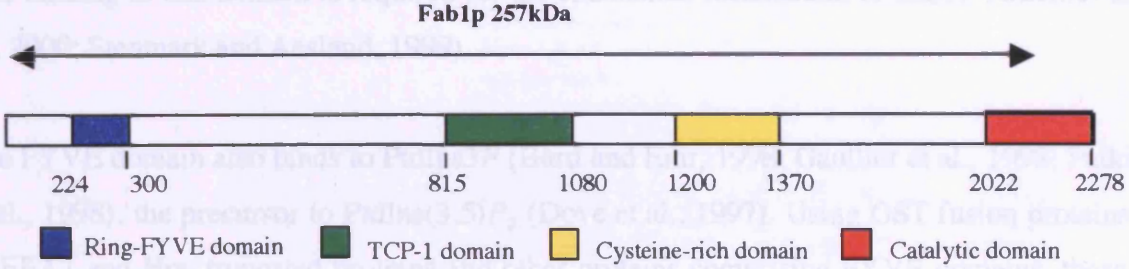

Figure 1.6. The domain topology of Fab1p showing the 4 domains and their amino acid positions within the protein (Gary et al., 2002). Other homologues of Fab1p, notably mammalian PIKfyve (Accession No. NP-055855) and *Drosophila melanogaster* (Accession No. AAF57789) also contain a DEP domain (Section 1.6.5). Fab1p does not contain this domain even though these domains occur in the yeast genome (Schultz et al., 1998). Fab1p domains were identified from the NCBI and Pfam databases (http://www.ncbi.nlm.nih.gov/entrez and http://www.sanger.ac.uk/Software/Pfam)

The primary structure of the FYVE domain contains eight conserved cysteines, which coordinate the binding of two zinc ions, and other conserved features. The most notable of these is the basic amino acid sequence motif R(R/K)HHCRxCG surrounding the third and fourth cysteine residues and several hydrophobic amino acid positions distributed around this motif (Stenmark et al., 1996) (Figure 1.6.1). In depth investigations reveal that deletion of this domain or mutation of conserved histidines and cysteines lead to a reduction in zinc binding with a simultaneous mislocalisation of EEA1 to the cytosol, demonstrating that zinc binding to this domain is required for the endosomal localisation of EEA1 (Gaullier et al., 2000; Stenmark and Aasland, 1999).

The FYVE domain also binds to PtdIns3*P* (Burd and Emr, 1998; Gaullier et al., 1998; Patki et al., 1998), the precursor to PtdIns(3,5)P_2 (Dove et al., 1997). Using GST fusion proteins of EEA1 and Hrs, truncated proteins and other proteins comprising FYVE domains, these domains direct selective binding of PtdIns3*P* both *in vivo and in vitro* (Burd and Emr, 1998; Gaullier et al., 1998; Patki et al., 1998). Hrs is the mammalian protein hepatocyte growth factor-regulated tyrosine kinase substrate that plays a role in endosome maturation (Komada et al., 1997). Additionally, upon the introduction of the PI3K inhibitor wortmannin, GFP-EEA1 fails to localise to early endosomes indicating that the FYVE domain binds to PtdIns3*P* *in vivo* and that this mechanism is required for the correct localisation of EEA1 (Patki et al., 1997; Stenmark et al., 1996).

In vitro analysis of the FYVE domain at the N-terminal of Fab1p shows that it binds to liposomes containing PtdIns3*P* but not liposomes enriched for other phosphoinositides (Burd and Emr, 1998). The FYVE domain of PIKfyve, the mammalian Fab1p homologue binds with high affinity to PtdIns3*P* enriched liposomes *in vitro* and this binding is sensitive to the presence of the PI3K inhibitor wortmannin (Sbrissa et al., 2002). Thus FYVE domains appear to target proteins to sites of PtdIns3*P* production (Gillooly et al., 2001).

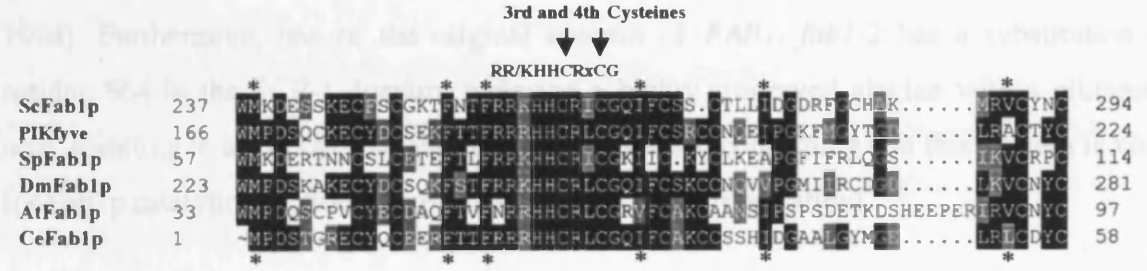

Figure 1.6.1. Alignment of FYVE domains in Fab1p homologues; PIKfyve, (Mammalian homologue) (Accession No. NP-055855), SpFab1p (*S. pombe*) (Accession No. 059722), DmFab1p (*Drosophila melanogaster*) (Accession No. AAF57789), AtFab1p, (*Arabadopsis thaliana*) (Accession Nos. NP-188044 and NP-195050), and CeFab1p, (*Caenorhabditis elegans*) (Accession No. T18961). Identical residues are shaded black whereas similar residues are grey. The FYVE domain is characterised by the presence of the basic amino acid sequence motif R(R/K)HHCRxCG surrounding the third and fourth cysteine residues as shown. Also shown with asterisks are some of the hydrophobic residues surrounding this motif. Adapted from McEwen *et al.* (McEwen et al., 1999).

1.6.2 The TCP-1/chaperonin-like domain

Fab1p contains a central domain containing conserved sequences similar to those present in chaperonin-containing T-complex proteins (CCT-1 proteins) (McEwen et al., 1999). These type II eight unit family of chaperonins are part of a larger family of TCP-1 related proteins (t-complex polypeptides), implicated in the binding and folding of newly synthesised actin and tubulin (Llorca et al., 1999; Vinh and Drubin, 1994). In yeast, mutations in CCT genes give rise to defects in microtubule function and segregation of nuclei (Vinh and Drubin, 1994). Furthermore, one of the original mutants of *FAB1, fab1-2* has a substitution at residue 864 in the TCP-1 domain, replacing a highly conserved glycine with a glutamic acid, resulting in a reduction of PtdIns(3,5)P_2 synthesis, confirming that this domain is vital for Fab1p catalytic function (Dr. F.Cooke, personal communication).

In PIKfyve, the region encompassing the TCP-1 domain was completely removed to generate *PIKfyveΔ560-1231* and analysed in COS cells (Sbrissa et al., 1999). Thin layer chromatography showed that kinase activity was greatly compromised in this mutant when compared to wild-type kinase activity implying that the TCP-1 domain is vital for PIKfyve function (Sbrissa et al., 1999). Whilst the TCP-1 domain appears to play a role in PtdIns(3,5)P_2 production, the exact role of the Fab1p TCP-1 domain has not yet been fully elucidated

1.6.3 The Cysteine-rich domain

This domain is found in all Fab1p homologues and is cysteine rich. There is no known role for this domain.

1.6.4 The Catalytic Domain

Initially it was speculated that the catalytic domain of Fab1p had PtdIns4*P* 5-OH kinase activity (Yamamoto et al., 1995). However the demonstration that Fab1p is required for PtdIns(3,5)P_2 production resolved this (Cooke et al., 1998). The generation of an extensive

array of catalytic domain mutants has proved that this domain is responsible for the PtdIns3*P* 5-OH kinase activity of Fab1p (Gary et al., 1998; McEwen et al., 1999).

Mutated residues and motifs within the catalytic domain of Fab1p, when expressed in *fab1*Δ cells exhibit variable PtdIns(3,5)P_2 production (Gary et al., 1998). Glycines at positions 2042 and 2045 were changed to valine (G2042V/G2045V) on the premise that these glycines are included in a highly conserved glycine rich loop common to the catalytic domain of several protein kinases (Grant et al., 1998; Hemmer et al., 1997). Similarly an aspartate at residue 2134 in the Fab1p putative catalytic domain was altered to an alanine (D2134R) on the basis that an analogous aspartate at position 386 of the c-Src protein is critical for catalytic activity (Xu et al., 1997) and also an analogous mutation of this residue in the yeast Vps34p kinase causes compromised PtdIns3*P* production (Schu et al., 1993). Subsequent analysis of these mutants in *fab1*Δ cells reveal that PtdIns(3,5)P_2 synthesis is duly compromised. In *fab1*Δ cells expressing the *fab1*$^{G2042V/G2045V}$ mutation, PtdIns(3,5)P_2 decreases 9-fold whereas in *fab1*^{D2134R}, PtdIns(3,5)P_2 is barely detectable in the presence of hyperosmotic stress (Gary et al., 1998).

Additionally, PtdIns(3,5)P_2 production in a *fab1-20* mutant is detectable but severely reduced under osmotic stress (Shaw et al., 2003) Sequencing of this mutant allele reveals a G2213E change, at a highly conserved glycine at the beginning of a conserved patch of residues within the catalytic domain, termed the activation loop (Kunz et al., 2000). This activation loop is responsible for substrate specificity in human type I and type II phosphoinositide phosphate kinases (Kunz et al., 2000). More specifically, the conserved residue D2216 in this loop and adjacent others, serve to coordinate divalent cations vital for positioning phosphates prior to phosphorylation of the substrates (Hanks and Hunter, 1995). Further catalytic residues have been identified that are believed to be important for the catalytic activity of various protein and phosphoinositide kinases, and in Fab1p these are Lys-2059, Asp-2196 and Asp-2216 (McEwen et al., 1999). The substitution of lysine at 2059 for methionine abolishes Fab1p PtdIns 3*P* 5-OH kinase activity *in vitro* (McEwen et al., 1999). Thus these data indicate that these residues are important for PtdIns(3,5)P_2 production and that the catalytic domain is responsible for the catalytic activity of Fab1p

(Gary et al., 1998; McEwen et al., 1999; Shaw et al., 2003; Yamamoto et al., 1995). The reduction of PtdIns(3,5)P_2 production in these strains containing catalytically compromised mutants of Fab1p is also accompanied by the appearance of a number of phenotypes associated with *fab1*Δ cells (see Section 1.10).

PIKfyve, the mammalian homologue of Fab1p, over-expressed in several mammalian cell lines, leads to increased intracellular PtdIns(3,5)P_2 production by approximately 30-50% (Ikonomov et al., 2001). Expression analyses of several PIKfyve catalytic domain mutants reveal that levels of both PtdIns5*P* and PtdIns(3,5)P_2 are significantly decreased when compared to wild-type cells (Ikonomov et al., 2002). Choice of sites to be mutated within this domain is dictated by the identification of conserved residues within the conserved loop region common to many human phosphoinositide kinases (Hanks and Hunter, 1995). A *PIKfyve*^{K1831E} mutant has no enzymatic activity *in vitro* and over-expression results in a "dominant-negative" phenotype *in vivo* (Sbrissa et al., 2000). Furthermore, the expression of *PIKfyve*^{K1999E}, *PIKfyve*^{K2000E} and *PIKfyve*$^{K1999E/K2000E}$ mutants cause significant reduction in both *in vitro* PtdIns5*P* and PtdIns(3,5)P_2 production, again with simultaneous defects in cellular morphology (Ikonomov et al., 2002). However as previously discussed (Section 1.5), there are considerable doubts that PtdIns5*P* is the functional output of PIKfyve and that it is more likely, PtdIns(3,5)P_2 is the sole physiological product of PIKfyve kinase (Cooke, 2002).

1.6.5 The DEP Domain

This is an ~100 amino acid motif of unknown function present in various signalling molecules including dishevelled, *Egl-10* and pleckstrin proteins from which it derives its acronym (Ponting and Bork, 1996). The domain is present in the Fab1p homologues, PIKfyve and *Drosophila melanogaster* DmFab1p (Shisheva, 2001), but is not found in Fab1p despite the DEP domain being widely reported in the yeast proteome (Schultz et al., 1998). No role for this domain in PIKfyve function has been described.

1.7 Regulation of Fab1p and PtdIns(3,5)P_2 synthesis

The identification of PtdIns(3,5)P_2 in yeast and the fact that levels increase transiently upon application of an hyperosmotic stress, suggest that this phospholipid is part of an osmoregulated signalling pathway and that PtdIns(3,5)P_2 production is tightly regulated (Dove et al., 1997). Similar observations are also seen in the plants, *Chlamydomonas moewussi*, alfalfa, pea and tomato (Meijer et al., 2001; Meijer et al., 1999). Intriguingly, two-fold PtdIns(3,5)P_2 production is detected in a CTLL-2 mouse T-lymphocyte cell line upon stimulation with both UV radiation and interleukin-2 (IL-2) (Jones et al., 1999). However, the molecular mechanisms underpinning activation of PtdIns(3,5)P_2 synthesis have not yet been determined.

In *S. cerevisiae*, two proteins appear to be upstream regulators of Fab1p: Vac7p and Vac14p (*vac*: vacuole inheritance mutants) (Bonangelino et al., 1997; Dove et al., 2002) (Figure 1.7). The *VAC7* gene was originally identified in a mutant screen for aberrant vacuolar segregation and inheritance where cells contained no vacuole or extremely small vacuoles in the bud (Gomes de Mesquita et al., 1996). Deletion of *VAC7* from *S. cerevisiae* results in phenotypes strikingly similar to *fab1*Δ cells (Bonangelino et al., 1997). These include defects in vacuole morphology where the vacuole of *vac7*Δ cells are grossly swollen, decrease in growth rates and defects in vacuole acidification and inheritance (Bonangelino et al., 1997). Additionally, electron density staining reveal that *vac7*Δ cells contain a single large vacuole and appear less-electron dense than wild-type cells and, *in vivo* PtdIns(3,5)P_2 in both resting and stressed cells is greatly reduced when compared to wild-type cells (Gary et al., 1998).

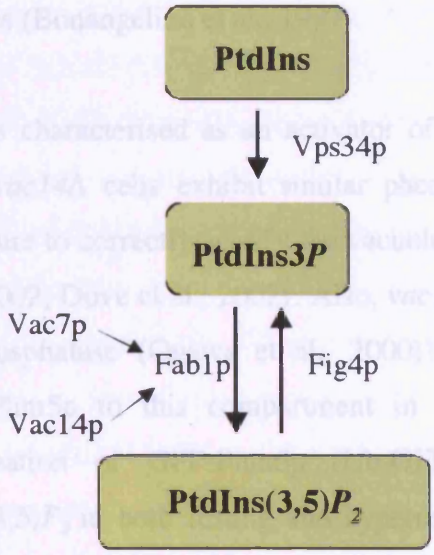

Figure 1.7. The steps leading to the synthesis of PtdIns(3,5)P_2 in *S. cerevisiae*. PtdIns is phosphorylated by Vps34p to PtdIns3*P*, which is a substrate of Fab1p. However Fab1p cannot synthesise PtdIns(3,5)P_2 efficiently without the presence of Vac14p and Vac7p (Bonangelino et al., 1997; Dove et al., 2002).

Expression of a *FAB1* mutant allele, *fab1-5* (contains undefined multiple mutations) in *vac7*Δ cells not only increases levels of PtdIns(3,5)P_2 four-fold (compared to wild-type), but also restores wild-type vacuole morphology (Gary et al., 2002). These results are therefore consistent with Vac7p acting as an activator of Fab1p activity. Database searches fail to show *VAC7* homologues in model organisms, however homologues do exist in other *Saccharomyces* species (Bonangelino et al., 1997).

The *VAC14* gene was characterised as an activator of Fab1p (Bonangelino et al., 2002; Dove et al., 2002). *vac14*Δ cells exhibit similar phenotypic defects to *fab1*Δ cells: an enlarged vacuole, failure to correctly acidify the vacuole and aberrant vacuole morphology (Bonangelino et al., 2002; Dove et al., 2002). Also, *vac14*Δ cells fail to traffic GFP-Phm5p (a polyphosphate phosphatase (Ogawa et al., 2000)) to the vacuole lumen. However trafficking of GFP-Phm5p to this compartment in *vac14*Δ cells is restored by the irreversible ubiquitination of GFP-Phm5p (Ub-GFP-Phm5p) (Dove et al., 2002). Furthermore, PtdIns(3,5)P_2 in both resting and hyperosmotically stressed *vac14*Δ cells is very low (Bonangelino et al., 2002; Dove et al., 2002). The absence of *VAC14* from these cells clearly causes a compromise in PtdIns(3,5)P_2 production in spite of having an intact *FAB1* gene, suggesting that Vac14p is acting as an upstream regulator of Fab1p (Dove et al., 2002). There are several potential homologues of Vac14p in other eukaryotes so it is reasonable to predict that Vac14p unlike Vac7p is a universal Fab1p regulator (Dove et al., 2002). Recently, mammalian Vac14 (hVac14) was found to regulate PIKfyve (Sbrissa et al., 2004). Using small interference RNA (siRNA) technology, endogenous hVac14 is knocked down, resulting in cell morphological defects similar to cells expressing PIKfyve mutants in which PtdIns(3,5)P_2 synthesis is compromised. *In vivo* PIKfyve activity is decreased whereas PIKfyve protein levels remain constant (Sbrissa et al., 2002). Depletion of hVac14 reduces intracellular PtdIns(3,5)P_2 whereas ectopic expression of hVac14 elevates PtdIns(3,5)P_2 levels (Sbrissa et al., 2002). Thus these data would suggest that the role of Vac14p is conserved in all eukaryotic cells.

1.8 Hydrolysis of PtdIns(3,5)P_2

FIG4, originally identified as a pheromone-induced gene (Erdman et al., 1998) was also identified as a potential regulator of PtdIns(3,5)P_2 levels in yeast (Gary et al., 2002) (Figure 1.7). The protein contains an N-terminal Sac phosphatase domain that defines a conserved phosphoinositide phosphatase enzymatic activity. *In vitro* studies on Sac1p reveal that this domain dephosphorylates PtdIns3*P*, PtdIns4*P* and PtdIns(3,5)P_2 (Guo et al., 1999; Hughes et al., 1999). Deletion of *FIG4* in *vac7*Δ cells (*fig4*Δ/*vac7*Δ) prompts a suppression of *vac7*Δ temperature sensitivity and vacuole morphology defects, and causes a sevenfold increase in PtdIns(3,5)P_2 levels when compared with *vac7*Δ cells (Gary et al., 2002). The identification and expression of a mutant allele of *FIG4*, *fig4-1* in *vac7*Δ cells similarly suppresses the temperature sensitivity of these cells, restoring growth at 38 °C and suppressing the enlarged vacuole morphology phenotype. But strikingly, the expression of the mutant allele restores PtdIns(3,5)P_2 levels to 2.5-fold greater than in *fig4*Δ/*vac7*Δ cells prompting the suggestion that Fig4p hydrolyses PtdIns(3,5)P_2 *in vivo* (Gary et al., 2002). This hypothesis was borne out when His-tagged-Fig4p displayed *in vitro* phosphatase activity only against PtdIns(3,5)P_2 (Rudge et al., 2004). GFP-Fig4p localises to the vacuole membrane consistent with it being a peripheral membrane-associated protein and this localisation is dependant on Vac14p, a known regulator of Fab1p (Dove et al., 2002; Rudge et al., 2004). Immunoprecipitation experiments confirm the interaction between the two suggesting a dual role for Vac14p in activating Fab1p kinase activity and also in regulating Fig4p phosphoinositide phosphatase (Rudge et al., 2004) (Figure 1.7). Consistent with these observations is the identification of Fig4p as interacting with Vac14p using the yeast two-hybrid technique (Dove et al., 2002).

Several other enzymes have been implicated in the hydrolysis of PtdIns(3,5)P_2. Amongst these are the synaptojanin yeast homologues Inp51p, Inp52p and Inp53p proteins and Sac1p, involved in actin cytoskeleton regulation, TGN secretion and microsomal ATP transport (Guo et al., 1999; Hughes et al., 2000). The Sac domains of Inp52p and Inp53p but not Inp51p possess polyphosphoinositide phosphatase activity (PPIPase) that hydrolyses PtdIns(3,5)P_2 to PtdIns *in vitro* (Guo et al., 1999; Hughes et al., 2000). The

deletion of Inp51p from yeast increases levels of cellular PtdIns(4,5)P_2 whereas the deletion of both Inp52p and Inp53p causes an increase in cellular levels of PtdIns(3,5)P_2 (Guo et al., 1999; Stolz et al., 1998b), suggesting that Inp52p and Inp53p have roles in PtdIns(3,5)P_2 metabolism (Srinivasan et al., 1997; Stolz et al., 1998a). The deletion of Sac1p from yeast prompts an increase in both PtdIns4P and PtdIns(3,5)P_2 but not PtdIns(4,5)P_2 suggesting that Sac1p has a role in the metabolism of PtdIns(3,5)P_2 (Guo et al., 1999; Hughes et al., 2000). Interestingly, the over-expression of Inp52p and Inp53p but not Inp51p in *sac1*Δ cells restores some growth defects and lipid levels (Hughes et al., 2000). In addition to the Sac1 domain, Inp51p, Inp52p and Inp53p also contain 5-phosphatase domains that remove phosphate from the D-5-hydroxyl position of phosphatidylinositol phosphates (Hughes et al., 2000). Thus the possibility that Inp52p, Inp53p and Sac1p have some role in PtdIns(3,5)P_2 metabolism must not be discounted.

1.9 Localisation of Fab1p in the yeast cell

Utilising differential centrifugation and western blotting techniques, Fab1p localises predominantly to the pellet fraction (70%) with 30% of protein being soluble in yeast cells (Gary et al., 1998). Using various cellular markers, soluble Fab1p localises to fractions containing endosomal and vacuolar membranes (Gary et al., 1998). However a caveat to this approach is that the authors use spheroplasting to lyse the cells, a procedure that strongly activates the production of PtdIns(3,5)P_2 (Dove et al., 1997); thus stimulating Fab1p may alter its localisation. Using indirect immunofluorescence, Fab1p co-localises with Vac8p, a protein associated with the vacuolar membrane (Wang et al., 1998) thus placing it at the vacuole and PVC (Gary et al., 1998). Similarly, using GFP-Fab1p expressed in wild-type BY4742 cells, GFP-Fab1p localises to FM4-64 positive vacuolar structures placing it at the vacuole (Dove et al., 2002). Thus it would appear that Fab1p localises predominantly to the vacuole membrane in *S. cerevisiae*.

1.10 Phenotype of *fab1*Δ cells and functions of PtdIns(3,5)P_2

When *FAB1* was first identified, a deletion allele was constructed (all but 41 of 2279 residues removed) and analysed in a diploid yeast strain (Yamamoto et al., 1995). This strain along with another expressing a temperature sensitive allele (*fab1-2*) yielded several distinct phenotypes (Yamamoto et al., 1995). Subsequent studies have demonstrated that PtdIns(3,5)P_2 production is critical for these functional outputs (Figure 1.10). A summary of *fab1*Δ-associated phenotypes is shown in Table 1.10.

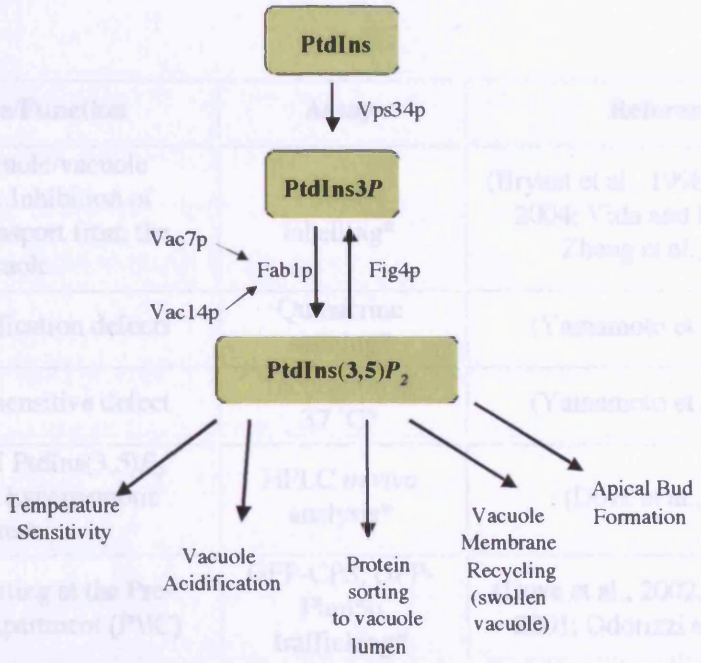

Figure 1.10. The proposed functional output of PtdIns(3,5)P_2 in *S. cerevisiae*. Does PtdIns(3,5)P_2 have one effector molecule that contributes to multiple cell functions, or are there several effectors of PtdIns(3,5)P_2 to explain these disparate functions?

Phenotype/Function	Assay	Reference
Swollen vacuole/vacuole morphology. Inhibition of retrograde transport from the vacuole	FM4-64 labelling*	(Bryant et al., 1998; Dove et al., 2004; Vida and Emr, 1995; Zheng et al., 1998)
Vacuole acidification defects	Quinacrine staining*	(Yamamoto et al., 1995)
Temperature sensitive defect	Incubation at 37 °C*	(Yamamoto et al., 1995)
Production of PtdIns(3,5)P_2 with/without hyperosmotic stress	HPLC *in vivo* analysis*	(Dove et al., 1997)
Protein missorting at the Pre-Vacuolar Compartment (PVC)	GFP-CPS, GFP-Phm5p trafficking*	(Dove et al., 2002; Epple et al., 2001; Odorizzi et al., 1998)
Abnormal apical bud formation	Direct Allele Replacement Technology (DART)	(Bidlingmaier and Snyder, 2002)

Table 1.10. The phenotypes displayed by *fab1*Δ cells and assays used to characterise them. These phenotypes are associated with the absence of *in vivo* PtdIns(3,5)P_2 in *fab1*Δ cells. Assays labelled with an asterisk were used in this study to help characterise *S. cerevisiae* effector and binding partners to Fab1p (Chapter 4).

1.10.1 FM4-64 staining/the swollen vacuole phenotype

The yeast vacuole is an acidic organelle and is required for yeast viability as it plays multiple roles in responses to various cellular stresses. It is also analogous to the mammalian lysosome and shares with it many functions such as degradation, storage, pH buffering of the cytoplasm and is important in water and ion homeostasis (Weisman, 2003).

One of the most striking features of the *fab1*Δ phenotype is the appearance of an enlarged vacuole visible by light microscopy (Yamamoto et al., 1995) (Figure 1.10.1a). The vacuole of *fab1*Δ cells swell to several times that of wild-type cells such that the only major visible organelle in the cell is the vacuole (Yamamoto et al., 1995).

Based on evidence that the enlarged vacuole phenotype observed in *vac7*Δ cells was caused by a retrograde blockage in traffic from the vacuole via the PVC to the TGN (Bryant et al., 1998), it was speculated that the *fab1*Δ swollen vacuole phenotype was caused by a similar retrograde blockage (Cooke, 2002; Cooke et al., 1998). The standard concept is that the vacuole is the final organelle for proteins destined for degradation (Bryant and Stevens, 1998; Kornfeld and Mellman, 1989); however this thinking has been altered with the possible existence of a retrograde pathway out of the vacuole to the TGN (Wilcox et al., 1992). Experimental proof to corroborate this concept was initiated by work on the Class III *vac* mutant *vac7-1* (Wang et al., 1996). As described, *VAC7* deletion mutants exhibit defects in vacuole morphology, vacuole acidification and vacuole inheritance, in a manner not dissimilar to *fab1*Δ cells (Bonangelino et al., 1997). The analysis of retrograde trafficking in *vac7* mutants was facilitated by the fusion of alkaline phosphatase (ALP) to a FXFXD motif, a localisation signal that mediates retrieval from the vacuole back to the TGN via the PVC. In wild-type cells, this fusion protein localises to the TGN through continual retrieval from the vacuole (Bryant and Stevens, 1997). In the *vac7-1* mutant, instead of localising to the TGN, the fusion protein mislocalises to the vacuolar membrane suggesting that *VAC7* is implicated in a transport step away from the vacuole to the TGN (Bryant et al., 1998). As Vac7p is a regulator of Fab1p, it was assumed that PtdIns(3,5)P_2 would be required for this step. This has now been shown to be the case (Dove et al., 2004).

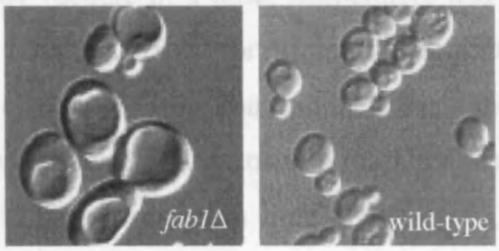

Figure 1.10.1a. Nomarski images of *fab1*Δ and wild-type cells. The *fab1*Δ vacuole is swollen and enlarged resulting in cells several times the size of wild-type. Taken from Dove *et al.* (Dove et al., 2002).

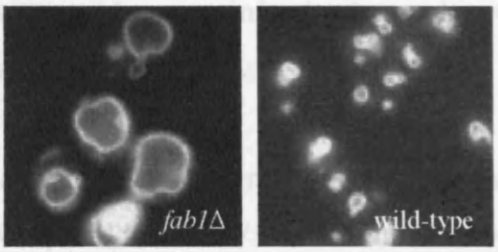

Figure 1.10.1b. FM4-64 fluorescence images of *fab1*Δ and wild-type cells. FM4-64 labelling show that the swollen *fab1*Δ vacuole is un-lobed and several times the size of wild-type cells. These cells have a lobed multi-membrane interior. Taken from Dove *et al.* (Dove et al., 2002).

While the swollen vacuole is one aspect of vacuole morphology easily observed using Nomarski optics, the development of the fluorescent lipophilic styryl compound, FM4-64 allows visualisation of subcellular dynamics and the spatial relationships between organelles (Vida and Emr, 1995). The dye can be used to follow membrane internalisation and transports to the yeast vacuole in a time, temperature and energy dependant manner. Yeast cells labelled with FM4-64 at 0 °C for 30 minutes exhibit staining exclusively at the cell perimeter indicative of FM4-64 insertion into the plasma membrane. No other staining is observed as at this temperature endocytosis is inhibited. Subsequently when cells are washed, warmed to 25 °C and observed at time points of 10, 20, 40 and 60 minutes, a gradual decrease in fluorescence is observed at the plasma membrane concomitant with a gradual increase in fluorescence initially in the cytoplasm and ultimately culminating in vacuolar membrane staining. Energy is required for this process. FM4-64 labelled yeast cells incubated in a glucose rich media at 30 °C with and without energy poisons to block ATP production (10 mM Sodium Fluoride (NaF) and 10 mM Sodium tri-nitrate (NaN_3)), exhibit altered labelling. Those cells growing in the absence of the energy poisons exhibit vacuolar membrane staining after 60 minutes whereas those growing in the presence of energy poisons, only plasma membrane staining is observed associated with a reduction in fluorescence intensity (Vida and Emr, 1995).

FM4-64 stained *fab1*Δ cells reveal an aberrant vacuole morphology (Bonangelino et al., 1997; Dove et al., 2002; Gary et al., 1998; Vida and Emr, 1995) . The vacuole appears as a single enlarged un-lobed organelle that comprises the majority of the cell volume (Figure1.10.1b).

The generation of several *FAB1* mutants reveals defects in FM4-64 staining (Gary et al., 1998). Analysis of *fab1*^{D2134R}, *fab1*$^{G2042V/G2045V}$ and *fab1-20* (*fab1*^{G2213E}) strains reveal phenotypes similar to *fab1*Δ cells (Gary et al., 1998; Shaw et al., 2003). As described previously, these mutants show a reduction or ablation in lipid kinase activity and FM4-64 data show that PtdIns(3,5)P_2 production is required to maintain wild-type vacuole morphology (Gary et al., 1998; Shaw et al., 2003).

Similarly, analysis of several Fab1p homologues reveals various vacuolar defects (Ikonomov et al., 2002; Morishita et al., 2002). Experiments with COS-7 cells expressing the mammalian catalytically dead *PIKfyve*^{K1831E} and *PIKfyve*$^{K1999E/K2000E}$ show defects in cell morphology such that cells became swollen, and accumulated large vacuole-like structures not dissimilar to the yeast *fab1*Δ phenotype (Ikonomov et al., 2002). Co-expression of wild-type PIKfyve with *PIKfyve*^{K1831E} transfected cells reverses the cell morphology of these cells suggesting that PIKfyve is crucial in maintaining correct cell morphology in mammalian cells (Ikonomov et al., 2001). Crucially, these cellular phenotypes are significantly corrected by the microinjection of PtdIns(3,5)P_2, but not PtdIns5*P* into these cells and whilst this correction is transient (48 hours), it demonstrates that not only is PtdIns(3,5)P_2 the likely functional output of PIKfyve but that this is sufficient to correct the aberrant vacuole morphology in these cells (Ikonomov et al., 2002). In *S. pombe*, *ste12*$^{+}$mutants contain abnormally enlarged vacuoles (Morishita et al., 2002) and deletion analysis of the *Candida albicans* homologue CaFab1p, displays defects in vacuole morphology (Morishita et al., 2002). Thus, Type III PIPkins and hence PtdIns(3,5)P_2 are likely to be required for vacuole homeostasis in all eukaryotes.

1.10.2 Quinacrine staining/vacuole acidity

*fab1*Δ cells also display non-acidification of the vacuole (Yamamoto et al., 1995). Using Nomarski imaging, this defect was originally highlighted by the apparent differences in refractivity between a *fab1* mutant and wild-type cells inferring *fab1* mutant strains have altered vacuole function and content (Yamamoto et al., 1995). One parameter of vacuole function is pH, which is qualitatively assayed by quinacrine (Yamamoto et al., 1995). Quinacrine is a basic hydrophobic fluorescent dye that crosses cell membranes by diffusion and concentrates due to protonation in acidified cellular compartments (Weisman et al., 1987). Thus *fab1*Δ vacuoles stain poorly, implying a failure to acidify this compartment correctly; conversely wild-type cells accumulate the dye, signifying a normal vacuolar pH (Yamamoto et al., 1995) (Gary et al., 1998). Yamamoto *et al* (Yamamoto et al., 1995) determined the pH of the *fab1*Δ vacuole was 7.0 or higher whereas the pH of the wild-type yeast vacuole was around 6.0 as reported previously (Preston et al., 1989).

Defects in acidification are present in cells expressing catalytically compromised *FAB1* mutants (Augsten et al., 2002; Gary et al., 1998; Shaw et al., 2003). Cells expressing *fab1*^{D2134R} exhibit weak vacuole acidification however those expressing *fab1*$^{G2042V/G2045V}$ exhibit wild-type staining as verified by electron microscopy (EM) (Gary et al., 1998). The transparency of the vacuole is likely to be a measure of vacuole acidification as inactivation of the vacuolar ATPase results in electron-transparent vacuoles (Wurmser and Emr, 1998). Thus by EM, *fab1*^{D2134R} vacuoles appear transparent similar to *fab1*Δ vacuoles whereas *fab1*$^{G2042V/G2045V}$ vacuoles are electron dense, similar to wild-type cells (Gary et al., 1998). Interestingly, the acidification defects observed in the *fab1*^{D2134R} strain when compared with the *fab1*$^{G2042V/G2045V}$ strain appear to correlate with PtdIns(3,5)P_2 in these strains. The *fab1*^{D2134R} strain contains barely traceable PtdIns(3,5)P_2 whereas the *fab1*$^{G2042V/G2045V}$ strain contains significantly higher levels than wild-type (Gary et al., 1998). Hence the presence of PtdIns(3,5)P_2 appears to be vital in the maintenance of vacuolar acidification in these cells (Gary et al., 1998). Similarly, *fab1-20* cells contain acidified vacuoles that are less severe than *fab1*Δ cells, again verified by EM (Shaw et al., 2003).

Deletion analysis of the *Candida albicans* homologue CaFab1p reveals defects in vacuole acidification as assayed by quinacrine (Augsten et al., 2002). Thus it appears that PtdIns(3,5)P_2 is required for the maintenance of an acidified vacuole in *Candida albicans*.

1.10.3 Growth of *fab1*Δ at 37 °C

As stated previously the initial isolation of a temperature sensitive *fab1* allele (*fab1-2*) resulted from a screen for abnormal nuclear segregation in yeast (Yamamoto et al., 1995). Both *fab1-2* and *fab1*Δ mutants grow at 23 °C but fail to grow at 37 °C (Yamamoto et al., 1995). Thus in *S. cerevisiae* PtdIns(3,5)P_2 is required for growth at 37 °C. However the mechanisms underlying this have yet to be determined.

1.10.4 GFP-CPS and GFP-Phm5p trafficking in wild-type and *fab1*Δ cells

In wild-type yeast cells, a number of integral membrane proteins such as carboxypeptidase S (CPS) (Odorizzi et al., 1998), Aut5/Cvt17p (Epple et al., 2001) and Phm5p (Reggiori and Pelham, 2001) traffic from the TGN via the PVC to the vacuole lumen (Cowles et al., 1997b; Odorizzi et al., 1998; Odorizzi et al., 2000). This process is assayed *in vivo* using GFP fusion-proteins of CPS and Phm5p (Figure 1.10.4a).

The type II integral membrane protein CPS was used to investigate protein trafficking in both *fab1*Δ and wild-type yeast cells (Odorizzi et al., 1998). In wild-type cells, this single trans-membrane domain vacuolar hydrolase, exits the endoplasmic reticulum (ER) and is transported from the TGN through the endocytotic pathway as an inactive precursor (proCPS). Transport of proteins to the vacuole via this pathway is mediated by the PVC (Cowles et al., 1997b; Odorizzi et al., 1998; Odorizzi et al., 2000). In preparation for a trafficking event, invagination of the PVC outer membrane occurs, followed by trafficking of integral membrane proteins such as proCPS into these invaginations. Vesicles then pinch off from the limiting membrane and bud into the lumen of the PVC. The PVC subsequently fuses with the vacuole releasing the invaginated vesicles into the vacuole lumen where they are digested by vacuolar hydrolases, proCPS is cleaved lumenal to its transmembrane domain to yield soluble active CPS (Odorizzi et al., 1998; Spormann et al., 1992). Thus in wild-type cells, this results in an even distribution of GFP within the vacuole (Odorizzi et al., 1998) (Figure 1.10.4a).

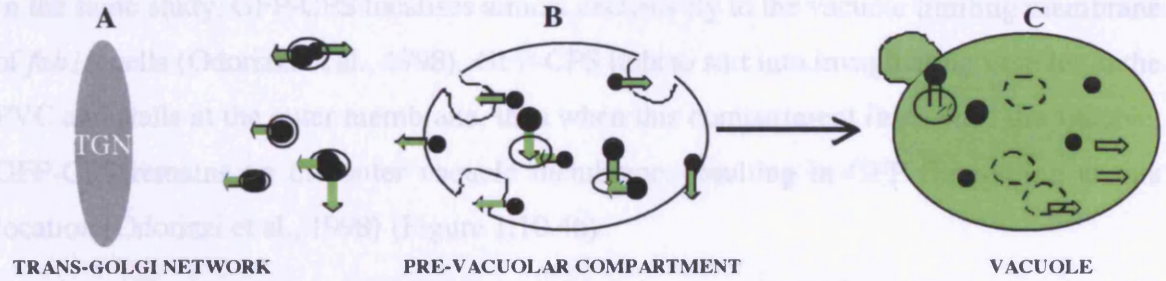

Figure 1.10.4a. Schematic of GFP tagged integral membrane protein trafficking in wild-type yeast cells. (A) Proteins traffic from the TGN and are incorporated into the membranes of vesicles that invaginate into the PVC (B). The mature PVC fuses with the vacuole releasing these vesicles, and digestion releases GFP tagged protein into the vacuole lumen (C). The vacuole fluoresces green.

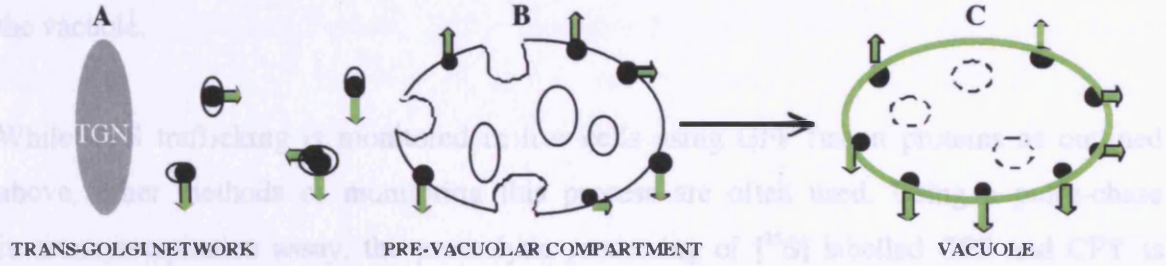

Figure 1.10.4b. Schematic of GFP tagged integral membrane protein trafficking in *fab1*Δ cells. (A) Integral membrane proteins traffic from the TGN to the PVC (B) vesicles are invaginated at the PVC however GFP-tagged proteins do not sort into invaginating vesicles but remain on the outer membrane. (C) When the PVC fuses with the vacuole, proteins remain on the outer vacuole membrane resulting in GFP fluorescing at the vacuole membrane.

In the same study, GFP-CPS localises almost exclusively to the vacuole limiting membrane of *fab1*Δ cells (Odorizzi et al., 1998). GFP-CPS fails to sort into invaginating vesicles at the PVC and stalls at the outer membrane, thus when this compartment fuses with the vacuole, GFP-CPS remains on the outer vacuole membrane, resulting in GFP fluorescing at this location (Odorizzi et al., 1998) (Figure 1.10.4b).

GFP-CPS trafficking is aberrant in the $fab1^{D2134R}$ mutant in which PtdIns(3,5)P_2 levels are compromised (Odorizzi et al., 1998). In this strain, GFP-CPS stalls at the outer vacuole membrane similar to *fab1*Δ cells whereas in the $fab1^{G2042V/G2045V}$ strain, GFP-CPS localises to the vacuole lumen (Odorizzi et al., 1998). Similarly GFP-CPS processing in *fab1-20* stalls at the outer vacuole membrane in a *fab1*Δ like manner (Shaw et al., 2003). Thus both these studies suggest that PtdIns(3,5)P_2 production is essential for correct GFP-CPS trafficking to the vacuole.

While CPS trafficking is monitored in live cells using GFP fusion proteins as outlined above, other methods of monitoring this process are often used. Using a pulse-chase immunoprecipitation assay, the proteolytic processing of [^{35}S] labelled CPS and CPY is assayed to give an indication of rate of production of mature enzyme (Klionsky et al., 1990). Both CPS and the soluble hydrolase carboxypeptidase Y (CPY) traffic from the TGN to the vacuole via the PVC and undergo a series of compartment specific modifications that are scored easily by changes in molecular weight (Klionsky et al., 1990). In *fab1*Δ cells, the formation of mature CPY is significantly delayed; even after 60 minutes chase, the majority of [^{35}S]-CPY is in the immature precursor form whereas wild-type cells contain 100% mature [^{35}S]-CPY after only 30 minutes chase (Yamamoto et al., 1995). Similarly, when the catalytically dead mutant, $fab1^{D2134R}$, with undetectable PtdIns(3,5)P_2 activity (Odorizzi et al., 1998) is assayed in the same manner with CPS, there is a significant delay in CPS maturation when compared to wild-type cells (Gary et al., 1998). The *FAB1* double mutant, $fab1^{G2042V/G2045V}$, in which levels of PtdIns(3,5)P_2 are 10% of wild-type (Odorizzi et al., 1998), exhibit wild-type CPS processing kinetics (Gary et al., 1998). However, there is a drawback to this technique: cells in these studies were lysed by

spheroplasting, a technique that strongly activates Fab1p (Dove et al., 1997) thus an allele with a partial loss of function could have wild-type trafficking restored.

1.10.4.1 Other cargos require Fab1p activity for correct trafficking

As mentioned previously, three other cargoes missort to the vacuole outer membrane in *fab1*Δ cells in a manner similar to CPS. Phm5p, a polyphosphate phosphatase, is an integral membrane protein required for the catabolism of polyphosphate in the yeast vacuole (Ogawa et al., 2000). Yeast cells accumulate large amounts of polyphosphate chains in the vacuole that are used as stores for phosphate metabolism (Urech et al., 1978). In wild-type cells, GFP-Phm5p traffics to the vacuole lumen (Reggiori and Pelham, 2001). Expressed in *fab1*Δ cells however, GFP-Phm5p trafficking is not restored to the vacuole lumen (Dove et al., 2002; Reggiori and Pelham, 2001). Interestingly, as with GFP-CPS (Katzmann et al., 2004), the fusion of an ubiquitin sequence to the N-terminus of the GFP-Phm5p sequence restores trafficking to the vacuole lumen in *fab1*Δ cells (Reggiori and Pelham, 2002).

Aut5/Cvt17p also missorts to the vacuole membrane in *fab1*Δ cells (Epple et al., 2001). This glycosylated integral membrane protein, tagged with haemagglutinin, missorts to the vacuole membrane as opposed to the vacuole lumen and suggests that Aut5/Cvt17p reaches the vacuole via the PVC in a similar manner to both CPS and Phm5p (Epple et al., 2001).

The α-pheromone receptor Ste3p, does not traffic efficiently into the PVC in both *fab1*Δ cells and a strain expressing a mutant allele of *FAB1* (*fab1-20*) (Shaw et al., 2003). In both instances the majority of GFP-Ste3p localises to the outer vacuole membrane (Shaw et al., 2003).

1.11 Ubiquitination of cargos is required for correct trafficking to the vacuole lumen

It is now clear that ubiquitination of cargos is essential for their delivery to the vacuole lumen (Hicke and Dunn, 2003; Katzmann et al., 2001; Reggiori and Pelham, 2001). However the speculation that de-ubiquitination also plays a role in this endosomal trafficking has been suggested in work with mutants lacking Doa4p, a late endosomal ubiquitin-specific protease that removes ubiquitin from protein conjugates prior to transport into the vacuole lumen (Amerik et al., 2000). In *doa4Δ* cells, reduced free ubiquitin disrupts ubiquitin related processes however these defects are restored by the provision of additional ubiquitin (Swaminathan et al., 1999). Both GFP-Phm5p and GFP-CPS mislocalise to the outer vacuole membrane in *doa4Δ* cells even though both are ubiquitinated *in vivo* (Reggiori and Pelham, 2001). Mutation of 4 lysines at the cytoplasmic domain of GFP-Phm5p abolishes attachment of ubiquitin chains, resulting in vacuolar membrane fluorescence hence trafficking is not restored in *doa4Δ* cells (Reggiori and Pelham, 2001). However, the covalent attachment of an ubiquitin to the N-terminus of GFP-Phm5p (Ub-GFP-Phm5p) results in wild-type trafficking, indicating that the trafficking defect in these cells is due to lack of ubiquitination of Phm5p at these residues (Reggiori and Pelham, 2001).

Recently, several molecules have emerged that are involved in the marking of incorrectly folded membrane proteins at the TGN for delivery into PVCs by the ubiquitination of their transmembrane domains (TMD) (Katzmann et al., 2001; Reggiori and Pelham, 2001). Tul1p (transmembrane ubiquitin ligase 1), a TGN resident protein, is required for the trafficking of GFP-CPS and GFP-Phm5p to the vacuole lumen but not for the trafficking of GFP-Sna3p and Ub-GFP-Phm5p (Reggiori and Pelham, 2002). In *tul1Δ* cells, GFP-Sna3p traffics in an ubiquitin independent manner into the vacuole lumen, as does Ub-GFP-Phm5p (Reggiori and Pelham, 2002). These data suggest that Tul1p tags certain proteins for entry into the PVC and ultimately the vacuole lumen and that this tagging may be carried out at the TGN where Tul1p is a resident protein (Reggiori and Pelham, 2002). Equally Fab1p is required to traffic GFP-CPS and GFP-Phm5p but not GFP-Sna3p and Ub-GFP-

2002). Whether Fab1p is involved in this process at the PVC or the TGN remains to be tested.

Rsp5p is an ubiquitin ligase that localises to the TGN, endosomal and plasma membranes in yeast (Katzmann et al., 2004). Rsp5p is an essential gene hence the analysis of GFP-CPS trafficking in a temperature sensitive Rsp5p strain (*mvb326*) (Katzmann et al., 2004). In *mvb326* cells GFP-CPS traffics to the outer vacuole membrane whereas Ub-GFP-CPS and GFP-Sna3p traffic to the vacuole lumen raising the possibility that Rsp5p like Tul1p tags certain proteins for entry to the vacuole lumen (Katzmann et al., 2004). However these workers also assessed the trafficking of GFP-CPS in *tul1*Δ in both SEY6210 and BY4742 backgrounds and observed no defects. This observation was in direct contrast to the work of Reggiori *et al.* where GFP-CPS trafficking was defective in *tul1*Δ in a BY4742 background (Reggiori and Pelham, 2002). A more recent report has suggested that trafficking of GFP-CPS depends on the genetic background of the yeast, some strains exhibit vacuolar staining, others exhibit partial staining between the vacuole and limiting membrane whereas others exhibit staining predominantly on the vacuolar membrane (Morvan et al., 2004). Thus these differences may be simply due to background strain or different methodologies used.

Notwithstanding these findings, Rsp5p binds to the WW domain (domains that recognise PPXY amino acid motifs (Sudol, 1996)) of Bsd2p, a protein that localises to the TGN (Hettema et al., 2004). Bsd2p contains three highly conserved transmembrane domains and is implicated in the vacuolar targeting of a manganese transporter and a mutant plasma membrane ATPase and appears to play a role in cell stress protection (Liu and Culotta, 1999; Liu et al., 1997). Also it would appear that Bsd2p and Tul1p function similarly but independently in the trafficking and ubiquitination of several substrates such as CPS and Phm5p and in *bsd2*Δ/*tul1*Δ cells, defects in trafficking of these cargos are more pronounced than in *bsd2*Δ and *tul1*Δ cells alone (Hettema et al., 2004). Thus, Tul1p and Bsd2p/Rsp5p both appear to contribute to the independent ubiquitination of these substrates and the interaction between Bsd2p and Rsp5p suggests that Bsd2p may serve as an adaptor linking Rsp5 to these substrates for ubiquitination (Hettema et al., 2004).

Clearly, there are several ubiquitination events along the TGN/PVC/vacuole pathway. Protein cargos would appear to be ubiquitinated at the TGN probably by Tul1p or Rsp5, for transport to the vacuole lumen. However, entry into invaginating vesicles would seem to require deubiquitination of these cargos possibly by Doa4p in order to prepare them for vacuole degradation and to maintain recycling ubiquitin in the cell (Hicke and Dunn, 2003). Clearly more investigation is required to resolve the mechanisms behind ubiquitination.

1.12 Effectors of PtdIns(3,5)P_2

The paradigm that phosphoinositides act as membrane-anchored mediators of a wide variety of intracellular functions has become widespread in recent years (Cullen et al., 2001; Hurley and Meyer, 2001; Lemmon, 2003). Phosphoinositide headgroups can be rapidly modified by phosphorylation or dephosphorylation to induce or ablate membrane-targeting signals at specific times and locations (Cullen et al., 2001). This diversity of function is increasing, seemingly exponentially, with the large amount of phosphoinositide recognising protein domains that have been identified (Cullen et al., 2001). Protein domains such as ENTH, ANTH, FYVE, PX, PH and FERM, which bind phosphoinositides, have ensured a huge and significant diversity at both a structural and functional level in intracellular signalling (Lemmon, 2003).

As discussed, the loss of PtdIns(3,5)P_2 is concomitant with the appearance of several distinct phenotypes unique to the *fab1*Δ strain (summarised in Figure 1.12), thus it is expected that there would be one or more PtdIns(3,5)P_2-specific binding proteins that would carry out these functions. This is borne out by the identification of several effector proteins for PtdIns(3,5)P_2 which when deleted from the yeast genome cause some but not all the phenotypes associated with the *fab1*Δ phenotype (Dove et al., 2004; Eugster et al., 2004; Friant et al., 2003). As deletion of these genes do not cause all the phenotypes associated with *fab1*Δ cells it is now obvious, as predicted (Cooke, 2002; Dove et al., 2002) that Fab1p regulates a number of independent cellular processes via PtdIns(3,5)P_2 production. Thus the efficacy of PtdIns(3,5)P_2 function is mediated via its interaction with several different effector proteins (Figure 1.12).

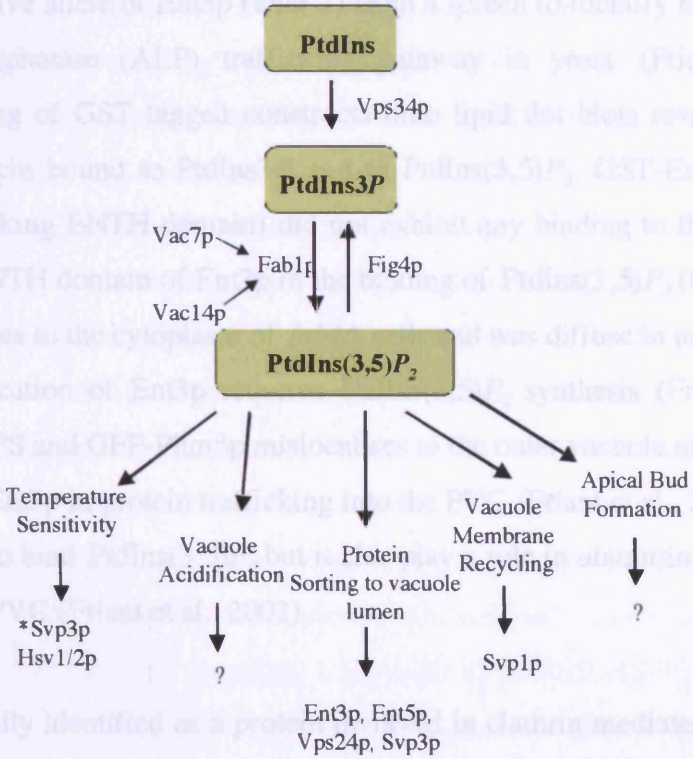

Figure 1.12. The involvement of Fab1p and PtdIns(3,5)P_2 and downstream effector proteins in various yeast cell functions. PtdIns(3,5)P_2 function in combination with the these effector proteins is pivotal to the cellular functions as outlined. *Svp3p and Hsv1/2p have not been fully described in the literature but have been mentioned by Dove *et al* (Dove et al., 2004).

Both Ent3p and Ent5p were identified as effector proteins of PtdIns(3,5)P_2 and were implicated in PVC protein trafficking (Eugster et al., 2004; Friant et al., 2003). Both contain epsin N-terminal homology (ENTH) domains that promote membrane recruitment by binding various phosphoinositides (De Camilli et al., 2002; Kay et al., 1999). The identification of Ent3p as an effector of PtdIns(3,5)P_2 stemmed from the isolation of a temperature sensitive allele of Ent3p (*ent3-1*) from a screen to identify mutants deficient in the alkaline phosphatase (ALP) trafficking pathway in yeast (Friant et al., 2003). Subsequent blotting of GST tagged constructs onto lipid dot blots revealed that a GST-Ent3p fusion protein bound to PtdIns3P and to PtdIns(3,5)P_2. GST-Ent3pΔ*ENTH* fusion protein (Ent3p lacking ENTH domain) did not exhibit any binding to these phospholipids implicating the ENTH domain of Ent3p in the binding of PtdIns(3,5)P_2 (Friant et al., 2003). Ent3p-GFP localises to the cytoplasm of *fab1*Δ cells and was diffuse in nature implying that the endosomal location of Ent3p requires PtdIns(3,5)P_2 synthesis (Friant et al., 2003). Similarly, GFP-CPS and GFP-Phm5p mislocalises to the outer vacuole membrane in *ent3-1* cells implicating Ent3p in protein trafficking into the PVC (Friant et al., 2003). Thus, Ent3p appears not only to bind PtdIns(3,5)P_2 but it also play a role in ubiquitin-dependent protein trafficking to the PVC (Friant et al., 2003).

Ent5p was originally identified as a protein involved in clathrin-mediated trafficking at the late TGN where it bound to the γ-subunit of AP-1 (Duncan et al., 2003). Based on homology with Ent3p, Ent5p was similarly investigated as an effector of PtdIns(3,5)P_2 and was also found to specifically bind to this phosphoinositide via its ENTH domain (Eugster et al., 2004). In *ent3*Δ/*ent5*Δ cells, GFP-CPS, GFP-Ste2p and GFP-Phm5p mislocalise to the outer vacuolar membrane suggesting that Ent3p and Ent5p are required for the correct trafficking of ubiquitinated cargo to the vacuole lumen (Eugster et al., 2004). Ent3p and Ent5p act in complex with Vps27p, a protein containing an ubiquitin-interacting motif (UIM) and implicated in the ESCRT I cascade in yeast (Katzmann et al., 2003) Thus the interaction between Ent3p/Ent5p/Vps27p is believed to facilitate the trafficking of ubiquitinated cargo into intralumenal vesicles at the PVC (Eugster et al., 2004).

SVP1 (swollen vacuole phenotype) was identified on the basis that the *svp1Δ* strain exhibit enlarged vacuoles similar to *fab1Δ* cells (Dove et al., 2004). GFP-Svp1p localises to the vacuole in a Fab1p-dependant manner suggesting that it may be an effector of PtdIns(3,5)P_2. On this premise, GST-Svp1 binds to PtdIns(3,5)P_2 but more stringent binding studies narrowed this specifically to a WD40 domain in Svp1p that folds as a β-propeller (Dove et al., 2004). WD40 repeats are found in a number of eukaryotic proteins that cover a wide variety of functions including adaptor/regulatory modules in signal transduction, pre-mRNA processing, cytoskeleton assembly and cell cycle control (Yaffe and Smerdon, 2004). The only common functional theme of WD40 domains is to serve as a stable propeller-like platform to which proteins can bind either stably or reversibly (Yaffe and Smerdon, 2004). This is the first example of a WD40 protein binding to phosphoinostides and may be indicative of a subset of these proteins (Dove et al., 2004). *svp1Δ* cells also exhibit a defect in membrane recycling from the vacuole, a phenotype observed in *fab1Δ* and *vac7Δ* cells prompting the formation of an enlarged vacuole (Bryant et al., 1998). That *svp1Δ* have enlarged vacuoles and similarly fail to recycle membrane to the late endosome implies that Svp1p/PtdIns(3,5)P_2 are important for this step (Dove et al., 2004). Homologues of Svp1p exist in *Drosophila, Arabadopsis, C. elegans* and mammals suggesting that this protein may constitute a large family of PtdIns(3,5)P_2–effector proteins (Dove et al., 2004). However, Svp1p does not appear to play a role in GFP-Phm5p trafficking nor vacuole acidification, therefore these PtdIns(3,5)P_2–dependant processes appear to be independent of Svp1p (Dove et al., 2004).

Mammalian Vps24p (mVps24p) was identified by screening a cDNA phage library with biotin tagged-PtdIns(3,5)P_2 immobilised onto NeutrAvidin beads (Whitley et al., 2003). mVps24p is homologous with *S. cerevisiae* Vps24p, which is a component of the oligomeric ESCRT III complex involved in the trafficking of transmembrane proteins into the PVC destined for transport to the vacuole lumen (Babst et al., 2002). His-tagged mVps24p binds with high selectivity to PtdIns(3,5)P_2 in lipid binding experiments and localisation experiments places mVps24p at endosomal membranes consistent with PtdIns(3,5)P_2 localisation (Whitley et al., 2003). However, these results have not yet been verified in *S. cerevisiae*.

Four other proteins are reported to bind PtdIns(3,5)P_2. Firstly, the Phox homology (PX) domain of the cytokine-independent survival kinase (CISK) binds to PtdIns(3,5)P_2, PtdIns(3,4,5)P_3 and to a lesser extent to PtdIns(4,5)P_2 *in vitro* whereas CISK is localised to endosomal compartments of vesicles in COS-7 cells (Xu et al., 2001). Secondly, the soybean Sec14p homologue Ssh1p, identified as a phosphatidylinositol transfer protein (PITP) binds to PtdIns(3,5)P_2 and to PtdIns(4,5)P_2 *in vitro* and can rescue functional defects in *sec14*Δ cells (Kearns et al., 1998). Thirdly, *S. cerevisiae* Gcs1p, identified as a homologue of centaurin α, binds PtdIns(3,5)P_2 *in vitro* with high affinity and specificity (Blader et al., 1999). *gcs1* mutants display vesicle trafficking defects and both *in vivo* and *in vitro* studies show that Gsc1p interacts with the actin cytoskeleton in *S. cerevisiae* (Blader et al., 1999). Lastly, the PX domain of sorting nexin 1 (SNX1) from eukaryotes binds PtdIns3P and PtdIns(3,5)P_2 *in vitro* (Cozier et al., 2002). GFP-SNX1 partially localises to the early endosomal compartment in HeLa cells consistent with the presence of PtdIns3P at this compartment. (Cozier et al., 2002).

This subset of PtdIns(3,5)P_2 interacting proteins may define new functions of PtdIns(3,5)P_2 biology not previously identified. However it is expected that disruption of genes for authentic PtdIns(3,5)P_2 binding proteins would exhibit some *fab1*Δ phenotypes hence, it will be interesting if deletion mutants of these proteins are analysed in terms of PtdIns(3,5)P_2 and Fab1p function. Certainly those proteins containing recognised phosphoinositide-binding motifs such as the PX containing CISK and SNX1 would appear likely candidates to be PtdIns(3,5)P_2 binding proteins; however as yet there is little data linking these or the other proteins to PtdIns(3,5)P_2 functions.

1.13 Summary and outline of project

The study of many eukaryotic metabolic and signalling processes has been greatly facilitated by use of the model organism *S. cerevisiae* (Botstein and Fink, 1988). Study of these processes in this organism offers many scientific and technical advantages over most other systems, *S. cerevisiae* is a simple unicellular system, grows rapidly over several generations and with the sequencing of the yeast genome completed, its genes can be easily

manipulated and studied (Winzeler et al., 1999). Thus the tractability of *S. cerevisiae* makes it ideal to study those phosphoinositide signalling systems that appear to be evolutionary well conserved between eukaryotes (Roth and Sternweis, 1997).

Fab1p and its putative homologues are the first PtdIns3*P* 5-kinases to be classified as type III PIPkins, establishing them as prototype enzymes of this class (Cooke et al., 1998). This distinguishes them from the type I and type II PIPkins which have different enzymological properties and are in general much smaller proteins (47-90kDa) than the type III PIPkins (Cooke et al., 1998). As outlined, the functional output of the type III PIPkins is derived from the 5-OH phosphorylation of PtdIns3*P* to produce PtdIns(3,5)P_2 which appears to be a conserved mechanism in all eukaryotic cell types investigated (Dove et al., 1997; Whiteford et al., 1997). The loss of Fab1p and PtdIns(3,5)P_2 from yeast causes several distinct phenotypes (Section 1.10), thus this phosphoinositide and PtdIns3*P* 5-kinase are now accepted as playing a pivotal role in a wide range of independent intracellular yeast functions (Section 1.10). The mechanisms behind these functions have not yet been fully elucidated despite several regulators of Fab1p (Section 1.7) and effectors of PtdIns(3,5)P_2 having been identified (Section 1.12). While analysis of these regulatory proteins have shed some light on several Fab1p/PtdIns(3,5)P_2 functions, there still remains unidentified regulators/effectors influencing these mechanisms.

Therefore, the remit of this project is to specifically identify effectors/regulators of Fab1p. The *FAB1* gene, individual domains and double adjacent domains will be used as bait in a yeast two-hybrid screen (Chapter 3). Potential interactors will be evaluated and their corresponding deletion mutants subject to phenotypic analyses. These analyses will incorporate several assays used to characterise the *fab1*Δ strain, the premise being that deletion mutants exhibiting defects similar to this strain are good candidates to be effectors/regulators of Fab1p (Chapter 4). Subsequent, more thorough investigations will focus on potential interactors on the strength and outcome of these phenotypic analyses (Chapter 5).

2 MATERIALS AND METHODS

Merck BDH and Sigma supplied most reagents. New England Biolabs supplied all restriction and modifying enzymes. Difco supplied chemicals used for solid and liquid media and synthetic drop-out media (SD) was supplied by Bio101.

2.1 Yeast Strains

PJ69-4α and PJ69-4a yeast strains (James et al., 1996) were used in the yeast two-hybrid screen and were used to express the bait (*GAL4*-DNA-binding domain fusion) and prey (*GAL4* activation domain fusion) respectively.

PJ69-4α Genotype: MATalpha *trp1-901; leu2-3, 112 ura3-52 his3-200 gal4Δ gal80Δ LYS2::GAL1-HIS3 GAL2-ADE2 met2::GAL7-lacZ*

PJ69-4a Genotype: MAT*a trp1-901; leu2-3, 112 ura3-52 his3-200 gal4Δ gal80Δ LYS2::GAL1-HIS3 GAL2-ADE2 met2::GAL7-lacZ*

All yeast manipulations were carried out in the BY4741 strain background and were supplied by Euroscarf, University of Frankfurt, Germany.

BY4741 Genotype: MAT*a; his3Δ1; leu2Δ0; met15Δ0; ura3Δ0.*

2.2 *E. coli* strains

DH5α® was the *E. coli* strain of choice for transformations and cloning.
Genotype: ϕ80d*lac*ZΔM1, *rec*A1, *end*A1, *gyr*A96, *thi*-1, *hsd*R17(r_k-,m_k+), *supE*44, *rel*A1, deoR, Δ(*lac*ZYA-*argF*)U169

2.3 Plasmids

YCplac111 (Gietz and Sugino, 1988)
YCplac33 (Gietz and Sugino, 1988)
pRS313 (Sikorski and Hieter, 1989)

Plasmids for expressing myc-tagged yeast proteins from the *MET25* promoter were constructed as follows. The *MET25* promoter and phosphoglycerate kinase (PGK) polyadenylation/termination sequence were amplified by PCR from pBridge (Clontech), and sub-cloned in pCR®-Blunt (Invitrogen). PCR fidelity was confirmed by sequencing. This fragment was excised by restriction enzyme digestion and ligated into YCplac33 (*URA3*). This plasmid was linearised, and primers coding for the myc-tag (9E10) epitope inserted to give a plasmid with a MET25/myc/PGK expression cassette. This cassette was then excised and ligated into YCplac111 (*LEU2*), and pRS313 (*HIS3*) to give three expression plasmids with different auxotrophic markers.

2.4 Yeast methods

Yeast cultures were grown in rich media or synthetic defined minimal media (SD). All liquid and solid media having been prepared according to manufacturers instructions/Maniatis in clean glassware was sterilised by autoclaving at 121 °C for 15 minutes at 103 kPa. 2 % bacto-agar was added to solutions to make solid media. Plates were poured using basic laboratory aseptic technique and were left to dry for 2-3 days at room temperature before use. Colonies from yeast transformations were routinely streaked onto fresh plates before analysis. Yeast strains were maintained as frozen stocks in 2xYPD supplemented with 15 % glycerol at –80 °C.

Solutions.

YAPD: 2 % D-glucose, 2 % bactopeptone, 1 % yeast extract.

SD: (Bio101) 0.67 g/L yeast nitrogen base (without amino acids), 2 % (w/v) D-glucose, 2 % (w/v) agar and specified weight of auxotrophic amino acids where required.

3-AT; filter sterilised through a 0.22 μm filter (Acrodisc) and added to cool media prior to pouring plates.

2.4.1 Monitoring yeast cell growth

Yeast cells grown in liquid media was periodically monitored by taking OD_{600nm} readings on a Hitachi U-1500 spectrophotometer (Hitachi Corporation, Japan) in 1 ml cuvettes (Sarstedt). Alternatively, cell density was monitored by counting cells using an improved Neunauer haemocytometer (Hawksley) on a light microscope.

2.4.2 High Efficiency Yeast Transformation

Plasmid DNA was transformed into yeast cells using the high efficiency yeast transformation protocol (Gietz and Woods, 2002). Briefly, yeast cells were inoculated from solid media into 10 ml YPD and incubated overnight at 30 °C or 24 °C with shaking. Next morning, 5 ml of the overnight culture was added to 50 ml YPD liquid culture and grown until the OD_{600nm} was between 0.75-1. The culture was centrifuged at 2500 rpm for 5 minutes, the supernatant decanted and the pellet washed with sterile distilled water and re-centrifuged as before. The supernatant was removed, 1 ml 100 mM lithium acetate added and the volume transferred to a micro-centrifuge tube. Cells were pelleted by brief centrifugation, the supernatant removed and 400 µl 100 mM lithium acetate added. After vortexing, 50 µl was removed and transferred to a clean sterile micro-centrifuge tube. To this tube the following was added in this order:

240 µl PEG 3320 (50 % v/v)
36 µl 1 M lithium acetate
25 µl pre-boiled Herring sperm DNA (2 mg/ml).
50 µl distilled water containing plasmid to be transformed (0.1-1 µg DNA)

The tube was vortexed vigorously for one minute and incubated at 30 °C or 24 °C for 30 minutes and then 42 °C for 20 minutes in order to heat shock. The cells were centrifuged briefly and the supernatant removed. 1 ml sterile distilled water was added to wash and the cells were centrifuged again. The pellet was resuspended in 1 ml sterile distilled water and approximately 200 µl spread onto appropriate selective media. Plates were incubated at 30 °C or 24 °C for several days after which single colonies were streaked onto fresh plates.

2.4.3 Yeast Two-Hybrid Assay

ORFs to be screened were cloned into a *GAL4* DNA binding domain bait vector (pOBD2) by homologous recombination using a PCR based strategy, transformed into the bait strain PJ69-4α, plated onto SD-Trp media and grown at 30 °C to select for transformants. Confirmation of positive transformants was assayed by PCR (Section 2.6.6).

To assay for self-activation, positive transformants were screened by streaking onto SD-Trp-His media plus 8 mM 3-amino-1,2,4-triazole (see below) and incubation at 30 °C for several days. Lack of growth indicated no self-activation by the bait fusion of the integrated *GAL4* promoter *HIS3* fusion promoter.

Bait fusions in strain PJ69-4α were grown up overnight in SD-Trp liquid media and mated to *GAL4* Activation domain fusions in the opposite mating type PJ69-4a. These latter strains were pinned on 16 SD-Leu plates, 384-format array which contained 6000+ ORFs (Uetz et al., 2000). Diploids were selected on SD-Trp-His after 3-5 days incubation at 30 °C. Protein-protein interactions were selected for by pinning diploids onto SD-Trp-His-Leu media (see below) supplemented with 8 mM 3-AT. Colonies were scored after 10 days incubation at 30 °C.

All replications and inoculations were carried out using the 384-pin replicator of a Biomek® 2000 Laboratory Automation Workstation (Beckman), with movements programmed using the Bioworks™ Version software (Beckman). Putative interacting partners were identified as reproducible two-hybrid positives that were observed twice from

duplicate high throughput two-hybrid screens. It was assumed that interacting proteins identified only once were the result of a non-reproducible false positive.

Media for yeast two-hybrid work

SD-Trp (Bio101):
0.67 g/L yeast nitrogen base (without amino acids), 2 % (w/v) D-glucose, 2 % (w/v) agar and 0.64 g/L SD–Trp media

SD-Trp-His (Bio101):
0.67 g/L yeast nitrogen base (without amino acids), 2 % (w/v) D-glucose, 2 % (w/v) agar and 0.62 g/L SD–Trp-His media

SD–Trp-His-Leu (Bio101):
0.67 g/L yeast nitrogen base (without amino acids), 2 % (w/v) D-glucose, 2 % (w/v) agar and 0.62 g/L SD –Trp-His-Leu

8 mM 3-AT, filter sterilised through 0.22 μm filter (Acrodisc) and added to cool media prior to pouring plates.

2.4.4 LacZ Assay

LacZ assays were carried out on bait (PJ69-4α) and prey (PJ69-4a) strains from the Fields library in order to assess protein-protein interactions. The method is adapted from Guarente *et al* (Guarente, 1983).

To mate the bait and the prey strains, yeast cells were inoculated into YPD and incubated overnight at 30 °C. Next day, cultures were centrifuged briefly at 14,000 rpm to pellet yeast, the supernatant removed and the pellet washed/resuspended in sterile distilled water. This volume was centrifuged briefly, and 200 µl spread onto SD-Leu-Trp plates. Plates were incubated at 30 °C.

For the assay, mated yeast cells were grown to mid log phase in SD–Leu-Trp liquid culture and $OD_{600\,nm}$ recorded. A prey only control was also assayed for LacZ activity. 20 ml was removed from the culture and centrifuged at 4000 rpm. This was done in triplicate. Pelleted cells were resuspended in 1 ml Z buffer (60 mM $Na_2HPO_4.7H_2O$, 35 mM $NaH_2PO_4.H_2O$, 10 mM KCL, 1 mM $MgSO_4.7H_2O$, 0.27 % v/v β-mercaptoethanol pH 7.0). Cells were lysed by adding 150 µl chloroform, 150 µl 0.1% (w/v) SDS, vortexing for 15 seconds and incubating at 28 °C for 5 minutes. The reaction was started by adding 200 µl O-nitrophenyl-β-D-galactopyranoside (4 mg/ml Z buffer) and the time noted. When a faint yellow colour was observed, 500 µl 1M Na_2CO_3 was added to stop the reaction and the time elapsed noted. The tubes were centrifuged at 14,000 rpm for 5 minutes after which the OD_{420nm} of the supernatant was recorded. β-galactosidase activity was calculated using the following equation and data was represented as arbitrary units.

1000 x (OD_{420nm}/ OD_{600nm} x volume assayed x time).

2.4.5 Extraction of total yeast cell protein

Yeast cells were grown to mid log phase (5-8 x 10^6 cells/ml) as determined by counting using a haemocytometer. Cultures were centrifuged at 4000 rpm in order to pellet the yeast and the supernatant discarded. To the pellet was added 0.4 mg of cold acid washed glass beads (425-600 micron, Sigma) along with an appropriate volume of cold extraction buffer (100 mM Tris pH 6.8, 150 mM NaCl, 10 mM EDTA, 1 % v/v Triton X-100, 1 mM DTT, 0.5 mM Benzamadine, and protease inhibitors, (Roche Biochemicals) to just cover both the cells and beads. Cells were disrupted by vortexing for 30 seconds and cooling for 30 seconds, repeated 5 times. Cellular debris was pelleted by centrifugation at 14,000 rpm leaving a clear supernatant.

2.4.6 Separation of proteins by SDS polyacrylamide gel electrophoresis

Individual proteins and complexes from a yeast extract can be separated using a discontinuous electrophoresis system. When electrophoresed, the lattice formed by

polymerised acrylamide molecules separates proteins on the basis of size difference. In this study, the Hoefer SE 400 series was used for this purpose (Amersham Pharmacia Biotech).

A resolving gel (% depended on the size of protein being separated) was allowed to polymerise between two glass plates onto which a 3 % stacking gel was poured, a comb inserted and the gel allowed to set.

Prior to loading, protein samples were boiled for 10 minutes in sample buffer (see below). A reference protein ladder (Amersham Pharmacia biotech) was also included. Samples were loaded into wells and electrophoresis proceeded at 30 V overnight in running buffer (see below).

Resolving Gel (for an 8 % gel)

8 ml Acrylamide (National Diagnostics)

3.2 ml Methylene bis-acrylamide (National Diagnostics)

0.15 ml 20 % (w/v) SDS

11.25 ml 1 M Tris HCl pH 8.8

0.15 ml 20 % w/v Ammonium persulphate } polymerising agents

10 µl v/v TEMED

Water to 30 ml

3 % Stacking Gel

1 ml Acrylamide (National Diagnostics)

0.4 ml Methylene bis-acrylamide (National Diagnostics)

0.05 ml 20 % (w/v) SDS

1.25 ml 1 M Tris HCl pH 6.8

0.05 ml 20 % (w/v) Ammonium persulphate } polymerising agents

10 µl (v/v) TEMED

0.0

Water to 10 ml

10 µl (v/v) TEMED

Water to 10 ml

Sample Buffer

10 % (w/v) SDS, 20 % (v/v) Glycerol, 1 M Tris pH 6.8, 0.1 M DTT, Bromophenol Blue

Running Buffer

0.025 M Tris, 0.192 M Glycine, 0.1 % (w/v) SDS

2.4.7 Direct staining of SDS gels

After electrophoresis, the gel was dismantled and the stacking gel cut away from the main gel. To visualise protein bands the gel was immersed in Coomassie Blue: 0.05 % (w/v) Coomassie blue, 50 % (v/v) methanol and 10 % (v/v) acetic acid. Gels were agitated for 30-60 minutes after which they were destained in 10 % (v/v) methanol and 7.5 % (v/v) acetic acid at room temperature.

2.4.8 Western Blotting of SDS gels

SDS-PAGE separated proteins were transferred onto nitrocellulose membranes (Schleicher & Schuell) by electrophoretic transfer using the Trans-Blot® Electrophoretic Transfer Cell (Biorad). Prior to transfer, the gel, several pieces of Whatmann filter paper, a section of nitrocellulose membrane and gel pads were soaked in chilled transfer buffer (25 mM Tris, 150 mM Glycine, 20 % (v/v) Methanol) in order to equilibrate all transfer apparatus. The apparatus was set up as a sandwich: padding, filter paper, gel, nitrocellulose filter, filter paper and padding and positioned in the transfer cell so that the gel was towards the cathode and membrane towards the anode. Transfer buffer was poured into the tank to allow for the application of 0.4 milli-Amps for 2 hours across the cell causing the transfer of negatively charged proteins from the gel onto the membrane.

After 2 hours the apparatus was dismantled. Transfer efficiency was ascertained by how well the pre-stained protein ladder had transferred to the filter and also by staining the nitrocellulose filter with Ponceau S. This transient stain is water-soluble, highlights the presence of protein on the filter and does not affect downstream processing.

2.4.9 Immunodetection of proteins on blotted membranes

The blot was incubated in blocking agent, 0.1 % Tween (v/v), 4 % Fat Free Milk (w/v) (Tesco) in phosphate buffered saline (PBS) (140 mM NaCl, 27 mM KCl, 100 mM Na_2HPO_4, 18 mM KH_2PO_4, pH 7.4) for 1 hour with agitation. This step was to saturate non-specific protein binding sites. Primary antibody (1:1000) in blocking buffer was added to the membrane and incubated at room temperature for 90 minutes. The blot was washed for 30 minutes in 4 % milk (w/v) with changes every 5 minutes. Horseradish peroxidase conjugated secondary antibody (Amersham) in 4 % milk (w/v) was added (1:5000) to the blot and incubated for 60 minutes at room temperature with shaking. The blot was then washed once in 4 % milk (w/v), in 0.1 % Tween (v/v) in PBS for 30 minutes with buffer changes every 5 minutes and finally in PBS for 2 x 5 minute washes.

2.4.10 Enhanced Chemiluminescence visualisation

Antibody binding was visualised by enhanced chemiluminescence (ECL). Equal volumes of reagent A and B were mixed and applied to the membrane for 1 minute after which localised fluorescence was detected by exposure to X-ray film (Amersham-Pharmacia).

Reagent A; 100 mM glycine pH 10 (NaOH), 0.4 mM luminol, 8 mM 4-iodophenol

Reagent B; 0.12 % (v/v) hydrogen peroxide in water

2.4.11 Yeast Genomic DNA Prep

Approximately 3-4 µg genomic DNA was obtained from a 1.5 ml overnight yeast culture grown to stationary phase using the MasterPure™ Yeast DNA purification kit (Cambio). DNA was resuspended in distilled water and stored at –20 °C.

2.4.12 *In vivo* phosphoinositide measurement in yeast

This protocol was carried out as described previously (Cooke et al., 1998; Dove et al., 1997; Stephens et al., 1991). Briefly, yeast cells were grown in synthetic complete supplementary medium without inositol (Bio101). An overnight culture was diluted to $5x10^4$ cells/ml and 10 μCi/ml [^{3}H]-inositol (Amersham) added. Cells were grown to a density of 2-$4x10^6$ cells/ml (12-16 hours), after which the cells were killed by the addition of an equal volume of MeOH. Yeast cells were harvested by centrifugation, disrupted by vortexing with ~ 0.4 g glass beads (425-600 micron, Sigma) in the presence of 200 μl MeOH, and lipids extracted and deacylated. The lipid head groups were analysed by HPLC, and peaks detected by liquid scintillation counting (Cooke et al., 1998; Dove et al., 1997; Stephens et al., 1991).

2.5 Microscope methods

2.5.1 Trafficking Assay

Yeast strains were transformed with plasmids encoding, Ub-GFP-Phm5p, GFP-Phm5p (gifts from Dr. Stephen Dove), GFP-CPS (gift from Professor Scott Emr) or GFP-Sna3p (gift from Professor Hugh Pelham), plated onto SD media and grown at 24 °C for several days. Cells were inoculated into SD liquid culture and grown overnight at 24 °C. Next day cells were diluted and grown until a cell density of $8x10^6$ cells/ml was reached. Cells were viewed on a Leica DM RXA2 microscope with a GFP filter cube. Fluorescent and Nomarski images were acquired with an ORCA digital camera (Hamamatsu, Japan) and processed in Open Lab (Improvision) and Adobe Photoshop.

2.5.2 Quinacrine Staining

Yeast cells were grown to $8x10^6$ cells/ml in sterile YPD liquid media, centrifuged briefly and incubated for 5 minutes in the dark at 24 °C in 100 mM Hepes/KOH (pH 7.5),

3% (w/v) glucose, 200 µm Quinacrine (Sigma). They were washed in Hepes/Glucose without Quinacrine, resuspended in 50 µl and viewed on a Leica DM RXA2 microscope with a GFP filter cube. Fluorescent and Nomarski images were acquired with an ORCA digital camera (Hamamatsu, Japan) and processed in Open Lab (Improvision) and Adobe Photoshop. This method is adapted from Wesiman *et al* (Weisman et al., 1987)

2.5.3 FM4-64 Staining

Yeast cells were grown to a density of $8x10^6$ cells/ml in YPD media, washed in PIPES buffered YPD pH 6.8 and 80 µm FM4-64 (Molecular Probes) added in 1 ml YPD. Cells were incubated for 1 hour at 24 °C in the dark after which they were washed twice and then chased for 2 hours in 1 ml YPD in the dark. Cells were viewed on a Leica DM RXA2 microscope with a Texas Red filter cube. Fluorescent and Nomarski images were acquired with an ORCA digital camera (Hamamatsu, Japan) and processed in Open Lab (Improvision) and Adobe Photoshop. This method is adapted from Vida *et al* (Vida and Emr, 1995).

2.6 Molecular biology methods

2.6.1 Preparation of competent *E. coli* cells

E. coli cells were inoculated into 10 ml sterile Luria Bertani broth (LB) (1 % (w/v) tryptone, 0.5 % (w/v) yeast extract and 1 % (w/v) NaCl) and grown overnight at 37 °C with shaking. Next day, 1 ml of the culture was inoculated into 100 ml sterile LB and grown until OD_{600nm} was 0.4-0.6. Cells were centrifuged at 4000 rpm and supernatant removed. Cells were subsequently washed and centrifuged in 2 x 50 ml aliquots of ice cold 0.1 M $MgCl_2$. The pellet was resuspended in 4 ml ice cold 0.1 M $CaCl_2$ and incubated on ice for at least 2 hours after which cells were used. Glycerol was added to a final concentration of 15 % to allow for freezing at –80 °C.

2.6.2 *E. coli* transformation

E. coli competent cells were thawed on ice and 100 µl pipetted into chilled microcentrifuge Plasmid DNA was added and the tubes incubated on ice for 30 minutes. Control plasmid DNA and no plasmid DNA controls were always included. After incubation, tubes were placed at 42 °C for 3 minutes, cooled on ice for 2 minutes, 1 ml pre-warmed LB added and all tubes incubated at 37 °C for 45 minutes. Tubes were centrifuged briefly and the pellet resuspended in approximately 200 µl of the supernatant. This volume was plated onto LB plates supplemented with ampicillin/kanamycin to a final concentration of 100 µg/ml and 30 µg/ml respectively. Plates were then incubated overnight at 37 °C.

2.6.3 Preparation of plasmid DNA from *E. coli* cells

Approximately 1-5 µg of high-copy plasmid DNA was obtained from 2 ml LB overnight cultures of *E. coli* using the Qiagen Miniprep kit (Qiagen) according to manufacturers instructions. Similarly a Qiagen Maxiprep kit was used to obtain DNA quantities of up to 500 µg. DNA was resuspended in distilled water and stored at -20° C.

2.6.4 Quantitation of DNA

DNA quantities were assayed for on a Hitachi U-1500 spectrophotometer (Hitachi Corporation, Japan). DNA was diluted 1:100 in distilled water and read against a water blank in a quartz cuvette at OD_{260nm}. DNA quantity in mg/ml was calculated using the following equation:

OD_{260nm} x 50 (coefficient relating to the absorption of 50 µg/ml double stranded DNA at an OD_{260nm} of 1) x dilution factor

2.6.5 Restriction enzyme digest

0.1-4 μg plasmid DNA in distilled water was digested with restriction endonucleases along with 1/10th volume appropriate restriction buffer for 2 hours at recommended temperature as specified by New England Biolabs.

2.6.6 Polymerase chain reaction (PCR)

PCR was used for amplification of DNA and site directed mutagenesis. Primers were dissolved in distilled water according to manufacturers instructions to give a concentration of 10 pmol/μl. The following reaction volume was made up:

0.5 μl DNA (0.1-0.5 μg/μl)
2.5 μl x 10 *Pfu* buffer (Stratagene)
1 μl Primer 1 (10 pmol/μl) (Operon)
1 μl Primer 2 (10 pmol/μl) (Operon)
1 μl dNTPs (10 mM) (Boehringer Mannheim, Germany)
18 μl distilled water
1 μl *Pfu* DNA polymerase (2.5 u/μl) (Stratagene)
25 μl Final volume

Pfu DNA polymerase was routinely added in a "hot start" manner, i.e. after the initial denaturation step. Typical parameters were as follows:

95 °C 5 minutes
95 °C 30 seconds
54 °C 2 minutes
72 °C 15 minutes 15-30 cycles
72 °C 10 minutes
10 °C pause.

These parameters were altered accordingly with respect to size of DNA template, primers used and type of DNA template. For instance, minimum extension time for *Pfu* DNA polymerase was 2 minutes + /kb, annealing temperatures were altered with respect to the melting temperatures of primers used and number of cycles were altered if using plasmid or genomic DNA.

2.6.7 Site-directed mutagenesis

HPLC purified primers (Operon), complimentary to opposite strands of the double stranded target DNA but incorporating the desired mutation(s) were used for PCR amplification of targeted plasmid (Section 2.6.6). Successive rounds of cycling incorporated the mutated DNA into the plasmid. PCR products were digested with the restriction endonuclease *Dpn1*. Non-mutated template plasmid was *dam* methylated and therefore susceptible to digestion by *Dpn1* however plasmid generated by PCR was unmethylated and therefore immune to digestion. 1 µl of this volume was then transformed into competent *E. coli* cells as described (Section 2.6.2), plated out onto LB plates supplemented with the appropriate antibiotic and incubated overnight at 37 °C. Colonies were picked, grown overnight and DNA extracted and prepared using the Qiagen Miniprep kit (Section 2.6.3). Incorporation of mutations was confirmed by sequencing. All sequencing reactions were carried out by the Sequencing Facility, Department of Biochemistry, University of Cambridge to their own specifications.

2.6.8 Site-directed mutagenesis of *APL2* and *APL4*

Both *APL2* and *APL4* genes were amplified by PCR from genomic BY4741 DNA using high fidelity *Pfu* polymerase (Stratagene) using parameters as described (Section 2.2.6). The primers used for the amplification of *APL2* were: gcg**ggatcc**atgccaccattggat and gagctaaataagact**ctcgag**cgc and for the amplification of *APL4:* gcg**ggatcc**atgggctcttcgttgagaagc and gcg**ctcgag**ttatagagtttcatcgaatttg. The highlighted sequences refer to 5' *BamHI* and 3' *XhoI* restriction sites introduced to facilitate a generic approach to cloning.

Site directed mutagenesis was carried out as described (Section 2.6.7) and mutations introduced sequentially into *APL2* using the following primer pairs:

ggctaacgatgatgtgctattggcagcagcagaaagagatgatgtaaca
and tgttacatcatctctttctgctgccaatagcacatcatcgttagcc

gtgtcacaggatctcctcgcagcagcatgactcgaggcgcctgaattcc
and ggaattcaggcgcctcgagtcatgctgctgcgaggagatcctgtgacac.

Mutations were introduced into *APL4* using the following primer pair:

tatctccaacgaaccagttgctgcggcgtcagctgcagcgggtgaggatagcaaggctga
and cagccttgctatcctcacccgctgcagctgacgccgcagcaactggttcgttggagataa.

Incorporation of mutations was verified by sequencing.

2.6.9 Agarose gel electrophoresis of DNA

DNA fragments between 0.5-25 kb were separated on 0.8 % agarose gels (Gibco BRL) in TAE buffer (40 mM Tris, 5 mM Na_2HPO_4, 5.7 % (v/v) glacial acetic acid). After microwaving, gels were cooled and poured into a sealed tray with an appropriate sized comb. When set, samples were mixed with DNA loading buffer (0.5 x TAE, 10 % (v/v) glycerol, 0.1 % (w/v) bromophenol blue). A reference 1 kb ladder (NEB) was also included. Generally gels were electrophoresed at 100 V for 1 hour or until the dye front had progressed sufficiently along the gel. The gel was placed into TAE buffer containing 10 mg/ml ethidium bromide and gently agitated for 10 minutes. DNA bands were visualised on a short wave UV transilluminator and photographed.

2.6.10 Isolation and purification of DNA fragments from agarose gels

DNA fragments were excised from gels using clean scalpel blades and placed into clean micro-centrifuge tubes for gel extraction. This was carried out using the Qiagen gel extraction kit (Qiagen Corporation) according to manufactures instructions.

2.6.11 Ligation of DNA fragments into plasmid vectors

Plasmids were restriction digested (Section 2.6.5) and electrophoresed on 0.8 % agarose gels as outlined (Section 2.6.9). Vectors and inserts were gel extracted accordingly (Section 2.6.10) and a ligation reaction set up. Typically reaction volumes contained an insert to vector molar ratio of 3:1.

	Vector+Insert	Vector Only
Insert	7 µl	0 µl
Vector	1 µl	1µl
Ligase (NEB)	1 µl	1 µl
X 10 Buffer	1 µl	1 µl
Water	0 µl	7 µl
Final Volume	10 µl	10 µl

In general, cohesive end ligations were incubated at room temperature for 2 hours and those with blunt ends were incubated overnight at 16 °C. After incubation, reaction volumes were transformed into competent *E. coli* cells, plated onto LB media supplemented with the appropriate antibiotic and incubated overnight at 37 °C (section 2.6.2). Colonies were picked into sterile LB broth and antibiotic and cultures grown overnight at 37 °C with shaking. Next day, DNA was extracted (Section 2.6.3) and subjected to restriction analysis (Section 2.6.5) and sequencing to confirm clones.

2.6.12 Ligation of inserts into pCR®-Blunt

As a matter of routine all ORFs amplified by PCR were blunt end cloned into the pCR®-Blunt vector (Invitrogen) according to manufacturers instructions. Positive clones were sequenced and stored at –20 °C thus providing a valuable source of high fidelity insert DNA for downstream plasmid construction.

3 YEAST TWO-HYBRID RESULTS

3.1 Introduction

Fundamental to many biochemical processes is the physical interaction between proteins in the cell. The understanding of how these interactions are mapped and brought about has been mediated in part by the advent of the yeast two-hybrid system (Fields and Song, 1989).

This system exploits the properties of the *GAL4* gene of *S. cerevisiae* (Fields and Song, 1989). Gal4p is a DNA binding transcriptional activator required for the transcription of *GAL* genes encoding proteins required for the utilisation of galactose (Lohr et al., 1995). The protein comprises two separable and functionally distinct domains: an N-terminal that binds specific DNA upstream activation sequences (UAS) and a C-terminal that is necessary to activate transcription. When Gal4p binds to UAS recognition sequence, transcription is activated and proteins are synthesised to allow metabolism of galactose (Fields and Song, 1989).

The DNA binding domain of *GAL4* is fused to a bait protein and the transcriptional activating domain is fused to a prey protein. If an interaction occurs, the respective domains come into proximity and lead to transcriptional activation of either *HIS3* or β-galactosidase (Figure 3.1).

We used a yeast two-hybrid library provided by Dr. Stan Fields (Uetz et al., 2000). Construction of this library resulted from the yeast genome-sequencing initiative which identified 6000+ ORFs (Goffeau et al., 1996). To make the library, these ORFs were amplified to yield PCR products containing 70bp sequences at the 3' and 5' ends compatible with the arms of a cloning vector. This allows for highly efficient recombination between the fragment and the cloning vector. Positive transformants were plated onto 16 microassay plates of 384 colonies each and screens carried out as described (Section 3.4.3).

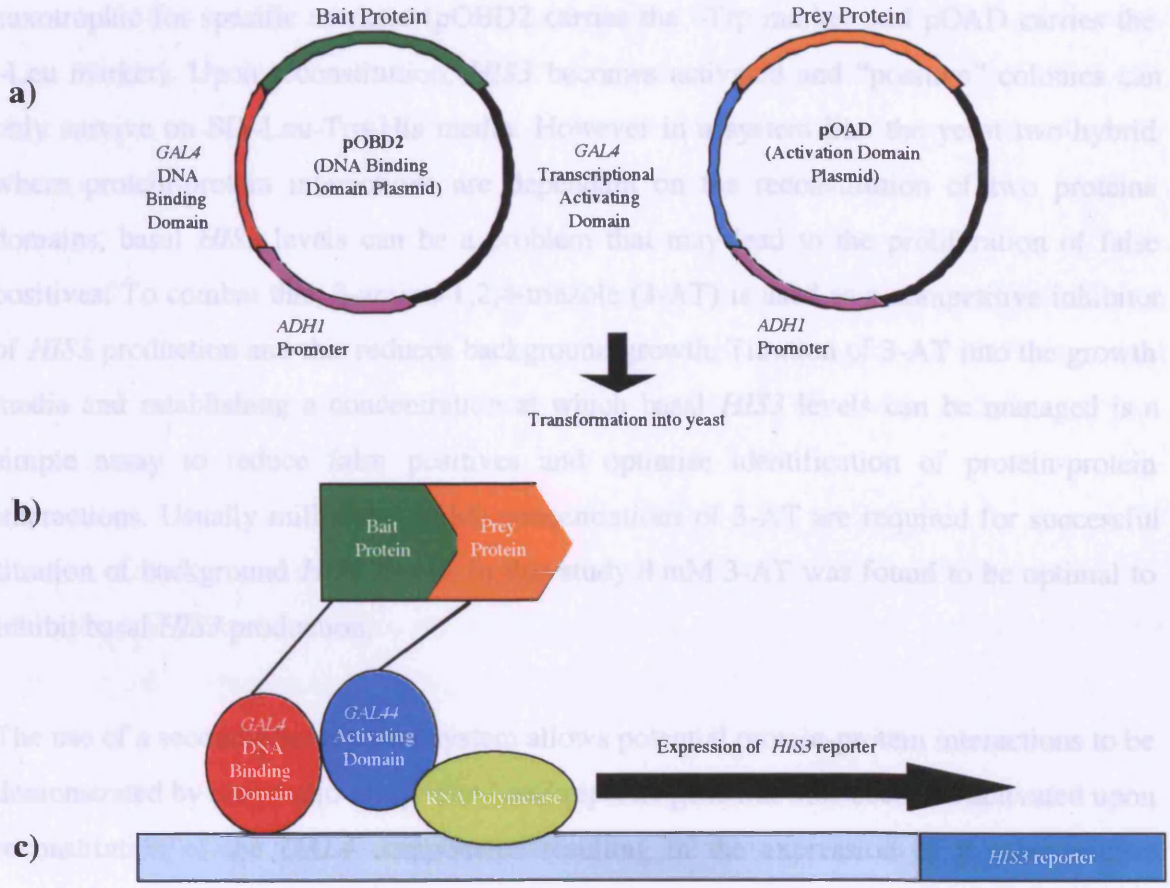

Figure 3.1. Strategy used to detect protein-protein interactions using the yeast two-hybrid *HIS3* reporter gene system, a) genes of interest cloned in frame to *GAL4* domains in cloning plasmids b) transformed and expressed as fusion proteins in yeast where bait and prey physically interact bringing *GAL4* domains into proximity and c) activation of downstream *HIS3* reporter gene.

3.2 Yeast two-hybrid; reporter genes

The yeast two-hybrid system used in this study incorporates two reporter gene systems to indicate potential protein-protein interactions (Fields and Song, 1989). The first, is used in a plate based growth assay where the *HIS3* reporter gene becomes activated upon reconstitution of the individual *GAL4* domains of the respective vectors, both of which are auxotrophic for specific markers (pOBD2 carries the –Trp marker and pOAD carries the –Leu marker). Upon reconstitution, *HIS3* becomes activated and "positive" colonies can only survive on SD–Leu-Trp-His media. However in a system like the yeast two-hybrid where protein-protein interactions are dependant on the reconstitution of two proteins domains, basal *HIS3* levels can be a problem that may lead to the proliferation of false positives. To combat this, 3-amino-1,2,4-triazole (3-AT) is used as a competitive inhibitor of *HIS3* production and this reduces background growth. Titration of 3-AT into the growth media and establishing a concentration at which basal *HIS3* levels can be managed is a simple assay to reduce false positives and optimise identification of protein-protein interactions. Usually millimolar (mM) concentrations of 3-AT are required for successful titration of background *HIS3* levels. In this study 8 mM 3-AT was found to be optimal to inhibit basal *HIS3* production.

The use of a second gene reporter system allows potential protein-protein interactions to be demonstrated by enzymatic assay. The LacZ reporter gene likewise becomes activated upon reconstitution of the *GAL4* components resulting in the expression of β-galactosidase. Production of this enzyme is monitored by its ability to cleave the substrate o-nitrophenol-D-galactopyranoside (ONPG) to produce o-nitrophenol, which can be assayed by absorbance at 420nm (Guarente, 1983).

The combination of two reporter gene systems to monitor protein-protein interactions allows for a more thorough investigation to be carried out. Therefore, identified interactors can be assayed both by growth assay and by an enzymatic assay.

3.3 Yeast two-hybrid; pros and cons

The yeast two-hybrid system has become a routine laboratory method for the study of protein-protein interactions and as such offers several advantages over *in vitro* biochemical techniques. For instance protein-protein interactions in the yeast two-hybrid occur *in vivo*, reflecting the true physiological state of interacting proteins within the cell. Also some proteins require post-translational modifications prior to interaction and this is achieved *in vivo*. The yeast two-hybrid can also detect weak and transient interactions more efficiently than conventional *in vitro* biochemical techniques, which may disrupt interactions by detergent extraction.

Potentially the time taken, reagents required and cost to complete a yeast two-hybrid screen is minimal. Essential requirements include the full-length gene, (or a partial functional cDNA), fusion vectors (readily available from the Fields laboratory) and the relevant solid/liquid media.

Finally, the technique is ideal for examining known interactions between two proteins and through site directed mutagenesis, the alteration of critical residues can affect binding affinities. Also domains of interaction can be mapped by this method.

Naturally there are caveats to the yeast two-hybrid technique; however if time and care is taken in addressing these concerns, their impact can be reduced. The construction of a chimeric protein e.g. *GAL4* DNA binding domain and "protein X" cannot be predicted with surety to interact with the prey in a natural physiological way. The introduction of a fusion protein may cause steric hindrance in binding, it may misfold and bind with limited activity or alternatively bind to a non-partner with augmented activity, or it may alter function of the association thus giving a false representation of the interaction. These factors will either destroy protein-protein interactions or severely affect interactions to such an extent they cannot be detected. One way to overcome this problem would be to section the protein of interest into its constitutive domains. Expressing smaller domains of a protein may increase the likelihood of achieving soluble expression.

Also, the yeast two-hybrid system permits *in vivo* interactions to occur inside the nucleus. For those proteins that are not nuclear in distribution and function this presents a problem in that proteins may be forced to interact regardless of their compartment of origin thus giving rise to spurious interactions.

Finally the technique is not suited to integral membrane proteins. Again the expression of truncations and certain domains may overcome this problem.

3.4 Yeast two-hybrid; the rationale

Having critically assessed the pros and cons of the yeast two-hybrid system, it appeared to be the ideal first step, in identifying Fab1p protein-protein interactions. The yeast two-hybrid is not the definitive tool for identifying these interactions, but it is an *in vivo* technique and as such is an excellent starting point from where a more detailed and thorough investigation can be launched.

Importantly, the system allows for the high throughput screening of proteins or protein domains that should increase the chances of identifying physiologically relevant protein-protein interactions. In this study, 7 screens were carried out (Table 3.4).

Our approach was to achieve maximum solubility of our fusion proteins therefore we identified the individual domains of Fab1p (Section 1.6), cloned and expressed these using a PCR based strategy. Fab1p is a 257kDa in size and its expression as a fusion protein was expected to cause problems in terms of solubility as is often the case with large proteins. Individual and double domains of *FAB1* were soluble, when expressed as GST fusions (Dr. F. Cooke previous work). Also it was decided to express the full-length Fab1p protein and use that in the screen. Although we had no functional assays for the Fab1p domain fusion proteins, a full-length Fab1p fusion protein complemented the phenotype of *fab1*Δ cells (data not shown).

Domain	Construct Type
Catalytic	Single Domain
FAB1	Full-Length
FYVE	Single Domain
FYVE-TCP	Double Domain
TCP	Single Domain
Zinc-F	Single Domain
Zinc-F-TCP	Double Domain
Zinc-F-Cat	Double Domain

Table 3.4. The domains/constructs of *FAB1* used in the yeast two-hybrid screen as bait. In all 7 screens were carried out, the double domain bait fusion Zinc-F-Cat was found to self activate and was not used.

3.5 Construction of bait plasmids

The template used for the construction of all plasmids was a 6.8 kb full-length *FAB1* ORF that had been previously cloned into a pBluescript plasmid (Stratagene) (Dr. F. Cooke previous work). This insert had been amplified with *Pfu* polymerase to maintain sequence fidelity and then sequenced to check for errors. None were found. Each domain to be amplified underwent two rounds of PCR (Section 2.6.6) in order to introduce sequences homologous to the arms of the cloning plasmid, pOBD2 (Figure 3.5).

This method of plasmid construction allowed for an easy and simple method of homologous recombination of the insert into plasmids. Also this method allowed a generic approach to amplifying inserts and cloning them into yeast two-hybrid plasmids.

3.5.1 Primers Used

All primers (Operon, Sigma) were synthesised to include a stop and start codon (ATG). The start codon allows transcription of the insert from the *ADH1* promoter. Primary and secondary primers are shown (Table 3.5.1a and 3.5.1b respectively).

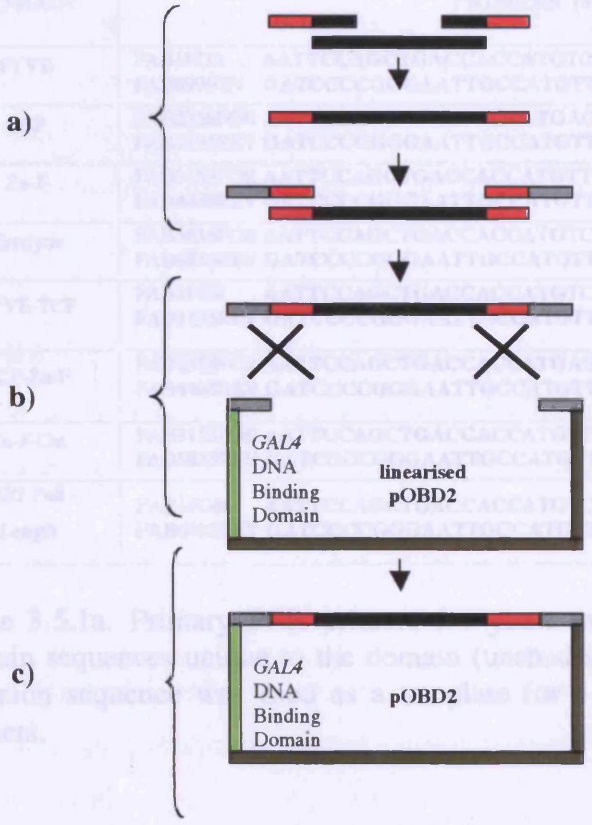

Figure 3.5. Strategy for the construction of yeast two-hybrid bait plasmids **a)** Primers designed to amplify template DNA include sequences (red) homologous to a second round of primers. This second round of primers amplifies the template and incorporates sequences homologous to the plasmid arms (grey). b) This template homologously recombines into a linearised plasmid. c) The template inserts itself in frame with the *GAL4* DNA binding domain allowing the formation of a bait plasmid.

DOMAIN	PRIMERS (5'-3')	PCR PRODUCT
FYVE	FAB1FOR **AATTCCAGCTGACCACCATG**TCATCGGAAGAACCCCAT FAB899REV **GATCCCCGGGAATTGCCATGTTA**TGTGTCTGCATGCTCATAACA	900bp
TCP	FAB2358FOR **AATTCCAGCTGACCACCATG**AGAGAATTAAATGAAGTCTCT FAB3195REV **GATCCCCGGGAATTGCCATGTTA**CAAATAAACATCTGTAGAAAG	837bp
Zn-F	FAB3153FOR **AATTCCAGCTGACCACCATG**TTTAACGATAATTTCATACAA FAB4488REV GATCCCCGGGAATTGCCATGTTATTTCAGCTGCTTGGCCGTGAT	1335bp
Catalytic	FAB5635FOR **AATTCCAGCTGACCACCATG**TCTGACTATAGAAATAAAATG FAB6835REV **GATCCCCGGGAATTGCCATGTTA**ATTTCCTTCCCTATACCA	1200bp
FYVE-TCP	FAB1FOR **AATTCCAGCTGACCACCATG**TCATCGGAAGAACCCCAT FAB3195REV **GATCCCCGGGAATTGCCATGTTA**CAAATAAACATCTGTAGAAAG	3195bp
TCP-Zn-F	FAB2358FOR **AATTCCAGCTGACCACCATG**AGAGAATTAAATGAAGTCTCT FAB4488REV **GATCCCCGGGAATTGCCATGTTA**TTTCAGCTGCTTGGCCGTGAT	2130bp
Zn-F-Cat	FAB3153FOR **AATTCCAGCTGACCACCATG**TTTAACGATAATTTCATACAA FAB6835REV **GATCCCCGGGAATTGCCATGTTA**ATTTCCTTCCCTATACCA	3682bp
FAB1 Full - Length	FAB1FOR **AATTCCAGCTGACCACCATG**TCATCGGAAGAACCCCAT FAB6835REV **GATCCCCGGGAATTGCCATGTTA**ATTTCCTTCCCTATACCA	6835bp

Table 3.5.1a. Primary PCR primers for yeast two-hybrid plasmid construction. Primers contain sequences unique to the domain (unshaded) and common sequence (in bold). This common sequence was used as a template for a second round of PCR using secondary primers.

Second forward primer (5'-3')	CTATCTATTCGATGATGAAGATACCCCACCAAACCCAAAAAAAGAGATC **GAATTCCAGCTGACCACCATG**
Second reverse primer (5'-3")	**GTACCGTTAAGGGCCCCTAGGCAGCTGGACGTCTCTAGATACTTAGCATCTATGA** CTTTTTGGGGCGTTC

Table 3.5.1b. Secondary PCR primers for yeast two-hybrid plasmid construction. Primers contain sequences homologous (bold) to common sequences in the primary primers (Table 3.5.1a). Flanking these sequences were sequences homologous to the vector arms of the cloning plasmid pOBD2.

3.6 Results of yeast two-hybrid screen with Fab1p and its domains.

Below are the results of the yeast two-hybrid screen with constructs containing the *FAB1* full-length fusion, constructs containing single domain fusions and constructs containing double domain fusions. It is worth noting that there are no results for the double Zinc Finger-Catalytic domain construct as this was found to self activate, i.e. it automatically activated the *GAL4* DNA binding domain by growing on media supplemented with 8 mM 3-AT. Also included are tables containing the number of ORFs identified by two or more screens.

As described, (Section 2.4.3) all plates containing interacting diploids were incubated for up to 10 days at 30 °C on SD–L-T-H media supplemented with 8 mM 3-AT. Positive colonies were scored and identified relative to a duplicate plate.

3.6.1 Results of the FYVE domain screen

From the FYVE screen (Table 3.6.1), 23 ORFs were identified by cross-referencing to an EXCEL spreadsheet containing details of approximately 6000+ ORFs from the Fields library (Uetz et al., 2000). Additional information such as location and function of identified ORFs was taken from the *Saccharomyces* Genome Database (http://www.yeastgenome.org/) and the Comprehensive Yeast Genome Database (http://mips.gsf.de/genre/proj/yeast/) (July 2002). This procedure was applied to all screens. Also, those ORFs highlighted in bold were chosen for further analysis, explanations for which, are given in Section 3.8.

ORF	FUNCTION
ATC1	Protein that interacts with Bud6p/Aip3p, Cation Homeostasis
CAT5	May encode a protein involved in one or more monoxygenase or hydroxylase steps of ubiquinone biosynthesis
CCT3	Component of Chaperonin-containing T-complex (TCP ring complex, TRiC), homologous to mouse *CCT3*
FCP1	TFIIF-interacting component of the C-terminal domain phosphatase
GCN20	Component of a protein complex required for activation of Gcn2p protein kinase in response to amino

	acid starvation, member of ATP-binding cassette (ABC) superfamily
GCN4	Transcription factor of the basic leucine zipper (bZIP) type, regulates general control in response to amino acid or purine starvation
HOM3	Aspartate kinase (L-aspartate 4-P-transferase), first step in the common pathway for methionine and threonine biosynthesis
MED2	Component of RNA polymerase holoenzyme and mediator subcomplex
ROX3	Component of RNA polymerase holoenzyme and mediator subcomplex
SNF11	Component of *SWI/SNF* global transcription activator complex, acts to assist gene-specific activators through chromatin remodeling
SPP2	Protein involved in pre-mRNA processing, high-copy suppresses of temperature-sensitive prp2 mutations
TFA2	RNA polymerase transcription initiation factor TFIIE (factor a), 43 kDa subunit
YCL073C	Member of the yeast-specific multidrug-resistance (MFS-MDR) family of the major facilitator superfamily (MFS)
YCR056W	Protein of unknown function
YHR199C	Protein with similarity to Yhr198p
YIP3	**COPII vesicle component involved in vesicle transport and membrane fusion**
YJL182C	Protein of unknown function
YML032Ca	Protein of unknown function
YMR103C	Protein of unknown function, questionable ORF (GB:Z49702)
YMR316W	Protein of unknown function, contains a zinc carboxypeptidase motif PS00133/Protein involved in invasive growth, mRNA abundance is reduced by the drug FK506 in a calcineurin- and immunophilin-dependent manner
YNL122C	Protein of unknown function
YNL203C	Protein with weak similarity to *Bacillus subtilis* CDPdiacylglycerol--serine O-phosphatidyltransferase
YPL098C	Protein of unknown function
YPL133C	Protein with similarity to transcription factors, has Zn[2]-Cys[6] fungal-type binuclear cluster domain in the N-terminal region

Table 3.6.1. 23 ORFs were identified when the FYVE domain construct was screened against the Fields library.

3.6.2 Results of the TCP domain screen

ORF	FUNCTION
CBS2	Translational activator of COB mRNA
ECM13	Protein possibly involved in cell wall structure or biosynthesis
FAL1	Putative ATP-dependent RNA helicase with similarity to eukaryotic initiation factor 4A subfamily of DEAD–box proteins
MSI4	Rab geranylgeranyltransferase regulatory component (component A) and rab guanine nucleotide dissociation inhibitor (Rab GDI)

MSS51	Protein possibly involved in translational activation of COX1 and COB mRNA
PGL1	Polygalacturonase, pectin-hydrolyzing enzyme
POL32	Small subunit of DNA polymerase delta
POP2	Components of the *CCR4* complex, required for glucose derepression
RFC2	Replication factor C, second subunit, homologous to human 37 kDa subunit
SAE2	Protein involved in meiotic recombination pathway
SGA1	Glucoamylase (glucan-alpha-1,4-glucosidase), sporulation-specific
SPS19	Peroxisomal 2,4-dienyol-CoA reductase
STE14	Farnesyl cysteine:carboxyl methyltransferase
SUL2	High-affinity sulfate transporter
UBP9	**Ubiquitin C-terminal hydrolase, has similarity to Ubp13p**
YBL006C	Protein of unknown function
YBR301W	Protein with similarity to Ykl224p and other members of the PAU1 family
YCL073C	Strong similarity to subtelomeric encoded proteins
YCR050C	Protein involved in mitochondrial function
YCR056W	Protein of unknown function
YDL186W	Protein of unknown function
YER028C	Protein with similarity to Mig2p
YGR045C	Protein of unknown function
YJU3	Weak similarity to *E. coli* hypothetical protein
YLR282C	Protein of unknown function
YML032C-A	Questionable ORF
YNL120C	Protein of unknown function, questionable ORF
YNL203C	Protein with weak similarity to *Bacillus subtilis* CDPdiacylglycerol--serine O-phosphatidyltransferase
YOR366W	Protein of unknown function
YPL137C	Protein with similarity to Mhp1p
YPL229W	Protein of unknown function
YPR197C	Questionable ORF
YVL053C	Questionable ORF

Table 3.6.2. 33 ORFs were identified when the TCP domain construct was screened against the Fields Library.

3.6.3 Results of the Zinc-Finger domain screen

ORF	FUNCTION
BLM3	Weak similarity to Mms19p
EGD2	Beta subunit of the EGD complex
FAT1	Fatty acid transporter, Very long-chain acyl-CoA synthetase (VLCS
HHF2	Histone H4 (HHF1 and HHF2 code for identical proteins)
HXT12	Protein with similarity to hexose transporters (YIL170W and YIL171W are both homologous to HXT genes and are separated by a frameshift mutation)
INP54	Inositol polyphosphate 5-phosphatase, may play a role in regulation of secretion
MPA43	Protein that affects leads to high levels of PDC1 expression when overproduced
MRS5	Essential component of the mitochondrial import machinery, required for transfer of hydrophobic inner membrane carrier proteins across the intermembrane space
MSI4	Rab geranylgeranyltransferase regulatory component (component A) and rab guanine nucleotide dissociation inhibitor (Rab GDI)
MYO5	Myosin type I, may play a role in cell growth or polarity that is partially redundant with Myo3p
NUP100	Nuclear pore protein (nucleoporin) of the GLFG family, may be involved in binding and translation of proteins during nucleocytoplasmic transport
RPC53	RNA polymerase III, fourth-largest essential subunit (C53)
RPL35A	Ribosomal protein L35A (rat L35) (RPL35A and RPL35B code for identical proteins)
SAN1	Protein that may antagonize the function of Spt16p and Sir4p
SGD1	Protein involved in the Hog1p pathway
TEL1	Protein involved in controlling telomere length, phosphatidylinositol 3-kinase homologue (PI kinase homologue)
VAN1	Vanadate resistance protein
YCK3	**Casein kinase I isoform**
YDL163W	Protein of unknown function
YDL196W	Protein of unknown function
YDR157W	Questionable ORF
YHR105W	Protein of unknown function
YLR057W	Weak similarity to mouse alpha-mannosidase
YMR266W	Protein of unknown function, probable integral membrane glycoprotein, Possible membrane transporter involved in tunicamycin sensitivity
YOL057W	Protein of unknown function/Protein with similarity to rat dipeptidyl peptidase III which is a zinc-binding metalloproteinase
YPL044C	Protein of unknown function
YPR177C	Protein of unknown function
YPR204W	Protein with similarity to other subtelomerically-encoded proteins

Table 3.6.3. 28 ORFs were identified when the Zinc-Finger domain construct was screened against the Fields Library.

3.6.4 Results of the Catalytic domain screen

ORF	FUNCTION
ARGR2	Component of the ARGR regulatory complex
ARP8	**Protein with similarity to actin and actin-related proteins Arp1p-Arp10p**
BSC5	**Protein with similarity to Bul1p ubiquitin ligase binding protein, may be a pseudogene or separated from YNR068C by sequencing errors**
DYS1	Deoxyhypusine synthase, first step in hypusine biosynthesis, carries out the conversion of lysine + spermidine into deoxyhypusine
IAH1	Isoamyl acetate-hydrolyzing esterase enzyme
KRE28	Weak similarity *Plasmodium* repeat organellar protein
RPL42B	Ribosomal protein L42B (yeast L41) (YL27) (YP44) (human L36A) (rat L36A) (RPL42A and RPL42B code for identical proteins)
VMA6	**Vacuolar H-ATPase (V-ATPase) 36 kDa subunit (subunit D) of membrane (V0) sector, required for V-ATPase assembly**
YCL020W	Ty2A Gag protein; the main structural constituent of virus-like particles (VLPs)
YCL065W	Protein of unknown function
YGL177W	Questionable ORF
YGR257C	Protein with similarity to members of the mitochondrial carrier family (MCF)/Member of the mitochondrial carrier family (MCF) of membrane transporters
YIL060W	Protein of unknown function
YNL099C	Protein required for cell cycle delay at G1 phase after treatment with linoleic acid hydroperoxide, has similarity to protein tyrosine phosphatases (PTPs)
YOR203W	Protein required for cell viability

Table 3.6.4. 15 ORFs were identified when the Catalytic domain construct was screened against the Fields Library

3.6.5 Results of the FYVE-TCP double domain screen

ORF	FUNCTION
AHC1	Ada Histone acetyltransferase complex component; protein of the Ada histone acetyltransferase complex
ARO2	Chorismate synthase
ARP8	**Protein with similarity to actin and actin-related proteins Arp1p-Arp10p**
BOP2	Overproduction suppresses a pam1 slv3 double null mutation
CBS2	Translational activator of COB mRNA
CDC73	RNA polymerase II accessory protein
CHO1	Phosphatidylserine synthase (CDP-diacylglycerol serine O-phosphatidyltransferase)
CLN1	G1/S-specific cyclin, interacts with Cdc28p protein kinase to control events at START

CRN1	**Coronin, actin-binding protein, has WD (WD-40) repeats**
CSR1	Phosphatidylinositol transfer protein with a potential role in lipid turnover; interacts specifically with thioredoxin peroxidase (Tsa2p) and may have a role in oxidative stress resistance
CTR2	Putative low-affinity copper transport protein
DBF4	Regulatory subunit for Cdc7p protein kinase, required for G1/S transition
DBP2	ATP-dependent RNA helicase of DEAD box family
DER1	Protein involved in degradation of misfolded soluble proteins in the endoplasmic reticulum
DUR1, 2	Urea amidolyase, contains urea carboxylase and allophanate hydrolase activities
EAF3	Esa1p-associated factor, nonessential component of the NuA4 acetyltransferase complex, homologous to *Drosophila* dosage compensation protein MSL3
ECM13	Protein possibly involved in cell wall structure or biosynthesis
ENA5	P-type ATPase involved in Na+ efflux
EXO70	Component of exocyst complex, 70 kDa, required for exocytosis
FMP36	Similarity to hypothetical protein *Neurospora crassa*
GAL83	Protein that plans a role in glucose repression through interaction with Snf1p and Snf4p
GCN4	Transcription factor of the basic leucine zipper (bZIP) type, regulates general control in response to amino acid or purine starvation
GCR2	Protein required for expression of glycolytic genes, causes same spectrum of enzymatic changes as does Gcr1p
HAC1	Transcription factor with basic leucine zipper (bZIP) domain that activates the unfolded protein response pathway, mRNA splicing is regulated by Ire1p.
HAP4	Transcription factor with acidic activation domain, component of Hap2p-Hap3p-Hap4p-Hap5p complex involved in activation of CCAAT-box containing genes
HIS1	ATP phosphoribosyltransferase, first step in histidine biosynthesis pathway
HXT17	Protein with similarity to hexose transporters including Hxt13p, Hxt16p, Hxt6p, Hxt7p, and Lgt1p
IES5	Protein that associates with the INO80 chromatin remodelling complex under low-salt conditions
ISA2	Protein required for maturation of mitochondrial and cytosolic Fe/S proteins, localizes to the mitochondrial intermembrane space, overexpression of ISA2 suppresses grx5 mutations
KAR5	Coiled-coil membrane protein, required for homotypic nuclear fusion
KEL2	Protein with similarity to Kel1p and Kel3p, contains six Kelch repeat domains
MAL13	Maltose pathway regulatory protein, contains a Zn[2]-Cys[6] fungal-type binuclear cluster domain
MATALPHA2	Homeodomain regulatory protein MATalpha2p, acts with Mcm1p to turn off a-specific genes (ALPHA2 and MATALPHA2 have the same coding sequence, but ALPHA2 is silenced)
MDJ2	Protein of the mitochondrial inner membrane with similarity to E. *coli* DnaJ and other DnaJ-like proteins, function partially overlaps that of Mdj1p
MEF1	Mitochondrial translation elongation factor G, promotes GTP-dependent translocation of nascent chain from A-site to P-site of ribosome
MMM1	Protein essential for establishment and maintenance of mitochondrial shape and structure
MMS21	Protein involved in DNA repair
MNS1	Alpha-mannosidase, specific for removal of one mannose from Man[9]GlcNac to produce a single isomer of Man[8]GlcNac
MOB2	Protein that acts with Mob1p in maintenance of ploidy, involved in localization of Ace2p and Cbk1p which leads to daughter-specific expression of multiple genes
MRPL4	Mitochondrial ribosomal protein MRPL4 of the large subunit (YmL4)

NDI1	NADH-ubiquinone oxidoreductase (rotenone insensitive)
NIP100	Nuclear import protein
NMD4	Nam7p/Upf1p-interacting protein
NNT1	Putative nicotinamide N-methyltransferase, has a role in rDNA silencing and in lifespan determination
NSA1	Constituent of 66S pre-ribosomal particles, involved in 60S ribosomal subunit biogenesis
PAF1	Protein associated with RNA polymerase II, involved in positive and negative regulation
PET100	Protein required for assembly of cytochrome c oxidase
PEX21	Peroxin; Pex18p and Pex21p are partially functionally redundant
POL5	DNA polymerase V that has motifs typical of DNA polymerase family
RFA1	DNA replication factor A, 69K subunit, binds single-stranded DNA
RFX1	DNA-binding protein, homologous to a family of mammalian RFX1-4 proteins which have a novel highly conserved DNA-binding domain
RNP1	Ribonucleoprotein 1, has 2 RNA recognition (RRM) domains which include RNP-1 octamer and RNP-2 hexamer domains
RPL12B	Ribosomal protein L12B (Yeast L15) (YL23) (E. *coli* L11) (rat L12a) (RPL12A and RPL12B code for identical proteins)
RPT1	ATPase component of the 26S proteasome complex, member of the AAA family of ATPases
SAE2	Protein involved in meiotic recombination pathway
SLG1	Plasma membrane protein required for maintenance of cell wall integrity and for the stress response
SNZ1	Stationary phase protein and member of the stationary phase-induced gene family which includes Snz2p and SnZ3p
SPO12	Sporulation protein required for chromosome division in meiosis I
SPS19	Peroxisomal 2,4-dienyol-CoA reductase
SPS2	Middle/late gene of meiosis
SPS4	Protein expressed in mid-late (8-14 hr) sporulation, possible cell wall component
SRB9	Component of RNA polymerase holoenzyme and Kornberg's mediator (SRB) subcomplex
SSP1	Meiosis-specific protein, required for proper completion of meiotic division and spore formation
TDH1	Glyceraldehyde-3-phosphate dehydrogenase 1, converts D-glyceraldehyde 3-phosphate to 1,3-diphosphoglycerate
TID3	Protein with similarity to myosin heavy chain, possible coiled-coil
TIM22	Essential mitochondrial inner membrane protein involved in import of mitochondrial inner membrane proteins
TOM40	Mitochondrial integral outer membrane protein involved in protein import, forms the outer membrane import channel
UBP9	**Ubiquitin C-terminal hydrolase, has similarity to Ubp13p**
UGA4	High-affinity permease with specificity for 4-aminobutyric acid (GABA)
VAN1	Vanadate resistance protein
VID21	**Component of the NuA4 histone acetyltransferase complex**
VPS45	Protein of the Sec1p family essential for vacuolar protein sorting
YAR070C	Protein of unknown function, has potential mitochondrial transit peptide
YBR007C	Protein of unknown function, has weak similarity to uncharacterized C. *albicans* Orf6.6027p
YBR051W	Protein of unknown function

YBR267W	Protein of unknown function, has a single C2H2-type zinc finger
YBR293W	Member of major facilitator superfamily (MFS) multidrug-resistance (MFS-MDR) protein family
YCL073C	Protein of unconfirmed function; displays a topology characteristic of the Major Facilitators Superfamily of membrane proteins
YDL011C	Protein of unknown function
YDL183C	Protein of unknown function, has potential mitochondrial import sequence
YDL241W	Protein of unknown function
YDR045C	Protein with similarity to *Sulfolobus acidocaldarius* transcription elongation factor tfs
YDR107C	Protein with strong similarity to Emp70p
YDR114C	Protein of unknown function
YDR269C	Protein of unknown function, questionable ORF
YER028C	Protein with similarity to Mig2p (Protein that contains two tandem C2H2-type zinc finger domains, has strong similarity to Mig2p, a Tup1p-dependent and glucose-dependent transcriptional repressor)
YGL152C	Protein with similarity to rat G protein-coupled glutamate receptor
YGL159W	Protein of unknown function
YGR002C	Protein with similarity to *Drosophila melanogaster* transcription initiation factor IID 230 K chain PIR:A47371
YGR045C	Protein required for normal growth on nonfermentable carbon sources and for normal pseudohyphal growth
YHL040C	Member of major facilitator superfamily (MFS) multidrug-resistance (MFS-MDR) protein family
YHR045W	Protein of unknown function, has 5 potential transmembrane domains
YHR218W	Protein with similarity to other subtelomerically-encoded proteins including Yhr219p and Yfl065p, probable pseudogene
YIL055C	Protein of unknown function
YIL089W	Protein of unknown function
YJL132W	Protein of unknown function
YJR129C	Putative S-adenosylmethionine-dependent methyltransferase of the seven beta-strand family
YKL029C	Protein with similarity to malate dehydrogenase (oxaloacetate-decarboxylating)
YKL046C	Protein of unknown function, has 2 predicted transmembrane domains
YKR021W	Protein of unknown function
YKR075C	Protein with similarity to Reg1p
YLR076C	Protein required for cell viability
YLR282C	Protein of unknown function
YLR290C	Protein of unknown function, has moderate similarity to uncharacterized *C. albicans* Orf6.8461p
YLR455W	Weak similarity to human G/T mismatch binding protein
YML013C-A	Protein of unknown function
YML023C	Weak similarity to Nmd2p
YMR103C	Protein of unknown function, questionable ORF (GB:Z49702)
YMR222C	Protein with similarity to *S. pombe* DFR1, dihydrofolate reductase (SP:P36591)

YNL203C	Protein with weak similarity to *Bacillus subtilis* CDPdiacylglycerol--serine O-phosphatidyltransferase
YOL085C	Protein of unknown function
YOR006C	Protein of unknown function
YOR060C	Protein of unknown function
YOR342C	Protein of unknown function
YPL137C	Protein with similarity to Mhp1p
YPL229W	Protein of unknown function
YPR169W	Protein containing two WD domains (WD-40 repeat), which may mediate protein-protein interactions, has moderate similarity to uncharacterized *C. albicans* ORF 6.4016p

Table 3.6.5. 117 ORFs were identified when the FYVE-TCP double domain construct was screened against the Fields Library.

3.6.6 Results of the TCP-Zinc-Finger double domain screen

ORF	FUNCTION
ADK2	Adenylate kinase (GTP:AMP phosphotransferase), mitochondrial
EMI5	Similarity to hypothetical *S. pombe* protein
GAL4	Transcription factor involved in expression of galactose-induced genes, phosphorylation correlates with activation activity
ILS1	Isoleucyl-tRNA synthetase
INM1	**Protein with similarity to inositol monophosphatase of *E. coli*, *Aspergillus nidulans*, and *Neurospora crassa*. Inositol monophosphatase, member of the inositol monophosphatase family, catalyzes hydrolysis of inositol-1-phosphate, involved in the inositol cycle of calcium signaling**
NUP84	Nuclear pore protein (nucleoporin)
PDR12	**Protein with similarity to Pdr5p and Snq2p, member of the ATP-binding cassette (ABC) superfamily/Protein required for weak organic acid resistance, member of the ATP-binding cassette (ABC) superfamily of membrane transporters**
PRP38	Protein required for pre-mRNA splicing, involved in U4/U6 snRNA dissociation before U6 snRNA integration into the splicosome active site
PRY3	Protein with similarity to plant pathenogenesis-related proteins
RPS26A	Ribosomal protein S26A (rat S26) (RPS26A and RPS26B code for nearly identical proteins)
SHE2	Protein required for mother cell-specific expression of HO
SLD5	Part of GINS, replication multiprotein complex
SSN8	Cyclin C homologue and component of RNA polymerase holoenzyme complex and Kornberg's mediator (SRB) subcomplex
SWP73	Component of SWI/SNF global transcription activator complex, acts to assist gene-specific activators through chromatin remodeling
TKL2	Transketolase 2
URE2	Nitrogen catabolite repression regulator which acts by inhibition of the Gln3p regulator in the presence of preferred nitrogen sources

YCL003W	Phosphatidylglycerophosphate synthase
YCR044C	Suppressor of cdc1-1 temperature-sensitive growth defect, involved in Mn++ homeostasis
YCR082W	Protein with similarity to Rbk1p/Sugar Kinase
YDR271C	Protein of unknown function, questionable ORF
YDR344C	Protein of unknown function
YIP2	Protein with similarity to human polyposis locus protein 1 (GB:Z49274)/Protein that acts together with Yip1p in membrane trafficking, has similarity to human polyposis locus protein 1
YIR025W	Protein of unknown function/Protein required for meiotic nuclear divisions
YJL017W	Protein of unknown function
YKR105C	Member of major facilitator superfamily (MFS) multidrug-resistance (MFS-MDR) protein family
YLR266C	Protein with similarity to transcription factors, has Zn[2]-Cys[6] fungal-type binuclear cluster domain in the N-terminal region
YMR014W	Protein of unknown function, has possible coiled-coil domain/Protein with possible role in bud site polarity
YPL206C	Protein with similarity to *Mycoplasma genitalium* glycerophosphoryl diester phosphodiesterase (glpQ)

Table 3.6.6. 28 ORFs were identified when the TCP-Zinc-Finger double domain was screened against the Fields Library.

3.6.7 Results of the *FAB1* full-length screen

ORF	FUNCTION
ACE2	Metallothionein expression activator with similarity to Swi5p
APL2	**Beta-adaptin, large subunit of the clathrin-associated protein (AP) complex**
ARGR2	Component of the ARGR regulatory complex
AUT4	**Protein required for degradation of autophagic vesicles inside vacuole**
BIK1	Microtubule-associated protein required for microtubule function during mitosis and mating
CDC73	RNA polymerase II accessory protein
CWC25	Component of a complex containing Cef1p, involved in pre-mRNA splicing; has similarity to *S. pombe* Cwf25p
DUR1, 2	Urea amidolyase, contains urea carboxylase and allophanate hydrolase activities
FYV10	Protein of unknown function, required for survival upon exposure to K1 killer toxin; involved in proteasome-dependent catabolite inactivation of fructose-1,6-bisphosphatase; contains CTLH domain
GFA1	Glucosamine--fructose-6-phosphate aminotransferase, isomerizing (hexosephosphate aminotransferase), first step in chitin biosynthesis pathway
ISR1	Serine-threonine protein kinase, involved in staurosporine resistance
IWR1	Interacts with RNA Polymerase II
JIP3	98% of ORF overlaps the verified gene *MID2*
KRE5	Appears to function early in (1,6)-beta-D-glucan synthesis pathway; involved in cell wall biogenesis

LCB3	Sphingoid base-phosphate phosphatase, a key regulator of sphingolipid metabolism and stress response
MDM31	Mitochondrial Distribution and Morphology
MET16	3'-Phosphoadenylylsulfate reductase, part of the sulfate assimilation pathway
MRPL36	Mitochondrial ribosomal protein of the large subunit (YmL36)
NCA2	Protein required for control of mitochondrial synthesis of Atp6p and Atp8p
NDI1	NADH-ubiquinone oxidoreductase (rotenone insensitive)
NUP49	Nuclear pore protein (nucleoporin) of the GLFG family, acts in a complex with Nic96p, Nsp1p, and Nup57p
OYE3	NAPDH dehydrogenase (old yellow enzyme), isoform 3
PAU1	Protein of the PAU1 family (PAU1 and YIL176C code for identical proteins)
PAU5	Protein with similarity to members of the PAU1 family (seripauperin (PAU) family)
PEX21	Peroxin; Pex18p and Pex21p are partially functionally redundant.;Peroxin Pex21p
PHB2	Protein required for normal lifespan, Prohibitin, involved in determination of replicative lifespan; member of the prohibitin complex with Phb1p
PMI40	Mannose-6-phosphate isomerase, generates mannose-6-phosphate for synthesis of GDP-mannose and dolichol-phosphate-mannose
POP2	Components of the CCR4 complex, required for glucose derepression
PSR2	**Protein containing a UBX domain, which are found in ubiquitin regulatory proteins**
PWP2	Periodic tryptophan protein, has eight WD (WD-40) repeats
RAD18	Multifunctional DNA repair protein, required for post-replication repair
REF2	Protein involved in mRNA 3'-end formation prior to polyadenylation, mutant has significantly lower usage of weak poly (A) sites
RHC18	Protein involved in recombination repair, homologous to *S. pombe rad18*
RNP1	Ribonucleoprotein 1, has 2 RNA recognition (RRM) domains which include RNP-1 octamer and RNP-2 hexamer domains
RPS10A	Ribosomal protein S10A (rat S10) (RPS10A and RPS10B code for similar gene products)
SAC2	Subunit of the VFT (Sac2p-Vps53p-Luv1p) complex, involved in protein trafficking in the late TGN
SAE2	Protein involved in meiotic recombination pathway
SCM4	Protein that suppresses temperature-sensitive allele of CDC4 when overexpressed
SEL1	**Plasma membrane phosphatase required for sodium stress response**
SHR3	Protein required for appearance of amino acid permeases on the cell surface, Protein required for exit of amino acid permeases from the endoplasmic reticulum and subsequent appearance on the cell surface
SIF2	**Protein involved in telomere silencing, interacts with Sir4p and targets Sir4p from telomeres to other sites, component of Set3p complex, has WD (WD-40) repeats**
SLG1	Plasma membrane protein required for maintenance of cell wall integrity and for the stress response
SOK1	Protein that can when overexpressed suppress mutants of cAMP-dependent protein kinase
SPP2	Protein involved in pre-mRNA processing, high-copy suppresses of temperature-sensitive prp2 mutations
SPS19	Peroxisomal 2,4-dienyol-CoA reductase
SRB7	Component of RNA polymerase holoenzyme and Kornberg's mediator (SRB) subcomplex

SRM1	GDP/GTP exchange factor for Gsp1p/Gsp2p
SSH4	Suppressor of shr3
THR1	Homoserine kinase (ATP:L-homoserine-O-P-transferase),first step in the threonine biosynthesis pathway
TIP20	Cytoplasmic protein that interacts physically with Sec20p, required for ER to TGN transport
TYS1	Tyrosyl-tRNA synthetase
URA7	CTP synthase, final step in pyrimidine biosynthesis pathway
YBL100C	Protein of unknown function
YDL009C	Protein of unknown function
YDL012C	Protein of unknown function
YDL114W	Protein with similarity to proteins of the short-chain alcohol dehydrogenase family
YDR048C	Questionable ORF
YDR210W	Protein of unknown function
YDR445C	Protein of unknown function
YDR476C	Protein of unknown function
YEL073C	Protein of unknown function
YFL030W	Putative alanine glyoxylate aminotransferase (serine pyruvate aminotransferase
YGR002C	Protein with similarity to *Drosophila melanogaster* transcription initiation factor IID 230 K chain PIR:A47371
YGR128C	Protein with similarity to *Haemophilus* glutamate-ammonia-ligase adenylyltransferase (glnE) PIR:G64046
YHR218W	Protein with similarity to other subtelomerically-encoded proteins including Yhr219p and Yfl065p, probable pseudogene
YIL079C	RING finger protein that inhibits arginine methylation of Npl3p
YIL121W	Member of major facilitator superfamily (MFS) multidrug-resistance (MFS-MDR) protein family
YIP3	**COPII vesicle component**
YJL206C-A	**Protein involved in non-classical protein export pathway for proteins that lack standard secretory signal sequences**
YKL059C	Essential conserved subunit of CPF, cleavage and polyadenylation factor
YKL115C	Protein of unknown function
YLR003C	Protein of unknown function
YLR282C	Protein of unknown function
YMR040W	Protein with similarity to Ykl065p
YMR044W	Protein of unknown function, has glu-rich domains
YMR093W	Protein of unknown function, has WD (WD-40) repeats
YMR153W	Protein with similarity to Asm4p
YNL018C	Protein of unknown function, nearly identical to Ynl034p
YNL123W	**Protein of unknown function, has possible serine protease domain**
YNL157W	Protein with similarity to Yhr132w-ap and with weak similarity to human ENSA alpha-endosulfine and

	human ARPP-19 cAMP-regulated phosphoprotein
YNL275W	Protein with similarity to human band 3 anion transport protein
YOR139C	Protein of unknown function
YOR186W	Protein of unknown function
YOR235W	Questionable ORF
YOR281C	Protein with weak similarity to phosducins, Phosducin homologue, essential protein likely to be involved in regulation of pheromone response
YPL146C	Protein of unknown function
YPL196W	Protein of unknown function, has moderate similarity to uncharacterized *C. albicans* Orf6.1270p
YPL229W	Protein of unknown function
YPR067W	Protein of unknown function. Mitochondrial protein required for iron metabolism
YPR105C	Component of the Sec34p-Sec35p complex involved in vesicular transport to the TGN
YPR169W	Protein containing two WD domains (WD-40 repeat), which may mediate protein-protein interactions, has moderate similarity to uncharacterized *C. albicans* Orf6.4016p
YPR188C	Protein with similar to calmodulin and calmodulin-related proteins, possible light chain for Myo1p myosin
YVL073C	Member of the yeast-specific multidrug-resistance (MFS-MDR) family of the major facilitator superfamily (MFS)

Table 3.6.7. 93 ORFs were identified when *FAB1* was screened against the Fields library.

3.6.8 ORFs identified by two constructs expressing different domains.

This table shows the total number of ORFs that were identified by two separate screens. 26 ORFs were identified twice and some of these were chosen as candidates in the final phenotypic analysis (Table 3.9)

ORF	DOMAINS	FUNCTION
ARGR2	CAT & *FAB1*	Component of the ARGR regulatory complex, contains a Zn [2]-Cys [6] fungal-type binuclear cluster domain
ARP8	**CAT & FYVE-TCP**	**Protein with similarity to actin and actin-related proteins Arp1p-Arp10p**
CBS2	FYVE-TCP & TCP	Mitochondrial translational activator, acts specifically on the COB mRNA encoding cytochrome b
CDC73	*FAB1* & FYVE-TCP	RNA polymerase II accessory protein
DUR 1,2	*FAB1* & FYVE-TCP	Urea amidolyase, contains urea carboxylase and allophanate hydrolase activities fused together in a single polypeptide
ECM2	FYVE-TCP & TCP	Protein possibly involved in cell wall structure or biosynthesis
GCN4	FYVE & FYVE-TCP	Transcription factor of the basic leucine zipper (bZIP) type, regulates general control in response to amino acid or purine starvation
MSI4	TCP & ZINC F	Rab geranylgeranyltransferase regulatory component (component A) and rab guanine nucleotide dissociation inhibitor (Rab GDI)
NDI1	*FAB1* & FYVE-TCP	NADH-ubiquinone oxidoreductase (rotenone insensitive)
PEX21	*FAB1* &FYVE-TCP	Peroxin; Pex18p and Pex21p are partially functionally redundant
POP2	*FAB1* & TCP	Components of the *CCR4* complex, required for glucose derepression component of the major cytoplasmic mRNA deadenylase
RNP1	*FAB1* & FYVE-TCP	Ribonucleoprotein 1, has 2 RNA recognition (RRM) domains which include RNP-1 octamer and RNP-2 hexamer domains and Major polyadenylated RNA-binding protein of nucleus and cytoplasm, contains three RNA recognition (RRM) domains and three Gln/Asn-rich regions
SLG1	*FAB1* & FYVE-TCP	Plasma membrane protein required for maintenance of cell wall integrity and for the stress response during vegetative growth
SPP2	*FAB1* & FYVE	Protein involved in pre-mRNA processing, high-copy suppresses of temperature-sensitive prp2 mutations
UBP9	**FYVE-TCP & TCP**	**Ubiquitin C-terminal hydrolase, has similarity to Ubp13p**
VAN1	FYVE TCP & ZINC F	Vanadate resistance protein, component of mannosyltransferase M-Pol I, which includes Mnn9p and Van1p
YER028C	FYVE-TCP & TCP	Protein that contains two tandem C2H2-type zinc finger domains, has strong similarity to Mig2p, a Tup1p-dependent and glucose-dependent transcriptional repressor
YGR002C	*FAB1* & FYVE-TCP	Protein with similarity to *Drosophila melanogaster* transcription initiation factor IID 230 K chain PIR:A47371
YGR045C	FYVE-TCP & TCP	Protein required for normal growth on nonfermentable carbon sources and for normal pseudohyphal growth

YHR218W	*FAB1* & FYVE-TCP	Protein with similarity to other subtelomerically-encoded proteins including Yhr219p and Yfl065p, probable pseudogene
YIP3	***FAB1* & FYVE**	**COPII vesicle component**
YMR103C	FYVE & FYVE-TCP	Protein of unknown function, questionable ORF (GB:Z49702)
YOR366W	*FAB1* & TCP	Protein of unknown function
YPL137C	FYVE-TCP & TCP	Protein with similarity to Mhp1p
YPR067W	*FAB1* & FYVE-TCP	Mitochondrial protein required for iron metabolism
YPR169W	*FAB1* & FYVE-TCP	Protein of unknown function

Table 3.6.8. 26 ORFs were identified by two constructs expressing different domains. (CAT: catalytic domain).

3.6.9 ORFs identified by three constructs expressing different domains.

In some cases three different screens identified the same ORFs. In total 6 were identified.

ORF	DOMAIN	FUNCTION
SAE2	*FAB1* & FYVE-TCP & TCP	Protein involved in meiotic recombination pathway, required for efficient double strand break repair
SPS19	*FAB1* & FYVE-TCP & TCP	Peroxisomal 2,4-dienyol-CoA reductase
YCL073C	*FAB1* & FYVE-TCP & FYVE	Strong similarity to subtelomeric encoded proteins
YLR282C	*FAB1* & FYVE-TCP & TCP	Protein of unknown function
YPL229W	*FAB1* & FYVE-TCP & TCP	Protein of unknown function
YNL203C	FYVE & FYVE-TCP & TCP	Protein with weak similarity to *Bacillus subtilis* CDP diacylglycerol--serine O-phosphatidyltransferase

Table 3.6.9. 6 ORFs were identified by three constructs expressing different domains.

3.7 Summary and conclusions to yeast two-hybrid analysis

In total, 338 ORFs were identified when the full-length *FAB1* gene, single domains of *FAB1* and adjacent domains of *FAB1* were screened in a yeast two-hybrid screen against the Fields' 6000+ ORF library (Table 3.7). This number refers to the total number of positive interactions, uncorrected for those ORFs that were identified in two or more individual screens. When this is taken into account the total falls to 306 ORFs.

This final number of ORFs identified was high. This was probably due to the culmination of 7 individual screens that included the full-length Fab1p protein (257kDa) and two large double domains of the protein. Together these domains account for 70% of the total ORFs identified. Conversely the 4 smaller domains account for only 30% (Figure 3.7). Simply interpreted, this ratio indicates that the larger a protein domain is, the greater the amount of interactions, with a simultaneous increase in the amount of spurious positives. Alternatively, the smaller a domain is, the fewer interactions there will be thus reducing spurious positives. Therefore these statistics suggest that sectioning a protein into its constitutive domains is the best way to achieve a balanced screen. By screening all 7 domain-fusions it was hoped to increase the chances of identifying authentic binding partners of Fab1p.

There can be no doubt that some of these interactions are spurious or false positives. It is believed that the major cause of spurious interactions is the transcriptional activation of the bait plasmid itself. Apart from one self-activating bait, (CAT-Zinc-F domain), no other baits were found to self-activate. Conversely a number of false positives are known to exist in the library, but are present as control mechanisms to test the fidelity of the array (data not shown). Not all false positives are catalogued and undoubtedly some ORFs identified here are included in this collection. To combat the threat of spurious interactions, stringent measures of testing baits on growth media containing 8 mM 3-AT were beneficial in reducing these numbers.

DOMAIN	ORFS
CAT DOMAIN	15
FAB1 FULL-LENGTH	93
FYVE	24
FYVE-TCP	117
TCP	33
ZINC-F	28
ZINC-TCP	28
TOTAL	338

Table 3.7. In total 338 ORFs were identified in this screen, but when corrected for the occurrence of those ORFs that were identified in two or more different screens this number falls to 306. Representation of the total ORFs identified by each domain fusion is important in its own right as this reflects potential binding partners specifically for that domain fusion and provides insights into likely binding sites to Fab1p.

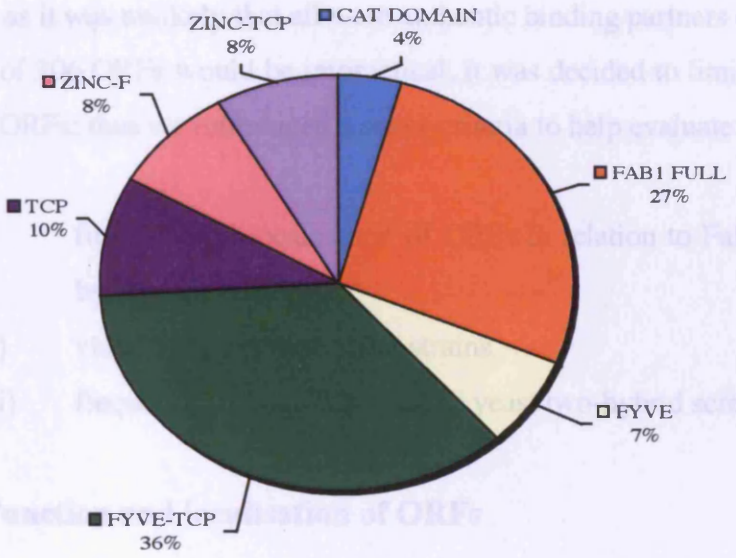

Figure 3.7. The classification of identified proteins according to domain. ORFs identified as interacting with each domain-construct were expressed as a percentage of the corrected total (306) to show the overall distribution with respect to domains screened.

An important factor was the scoring of positive colonies. Because all screens were carried out in duplicate, a colony not matched on its counterpart plate was not regarded as an authentic positive. The principle that duplicate positive colonies were inducing the *HIS3* gene product as a result of functional *GAL4* reconstitution bore no reflection to the size of colonies. It was assumed that large colony size reflected strong protein-protein interaction and likewise smaller colonies weaker or transient interactions; however the overruling criteria were that colonies of all sizes were chosen as long as they were duplicated.

3.8 Choosing ORFs for further analysis

When all data was tabulated, ORFs were chosen for further characterisation in terms of Fab1p phenotypes/function/localisation. That 306 ORFs had been identified presented a problem, as it was unlikely that all were authentic binding partners of Fab1p. As phenotypic analyses of 306 ORFs would be impractical, it was decided to limit our initial investigation to 15-20 ORFs; thus we introduced a set of criteria to help evaluate our results. These were:

i) function and localisation of ORFs in relation to Fab1p function as assigned by the SGD database
ii) viability of deletion yeast strains
iii) frequency of occurrence in the yeast two-hybrid screen

3.8.1 Function and localisation of ORFs

To assist in this selection, a pie chart showing the functional categories as identified from the screen was constructed (Figure 3.8.1a). The screen yielded a diverse number of functional groups such as cell polarity and structure, protein transport, signalling and energy metabolism. These groups accounted for roughly 40% of the ORFs identified however selection was based on relevant information we knew about Fab1p at the time of undertaking these studies (Chapter 1). More specific and detailed reasons are presented later (Table 3.9).

In terms of localisation, a pie chart was also constructed to represent the categories from which all ORFs were derived (3.8.1b). The number of categories was small, however our final choices included proteins localised to the vacuole/PVC compartment, trafficking pathways and the plasma membrane as these were areas in which Fab1p was believed to localise and function (Chapter 1, section 1.9). The large nuclear component (25%) of the screen may have been due to spurious interactions as yeast two-hybrid analysis requires that proteins are imported into the nucleus, a caveat of the yeast two-hybrid as already discussed (Section 3.3). However some of these proteins were selected in light of their functions. On the other hand, those proteins expressed in the mitochondria were not considered, as there was no evidence that Fab1p had a function in this compartment.

Both functional and location pie charts revealed that 32% and 38% of the ORFs identified could not be assigned either function and location respectively when using the SGD as a resource (July 2002). These statistics underline the fact that many ORFs identified by the yeast genome sequencing collaboration still need to be characterised.

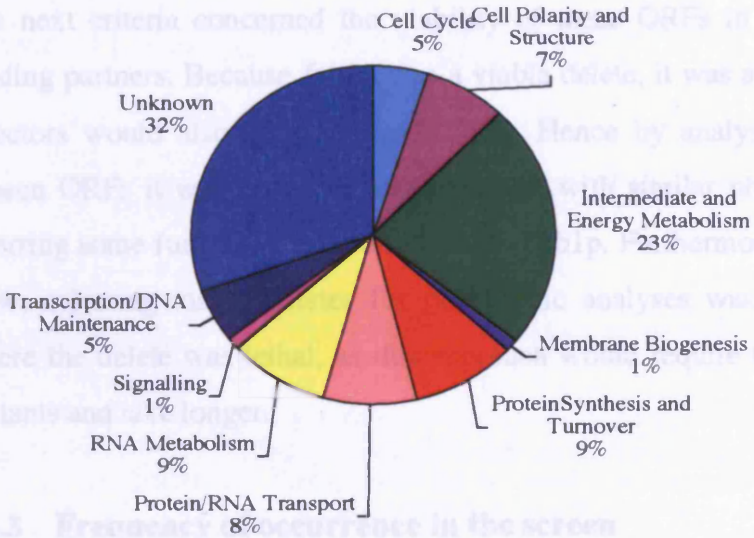

Figure 3.8.1a. The classification of identified proteins according to function. The function of each ORF was assigned using the SGD website (July 2002) and functional categories established for ORFs. These were expressed as a percentage of the total number of ORFs.

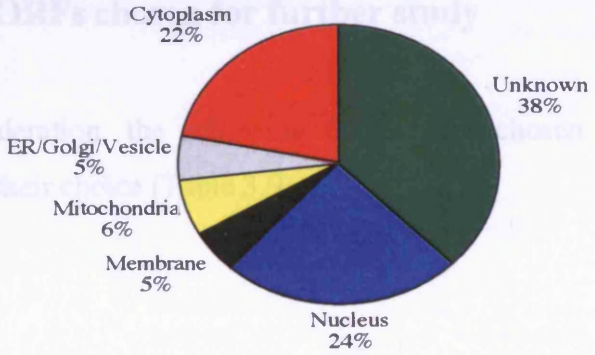

Figure 3.8.1b. The classification of identified proteins according to location. The cellular location of each ORF was identified using the SGD website (July 2002) and expressed as a percentage of the total ORFs identified.

3.8.2 Viability of ORFs

The next criteria concerned the viability of these ORFs in deletion strains of potential binding partners. Because *fab1Δ* was a viable delete, it was assumed that any regulators or effectors would also be viable as deletes. Hence by analysing deletion mutants of the chosen ORFs it was hoped to identify some with similar phenotypes to *fab1Δ* cells thus inferring some functional relationship with Fab1p. Furthermore, from a procedural point of view, selecting viable deletes for phenotypic analyses was easier than choosing ORFs where the delete was lethal, as this approach would require the acquisition of conditional mutants and take longer.

3.8.3 Frequency of occurrence in the screen

Finally, it was felt that any ORF that appeared twice or three times was of interest as statistically the chances of these being authentic binding partners of Fab1p were greater than those appearing once.

3.9 The ORFs chosen for further study

After consideration, the following ORFs were chosen for further analysis along with reasons for their choice (Table 3.9).

ORF	*DOMAIN*	*FUNCTION*	*REASON FOR CHOOSING ORF*
APL2	*FAB1*	Beta-adaptin, large subunit of the clathrin-associated protein (AP-1) complex	Involved in vesicle trafficking from TGN. Also, Apl4p, Gamma-adaptin of AP-1 complex binds to Vac14p, activator of Fab1p (Dove et al., 2002)
ARP8	Catalytic & FYVE-TCP	Protein with similarity to actin and actin-related proteins Arp1p-Arp10p	Identified by two separate screens. TCP domain in Fab1p homologous to actin binding chaperonin containing T-complex protein (CCT-1) (McEwen et al., 1999)
AUT4	*FAB1*	Protein required for degradation of autophagic vesicles inside vacuole	Targets proteins to vacuole via CVT pathway. Other protein in pathway is *AUT10*, shown to be PtdIns(3,5)P_2 binding protein (Dove et al., 2004)
BSC5	Catalytic	Protein with similarity to Bul1p ubiquitin ligase binding protein, may be a pseudogene or separated from YNR068C by sequencing errors	Chosen due to similarity to ubiquitin ligase. Speculation Fab1p may regulate such a ligase at MVB (Cooke, 2002)
CRN1	FYVE-TCP	Coronin, actin-binding protein, interacts with Arp2/Arp3 and involved in endocytosis and cell polarity, has WD (WD-40) repeats	TCP domain in Fab1p homologous to actin binding chaperonin containing T-complex protein (CCT-1) (McEwen et al., 1999)
INM1	Zinc-F-TCP	Protein with similarity to inositol monophosphatase of *E. coli*, *Aspergillus nidulans*, and *Neurospora crassa*. Member of the inositol monophosphatase family, catalyzes hydrolysis of inositol-1-phosphate, involved in the inositol cycle of calcium signaling	Chosen as protein involved in the biosynthesis of inositol and intracellular signaling (Lopez et al., 1999)
PDR12	Zinc-F-TCP	Protein with similarity to Pdr5p and Snq2p, member of the ATP-binding cassette (ABC) superfamily of membrane transporters Protein required for weak organic acid resistance.	Fab1p believed to be regulated by weak acid stress. (F.Cooke unpublished data)
PSR2	*FAB1*	Plasma membrane phosphatase required for sodium stress response	A regulator of salt stress response in yeast (Siniossoglou et al., 2000)
SEL1	*FAB1*	Protein containing a UBX domain, which are found in ubiquitin regulatory proteins	Similar to ubiquitin ligase. Speculation Fab1p may regulate such a ligase at MVB (Cooke, 2002)
SIF2	*FAB1*	Protein involved in telomere silencing, interacts with Sir4p and targets Sir4p from telomeres to other sites, component of Set3p complex, has WD-40 repeats	A nuclear protein containing 4 WD40 repeats that have been implicated in protein-protein interactions.
UBP9	FYVE-TCP & TCP	Ubiquitin C-terminal hydrolase, has similarity to Ubp13p	Identified in two separate screens. Similar to ubiquitin ligase. Speculation Fab1p may regulate such a ligase at MVB (Cooke, 2002)
VID21	FYVE-TCP	Component of the NuA4 histone acetyltransferase complex	Vacuolar Importation Degradation 21, potential vacuolar function.
VMA6	Catalytic	Vacuolar H-ATPase (V-ATPase) 36 kDa subunit (subunit D) of membrane (V0) sector, required for V-ATPase assembly	Interacts with catalytic domain of Fab1p. Is hydrogen transporter, blockage of channel or defect may increase pH in vacuole. Vacuolar

			acidification defect in *fab1Δ* seen in *vma6Δ* (Bauerle.,et al 1993)
YCK3	Zinc-F	Casein kinase I isoform	Localises to plasma membrane. Casein kinase I may phosphorylate Fab1p. (FTC unpublished data)
YIP3	*FAB1* & FYVE	COPII vesicle component involved in vesicle transport and membrane fusion	Identified by two separate screens, Vesicle protein found on COPII vesicles (Otte et al., 2001)
YJL206C	*FAB1*	Protein involved in non-classical protein export pathway for proteins that lack standard secretory signal sequences, putative regulatory zinc-finger protein	Involved in protein export (http://mips.gsf.de/)
YNL123W	*FAB1*	Protein having possible serine protease domain and PDZ domain	Contains PDZ domain. Motif involved in cell signaling (Jelen et al., 2003)

Table 3.9. 17 ORFs were chosen for further analysis based on criteria outlined (Section 3.8).

3.10 LacZ assay on chosen ORFs

As stated (Section 3.2), the yeast two-hybrid assay used in this screen has two reporter systems, one which allows for the identification of potential interactors by a plate based growth assay and one which allows for identification of potential interactors by enzymatic assay. After evaluation by the growth assay using the *HIS3* gene reporter system, we used the enzymatic assay LacZ gene reporter gene system to evaluate our chosen ORFs. The LacZ assay will not confirm these ORFs as bona fide interactors of Fab1p; instead the assay will enzymatically confirm the results of the growth assay.

The assay consisted of mating each of the 17 ORF strains from the Fields Library (prey cloned in frame with the *GAL4* activation domain and cloned into the pOAD vector on a leucine marker) to a strain expressing the Fab1p full-length (bait cloned in frame to the *GAL4* DNA binding domain into the pOBD2 vector on a tryptophan marker). For the assay, mated diploids were cultured into –L-T media and unmated ORF strains cultured into –Leu media. The latter step was included so as to account for background enzymatic activity from the unmated ORF. The assay was carried out as described (Section 2.4.4) (Figure 3.10).

These results indicate that the ORFs strains when mated to the bait Fab1p strain expressed β-galactosidase. None presented zero levels indicating that protein-protein interactions were occurring in all strains.

The selection of our ORFs complete, the next step involved characterisation of these proteins in terms of *fab1*Δ function using several phenotypic analyses as described (Section 1.10).

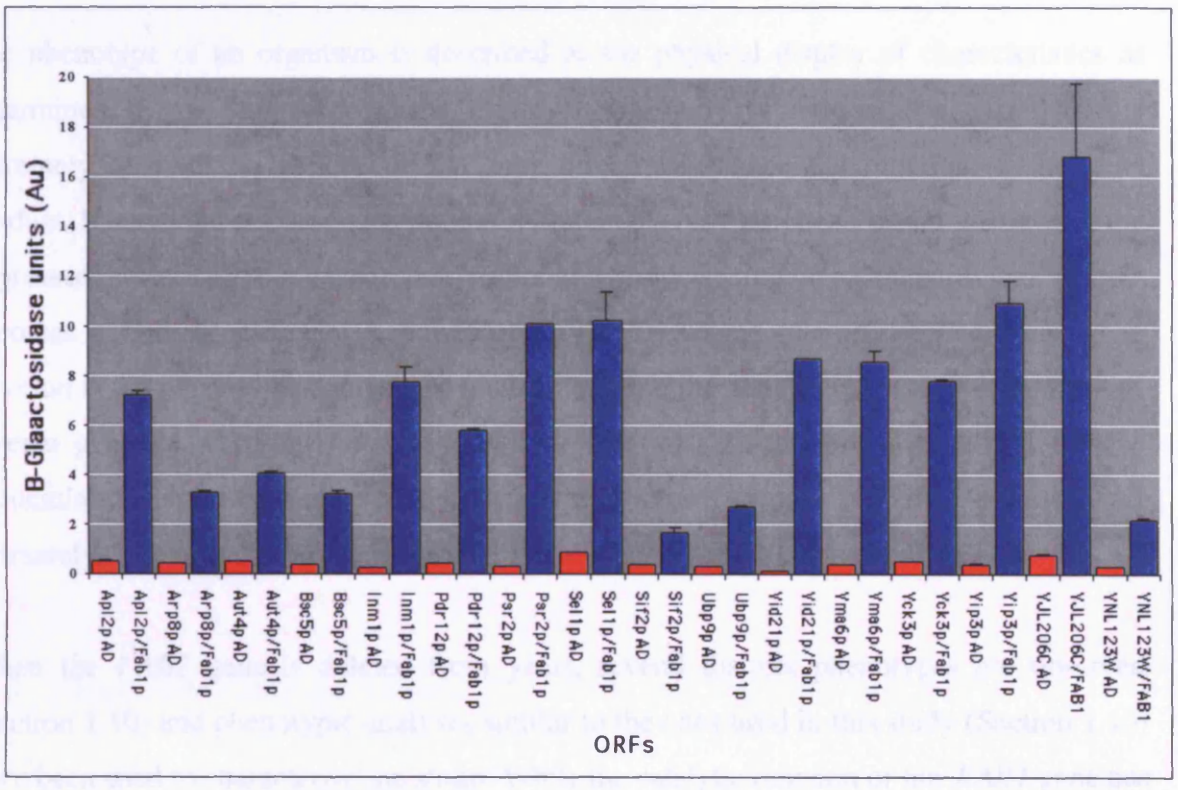

Figure 3.10. LacZ assay of Fab1p and ORFs using the yeast two-hybrid β-galactosidase reporter gene system. Strains expressing prey alone (red) and mated bait and prey (blue) were assayed in triplicate for β-galactosidase activity as described (Section 2.4.4). β-galactosidase activity units are given as arbitrary.

4 PHENOTYPIC ANALYSES OF ORF DELETION MUTANTS

4.1 Introduction

The phenotype of an organism is described as the physical display of characteristics as determined by its expressed genes. However the study of native gene expression is extremely complex as factors *in situ* may directly influence the function of the gene product. Interactors, effectors, transcription factors etc may all play a part in the role of the expressed protein to the extent that deciphering precise role(s) of a particular protein becomes extremely difficult. A powerful way to overcome this and to determine gene function is the phenotypic analysis of mutants missing the gene of interest. This concept of reverse genetics, carrying out phenotypic studies on deletion mutants, allows for the accumulation of information and data relating to gene function, protein expression and ultimately the physical characterisation of the mutant strain (Winzeler et al., 1999).

When the *FAB1* gene is deleted from yeast, several distinct phenotypes are observed (Section 1.10) and phenotypic analyses similar to the ones used in this study (Section 1.10) have been used to characterise the strain. While the catalytic function of the *FAB1* gene has been determined (Section 1.4), protein interactors and effectors of Fab1p have not been identified to explain the different phenotypes displayed by *fab1*Δ cells. It is likely that the phenotypes observed are regulated by independent mechanisms, suggesting several Fab1p effector/interactor proteins exist, accounting for these events (Dove et al., 2004).

In this study we have chosen 17 ORFs identified from a yeast two-hybrid analysis with Fab1p (Chapter 3). We have chosen to carry out phenotypic analyses in yeast strains in which each ORF has been deleted. This panel of deletion mutants has been chosen on the basis that the corresponding gene product is a potential candidate effector or interactor to Fab1p (Section 3.9). Our premise is that deletion of genes coding for authentic effectors

and/or activators of Fab1p would display one or more of the phenotypes associated with *fab1*Δ cells.

4.2 Phenotypic Analyses

The following phenotypic analyses were used to characterise the panel of deletion ORFs.

1) Temperature sensitivity

2) Protein trafficking assay using GFP-Phm5p

3) Protein trafficking assay using GFP-CPS

4) Quinacrine assay

5) FM4-64 assay

4.3 Phenotypic Analyses using the Euroscarf Deletion Library

Phenotypic analyses were carried out on deletion mutants obtained from the Euroscarf deletion library: http://web.uni-frankfurt.de/fb15/mikro/euroscarf/col_index.html.

The Euroscarf (European *Saccharomyces cerevisiae* archive for functional analyses) deletion library consists of individual ORFs that have been deleted from the yeast genome and replaced with the *KAN*MX4 cassette: a kanamycin resistance gene that contains G418 resistance to the *S. cerevisiae* strain (Baudin et al., 1993; Wach et al., 1994). This PCR based gene deletion strategy deletes the ORF and simultaneously incorporates a 20 base pair sequence tag unique to that ORF (Shoemaker et al., 1996). ORF deletions were confirmed by identification of these unique sequences from genomic DNA extraction and sequencing (data not shown).

4.4 Phenotypic Analyses Results

4.4.1 Temperature sensitivity of ORF deletion mutants at 37 °C

The *fab1*Δ mutant is inviable at 37 °C implying the gene is essential for growth at this temperature (Yamamoto et al., 1995). All deletion mutants were streaked onto YAPD plates and incubated at 37 °C for growth (Table 4.4.1).

The temperature sensitivity at 37 °C of *fab1*Δ cells is not a specific phenotype; it has been proposed that the phenomenon is due to steric hindrance caused by the swollen vacuole (Yamamoto et al., 1995). Growth of *vma6*Δ and *sel1*Δ cells are compromised at this temperature so it is possible a similar mechanism of steric hindrance is occurring here. It would appear that Arp8p is essential for growth at 37 °C.

Deletion Mutant	Growth at 37 °C	Deletion Mutant	Growth at 37 °C
apl2Δ	growth	*sif2Δ*	growth
arp8Δ	**no growth**	*ubp9Δ*	growth
aut4Δ	growth	*vid21Δ*	growth
bsc5Δ	growth	*vma6Δ*	**poor growth**
crn1Δ	growth	*yck3Δ*	growth
inm1Δ	growth	*yip3Δ*	growth
pdr12Δ	growth	yjl206cΔ	growth
psr2Δ	growth	ynl123wΔ	growth
sel1Δ	**poor growth**		

Table 4.4.1. Growth of deletion mutants on YAPD at 37 °C. *arp8Δ* cells do not grow at this temperature while two strains, *sel1Δ* and *vma6Δ* grew extremely poorly.

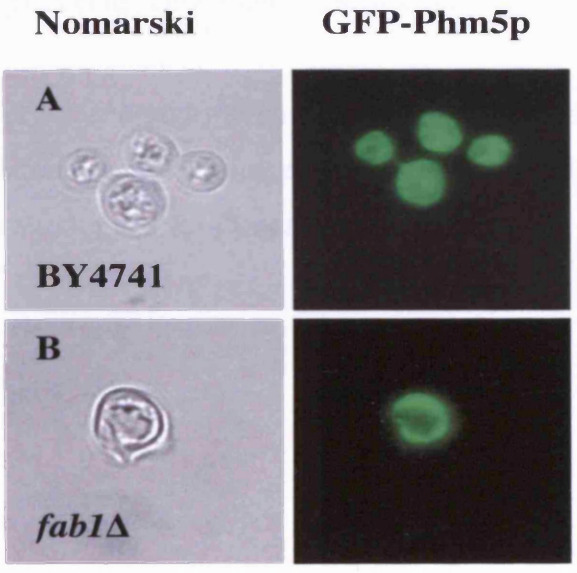

Figure 4.4.2.1. Localisation of GFP-Phm5p in BY4741 wild-type and *fab1*Δ cells. Cells expressing GFP-Phm5p were grown at 24 °C to a cell density of $8x10^6$ cells/ml. Cells were viewed on a Leica DM RXA2 microscope with a GFP filter cube and images recorded and processed in Adobe Photoshop. (A) GFP-Phm5p traffics to the vacuole lumen in BY4741 wild-type cells. (B) GFP-Phm5p traffics incorrectly in *fab1*Δ cells, the protein stalls at the outer vacuole membrane.

4.4.2.2 GFP-Phm5p trafficking in deletion mutants

GFP-Phm5p traffics to the vacuole lumen in all deletion mutants with the exception of *apl2*Δ (Figure 4.4.2.2). In these cells, GFP-Phm5p stalls at the outer vacuole membrane in a manner similar to *fab1*Δ cells (Figure 4.4.2.1).

Viewing these cells under Nomarski, it appears that the over-expression of GFP-Phm5p at least in this strain background (BY4741) affects cell morphology. Interestingly, these morphological effects were not noted in the studies of other workers. Different strain backgrounds were used; SEY6210 (Reggiori and Pelham, 2001) and BY4742 (Dove et al., 2002), suggesting that this observation is unique to the BY4741 strain. Nonetheless, in *apl2*Δ cells, GFP-Phm5p traffics to the outer vacuole membrane similar to *fab1*Δ.

As the aberrant morphology of the GFP-Phm5p over-expressing cells made it difficult to determine the phenotypes of some of the deletion strains, it was decided to investigate the trafficking of another cargo, GFP-CPS.

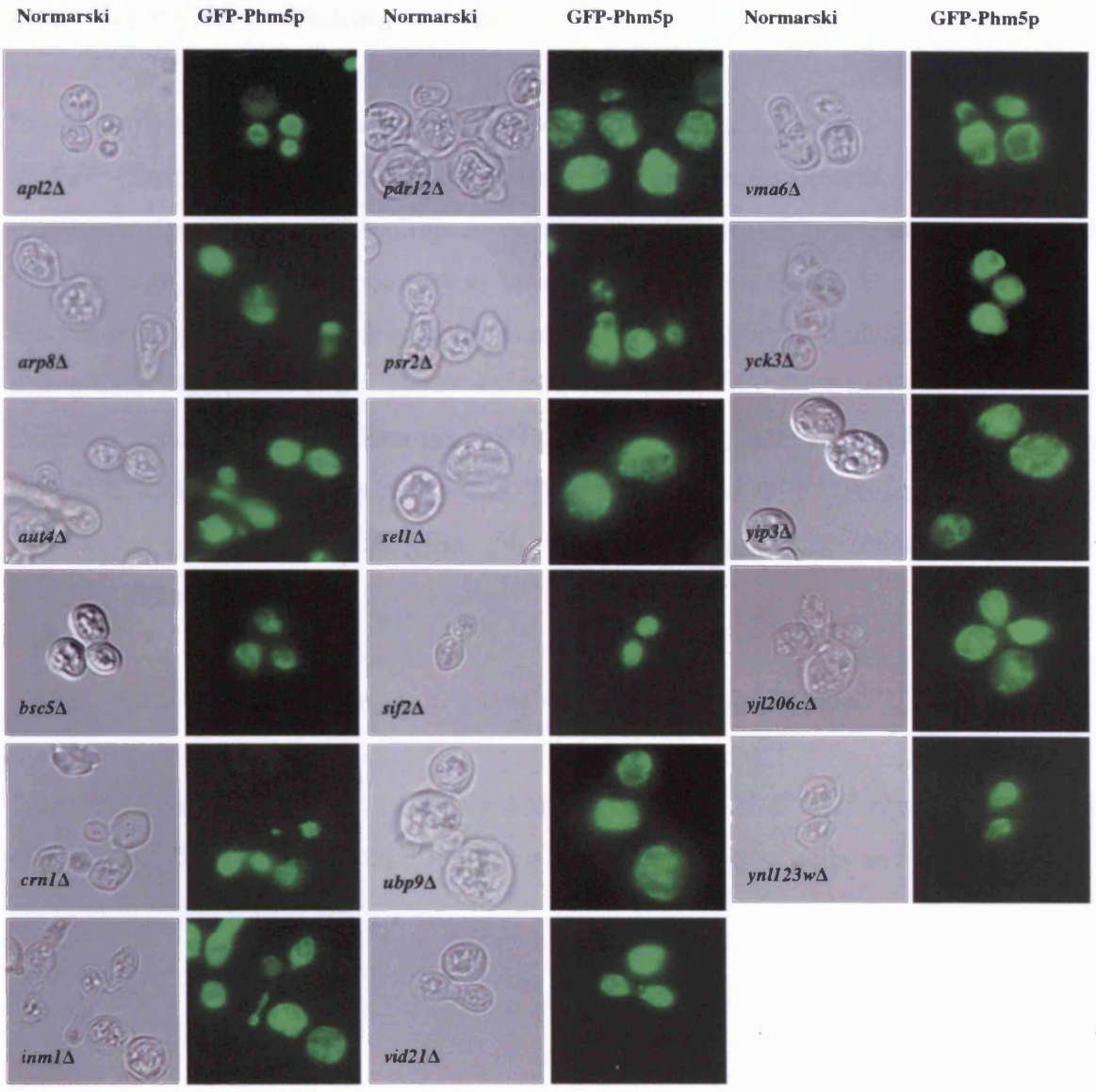

Figure 4.4.2.2. Localisation of GFP-Phm5p in deletion mutants. Cells were grown at 24 °C to a cell density of $8x10^6$ cells/ml. They were viewed on a Leica DM RXA2 microscope with a GFP filter cube and images recorded and processed in Adobe Photoshop. All deletion mutants traffic GFP-Phm5p to the vacuole except *apl2*Δ cells. Here, GFP-Phm5p stalls at the vacuole membrane.

4.4.3 GFP-CPS trafficking in yeast

In order to overcome the cell morphological difficulties encountered with over-expression of GFP-Phm5p, we decided to use the integral membrane protein, CPS. The single membrane domain vacuolar hydrolase, carboxypeptidase S (CPS) is transported from the TGN through the secretory pathway as an inactive precursor (proCPS). Once delivered to the vacuole, the protein is cleaved lumenal to a transmembrane domain to yield soluble active CPS (Spormann et al., 1992). In wild-type cells, GFP-CPS traffics to the vacuole lumen in vesicles delivered from the TGN (Odorizzi et al., 1998). However, in *fab1*Δ cells GFP-CPS stalls at the vacuole membrane. The mechanism of GFP-CPS trafficking from the TGN to the vacuole in both BY4741 wild-type and *fab1*Δ cells is similar to that in GFP-Phm5p (Figure 4.4.2.1)

4.4.3.1 GFP-CPS trafficking in BY4741 wild-type and *fab1*Δ cells

Like GFP-Phm5p, GFP-CPS trafficking was assayed in BY4741 wild-type and *fab1*Δ cells. GFP-CPS traffics to the vacuole lumen in BY4741 wild-type cells and was found to be aberrant in *fab1*Δ cells (Figure 4.4.3.1).

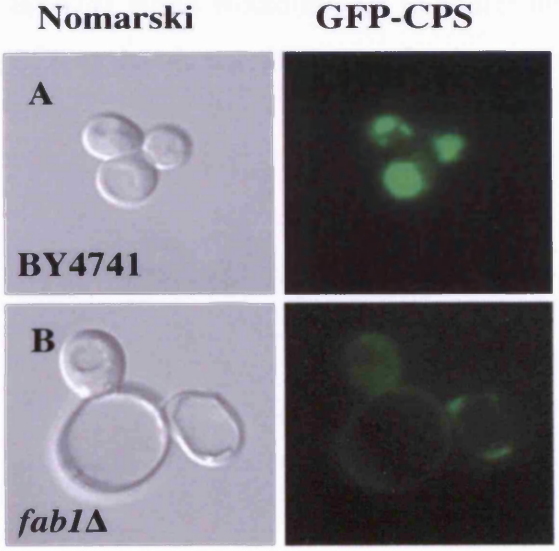

Figure 4.4.3.1. Localisation of GFP-CPS in BY4741 wild-type and *fab1*Δ cells. Cells were grown at 24 °C to a cell density of $8x10^6$ cells/ml. They were viewed on a Leica DM RXA2 microscope with a GFP filter cube and images recorded and processed in Adobe Photoshop. (A) BY4741 wild-type cells traffic GFP-CPS to the vacuole lumen whereas (B) GFP-CPS trafficking in *fab1*Δ cells stalls at the vacuole membrane.

4.4.3.2 GFP-CPS trafficking in deletion mutants

The panel of deletion mutants were assayed for GFP-CPS trafficking and all traffic GFP-CPS in a manner similar to wild-type cells with the exception of *apl2*Δ (Figure 4.4.3.2) These cells presented a similar phenotype to *fab1*Δ cells (Figure 4.4.3.1).

The Nomarski images appeared to indicate that expression of GFP-CPS in these cells had little effect on cell morphology in direct contrast to expression of GFP-Phm5p. However, the finding that the deletion mutant *apl2*Δ incorrectly trafficked GFP-CPS was important as these cells also incorrectly trafficked GFP-Phm5p. Hence the absence of Apl2p from the BY4741 strain would appear to confer an inability to traffic both GFP-Phm5p and GFP-CPS to the vacuole lumen, a phenotype coincidental with the loss of Fab1p from the same strain.

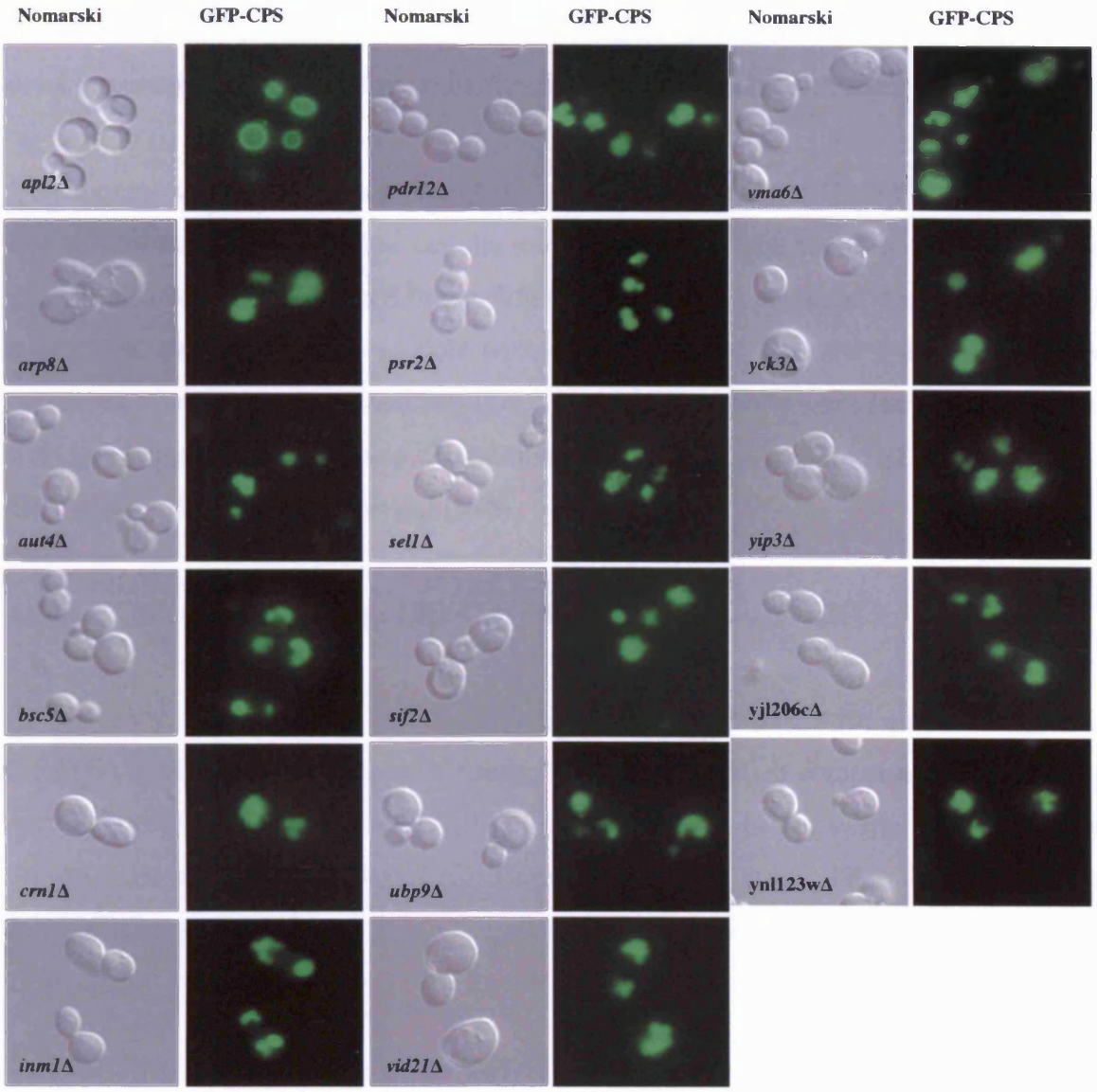

Figure 4.4.3.2. Localisation of GFP-CPS in deletion mutants. Cells were grown at 24 °C to a cell density of $8x10^6$ cells/ml and were viewed on a Leica DM RXA2 microscope with a GFP filter cube. Images were recorded and processed in Adobe Photoshop. Deletion mutants traffic GFP-CPS to the vacuole with the exception of *apl2*Δ. In these cells GFP-CPS was localises to the vacuole membrane similar to *fab1*Δ cells (Figure 4.4.3.1)

4.4.4 Assessment of vacuole acidification by quinacrine staining

Quinacrine is a basic fluorescent dye that crosses membranes by diffusion and concentrates due to protonation in acidified cellular compartments (Weisman et al., 1987). Because vacuole size was so pronounced in the *fab1*Δ mutant, it was proposed that this abnormality might have had an effect on vacuole content and function. The pH of a cell is one such parameter of vacuole content and function. Thus *fab1*Δ vacuoles were found to stain poorly with quinacrine, implying these compartments were poorly acidified (Dove et al., 2004; Gary et al., 1998; Yamamoto et al., 1995).

4.4.4.1 Quinacrine staining of BY4741 wild-type and *fab1*Δ cells

In this assay, BY4741 wild-type and *fab1*Δ cells were stained with quinacrine (Section 2.5.2) BY4741 wild-type cells accumulated the dye in acidified compartments indicating a correct intracellular pH. In contrast, in *fab1*Δ cells, uptake of quinacrine was reduced and the cells did not fluoresce as described previously (Gary et al., 1998; Yamamoto et al., 1995) (Figure 4.4.4.1)

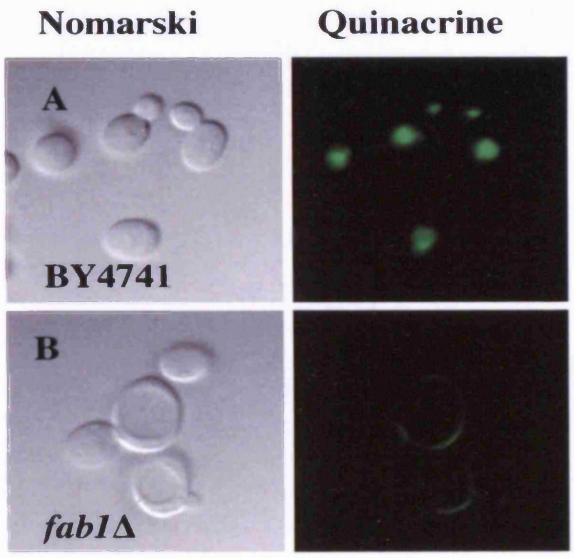

Figure 4.4.4.1. Quinacrine staining in BY4741 wild-type and *fab1*Δ cells. Yeast cells were grown to $8x10^6$ cells/ml at 24 °C in YPD, incubated in media containing 200 μm quinacrine in the dark for 5 minutes and viewed on a Leica DM RXA2 microscope with a GFP filter cube. Fluorescent and Nomarski images were acquired with an ORCA digital camera and processed in Open Lab and Adobe Photoshop. (A) BY4741 wild-type cells accumulated quinacrine in acidified vacuoles whereas (B) *fab1*Δ cells failed to accumulate quinacrine, indicating poorly acidified vacuoles.

4.4.4.2 Quinacrine staining in deletion mutants

Deletion mutants were assayed for vacuole acidification by quinacrine staining (Figure 4.4.4.2). Six deletion mutants did not accumulate the dye indicating poorly acidified vacuoles. These were: *arp8*Δ, *bsc5*Δ, *inm1*Δ, *sif2*Δ, *vma6*Δ and ynl123wΔ.

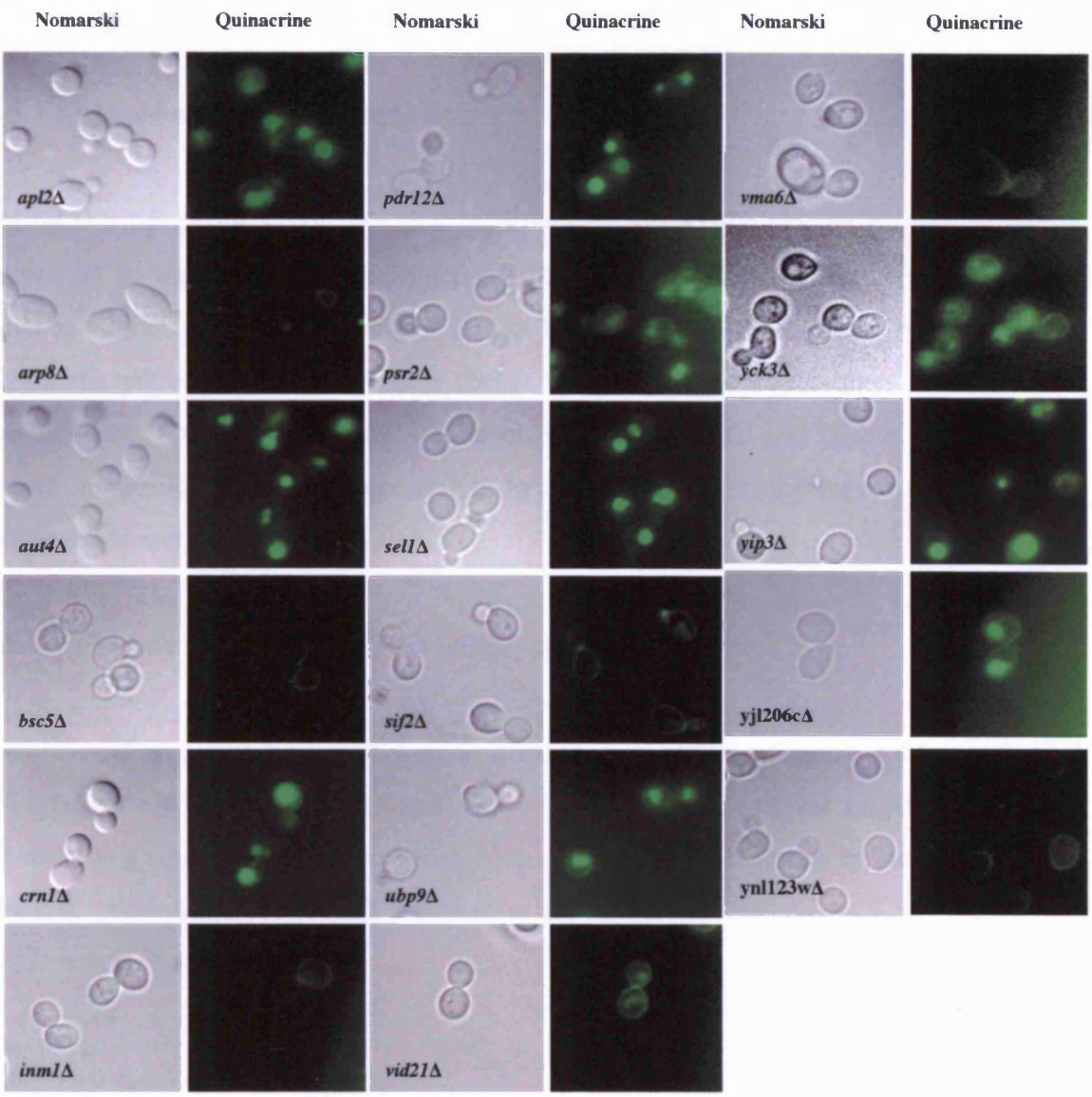

Figure 4.4.4.2. Quinacrine staining in deletion mutants. Yeast cells were grown to $8x10^6$ cells/ml at 24 °C in YAPD, incubated in 200 μm quinacrine in the dark for 5 minutes and viewed on a Leica DM RXA2 microscope with a GFP filter cube. Nomarski and fluorescence images were acquired with an ORCA digital camera and processed in Open Lab and Adobe Photoshop. Six deletion mutants failed to accumulate quinacrine in their vacuoles in a manner similar to *fab1*Δ. These were *arp8*Δ, *bsc5*Δ, *inm1*Δ, *sif2*Δ, *vma6*Δ and ynl123wΔ.

4.4.5 FM4-64 staining in yeast

FM4-64 is a lipophillic styryl dye that incorporates into a cells plasma membrane and is transported by endocytosis to the vacuole. The stain reveals subcellular dynamics and spatial relationships of organelles that cannot be observed in fixed cells. By labelling the cells in the presence of FM4-64 at a certain temperature and subsequent chasing for a specified time, FM4-64 can be used to label the yeast vacuole and is thus used to study vacuole morphology. This process occurs in a time, energy and temperature dependant manner (Vida and Emr, 1995).

4.4.5.1 FM4-64 staining in BY4741 wild-type and *fab1*Δ cells

BY4741 wild-type and *fab1*Δ cells were labelled with FM4-64 (Figure 4.4.5.1). BY4741 wild-type cells were found to contain a multilobed vacuole whereas in *fab1*Δ cells, the vacuole was a single large structure that often constituted the majority of the cells internal volume as previously described (Yamamoto et al., 1995).

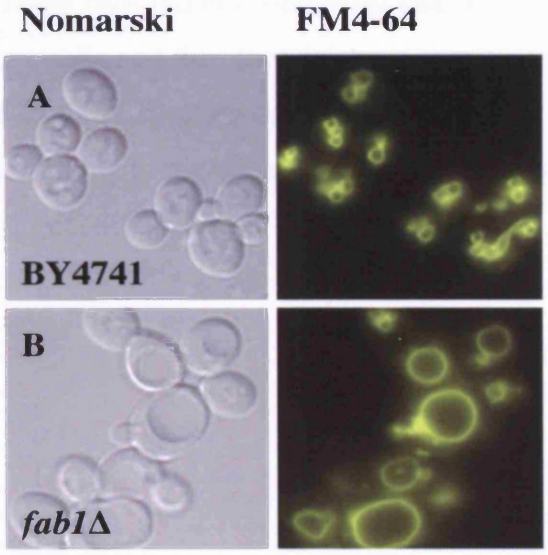

Figure 4.4.5.1. FM4-64 labelling of BY4741 wild-type and *fab1*Δ cells. Yeast cells were grown to a density of $8x10^6$ cells/ml in YPD media at 24 °C, washed in PIPES buffered YPD pH 6.8 and 80 μm FM4-64 added in 1 ml YPD. Cells were incubated for 1 hour at 24 °C in the dark, washed twice and chased for 2 hours in 1 ml YPD in the dark. Cells were viewed on a Leica DM RXA2 microscope with a Texas Red filter cube and images acquired with an ORCA digital camera and processed in Open Lab and Adobe Photoshop. (A) BY4741 wild-type vacuoles are multilobed organelles whereas (B) the *fab1*Δ vacuole is a large single entity filling most of the cell interior (Yamamoto et al., 1995).

4.4.5.2 FM4-64 staining in deletion mutants

Deletion mutants were assayed for vacuole morphology by FM4-64 labelling (Figure 4.4.5.2).

Of seventeen deletion mutants, three were found to present aberrant FM4-64 staining, *apl2*Δ, *vma6*Δ and *sel1*Δ. These cells did not contain the characteristic multi-lobed vacuolar staining as seen in wild-type cells and the other deletion mutants. Instead, vacuole staining was more rounded and *fab1*Δ-like indicating defects in vacuole morphology, however none of these cells had vacuolar swelling to the same extent as *fab1*Δ cells.

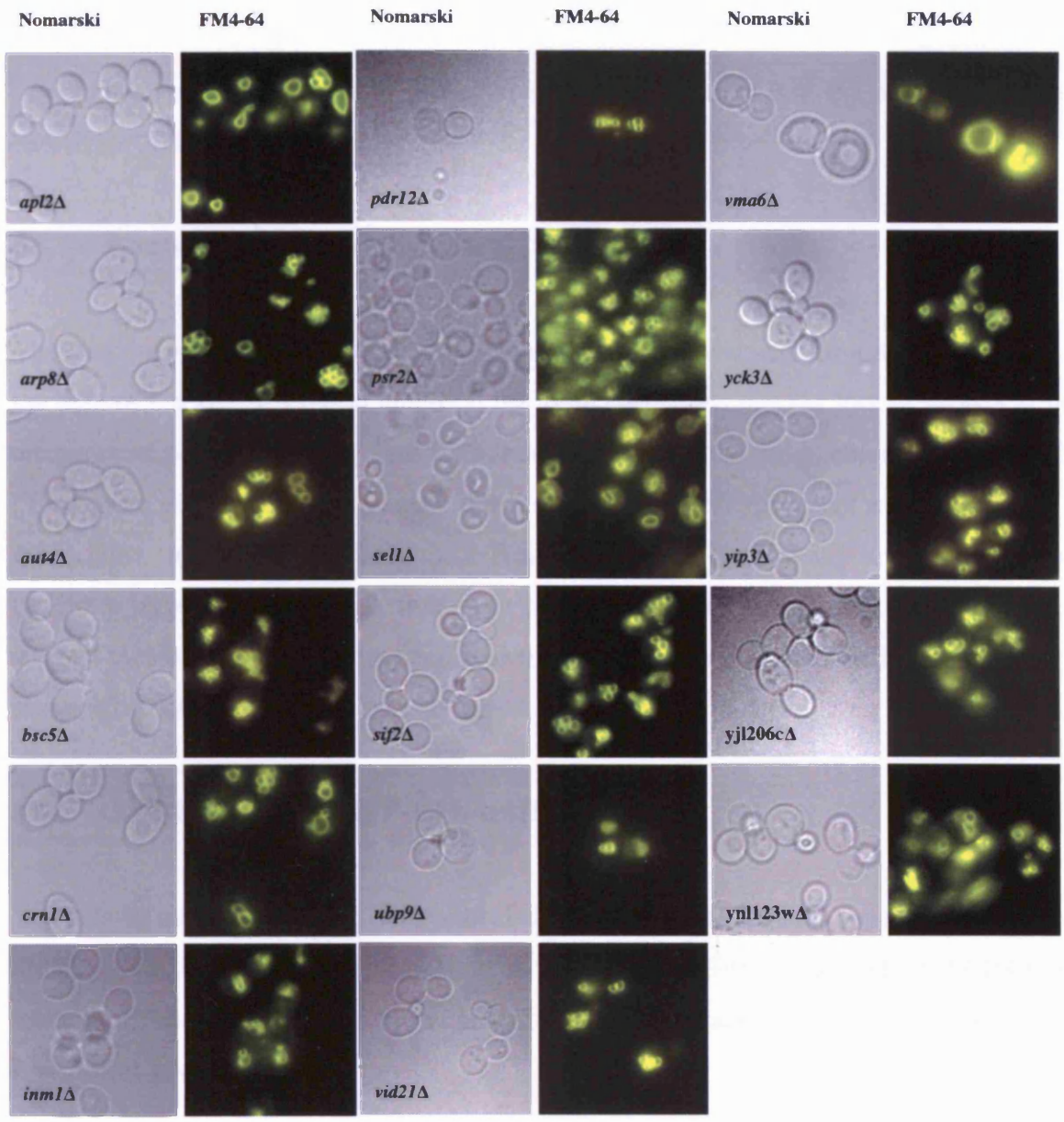

Figure 4.4.5.2. FM4-64 labelling of deletion mutants (Section 2.5.3). Three deletion mutants were found to exhibit altered vacuole morphology, *apl2*Δ, *sel1*Δ and *vma6*Δ.

4.5 Conclusions

These phenotypic analyses have yielded new information about 8 of the deleted ORFs in *S. cerevisiae* (Table 4.5).

4.5.1 Temperature sensitivity assay

The strain *arp8*Δ did not grow at 37 °C, whilst *sel1*Δ and *vma6*Δ grew extremely poorly. In the case of the *fab1*Δ deletion mutant it has been speculated that the loss of growth at this temperature is as a result of steric hindrance caused by the enlargement of the vacuole (Yamamoto et al., 1995), suggesting this temperature phenotype is not entirely specific to *fab1*Δ cells. In the case of *vma6*Δ, this temperature may be contributory to poor growth as it too has a large vacuole. The lack of growth for *arp8*Δ and poor growth in *sel1*Δ at 37 °C suggest these genes are required for growth at this temperature, although it is difficult to assess what roles these genes are playing (if any) in Fab1p function.

4.5.2 GFP-Phm5p and GFP-CPS trafficking assay

The protein trafficking assays have indicated that all deletion mutants with the exception of *apl2*Δ, correctly traffic both integral membrane proteins GFP-Phm5p and GFP-CPS to the vacuole. In *apl2*Δ cells these proteins stall at the outer vacuole membrane as shown by fluorescent microscopy.

Yeast Apl2p is the β-subunit of the yeast heterotetrameric AP-1 (adaptor protein) complex, which is involved in the formation of vesicular transport intermediates and the selection of cargo molecules for inclusion into these intermediates (Boehm et al., 2002). More specifically the AP-1 complex is involved in the assembly of clathrin-coated vesicles that originate from the TGN, ultimately ending up in early and late endosomes (Doray and Kornfeld, 2001). Integral membrane protein missorting has not been observed in *apl2*Δ cells before, therefore these data are the first to show that Apl2p may be involved in Fab1p-dependant trafficking to the vacuole lumen.

Cells	Growth at 37 °C	GFP-Phm5p trafficking	GFP-CPS trafficking	Quinacrine staining	FM4-64 labelling
apl2Δ	growth	**not wild-type**	**not wild-type**	staining	**aberrant vacuole morphology**
arp8Δ	**no growth**	wild-type	wild-type	**no staining**	wild-type
aut4Δ	growth	wild-type	wild-type	staining	wild-type
bsc5Δ	growth	wild-type	wild-type	**no staining**	wild-type
crn1Δ	growth	wild-type	wild-type	staining	wild-type
inm1Δ	growth	wild-type	wild-type	**no staining**	wild-type
pdr12Δ	growth	wild-type	wild-type	staining	wild-type
psr2Δ	growth	wild-type	wild-type	staining	wild-type
sel1Δ	**poor growth**	wild-type	wild-type	staining	**aberrant vacuole morphology**
sif2Δ	growth	wild-type	wild-type	**no staining**	wild-type
ubp9Δ	growth	wild-type	wild-type	staining	wild-type
vid21Δ	growth	wild-type	wild-type	staining	wild-type
vma6Δ	**poor growth**	wild-type	wild-type	**no staining**	**aberrant vacuole morphology**
yck3Δ	growth	wild-type	wild-type	staining	wild-type
yip3Δ	growth	wild-type	wild-type	staining	wild-type
YJL206CΔ	growth	wild-type	wild-type	staining	wild-type
YNL123WΔ	growth	wild-type	wild-type	**no staining**	wild-type

Table 4.5. Summary of phenotypic analyses carried out on the deletion mutants. In total 8 were found to share characteristics with the *fab1Δ* mutant strain.

4.5.3 Quinacrine assay

When deletion mutants were assayed for vacuole acidification using quinacrine at 24 °C, several displayed poorly acidified vacuoles. These deletion mutants were *arp8*Δ, *bsc5*Δ, *inm1*Δ, *sif2*Δ, *vma6*Δ and ynl123wΔ and these acidification defects were original observations in 5 out of 6 of these deletion mutants.

The function of yeast Arp8p (actin related protein) is unknown. It is a member of the *INO80* chromatin-remodelling complex, is required for DNA binding and when deleted causes the inactivation of Arp4p and actin in this complex. *arp8*Δ cells are defective for growth in media lacking inositol and hypersensitive to hydroxyurea (Shen et al., 2003). This defect in vacuolar acidification has not been described in *arp8*Δ cells.

Yeast Bsc5p (Bypass of stop codon) has yet to be characterised and as such this defect in vacuole acidity is a novel observation.

Inm1p is an inositol monophosphatase that plays a role in the *de novo* biosynthesis of inositol and in the phosphoinositide second messenger-signalling pathway. In *inm1*Δ mutants, inositol monophosphatase activity is reduced but not completely ablated with little effect on growth in the presence of lithium or valproate and no effect on growth in the absence of inositol (Murray and Greenberg, 2000). This defect in vacuole acidity has not been described before in *inm1*Δ cells.

S. cerevisiae Sif2p interacts with Sir4p and is a WD40-repeat containing protein that disrupts telomeric silencing when over-expressed (Neer et al., 1994). Deletion of the protein improves telomeric repression and mutants were hypersensitive to a range of stress conditions (Cockell et al., 1998). Defects in vacuole acidity have not been reported in *sif2*Δ cells before.

The yeast YNL123W protein has not been assigned any function or location by the SGD database (http://www.yeastgenome.org/) hence this defect in vacuole acidity is novel.

Vma6p is a 36 kDa subunit of the vacuolar (H^+)-ATPase multi-subunit complex, which regulates the acidification of intracellular compartments in eukaryotic cells (Stevens and Forgac, 1997). Deletion of Vma6p from yeast causes a defect in vacuolar acidification as previously reported (Bauerle et al., 1993). The absence of Vma6p prohibits the assembly of the V_0 subunits of the vacuolar (H^+)-ATPase complex thus preventing this complex from reaching the vacuole and hence a loss of acidification (Graham et al., 2000). Similarly when Vma4p, another component of the (H^+)-ATPase multi-subunit complex was deleted from yeast, acidification defects resulted as indicated by electron-transparent vacuoles (Odorizzi et al., 1998). Therefore, loss of acidification was expected in *vma6*Δ cells.

4.5.4 FM4-64 Assay

Three deletion mutants stained with FM4-64 were found to have significantly altered vacuole morphology when compared to BY4741 wild-type cells. These were *apl2*Δ, *sel1*Δ and *vma6*Δ cells and were characterised by a loss of multilobing, a morphology similar to *fab1*Δ cells. Vacuoles of *apl2*Δ but not *sel1*Δ cells were slightly larger than wild-type cells whereas vacuoles of *vma6*Δ cells were similar to *fab1*Δ cells. The large un-lobed swollen vacuole defect seen in *fab1*Δ cells has been proposed to be caused by retrograde blockage in traffic from the vacuole via the PVC to the TGN (Bryant et al., 1998) however the role (if any) of Apl2p and Sel1p in this process remains unknown.

Apl2p as previously mentioned is the β-subunit of the AP-1 complex and is involved in the formation of clathrin-coated vesicles at the TGN (Yeung et al., 1999). The vacuoles of *apl2*Δ cells were found to be slightly larger in size than BY4741 wild-type, but not as large as *fab1*Δ cells (Figure 4.4.5.2). Therefore the defects seen in *apl2*Δ cells are not typical of Class III mutants but Class II vacuole mutants, which contain a single un-lobed vacuole. Thus, while the observation of a defect in vacuole morphology in the *apl2*Δ phenotype has not been observed before, the phenotype can possibly be attributed to the Class II vacuole inheritance mutants (Weisman, 2003).

Sel1p in *S. cerevisiae* as in *S. pombe* has been shown to interact with Cdc48p, an ATPase involved in membrane fusion, protein transport and protein degradation (Hartmann-Petersen et al., 2004; Schuberth et al., 2004). Sel1p contains an ubiquitin regulatory X domain (UBX), an ubiquitin-associated domain (UBA), an ubiquitin interaction motif (UIM) and a domain of unknown function that is found in several UBX domain containing proteins. The identification of a defect in vacuole morphology in *sel1*Δ in *S. cerevisiae* has not been observed before, however unlike the defect seen in *apl2*Δ cells, *sel1*Δ mutant cells do not have enlarged vacuoles and therefore do not fall into any class of vacuole inheritance mutants previously described (Weisman, 2003).

The observation that *vma6*Δ cells have a defect in vacuole morphology has not been described before. These cells contain enlarged vacuoles but were not as large as *fab1*Δ cells, however from observations with other *Vma* mutants, it was expected that *vma6*Δ cells would display this phenotype (Odorizzi et al., 1998).

We have found a number of proteins that not only interact with Fab1p by yeast two-hybrid analysis but whose corresponding deletion mutants have phenotypes co-incidental with those displayed by a *fab1*Δ strain (Table 4.5). These are potentially good candidates to be effectors/regulators of Fab1p. Furthermore, the identification of 8 potential effectors/regulators of Fab1p, confirms that our approach to investigating Fab1p biology was valid. We thus decided that Apl2p would be chosen for further study.

The reason for choosing Apl2p was firstly based on the evidence that Vac14p was found to interact with Apl4p (Dove et al., 2002). Vac14p is essential for the synthesis of PtdIns(3,5)P_2 by Fab1p, trafficking Phm5p and CPS to the vacuole lumen and for correct vacuole morphology and acidity (Dove et al., 2002). *vac14*Δ cells are phenotypically identical to *fab1*Δ cells thus it is likely that Vac14p is a universal activator of Fab1p (Dove et al., 2002). Apl4p is the γ-adaptin subunit of the AP-1 complex (Yeung et al., 1999). As we have identified Apl2p, the β-adaptin subunit of the AP-1 complex as a potential interactor with Fab1p, these data reinforce the hypothesis that the AP-1 complex is required for some aspect of Fab1p biology.

Secondly, the AP-1 complex and the adaptins in general have been relatively well studied to date (Yeung et al., 1999, Boehm et al., 2001, Boehm et al., 2002, Valdivia et al., 2002): therefore there is functional and structural information known about this complex. The information known about AP-1 and the data gathered from these phenotypic analyses make Apl2p an excellent candidate to study as a potential effector/interactor with Fab1p.

5 APL2P AND THE AP-1 COMPLEX

5.1 Introduction

As stated in the previous chapter, the β-subunit of AP-1, Apl2p was chosen as a potential regulator/effector with Fab1p on the strength of the phenotypic analyses carried out in this study and also on the evidence that, the γ-subunit of AP-1, Apl4p interacts with Vac14p, a known regulator of Fab1p (Dove et al., 2002). Our phenotypic analyses have revealed that Apl2p is required for trafficking the integral membrane proteins GFP-Phm5p and GFP-CPS to the vacuole lumen, a process that also requires Fab1p (Sections 4.4.2.2 and 4.4.3.2). Furthermore, Apl2p is required for correct vacuole morphology (Section 4.4.5.2). Deletion of *APL2* does not cause defects in vacuole acidification nor does it abolish growth at 37 °C. These data suggest that AP-1 is required for some, but not all Fab1p-dependant functions.

Apl2p is the β-subunit of the *S. cerevisiae* AP-1 adaptor complex that acts in concert with 3 other subunits to effect adaptin mediated clathrin coat assembly and cargo recruitment at the TGN (Schroder and Ungewickell, 1991; Valdivia et al., 2002). The other subunits of the AP-1 heterotetramer are: the γ-subunit, Apl4p; the μ-subunit, either Apm1p or Apm2p and; the σ-subunit, Aps1p (Figure 5.1). There are two possible μ-subunits. Apm2p has been shown to interact with Apl4p and it displays homology to Apm1p however Apm2p cannot complement for Apm1p in *apm1Δ* cells suggesting an alternative AP-1 complex lacking Apm1p exists in yeast (Stepp et al., 1995; Yeung et al., 1999). Therefore in considering Apl2p as a potential regulator/effector of Fab1p, it was decided to investigate whether the other subunits of the AP-1 complex were involved in Fab1p function.

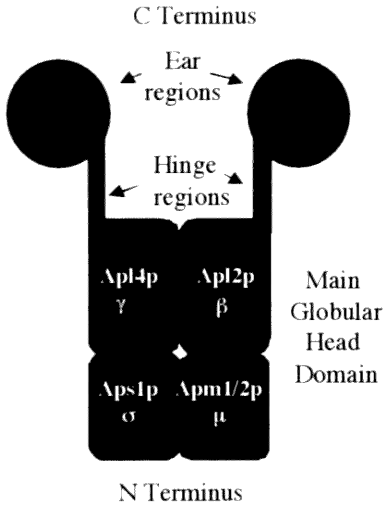

Figure 5.1. Schematic arrangement of the AP-1 complex components in *S. cerevisiae*. The complex consists of a main globular head domain comprising two large subunits Apl4p (γ) and Apl2p (β) (90-130kDa), one medium subunit Apm1p/Apm2p (μ) (~50kDa) and a small subunit Aps1p (σ) (~20kDa). This core is attached to two small globular ear regions via protease sensitive hinge regions (Schroder and Ungewickell, 1991).

5.2 The AP-1 complex is part of a large well-conserved family of adaptins

In eukaryotic cells, transport vesicles mediate protein transport between membrane-bound organelles e.g. the TGN, PVC/vacuole and the plasma membrane (Schmid, 1997). Targeted proteins use these vesicles as transporters to access various compartments, where they can undergo post-translational modifications, degradation, mediate signal transduction or a variety of other functions. Adaptins are molecules that co-ordinate targeted cargo recruitment to transport vesicles, providing a structural bridge between cargo and coat proteins, typically clathrin (Robinson, 2004). The term adaptin was originally used to describe a group of ~100kDa proteins that co-fractionated with clathrin during the purification of clathrin coated vesicles from pig brain (Pearse, 1975). Further work identified these proteins as two related AP complexes, termed AP-1 and AP-2 that associate with clathrin in mammalian cells (Keen, 1987; Pearse and Robinson, 1984). Both complexes share very similar component topology but differ in terms of cellular distribution: AP-1 localises to the TGN and endosomes (Robinson, 1987), whereas AP-2 localises to the plasma membrane (Ahle et al., 1988). By using platinum-shadowing (an electron microscopy method) the mammalian AP-2 complex has two small globular appendages attached to a large globular core via a protease sensitive flexible linker region (Heuser and Keen, 1988; Kirchhausen et al., 1989). Similarly by proteolysis experiments and subunit sequence similarities the AP-1 complex was found to have a similar structure (Schroder and Ungewickell, 1991). The AP acronym used to describe these complexes originally referred to "assembly polypeptides" (Zaremba and Keen, 1983) however the term "adaptor proteins" is now widely accepted.

In recent years, as a consequence of genome sequencing initiatives, two new AP complexes have been identified: AP-3 and AP-4. Both have similar subunit structure and topology to the AP-1 and AP-2 complexes (Dell'Angelica et al., 1999; Dell'Angelica et al., 1997) and both AP-3 and AP-4 associate with the TGN. Thus 4 adaptor complexes exist in eukaryotic cells to help mediate the large volume of post-TGN trafficking events in cells (Boehm and Bonifacino, 2002) (Figure 5.2).

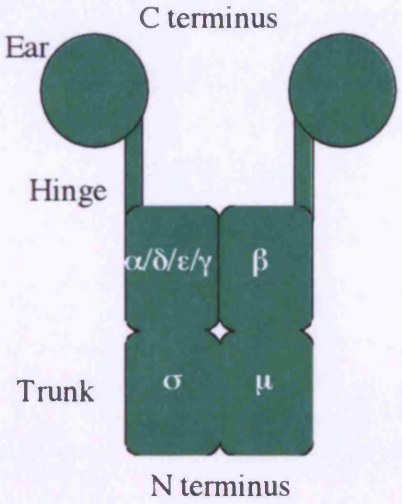

Figure 5.2. Schematic diagram of a generic AP complex identified from eukaryotes. Complexes comprise a large globular core that is attached to small globular ear appendages via hinge regions. The β- and γ-subunits are the most divergent with ~ 30% sequence similarity whereas μ- and σ-subunits share approximately 50% sequence similarity. The β regions share ~ 90% homology to each other and may be interchangeable (Kirchhausen, 1999; Schmid, 1997).

The four AP complexes have high homology to one another with 21-83% identity at the amino acid level (Boehm and Bonifacino, 2001). AP-1, AP-2 and AP-3 are expressed in all eukaryotic cells examined to date, whereas AP-4 is found in man (*Homo sapiens*), mouse (*Mus musculus*), chicken (*Gallus gallus*), and the plant *Arabadopsis thaliana,* but not in the fruit fly (*Drosophila melanogaster*), the nematode (*Caenorhabditis elegans*) nor the yeasts *S. cerevisiae* and *S. pombe* (Table 5.2).

Adaptins	*H. sapiens*	*M. musculus*	*A. thaliana*	*D. melanogaster*	*C. elegans*	*S. cerevisiae*	*S. pombe*
AP-1							
Large Subunit	γ1, γ2, β1	γ1, γ2, β1	γ-I-III β1/2-I-III	γ, β1/2	γ, β1/2	γ β1	γ β1
Medium Subunit	μ1A, μ1B	μ1A, μ1B	μ1	μ1	μ1-1, μ1-II	μ1-1, μ1-II	μ1
Small Subunit	σ1A, σ1B σ1C	σ1A, σ1B σ1C	σ1-I, σ1-II	σ1	σ1	σ1	σ1
AP-2							
Large Subunit	α1,α2,β2	α1,α2.β2	α β1/2-I-III	α, β1/2	α, β1/2	α β2	α, β2
Medium Subunit	μ2	μ2	μ2	μ2	μ2	μ2	μ2
Small Subunit	σ2	σ2	σ2	σ2	σ2	σ2	σ2
AP-3							
Large Subunit	δ, β3A,β3B	δ, β3A, β3B	δ, β3	δ, β3	δ, β3	δ, β3	δ, β3
Medium Subunit	μ3A, μ3B	μ3A, μ3B	μ3	μ3	μ3	μ3	μ3
Small Subunit	σ3A, σ3B	σ3A, σ3B	σ3	σ3	σ3	σ3	σ3
AP-4							
Large Subunit	ε β4	ε β4	ε β4	not found	not found	not found	not found
Medium Subunit	μ4	μ4	μ4				
Small Subunit	σ4	σ4	σ4				

Table 5.2. The distribution of adaptins among eukaryotes. Human and mice AP-1 complex contain two γ-subunits, two μ-subunits, one β-subunit and three σ-subunits. Existence of two or more genes for these subunits is believed to result from alternative gene splicing (Boehm and Bonifacino, 2001).

Of the three AP complexes in *S. cerevisiae* only AP-1 binds to and interacts with clathrin (Yeung and Payne, 2001). It is likely that AP-2 and AP-3 function in a clathrin independent manner as deletions of AP-2 and AP-3 do not exhibit any genetic interactions with the temperature-sensitive clathrin heavy chain mutant, *chc1*^{ts} (Phan et al., 1994; Rad et al., 1995; Stepp et al., 1995). Deletion of AP-3 components do however cause distinct phenotypes: the vacuolar transmembrane protein alkaline phosphatase (ALP) accumulates in cytoplasmic vesicles and tubules and the vacuolar t-SNARE Vam3p mislocalises to the vacuole, whereas trafficking of CPY and CPS to the vacuole remains unaffected (Cowles et al., 1997a; Stepp et al., 1997). Hence strains with deletions of AP-3 components appear to be defective in the clathrin-independent targeting of ALP to the vacuole (Boehm and Bonifacino, 2002; Cowles et al., 1997a). In *S. cerevisiae* the function of AP-2 has been investigated but component gene deletions reveal no effects on endocytosis or any other protein trafficking steps (Munn, 2001). Thus the role of AP-2 in yeast remains equivocal.

5.3 Overview of AP-1 complex formation with clathrin

The formation of clathrin transport vesicles involves the construction of a proteinaceous coat consisting of an outer polyhedral lattice of clathrin, comprising trimers of clathrin heavy chain (Chc) and clathrin light chains (Clc), and an inner layer of heterotetrameric adaptor protein (AP) complexes (Figure 5.3). The clathrin lattice envelops a layer of AP molecules that forms a bridge between the lattice and the vesicle membrane (Hirst and Robinson, 1998; Rad et al., 1995; Robinson, 2004). This mediated assembly of clathrin by the AP-1 complex occurs at the cytoplasmic surface of a donor organelle membrane where cargo molecules have been targeted for transport. AP-1 mediates both the recruitment of clathrin to organelle membranes and recognition of trafficking signals within the cytosolic tails of transmembrane cargo molecules (Bonifacino and Dell'Angelica, 1999). When the clathrin/AP complex scaffolding is in place on the cytoplasmic surface, a vesicle containing cargo for transport can bud from the membrane into the clathrin pit. After vesicle release from the donor membrane, clathrin coat disassembly occurs by a process that requires ATP hydrolysis (Greene and Eisenberg, 1990) and the vesicle travels to the acceptor membrane where fusion and delivery of the cargo occurs (Robinson, 2004).

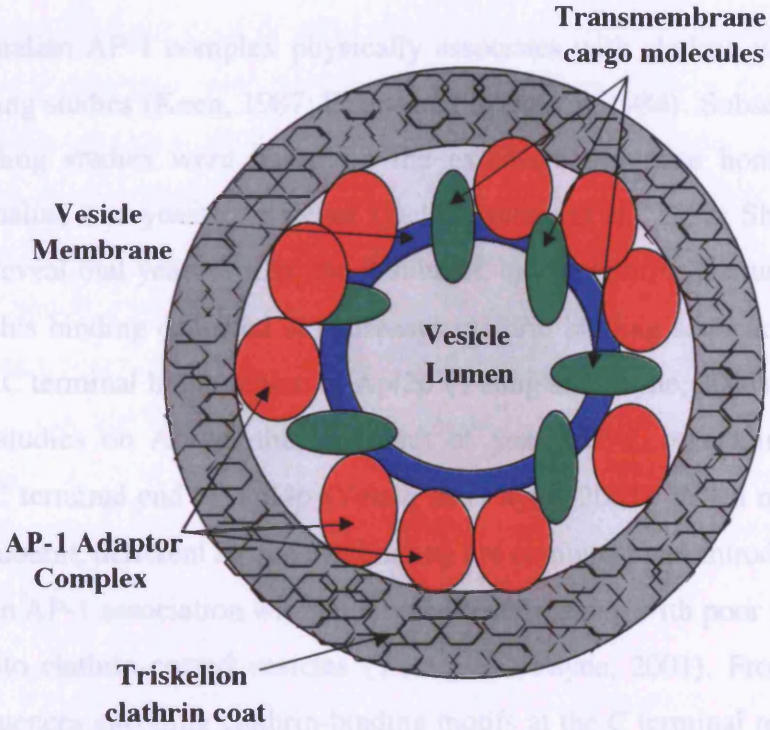

Figure 5.3. A diagrammatic representation of an AP-1/clathrin coated vesicle. Clathrin coated vesicles have two coats, the outer consists of triskelions of clathrin formed into a polyhedral lattice and the inner consists of a layer of AP-1 adaptor molecules. These adaptor molecules bind to transmembrane cargo molecules thus facilitating a connective link between clathrin and integral membrane proteins destined for transport. (Diagram adapted from Genes VII by Benjamin Lewin).

5.4 *S. cerevisiae* AP-I complex interacts physically and genetically with clathrin

5.4.1 AP-1 interacts physically with clathrin

That the mammalian AP-1 complex physically associates with clathrin was evident from very early binding studies (Keen, 1987; Pearse and Robinson, 1984). Subsequent yeast AP-1 clathrin binding studies were based on the extensive sequence homology observed between mammalian and yeast complexes (Dell'Angelica et al., 1998; Shih et al., 1995). Investigations reveal that yeast Apl2p, the β-subunit, binds clathrin [Gallusser, 1993 #484] and moreover this binding occurred at consensus clathrin binding sequences (LLDLF and LLDFD) at the C terminal hinge region of Apl2p (Yeung and Payne, 2001). Furthermore *in vitro* deletion studies on Apl4p, the γ-subunit of yeast AP-1, reveal interactions with clathrin at the C terminal end of Apl4p (Yeung and Payne, 2001). When mutants of the β-subunit and γ-subunit, deficient in clathrin binding are combined and introduced into yeast, severe defects in AP-1 association with membranes occur, along with poor incorporation of the complex into clathrin-coated vesicles (Yeung and Payne, 2001). From this it would appear that sequences encoding clathrin-binding motifs at the C terminal regions of Apl2p and Apl4p are instrumental in the binding of clathrin to promote AP-1/clathrin mediated protein transport.

Concomitant with binding clathrin, is the ability of AP-1 to target specific proteins destined for transport to various cellular compartments for downstream processing. Initial studies with vesicles isolated from calf brain suggest that Apl2p, the β-subunit is important in protein targeting as it interacts with a dileucine motif-sorting signal found in some transmembrane proteins thus promoting sequestration of vesicle cargoes in coated vesicles (Rapoport et al., 1998). Further characterisation of AP-1 protein targeting capabilities also reveal that yeast Apm1p, the μ-subunit recognises tyrosine-based signals in several integral membrane proteins thus mediating clathrin dependent trafficking (Ohno et al., 1995).

5.4.2 AP-1 interacts genetically with clathrin

Systematic genetic deletional analysis of *APL2*, *APL4*, *APM1*, *APM2* and *APS1* yields no obvious phenotypes in *S. cerevisiae* (Phan et al., 1994; Rad et al., 1995; Stepp et al., 1995; Yeung et al., 1999) prompting the suggestion that there are other factors contributing to adaptor functioning in the absence of AP-1 complex components. However, combined AP-1 component gene deletions with the temperature sensitive clathrin heavy chain allele (*chc1^{ts}*) compromise growth at the restrictive temperature of 37 °C (*chc1^{ts}* cells grow poorly at 37 °C) (Phan et al., 1994; Rad et al., 1995; Yeung et al., 1999). Mutant strains *chc1^{ts}/apm1*Δ and *chc1^{ts}/apl2*Δ fail to grow at 37 °C whereas the growth of *chc1^{ts}/aps1*Δ and *chc1^{ts}/apl4*Δ is limited when compared with *chc1^{ts}* cells, suggesting that loss of *APM1* and *APL2* is more deleterious to growth of *chc1^{ts}* cells than the loss of the *APS1* and *APL4*. Likewise, deletion of the AP-1 complex (*apl-1-null*) and analysis in *chc1^{ts}* cells inhibits growth completely at 37 °C (Yeung et al., 1999). Thus AP-1 complex component deletion mutants in combination with the *chc1^{ts}* allele, exhibit severe growth defects suggesting that clathrin plays an important role in AP-1 function (Yeung et al., 1999).

Similarly, AP-1 complex component deletion mutants in combination with the *chc1^{ts}* allele also exhibit protein-trafficking defects (Phan et al., 1994; Rad et al., 1995; Yeung et al., 1999). Yeast deficient in the clathrin heavy chain (*chc*) secrete a precursor form of the α-factor peptide-mating pheromone (Payne and Schekman, 1989). In wild-type cells, processing of the precursor α-factor is carried out by the endopeptidase Kex2p at the TGN (Redding et al., 1996). Kex2p cycles between this compartment and endosomes (Brickner and Fuller, 1997; Redding et al., 1991). In cells expressing a defective clathrin heavy chain, Kex2p mislocalises to the plasma membrane and a highly glycosylated precursor form of the α-factor is secreted (Payne and Schekman, 1989). Thus the mislocalisation of Kex2p to the plasma membrane and the depletion of Kex2p at the TGN prevent full maturation of the α-factor in this compartment. Analysis of AP-1 complex component deletion mutants in *chc1^{ts}* cells at 25 °C and 30 °C reveal slight α-factor maturation defects in *chc1^{ts}/aps1*Δ and *chc1^{ts}/apl4*Δ strains and severe defects in *chc1^{ts}/apm1*Δ and *chc1^{ts}/apl2*Δ strains. Simultaneous missorting of the endopeptidase Kex2p accompanied these α-factor

maturation defects in these cells indicating a role for AP-1 in Kex2p retrieval to the TGN in *chc1*^{ts} cells (Phan et al., 1994; Rad et al., 1995; Yeung et al., 1999).

In *chc1*^{ts} cells, the soluble hydrolase carboxyeptidase Y (CPY) exhibits a severe defect in trafficking to the vacuole at 37 °C but not 24 °C; however, after prolonged periods at the restrictive temperature trafficking ability is regained (Rad et al., 1995). In wild type and *chc1*^{ts} cells at 24 °C, the 67 kDa precursor CPY is synthesised and translocated to the ER where it undergoes signal sequence cleavage and core glycosylation (Stevens et al., 1982). From the ER, the modified CPY 67 kDa p1 precursor is transported to the TGN where it undergoes addition of mannose residues to yield the CPY 69 kDa p2 form. From here the p2 form proceeds to the vacuole via the PVC where it undergoes proteolysis to the active mature form of the protein (Vida et al., 1993). However in *chc1*^{ts} cells at 37 °C, the p2 precursor does not proceed to the vacuole and is secreted into the culture medium (Seeger and Payne, 1992). Investigation of CPY trafficking in *chc1*^{ts}*/apl2Δ/aps1Δ* cells revealed that nearly 75% of CPY was detected in the mature active form in contrast to 34% mature CPY in *chc1*^{ts} cells thus implying trafficking of CPY in *chc1*^{ts}*/apl2Δ/aps1Δ* cells is less severely disrupted than trafficking in *chc1*^{ts} cells (Rad et al., 1995).

Further genetic studies reveal a "retention mechanism" for AP-1 in a set of late TGN membrane proteins (Valdivia et al., 2002). In wild-type cells, the chitin synthase III, Chs3p cycles between the TGN and early endosomes and distributes to the plasma membrane. This trafficking is altered in *chs6Δ* cells; Chs3p becomes trapped at the TGN/early endosomes preventing the protein from trafficking to the plasma membrane (Ziman et al., 1998). This defect is overcome when AP-1 component genes are disrupted in the *chs6Δ* background. Using the fluorescent dye calcofluor, which interacts with chitin, this defect can be monitored in growth and microscope assays (Valdivieso et al., 1991). *chs6Δ* cells are growth resistant to calcofluor whereas deletion of AP-1 complex components in *chs6Δ* cells restores growth sensitivity to this dye. Simultaneous expression of GFP-Chs3p in *chs6Δ* cells reveals accumulation of the fusion protein in large punctate structures consistent with a TGN location whereas in AP-1 mutants in combination with *chs6Δ* this staining became more diffuse and less punctate (Valdivia et al., 2002). Furthermore subcellular fractionation

demonstrates that *chs6Δ/apl2Δ* cells restore localisation of Chs3p to the plasma membrane. Thus when Chs3p transport to the PM is blocked in *chs6Δ* cells, retention at the TGN/early endosome appears to require the function of AP-1 (Valdivia et al., 2002).

The soluble N-ethylmaleimide sensitive factor-attachment protein receptor (SNARE) Tlg1p is involved in several different functions in the secretory pathway including endocytosis and recycling of endocytosed proteins and lipids (Coe et al., 1999; Holthuis et al., 1998). In *sec6-4^{ts}* mutants, which accumulate transport vesicles at the restrictive temperature, subcellular fractionation reveal that 15-20% Tlg1p accumulates in dense vesicle fractions whereas in *sec6-4^{ts}/apm1Δ* cells, ~70% Tlg1p accumulates in dense vesicle fractions. Similarly in *end4-1^{ts}* mutants, which are deficient in endocytosis at the restrictive temperature, 5-10% Tlg1p accumulates in plasma membrane fractions whereas in *end4-1^{ts}/apm1Δ* cells, 25-30% of Tlg1p accumulates in similar fractions (Valdivia et al., 2002). These data suggest that Tlg1p mislocalises to various dense membrane fractions in AP-1 deficient cells (Valdivia et al., 2002).

Thus several studies indicate that the *S. cerevisiae* AP-1 complex interacts both physically and genetically with clathrin. Evidence suggests that at least some AP-1 functions will require binding of AP-1 to clathrin to mediate aspects of protein transport in yeast, probably the retention of proteins at the TGN by retrieval from the secretory/endosomal trafficking pathways (Valdivia et al., 2002).

5.5 AP-1 Component Phenotypic Analysis Results

As stated in the introduction to this chapter, *apl2Δ* cells exhibit similar phenotypes to *fab1Δ* cells in terms of GFP-CPS and GFP-Phm5p trafficking and vacuole morphology. However, as Apl2p is also a component of the heterotetrameric AP-1 complex, we studied all AP-1 complex component deletion mutants with respect to Fab1p function.

AP-1 complex component deletion mutants obtained from the Euroscarf deletion library (Section 4.3) were subjected to the following phenotypic analyses;

1) HPLC analysis of phosphoinositide complement including PtdIns(3,5)P_2

2) GFP-CPS trafficking

3) GFP-Phm5p trafficking

4) FM4-64 labelling for vacuole morphology

5) Quinacrine staining for Vacuole acidification

In addition, yeast two-hybrid analysis using the β-galactosidase reporter gene system was carried out to investigate physical interactions between Fab1p and the other subunits of the AP-1 complex. This assay is more sensitive than the *HIS3* growth assay used in the original screen.

5.5.1 LacZ assay on AP-1 subunits

In the yeast two-hybrid technique the LacZ gene reporter system is used to enzymatically assay for the production of the reporter gene β-galactosidase, indicating protein-protein interaction (Guarente, 1983). Strains expressing clones for each AP-1 subunit were mated to the strain expressing Fab1p and β-galactosidase activity assayed (Figure 5.5.1).

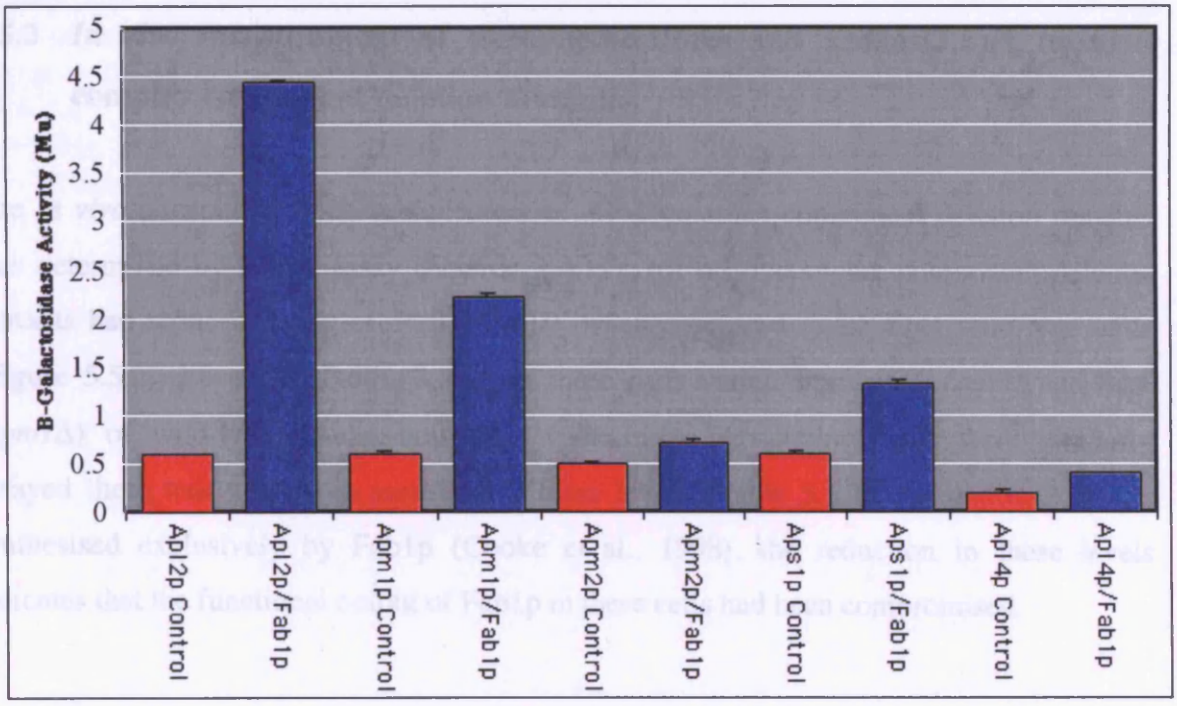

Figure 5.5.1. LacZ assay of Fab1p and AP-1 subunits using the yeast two-hybrid reporter gene β-galactosidase. Prey strains expressing each AP-1 subunit (red) and mated strains (blue) were assayed in triplicate for β-galactosidase activity (Section 2.4.4). β-galactosidase activity is given in arbitrary units. The increase in LacZ reporter gene activity in the bait and prey versus prey alone is indicative of an interaction between bait and prey.

Levels of β-galactosidase activity were greatest for cells expressing Apl2p and Fab1p supporting the premise that an interaction exists between these proteins. No other subunit of the AP-1 complex was identified from the initial yeast two-hybrid screen with Fab1p. The LacZ assay also reveals that one other AP-1 subunit appears to be interacting with Fab1p. Apm1p is one of the μ-subunits of the AP-1 complex and was not identified in the initial screen with Fab1p. This may have been due to Apm1p exhibiting weaker binding to Fab1p, and thus was below the level of detection of the original *HIS3* gene reporter growth assay. However, the more sensitive LacZ assay has detected a potential interaction. The remaining AP-1 complex subunits show only very weak interactions with Fab1p.

5.5.2 *In vivo* measurement of phosphoinositides and PtdIns(3,5)P_2 in AP-1 complex component deletion mutants.

The *in vivo* phosphoinositide complement of AP-1 complex component deletion mutants was determined by HPLC assay (Section 2.4.12). All AP-1 complex component deletion mutants had reduced levels of PtdIns(3,5)P_2 when compared to BY4741 wild-type cells (Figure 5.5.2). Levels of PtdIns(3,5)P_2 in these cells varied from 65% (*aps1*Δ) to 84% (*apm1*Δ) of wild-type levels; however, when other phosphoinositides were similarly assayed there was very little variation in these levels (Table 5.5.2). As PtdIns(3,5)P_2 is synthesised exclusively by Fab1p (Cooke et al., 1998), the reduction in these levels indicates that the functional output of Fab1p in these cells had been compromised.

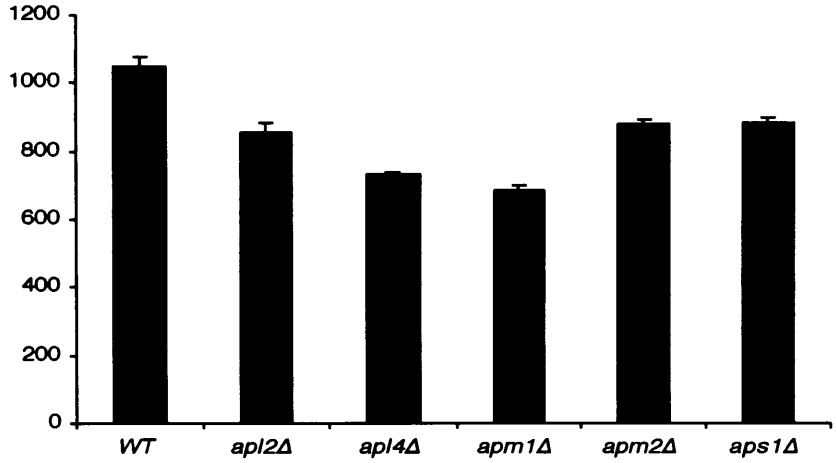

Figure 5.5.2. *In vivo* measurement of PtdIns(3,5)P_2 levels in AP-1 complex component deletion mutants. Mutants were labelled with [^{3}H]-inositol for 12-16 hours, killed, lysed and lipids extracted and deacylated. Lipid head groups were analysed by HPLC and peaks detected by liquid scintillation counting (Cooke et al., 1998; Dove et al., 1997; Stephens et al., 1991). Data on the vertical axis are shown as total counts per minute (cpm) incorporated into PtdIns(3,5)P_2 and error bars represent the s.e.m. (n=4).

Strain	PtdIns*3P*	PtdIns*4P*	PtdIns(3,5)P_2	PtdIns(4,5)P_2
BY4741	21402 ± 127	13932 ± 178	1049 ± 26	8100 ± 43
apl2Δ	17664 ± 176	14677 ± 239	855 ± 27	7659 ± 105
apl4Δ	17819 ± 146	13498 ± 152	731 ± 7	7741 ± 94
apm1Δ	22788 ± 160	12982 ± 243	687 ± 14	6910 ± 85
apm2Δ	19502 ± 147	13002 ± 147	877 ± 18	7704 ± 66
aps1Δ	21023 ± 262	15511 ± 91	884 ± 14	9156 ± 88

Table 5.5.2. Phosphoinositide levels in AP-1 complex component deletion mutants. Assayed levels of *in vivo* phosphoinositides remained static when compared to levels of *in vivo* PtdIns(3,5)P_2. [^{3}H]-PI levels were measured in 1.8 ml aliquots of cells labelled and analysed as described in the materials and methods. Data are given as total cpm and error bars represent the s.e.m. (n=4). All data were corrected to control PtdIns levels, which were: wild-type, 412,266 ± 2,928 cpm; *apl2Δ* 431,997 ± 5335 cpm; *apl4Δ* 406,500 ± 4,311 cpm; *apm1Δ* 287,527 ± 6,511 cpm; *apm2Δ* 320,379 ± 4,478 cpm; and *aps1Δ* 303,169 ± 3,342 cpm.

5.5.3 GFP-CPS trafficking in AP-1 complex component deletion mutants

GFP-CPS localises to the vacuole lumen in BY4741 wild-type cells whereas in *fab1*Δ cells, the protein traffics to the outer vacuole membrane (Odorizzi et al., 1998). As in *fab1*Δ cells, *apl2*Δ cells also traffic GFP-CPS to the outer vacuole membrane (Section 4.4.3.2). AP-1 complex component deletion mutants were assayed for GFP-CPS trafficking (Figure 5.5.3).

As in *fab1*Δ cells, *apl2*Δ, *apl4*Δ and *aps1*Δ cells clearly missorted GFP-CPS to the outer vacuole membrane. The trafficking defect of *apm1*Δ and *apm2*Δ cells was less transparent. There are two explanations for this: these are the two μ-subunits of the AP-1 complex and they may be partially redundant in function, thus deletion of both subunits may reveal a more pronounced GFP-CPS trafficking defect; alternatively, the wild-type vacuole morphology of these cells may have concentrated the GFP-CPS into a smaller volume making it difficult to define a clear phenotype.

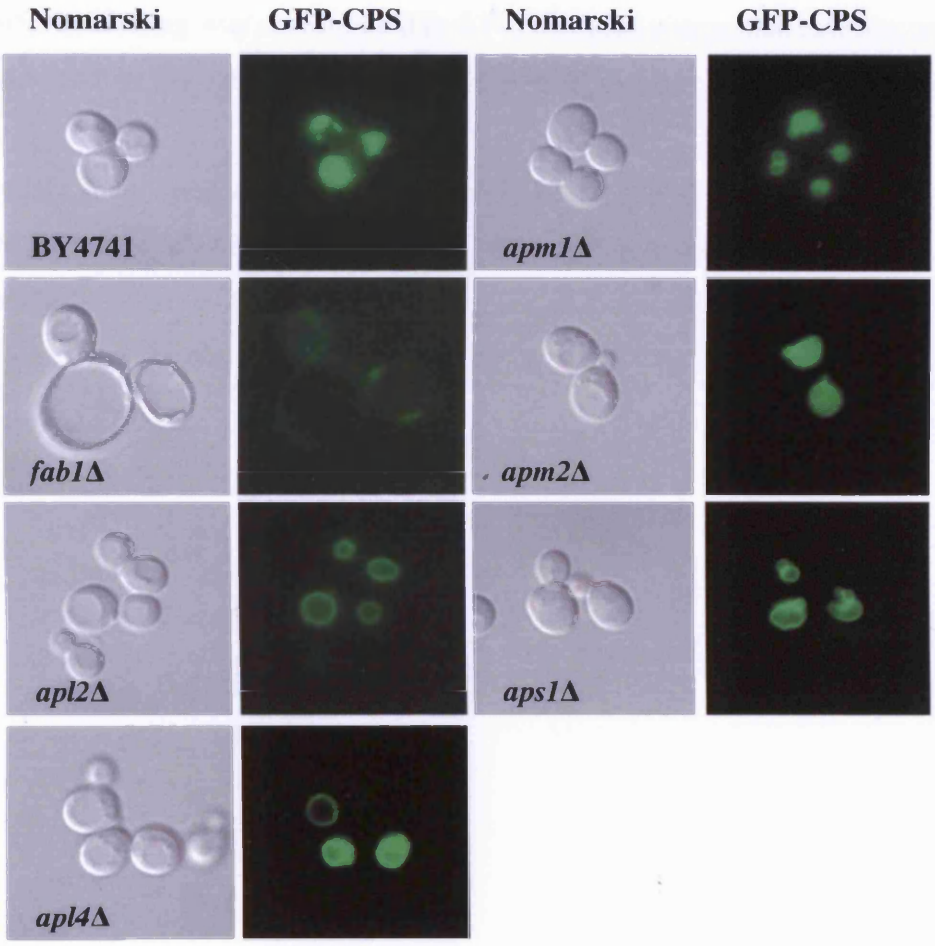

Figure 5.5.3. Trafficking of GFP-CPS in BY4741 wild-type, *fab1*Δ and AP-1 complex component deletion mutants. Cells were grown as described previously (Section 2.5.1). BY4741 wild-type and *fab1*Δ cells were included for comparison. All AP-1 complex component deletion mutants traffic GFP-CPS to the outer vacuole membrane.

5.5.4 GFP-Phm5p trafficking in AP-1 complex component deletion mutants

GFP-Phm5p traffics to the vacuole in a Fab1p-dependant manner (Dove et al., 2002). This cargo was found to stall at the outer vacuole membrane in *apl2*Δ cells (Section 4.4.2.2). GFP-Phm5p trafficking was investigated in AP-1 complex component deletion mutants and was found to stall at the outer vacuole membrane in all deletion strains (Figure 5.5.4).

As previously mentioned (Chapter 4, section 4.4.2.2), the expression of GFP-Phm5p in these cells altered cellular morphology. The GFP signal in some fields was extremely weak but nonetheless there is aberrant trafficking of GFP-Phm5p indicating that the AP-1 complex is required for the Fab1p-mediated trafficking of GFP-Phm5p.

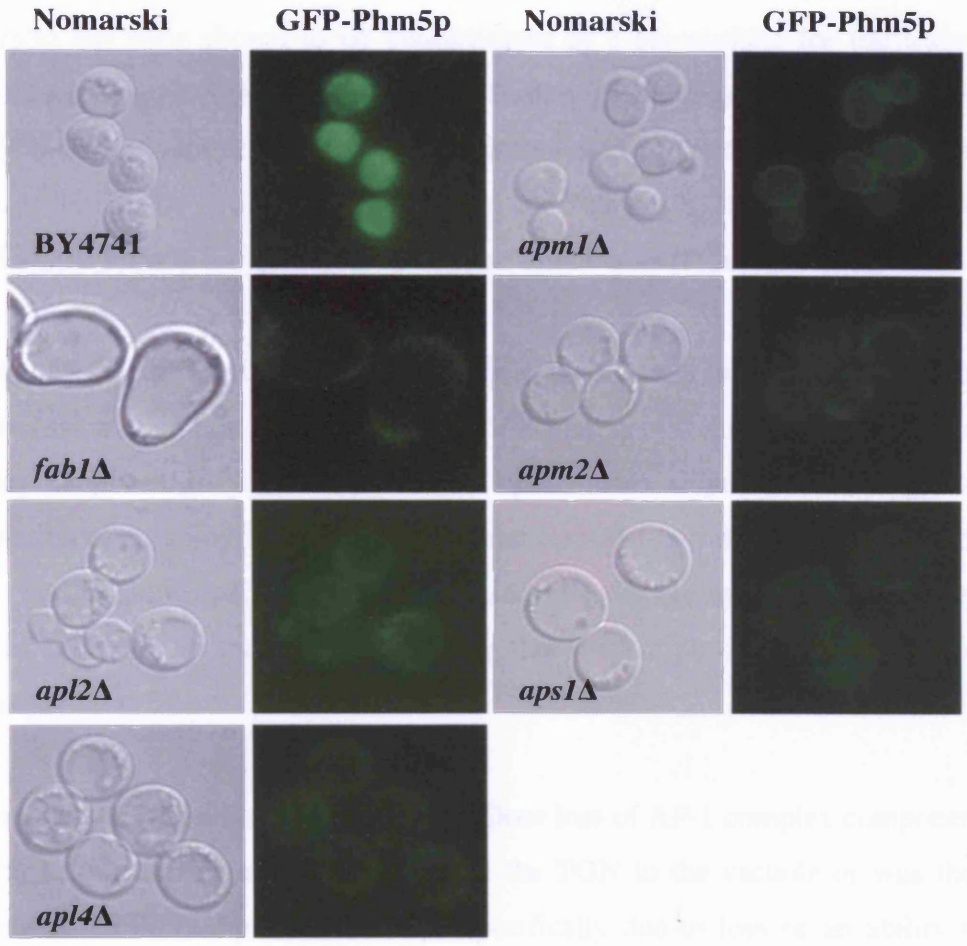

Figure 5.5.4. Trafficking of GFP-Phm5p in BY4741 wild-type, *fab1*Δ and AP-1 complex component deletion mutants. Yeast cells were grown as described previously (Section 2.5.1). BY4741 wild-type and *fab1*Δ cells were included for comparison. In all mutant AP-1 complex components deletion mutants GFP-Phm5p fails to traffic to the vacuole lumen.

5.5.5 Ub-GFP-Phm5p and GFP-Sna3p trafficking in AP-1 complex component deletion mutants

GFP-Phm5p has been shown to be ubiquitinated as a prerequisite for trafficking to the vacuole lumen (Reggiori and Pelham, 2001). Fusion of ubiquitin to the N-terminus of GFP-Phm5p (Ub-GFP-Phm5p) bypasses the requirement of Fab1p in trafficking of this protein to the vacuole lumen (Dove et al., 2002; Reggiori and Pelham, 2001). Therefore we decided to assess Ub-GFP-Phm5p trafficking in *apl2*Δ and *apl4*Δ cells (Figure 5.5.5a).

These data show that Ub-GFP-Phm5p traffics to the vacuole lumen in all cells examined. Therefore fusion of an ubiquitin sequence to GFP-Phm5p overcame the trafficking defect as previously observed in *fab1*Δ, *apl2*Δ and *apl4*Δ cells (Figure 5.5.4) suggesting that ubiquitination of cargo bypasses the requirement for AP-1 in trafficking GFP-Phm5p to the vacuole. Furthermore *apl2*Δ, *apl4*Δ and *fab1*Δ cells display an identical phenotype with respect to GFP-Phm5p trafficking indicating that they might be deficient in a common mechanism.

Our results also raise an important question. Does loss of AP-1 complex components cause disruption to the trafficking machinery from the TGN to the vacuole or was the altered trafficking of GFP-Phm5p and GFP-CPS specifically due to loss of an ability to traffic ubiquitinated cargoes? To test this, we assayed trafficking of the cargo, GFP-Sna3p. This protein was identified from vesicles derived from the PVC, functions in sodium ion uptake in cells and traffics to the vacuole lumen via the same pathway as GFP-CPS and GFP-Phm5p but in an ubiqiuitin and Fab1p-independent manner (Reggiori and Pelham, 2001) (Figure 5.5.5b).

GFP-Sna3p traffics to the vacuole lumen in all cells examined, indicating that the protein trafficking machinery from the TGN to the vacuole is intact in *apl2*Δ, *apl4*Δ and *fab1*Δ cells.

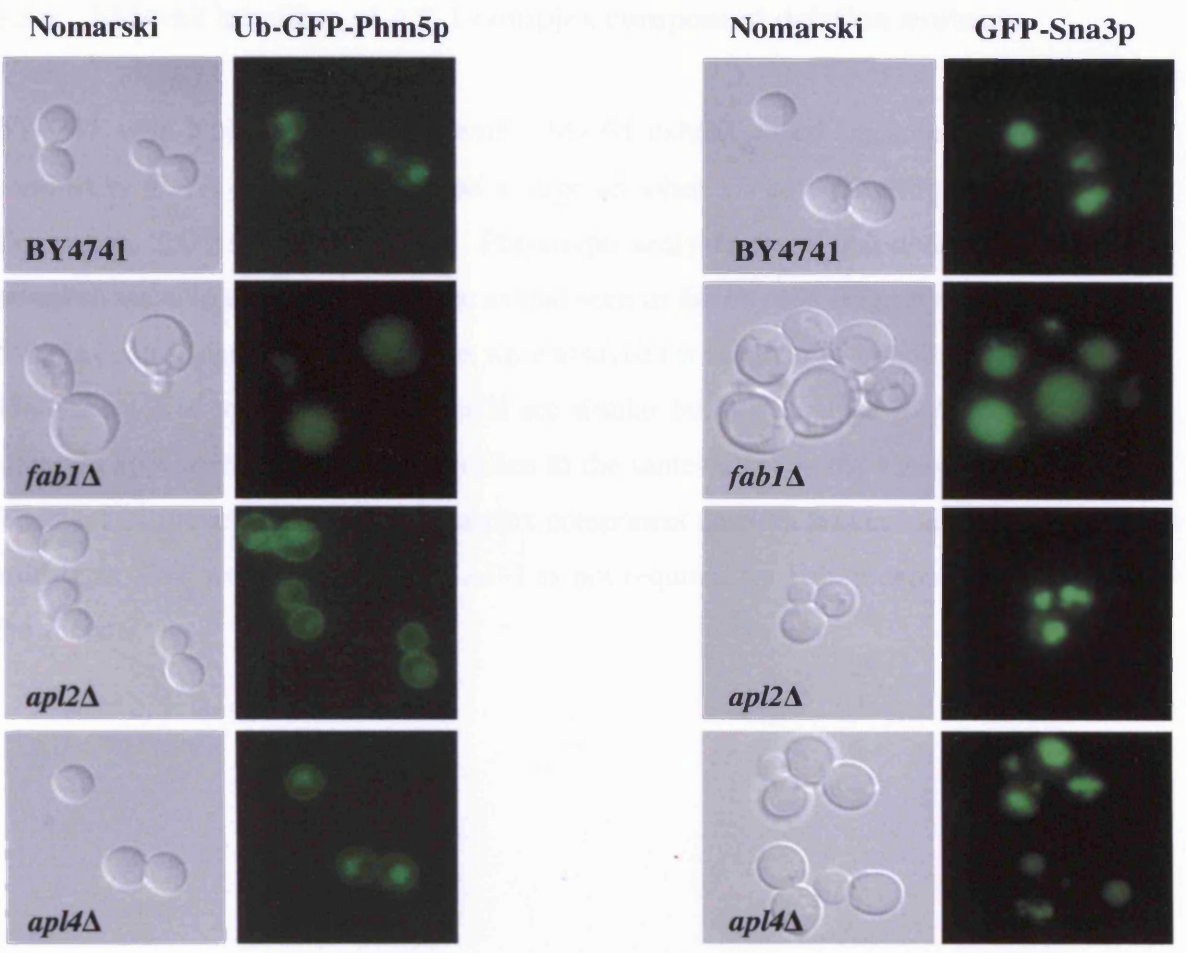

Figure 5.5.5a and 5.5.5b. Localisation of Ub-GFP-Phm5p (5.5.5a) and GFP-Sna3p (5.5.5b) in BY4741 wild-type, *fab1*Δ, *apl2*Δ and *apl4*Δ cells. Ub-GFP-Phm5p traffics to the vacuole lumen in all cells as does GFP-Sna3p in an ubiquitin-independent manner. Cells were grown as previously described (Section 2.5.1).

5.5.6 FM4-64 labelling of AP-1 complex component deletion mutants

BY4741 wild-type cells labelled with FM4-64 exhibit lobed vacuolar morphology, in contrast to *fab1*Δ cells which exhibit a large un-lobed vacuole (Bonangelino et al., 1997; Dove et al., 2002; Gary et al., 1998). Phenotypic analyses reveal that *apl2*Δ cells contain an un-lobed vacuole though not as large as that seen in *fab1*Δ cells (Figure 4.4.5.2). The AP-1 complex component deletion mutants were assayed for vacuolar morphology (Figure 5.5.6). The vacuoles of *apl2*Δ and *apl4*Δ cells are similar but not identical to *fab1*Δ cells. These vacuoles appear un-lobed but not swollen to the same extent as the vacuole of *fab1*Δ cells. Vacuoles of the remaining AP-1 complex component deletion mutants are multi-lobed and wild-type. This would suggest that AP-1 is not required for Fab1p dependant functions at the vacuole.

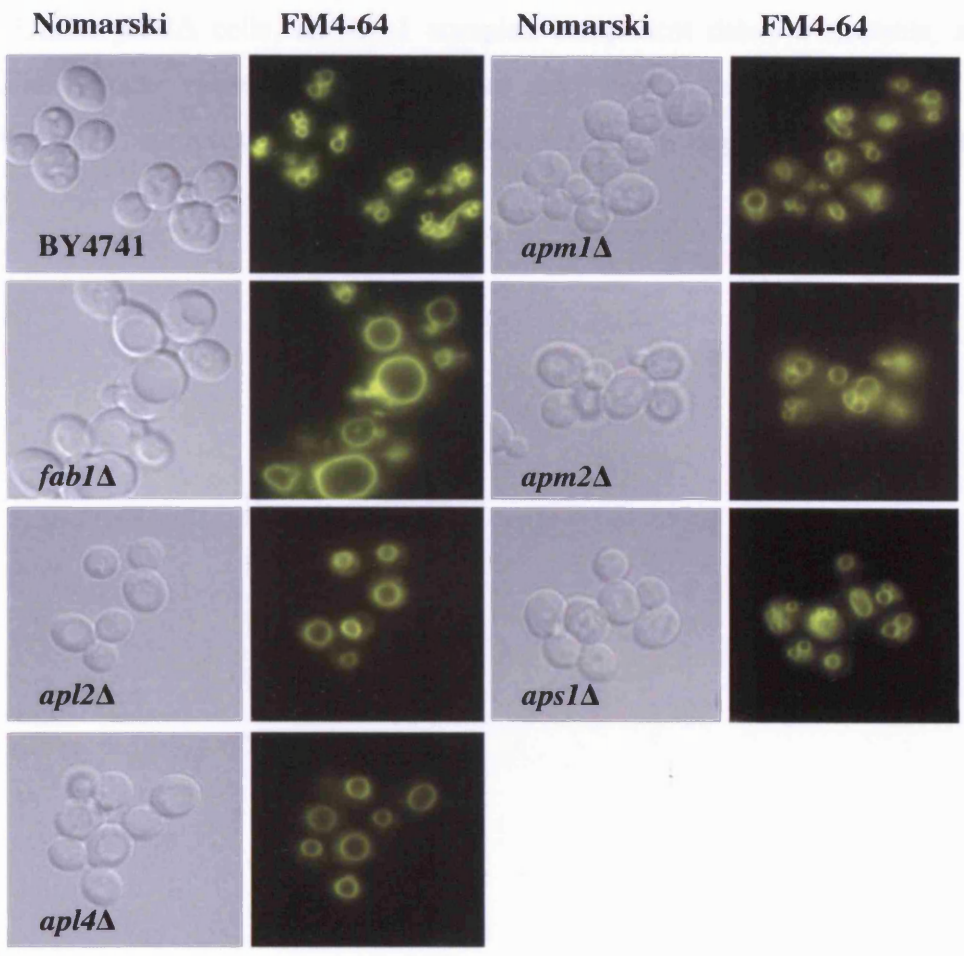

Figure 5.5.6. FM4-64 labelling in BY4741 wild-type, *fab1*Δ cells and AP-1 complex component deletion mutants. Yeast cells were grown as described previously (Section 2.5.3). Only *apl2*Δ and *apl4*Δ cells exhibit altered vacuole morphology. *apm1*Δ, *apm2*Δ and *aps1*Δ cells have a wild-type vacuole morphology.

5.5.7 Quinacrine staining of AP-1 complex component deletion mutants

*fab1*Δ cells do not accumulate quinacrine indicating a poorly acidified vacuole (Figure 4.4.4.1) whereas *apl2*Δ cells contain a wild-type acidified vacuole (Figure 4.4.4.2). All AP-1 complex component deletion mutants were assayed for vacuole acidification (Figure 5.5.7). Unlike *fab1*Δ cells, all AP-1 complex component deletion mutants, accumulate quinacrine in their vacuoles suggesting that these compartments are properly acidified. Thus the AP-1 complex is not required for the Fab1p dependant acidification of the vacuole.

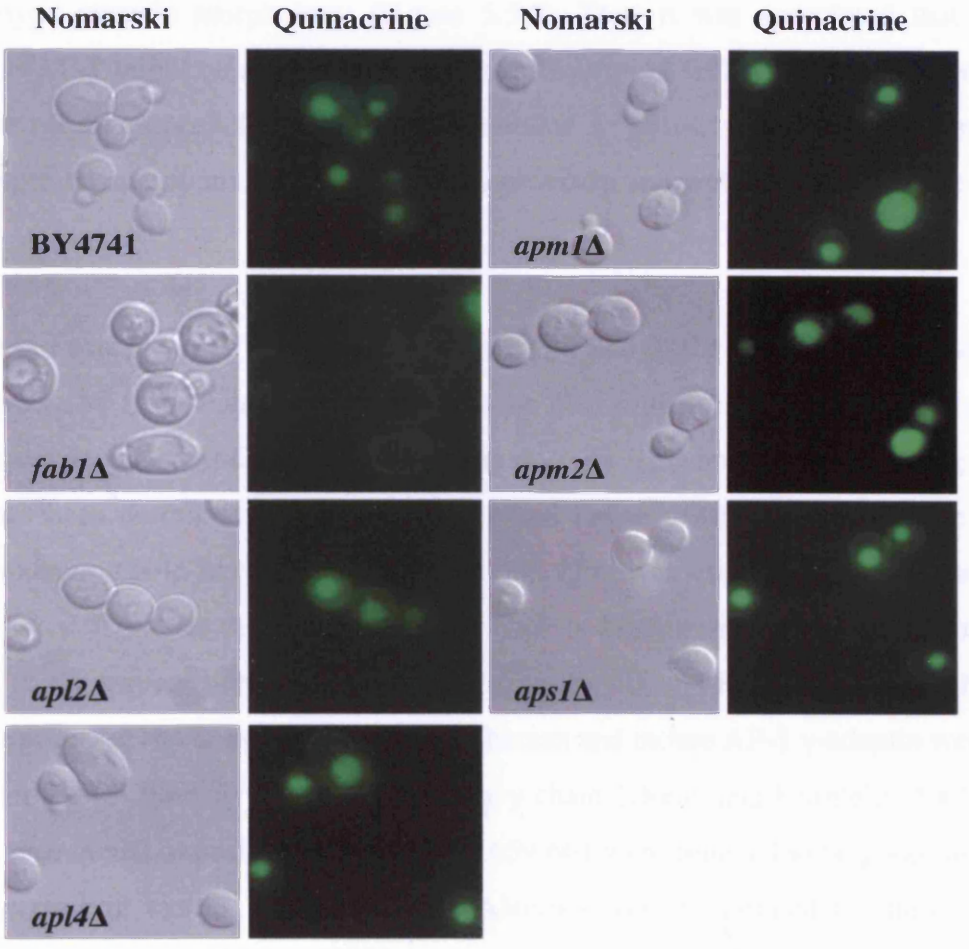

Figure 5.5.7. Quinacrine staining in BY4741 wild-type, *fab1*Δ cells and AP-1 complex component deletion mutants. Yeast cells were grown and stained as previously described (Section 2.5.2). BY4741 wild-type and *fab1*Δ cells were included for comparison. Unlike *fab1*Δ cells, all AP-1 complex component deletion mutant vacuoles are correctly acidified

5.6 Generation of non-clathrin binding mutants of Apl2p and Apl4p

Apl2p and Apl4p bind clathrin (Gallusser and Kirchhausen, 1993; Yeung and Payne, 2001; Yeung et al., 1999) to mediate recruitment of cargo to clathrin coated vesicles at the TGN (Schroder and Ungewickell, 1991). In this study both Apl2p and Apl4p are required for GFP-CPS trafficking to the vacuole lumen (Figure 5.5.3) and important in the maintenance of wild-type vacuole morphology (Figure 5.5.6). Thus it was speculated that clathrin binding to AP-1 might be required for correct trafficking of GFP-CPS and maintenance of wild-type vacuole morphology. As clathrin mutants are severely growth compromised we addressed this issue by making point mutants of Apl2p and Apl4p that are unable to bind clathrin.

Site directed mutagenesis was carried out on *APL2* and *APL4* (Section 2.6.8). Mutations were introduced into sequences predicted to be clathrin-binding sites of both genes to generate the mutants, *apl2-1* and *apl4-1* (Figure 5.6). The non-clathrin binding mutant, *apl2-1* has been described previously (Yeung and Payne, 2001) whereas precise clathrin binding sites in Apl4p have yet to be determined. However site directed mutagenesis was carried out on *APL4* on the strength that the clathrin binding sites were mapped to the C terminal of the protein between residues 609-678 (Yeung and Payne, 2001). Furthermore, dileucine motifs in the homologous region of human and mouse AP-1 γ-adaptin were found to be essential for binding to the clathrin heavy chain (Doray and Kornfeld, 2001). Thus, DLL clathrin motifs at positions 655-657 and 659-661 were believed to be good candidates to be the clathrin binding sites of Apl4p. Alanines were substituted for these clathrin-binding motifs in both *APL2* and *APL4* to generate *apl2-1* and *apl4-1* respectively (Figure 5.6). Western blotting indicated that both were expressed as full-length proteins and expression was similar to that of wild–type proteins (data not shown).

Thus these mutants allowed us to assess whether clathrin binding was required for GFP-CPS trafficking and the maintenance of vacuole morphology in *apl2*Δ and *apl4*Δ cells.

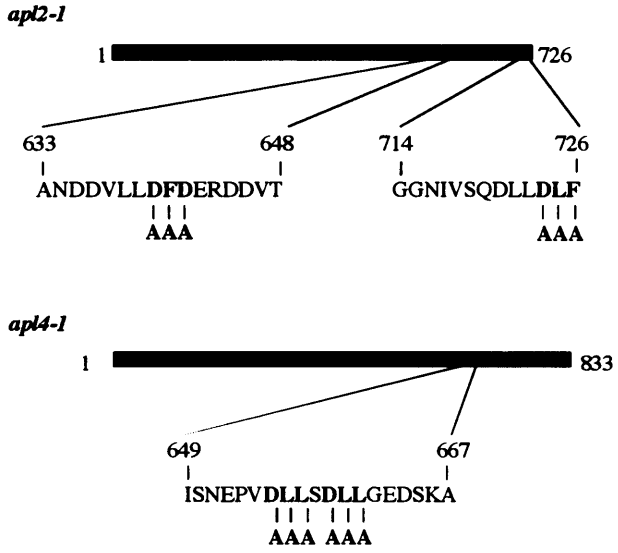

Figure 5.6. Site directed mutagenesis of *APL2* and *APL4* to generate *apl2-1* and *apl4-1* respectively. Clathrin binding motifs were mutated to alanines to abolish predicted clathrin binding sites in *APL2* and *APL4*. Mutants were generated by PCR on sub-cloned *APL2* and *APL4* in pCR®-Blunt (Invitrogen) using high fidelity *Pfu* and HPLC purified primers incorporating the mutated sequences (Section 2.6.8). Mutations were verified by restriction enzyme digestion and sequencing. *apl2-1* and *apl4-1* ORFs were then cloned into the expression vectors YCplac111Met(*apl2-1*) and pRS313Met(*apl4-1*) (Section 2.3).

5.6.1 GFP-CPS trafficking and wild-type vacuole morphology in *apl2Δ* cells expressing the non-clathrin binding mutant *apl2-1*

Plasmids (YCplac111Met) (Section 2.3) expressing *APL2*, *apl2-1* and an empty plasmid control were transformed into *apl2Δ* cells (Section 2.4.2). Empty plasmid was also transformed into BY4741 wild-type as a further control. To assay for trafficking, GFP-CPS was co-transformed into these strains. In a separate experiment cells were also labelled with FM4-64 (Figure 5.6.1)

The empty plasmid did not cause adverse effects on the expression and trafficking of GFP-CPS in the BY4741 wild-type strain and as expected GFP-CPS was found in the vacuole lumen; similarly this plasmid did not restore wild-type GFP-CPS trafficking in *apl2Δ* cells. In *apl2Δ* cells expressing *APL2*, GFP-CPS trafficking was restored to the vacuole lumen as expected. However, in *apl2Δ* cells expressing *apl2-1*, GFP-CPS stalled at the vacuole membrane.

As expected, FM4-64 staining of BY4741 wild-type cells expressing empty plasmid contained a wild-type multi-lobed vacuole whereas the vacuole of *apl2Δ* cells, similarly transformed, appeared largely un-lobed. As expected *apl2Δ* cells expressing *APL2* restored wild-type vacuole morphology however cells expressing *apl2-1* contained a large un-lobed vacuole.

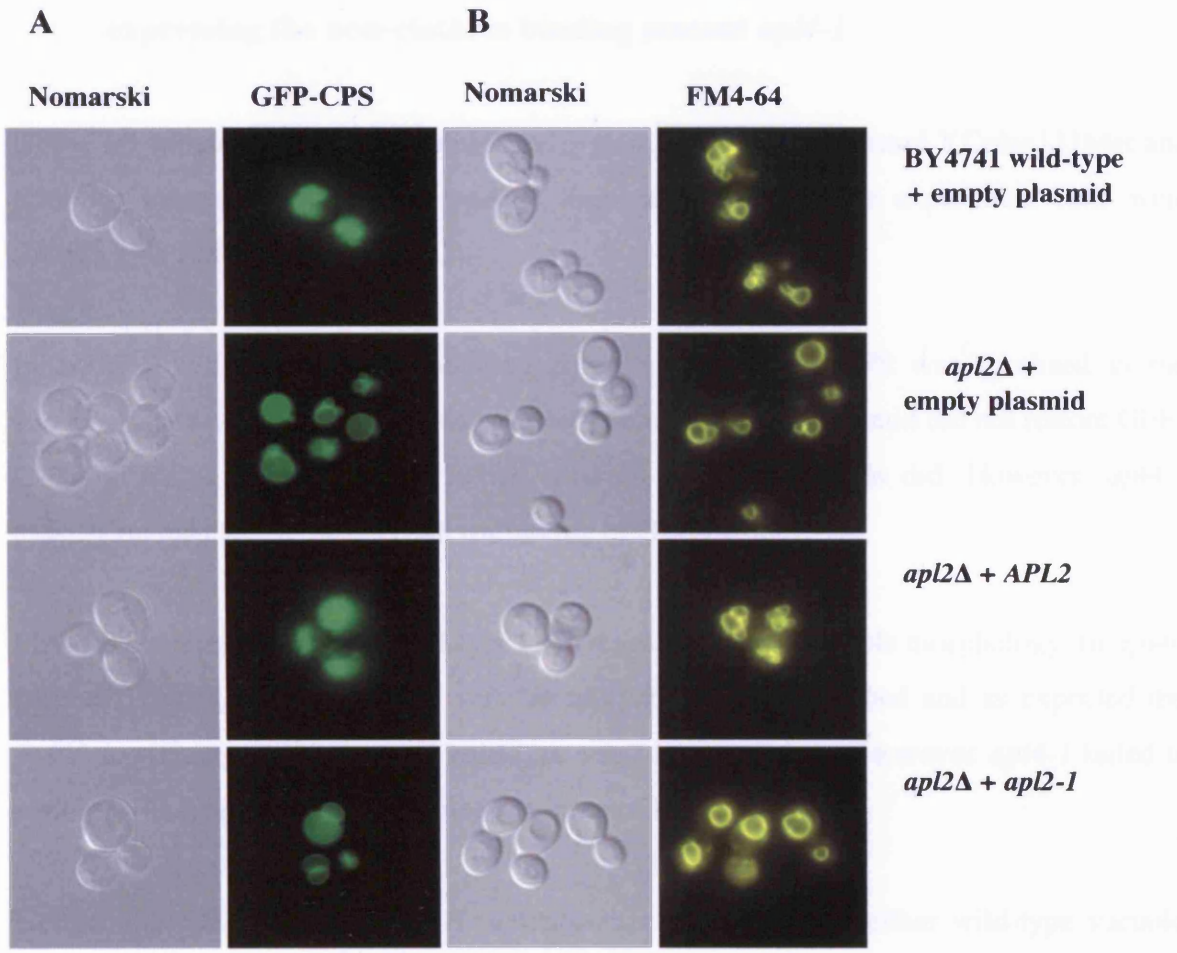

Figure 5.6.1. The non-clathrin binding mutant *apl2-1* displays aberrant trafficking of GFP-CPS and vacuole morphology in *apl2*Δ cells. Cells were grown and assayed as previously described (Sections 2.5.1 and 2.5.3). Panel A. *apl2*Δ cells were transformed with empty plasmid (YCplac111Met), or plasmids for *APL2*, or *apl2-1* expression. The BY4741 wild-type is included for comparison. The *apl2-1* mutant does not restore wild-type GFP-CPS trafficking. Panel B. Similarly *apl2*Δ cells were transformed with the same plasmids and stained for FM4-64. The *apl2-1* mutant exhibits aberrant vacuole morphology.

5.6.2 GFP-CPS trafficking and wild-type vacuole morphology in *apl4Δ* cells expressing the non-clathrin binding mutant *apl4-1*

GFP-CPS was transformed into *apl4Δ* cells along with empty plasmid YCplac111Met and plasmids expressing *APL4* and *apl4-1*. Similarly, in a separate experiment cells were stained with FM4-64 (Figure 5.6.2).

In BY4741 wild-type cells containing empty plasmid, GFP-CPS was localised to the vacuole lumen. As expected, *apl4Δ* cells containing the empty plasmid did not restore GFP-CPS trafficking to the vacuole lumen whereas *APL4* expression did. However, *apl4-1* expression resulted in the aberrant trafficking of GFP-CPS.

FM4-64 staining of BY4741 wild-type cells revealed normal vacuole morphology. In *apl4Δ* cells expressing empty plasmid, vacuole morphology was un-lobed and as expected the *apl4Δ* expressing *APL4* restored wild-type vacuole morphology. However *apl4-1* failed to restore wild-type vacuole morphology in these cells.

Neither the *apl2-1* nor the *apl4-1* mutants were able to restore either wild-type vacuole morphology or GFP-CPS trafficking in their respective deletion strains indicating that clathrin binding to both Apl2p and Apl4p is required for these aspects of AP-1 function.

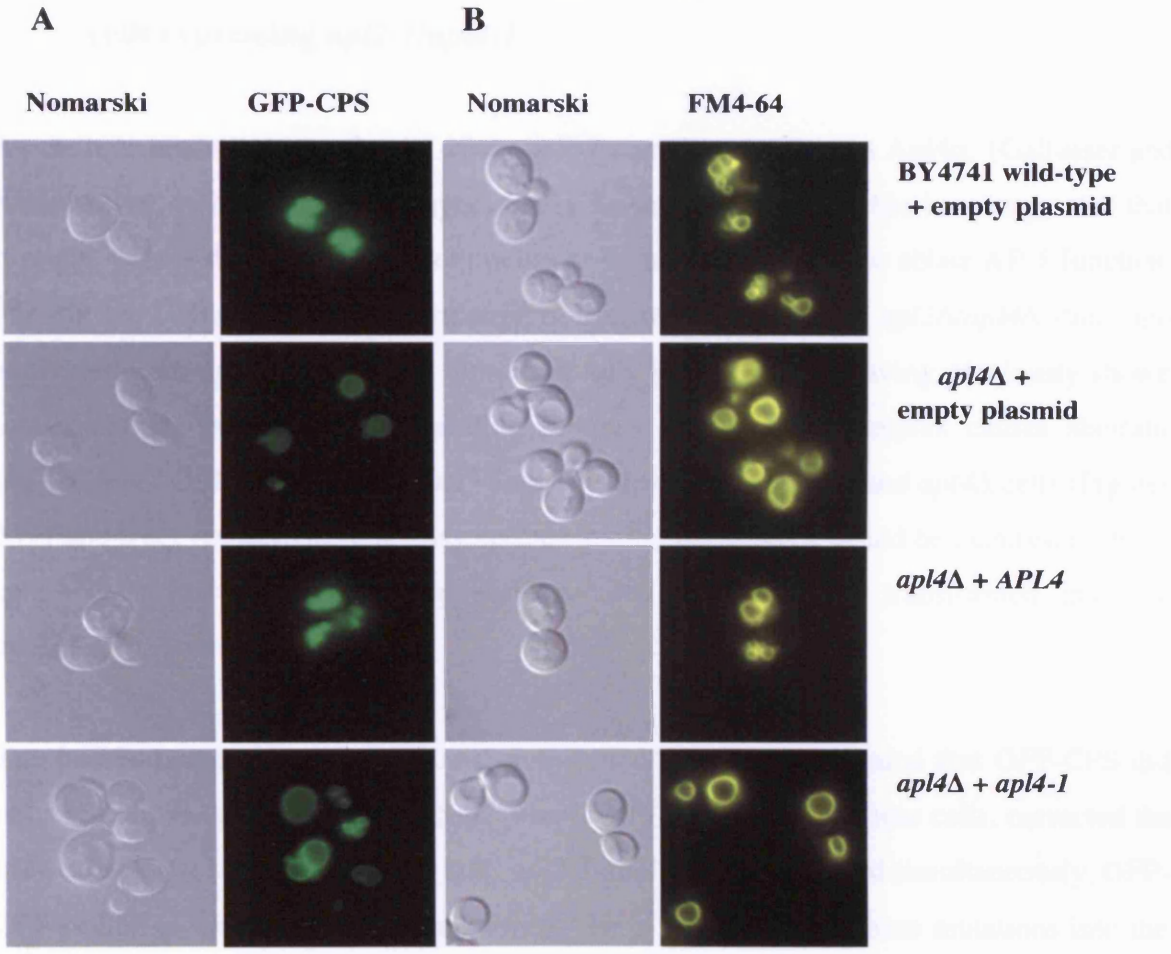

Figure 5.6.2. The putative non-clathrin binding mutant *apl4-1* displays aberrant trafficking of GFP-CPS and vacuole morphology in *apl4*Δ cells. Cells were grown and assayed as previously described (Sections 2.5.1 and 2.5.3). Panel A. *apl4*Δ cells were transformed with GFP-CPS along with empty plasmid, or plasmids for *APL4*, or *apl4-1* expression. The *apl4-1* mutant is unable to support wild-type GFP-CPS trafficking. Panel B. Similarly *apl4*Δ cells were transformed with the same plasmids and stained for FM4-64. The *apl4-1* mutant exhibited aberrant vacuole morphology.

5.6.3 GFP-CPS trafficking and wild-type vacuole morphology in *apl2Δ/apl4Δ* cells expressing *apl2-1/apl4-1*

As clathrin binds to two subunits of the AP-1 complex, Apl2p and Apl4p, (Gallusser and Kirchhausen, 1993; Yeung and Payne, 2001; Yeung et al., 1999) it has been suggested that it might require clathrin sites in both genes to be mutated in order to ablate AP-1 function (Yeung and Payne, 2001). In anticipation of this, we constructed an *apl2Δ/apl4Δ* strain and expressed both *apl2-1* and *apl4-1* simultaneously in these cells. Having previously shown that mutations in both clathrin-binding subunits of the AP-1 complex causes aberrant trafficking of GFP-CPS and aberrant vacuole morphology in *apl2Δ* and *apl4Δ* cells (Figures 5.6.1 and 5.6.2 respectively), it was expected similar phenotypes would be manifest in these cells. Thus plasmids expressing both mutated proteins were transformed into the *apl2Δ/apl4Δ* strain (Figure 5.6.3).

The transformation of empty plasmids into *apl2Δ/apl4Δ* cells revealed that GFP-CPS did not traffic to the vacuole lumen. Expression of *APL2* and *APL4* in these cells, corrected the trafficking defect. However, when both *apl2-1/apl4-1* were expressed simultaneously, GFP-CPS stalled at the outer vacuole membrane. Thus by introducing these mutations into the clathrin-binding domains of these proteins, clathrin binding was disrupted affecting protein trafficking of GFP-CPS (Figure 5.6.3).

FM4-64 staining of *apl2Δ/apl4Δ* alone cells revealed a defect in vacuole morphology. The introduction of empty plasmids had no effect on this morphology whereas the expression of plasmids containing wild-type genes reverted the defect in vacuole morphology. However the expression of *apl2-1/apl4-1* in these cells did not restore wild-type vacuole morphology (Figure 5.6.3). Given the data with the single deletions, these results were entirely expected.

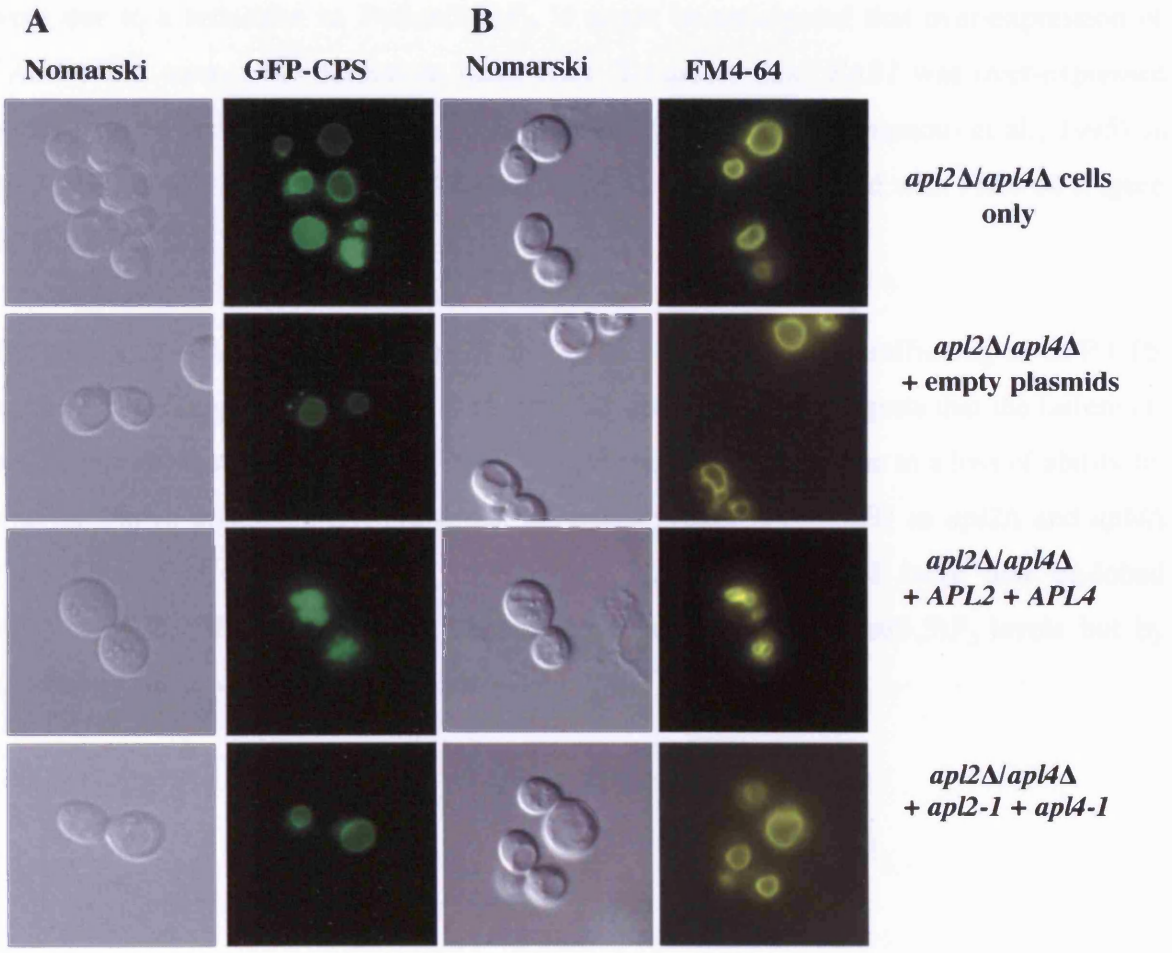

Figure 5.6.3. The mutants *apl4-1/apl2-1* display aberrant trafficking of GFP-CPS and vacuole morphology in *apl2Δ/apl4Δ* cells. Cells were grown and assayed as previously described (Sections 2.5.1 and 2.5.3). Panel A. *apl2Δ/apl4Δ* cells were transformed with GFP-CPS along with empty plasmids, or plasmids expressing *APL2* and *APL4* or *apl2-1* and *apl4-1*. *apl2Δ/apl4Δ* cells expressing *apl2-1/apl4-1* were unable to support wild-type GFP-CPS trafficking. Panel B. Similarly *apl2Δ/apl4Δ* cells were transformed with the same plasmids and stained for FM4-64. *apl2Δ/apl4Δ* cells expressing *apl2-1/apl4-1* exhibit aberrant vacuole morphology.

5.7 GFP-CPS trafficking is restored but not wild-type vacuole morphology in *apl2Δ* and *apl4Δ* cells over-expressing Fab1p

If the defects in trafficking of GFP-CPS and vacuole morphology in *apl2Δ* and *apl4Δ* cells were due to a reduction in PtdIns(3,5)P_2, it might be anticipated that over-expression of *FAB1* could correct the defects in these cells. To assess this, *FAB1* was over-expressed under its own promoter on a multicopy plasmid (pEMY105) (Yamamoto et al., 1995) in *apl2Δ* and *apl4Δ* cells expressing GFP-CPS and also in cells labelled with FM4-64 (Figure 5.7).

The over-expression of *FAB1* in *apl2Δ* and *apl4Δ* cells restores the trafficking of GFP-CPS to the vacuole lumen in at least 50% of the cells observed. This suggests that the failure of *apl2Δ* and *apl4Δ* cells to traffic GFP-CPS to the vacuole lumen is due to a loss of ability to activate Fab1p appropriately. However, the over-expression of *FAB1* in *apl2Δ* and *apl4Δ* cells has no effect on vacuole morphology; vacuoles appeared large and un-lobed suggesting that this defect is not caused by a reduction in PtdIns(3,5)P_2 levels but by another as yet unidentified mechanism.

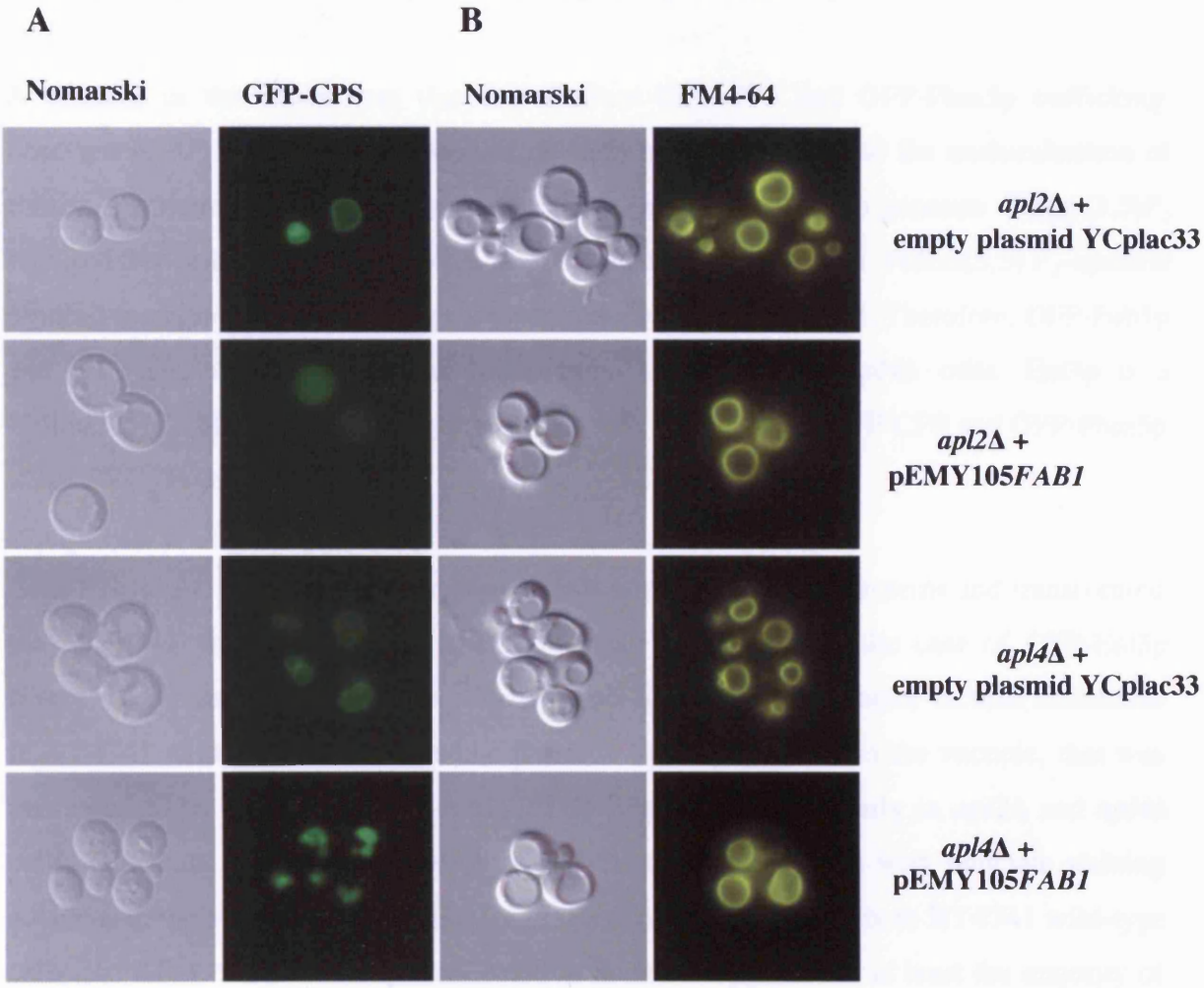

Figure 5.7 Over-expression of *FAB1* in *apl2*Δ and *apl4*Δ cells. Cells were grown as previously described (Sections 2.5.1 and 2.5.3). Panel A. Over-expression of *FAB1* restores GFP-CPS trafficking in *apl2*Δ and *apl4*Δ cells suggesting that the defects in these cells are due to depleted PtdIns(3,5)P_2 levels. Panel B. Over-expression of *FAB1* does not restore vacuole morphology in *apl2*Δ and *apl4*Δ cells suggesting that these defects are independent of *FAB1* function.

5.8 Localisation of Fab1p and Ent3p in *apl2Δ* and *apl4Δ* cells

A concern in this study was that the aberrant GFP-CPS and GFP-Phm5p trafficking observed in AP-1 complex components deletion mutants was due to the mislocalisation of Fab1p. Furthermore, if AP-1 was required for Fab1p activation to generate PtdIns(3,5)P_2 required for trafficking of proteins to the vacuole lumen, then PtdIns(3,5) P_2–specific binding proteins involved in this process might also be mislocalised. Therefore, GFP-Fab1p and GFP-Ent3p localisation was investigated in *apl2Δ* and *apl4Δ* cells. Ent3p is a PtdIns(3,5)P_2–binding protein required for protein trafficking of GFP-CPS and GFP-Phm5p at the PVC (Friant et al., 2003).

Both Fab1p and Ent3p were expressed as functional GFP-fusion proteins and transformed into BY4741 wild-type, *apl2Δ*, *apl4Δ* and also *fab1Δ* cells in the case of GFP-Ent3p (Figures 5.8a and 5.8b). GFP-Fab1p localises predominantly to the outer vacuole membrane in BY4741 wild-type cells with some punctate staining adjacent to the vacuole, that was presumed to be the PVC (Dove et al., 2002) (Figure 5.8a). Similarly in *apl2Δ* and *apl4Δ* cells, GFP-Fab1p localises to the outer vacuole membrane, again with punctate staining adjacent to the vacuole. The similar localisation of GFP-Fab1p in both BY4741 wild-type cells and AP-1 complex component deletion mutants suggests that at least the majority of Fab1p is localised correctly in these cells. Hence the GFP-CPS and GFP-Phm5p missorting phenotypes observed in AP-1 complex component deletion mutants are unlikely to be due to a gross mislocalisation of Fab1p.

Ent3p has been shown to bind PtdIns(3,5)P_2 and is required for trafficking of GFP-CPS and GFP-Phm5p at the PVC (Friant et al., 2003) hence disruption of Fab1p activity in *apl2Δ* and *apl4Δ* cells might alter the localisation of Ent3p. Thus in a similar experiment to the previous, GFP-Ent3p localisation was investigated in BY4741 wild-type, *apl2Δ*, *apl4Δ* and *fab1Δ* cells (Figure 5.8b).

GFP-Ent3p localisation in BY4741 wild-type cells was punctate throughout the cell consistent with a late endosomal/PVC localisation suggesting that Ent3p localises correctly

in these cells (Friant et al., 2003). A similar localisation was observed in *apl2*Δ and *apl4*Δ cells suggesting that GFP-Ent3p localisation is not disrupted in these cells. However, when GFP-Ent3p was observed in *fab1*Δ cells, a punctate staining was seen in the cytoplasm of the cells. It has been reported that endosomal localisation of Ent3p requires the presence of PtdIns(3,5)P_2, hence, in *fab1*Δ cells which contains no PtdIns(3,5)P_2, GFP-Ent3p has a cytoplasmic distribution reflecting the absence of PtdIns(3,5)P_2 (Friant et al., 2003). This along with other evidence (Section 1.12) suggests that Ent3p is an effector of PtdIns(3,5)P_2 and is required for protein trafficking to the PVC (Friant et al., 2003). However, our data are not consistent with GFP-Ent3p localisation in this study and would suggest that PtdIns(3,5)P_2 is not required for GFP-Ent3p localisation.

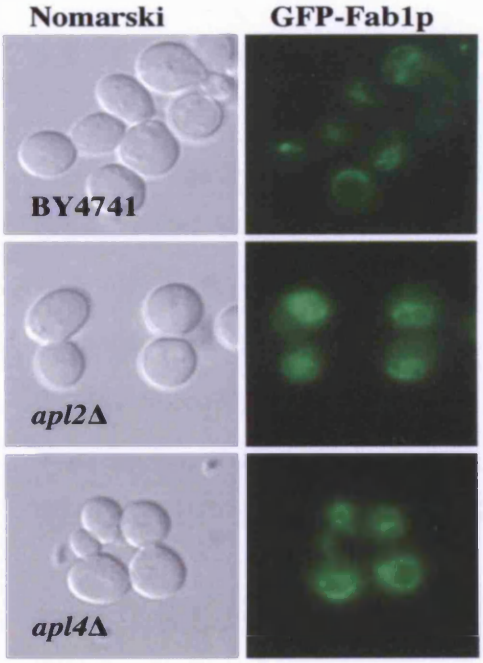

Figure 5.8a. Localisation of GFP-Fab1p in BY4741 wild-type, *apl2*Δ and *apl4*Δ cells. Cells were grown as described previously (Section 2.5.1). GFP-Fab1p localises predominantly to the outer vacuole membrane in BY4741 wild-type cells and in *apl2*Δ and *apl4*Δ cells.

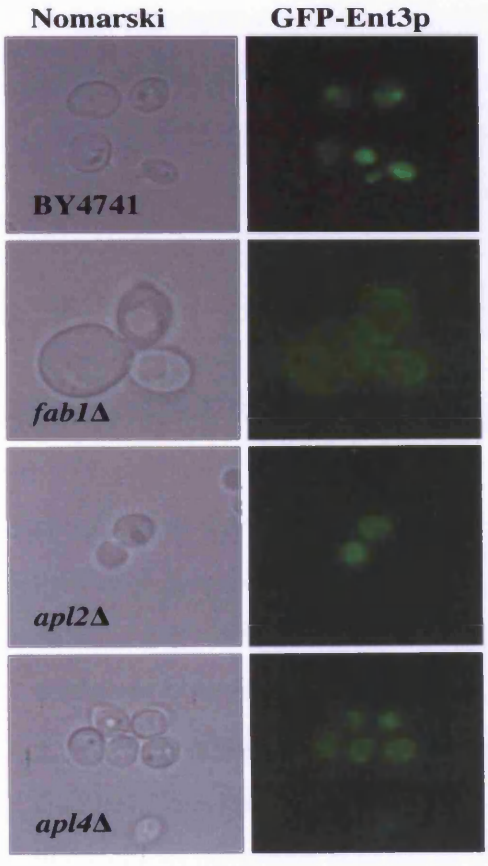

Figure 5.8b. Localisation of GFP-Ent3p in BY4741 wild-type, *fab1*Δ, *apl2*Δ and *apl4*Δ cells. Cells were grown at 30 °C to a density of $5x10^6$ then induced with galactose for 3-4 hours, harvested and viewed as previously described (Section 2.5.1). In all cells, GFP-Ent3p has a punctate cytoplasmic staining.

5.9 Conclusions

From the yeast two-hybrid data showing that Apl2p (the β-subunit of AP-1) potentially interacts with Fab1p and data suggesting that Vac14p, a known regulator of Fab1p interacts with Apl4p (the γ-subunit of AP-1) (Dove et al., 2002), it was postulated that AP-1 is either a regulator or effector of Fab1p function. Thus, in this chapter all AP-1 complex component deletion mutants were assayed for phenotypes coincident to *fab1*Δ phenotypes. If AP-1 is required for Fab1p related functions it would be expected that AP-1 complex component deletion mutants would be deficient in one or more Fab1p related functions.

5.9.1 LacZ Assay

Yeast two-hybrid analysis of Fab1p/AP-1 interactions was carried out using the β-galactosidase reporter gene system (Figure 5.5.1). This reveals that β-galactosidase levels were highest in the mating between Apl2p and Fab1p containing strains, corroborating the initial yeast two-hybrid data showing that Apl2p interacts with Fab1p. Also the LacZ assay identified Apm1p as potentially binding to Fab1p. This was not observed during the less sensitive *HIS3* growth reporter gene assay and will require further investigation.

5.9.2 HPLC Analysis of Phosphoinositides

HPLC assay was used in this study to assay for PtdIns(3,5)P_2 and other phosphoinositides in the AP-1 complex component deletion mutants (Figure 5.5.2). This shows that there was a reduction of PtdIns(3,5)P_2 in all mutants, ranging from 65% (*aps1*Δ) to 84% (*apm1*Δ) of wild-type PtdIns(3,5)P_2 levels. The changes in PtdIns(3,5)P_2 in these cells however are not matched in changes in other phosphoinositides assayed, (Table 5.5.2), indicating that the changes observed in PtdIns(3,5)P_2 levels are due to a reduction in Fab1p activity and not due to gross metabolic disruption of phosphatidylinositol metabolism.

From these data it would appear that the AP-1 complex is required to maintain wild-type PtdIns(3,5)P_2 production in yeast. Deletion of AP-1 complex components does not cause

the complete loss of PtdIns(3,5)P_2 implying that Fab1p kinase activity is compromised but not completely ablated. This modest reduction in PtdIns(3,5)P_2 could represent a significant loss of a local pool of PtdIns(3,5) P_2 production that may alter or compromise one or more but not all, Fab1p-dependent cellular functions in AP-1 complex component deletion mutants. By implication this suggests that AP-1 is not a universal regulator of Fab1p function, and thus it would be expected that AP-1 complex component deletion mutants would not display all the phenotypes of *fab1*Δ cells. This was found to be the case.

5.9.3 Trafficking in AP-1 complex component deletion mutants.

AP-1 complex component deletion mutants were assayed for trafficking of the ubiquitinated cargoes, GFP-CPS and GFP-Phm5p to the vacuole lumen. Both cargos stall at the outer vacuole membranes in a similar fashion to *fab1*Δ cells (Figures 5.5.3 and 5.5.4 respectively). Interestingly, the expression of GFP-Phm5p appears to alter the morphology of these cells in that the vacuole is slightly larger than wild-type. This is consistent with observations made in Chapter 4 where a panel of deletion mutants were similarly screened using GFP-Phm5p (Figure 4.4.2.1) In both screens cell viability is greatly compromised and the GFP signal extremely poor. Thus it appears that GFP-Phm5p is slightly toxic to these cells resulting in poor expression, compromising vacuole morphology and reducing cell viability. Nonetheless, AP-1 complex component deletion mutants did exhibit aberrant trafficking of GFP-Phm5p.

To overcome the morphological defects observed with GFP-Phm5p, AP-1 complex component deletion mutants were assayed for GFP-CPS trafficking. All deletion strains, *apl2*Δ, *apl4*Δ and *aps1*Δ clearly missort GFP-CPS to the outer vacuole membrane (Figure 5.5.3). A GFP-CPS trafficking defect was less transparent in *apm1*Δ and *apm2*Δ. Two possibilities were considered for this result. Firstly, as both Apm1p and Apm2p are subunits of AP-1, there could be some redundancy in function. Secondly, the wild-type vacuole morphology of these cells could make GFP-CPS trafficking defects less obvious by concentrating GFP-CPS. Interestingly, these cells were found to have defects in the

trafficking of GFP-Phm5p (Figure 5.5.4) implying that the latter explanation is the more likely.

Defects in trafficking of CPS have been recorded for AP-1 complex component deletion mutants (Rad et al., 1995; Valdivia et al., 2002; Yeung et al., 1999) (Section 5.4.2). In cells with combined deletions of *APL2* and *APL1* (AP-2 complex) and other combinational deletes of AP-1 and AP-2, CPS processing is delayed (Cowles et al., 1997a). These data indicate that deletion of AP-1 components in conjunction with other gene deletions, temperature sensitive alleles such as *chc1*^{ts} and *sec6-4*^{ts} cause defects in trafficking (Valdivia et al., 2002; Yeung et al., 1999). However the data presented here show for the first time that single AP-1 complex component deletion mutants also cause trafficking defects of GFP-CPS and GFP-Phm5p (Section 5.5.3 and 5.5.4). It was theorised that if AP-1 complex component deletion mutants fail to activate Fab1p, over-expression of *FAB1* might correct the GFP-CPS trafficking defect observed in *apl2*Δ and *apl4*Δ cells. GFP-CPS localises to the vacuole lumen in over 50% of *apl2*Δ and *apl4*Δ over-expressing *FAB1* (Figure 5.7). Thus the failure of *apl2*Δ and *apl4*Δ cells to traffic GFP-CPS to the vacuole lumen is due to an inability to activate Fab1p, further linking the AP-1 complex with Fab1p function. Similarly, *FAB1* over-expression also restores the vacuole morphology defects in *vac14*Δ cells (Dove et al., 2002).

Trafficking of GFP-Phm5p to the vacuole lumen is restored in *fab1*Δ cells by the fusion of an ubiquitin sequence to the N-terminus of these cargos. Similarly, fusion of ubiquitin to the N-terminus of GFP-CPS also allows ubiquitin independent trafficking into the vacuole lumen (Katzmann et al., 2004). As in *fab1*Δ cells, Ub-GFP-Phm5p traffics to the vacuole lumen in *apl2*Δ and *apl4*Δ cells (Figure 5.5.5a) These data suggest that *apl2*Δ and *apl4*Δ cells have lost the ability to sort ubiquitinated cargoes to the vacuole lumen in a manner similar to *fab1*Δ cells. Furthermore, as the phenotype of *fab1*Δ, *apl2*Δ and *apl4*Δ cells are identical with respect to GFP-CPS/GFP-Phm5p trafficking, it is likely that these cells are deficient in the same process.

That loss of AP-1 complex components causes a compromise in the transport machinery between the TGN and the vacuole was a distinct possibility. Expressing GFP-Sna3p in BY4741 wild-type, *fab1*Δ, *apl2*Δ and *apl4*Δ cells, tested this. GFP-Sna3p traffics to the vacuole lumen via the same pathway as GFP-CPS and GFP-Phm5p but in an ubiquitin-independent manner (Reggiori and Pelham, 2001). GFP-Sna3p traffics to the vacuole lumen in all cells assayed (Figure 5.5.5b), suggesting that the TGN/PVC/vacuole trafficking pathway is still intact in these cells. These data strongly suggest that loss of AP-1 complex component function confers a specific loss in the ability to correctly traffic a number of ubiquitinated cargoes from the TGN to the vacuole lumen.

We also investigated the localisation of GFP-Fab1p in *apl2*Δ and *apl4*Δ cells (Figure 5.8a). The localisation of GFP-Fab1p in BY4741 wild-type cells is in agreement with previous work (Dove et al., 2002). Similar localisation was also observed in *apl2*Δ and *apl4*Δ cells suggesting that the majority of GFP-Fab1p is correctly localised at the vacuole membrane /PVC in these cells. However the mislocalisation of a small proportion of Fab1p could not be discounted.

Ent3p is proposed to be a PtdIns(3,5)P_2-specific binding protein that is required for the trafficking of GFP-CPS to the vacuole lumen (Friant et al., 2003). The expression of GFP-Ent3p in BY4741 wild-type cells is in agreement with previous work; GFP-Ent3p localises to punctate structures in the cell consistent with a late endosomal/PVC localisation (Friant et al., 2003) (Figure 5.8b). A similar localisation is observed for *apl2*Δ and *apl4*Δ cells. In *fab1*Δ cells, which contain no PtdIns(3,5)P_2, GFP-Ent3p is reported to have a diffuse cytoplasmic staining, indicating its endosomal location requires PtdIns(3,5)P_2 (Friant et al., 2003). However, our data do not appear to agree with these findings; in *fab1*Δ cells we observe punctate GFP-Ent3p staining in the cytoplasm suggesting that localisation of GFP-Ent3p is independent of PtdIns(3,5)P_2 production. Furthermore, preliminary data from other laboratories would appear to imply that Ent3p is not a *bona fide* PtdIns(3,5)P_2 binding protein. [Dr. S.K Dove, personal communication]. Thus we did not pursue further work with Ent3p.

5.9.4 Clathrin-binding in AP-1 complex component deletion mutants.

Mutational analyses have shown that Apl2p and Apl4p of the AP-1 complex bind clathrin (Yeung and Payne, 2001). Therefore we assessed whether clathrin binding to AP-1 is required for both trafficking of GFP-CPS and vacuole morphology. The mutants, *apl2-1* and *apl4-1* were expressed in their respective deletion and double deletion strains. Neither *apl2-1* nor *apl4-1*, nor *apl2-1/ apl4-1* combined mutants restores wild-type trafficking of GFP-CPS nor maintains wild-type vacuole morphology in their respective deletion strains (Figures 5.6.1, 5.6.2 and 5.6.3 respectively). These data suggest that clathrin binding to both Apl2p and Apl4p is required for the trafficking of GFP-CPS to the vacuole lumen and vacuole morphology and that clathrin is an important component in this pathway.

5.9.5 Vacuole morphology in AP-1 complex component deletion mutants

*fab1*Δ cells have a large un-lobed vacuole (Yamamoto et al., 1995). Of the AP-1 complex component deletion mutants only *apl2*Δ and *apl4*Δ cells exhibit aberrant vacuole morphology, the other AP-1 complex component deletion mutants are all wild-type (Figure 5.5.6). The vacuole morphology in *apl2*Δ and *apl4*Δ cells is not identical to those seen in *fab1*Δ cells; while being un-lobed, they are much smaller than *fab1*Δ but slightly larger than wild-type vacuoles. The vacuoles of *apl2*Δ and *apl4*Δ cells are similar to those seen in class II vacuole inheritance mutants (Weisman, 2003). This class of mutants are characterised by un-lobed vacuoles whereas class III, which *fab1*Δ falls into, have exceptionally large, poorly acidified vacuoles (Weisman, 2003). Class II mutants are further differentiated into those mutants that sort correctly CPY (non-vacuole protein sorting mutants, non-*vps*) and those defective in this process (*vps* mutants). AP-1 complex component deletion mutants have been shown to traffic CPY to the vacuole, albeit with a slight delay (Cowles et al., 1997a), therefore *apl2*Δ and *apl4*Δ could be classified into the non-*vps* class II vacuole inheritance mutants. Three non-*vps* class II mutants *vac6, vac11* and *vac12* have been described but no genes have been assigned to these mutants (Weisman, 2003) hence it is possible that *APL2* and/or *APL4* could be one of these genes.

The vacuole morphology of *apm1*Δ, *apm2*Δ and *aps1*Δ cells is wild-type in contrast to *apl2*Δ and *apl4*Δ cells, despite these cells having reduced PtdIns(3,5)P_2 levels when compared to wild-type. If AP-1 is regulating a pool of PtdIns(3,5)P_2 responsible for correct vacuole morphology, it is likely all mutant AP-1 complex components would exhibit these morphological defects. These data suggest that AP-1 is not essential for regulating the pool of PtdIns(3,5)P_2 responsible for correct vacuole morphology. This observation is further supported by the over-expression of *FAB1* in *apl2*Δ and *apl4*Δ cells (Figure 5.7). It was theorised that over-expression of *FAB1* might restore wild-type PtdIns(3,5)P_2 levels in *apl2*Δ and *apl4*Δ cells thus correcting the vacuole morphology defect. However this is not the case, even in cells where GFP-CPS trafficking had been restored (Figure 5.7). These data suggest that the vacuole defects observed in *apl2*Δ and *apl4*Δ cells are independent of Fab1p function and are caused by an unknown mechanism. It is noteworthy however, that deletion of only the clathrin binding subunits of AP-1 (Apl2p and Apl4p) causes a defect in vacuole morphology. Thus the role of AP-1 and clathrin in vacuole function merits further investigation.

5.9.6 Quinacrine staining in AP-1 complex component deletion mutants

Lack of quinacrine accumulation in *fab1*Δ cells indicates a loss of vacuole acidification (Yamamoto et al., 1995). All AP-1 complex component deletion mutants accumulate quinacrine in their vacuoles implying that the vacuoles of these cells unlike those of *fab1*Δ cells are acidified correctly (Figure 5.5.7). Thus it is unlikely that AP-1 regulates Fab1p to promote correct vacuole acidification.

5.10 Summary

These data presented here would suggest that the *S. cerevisiae* AP-1 complex is required for some but not all Fab1p-dependent biology. AP-1 complex component deletion mutants have reduced levels of PtdIns(3,5)P_2 and hence the functional output of Fab1p is compromised. That PtdIns(3,5)P_2 is not completely absent from AP-1 complex component deletion mutants indicates that AP-1 is not a universal regulator of Fab1p, otherwise it

would be expected that mutant AP-1 complex components would display all the phenotypes of *fab1*Δ cells, which is clearly not the case.

We postulate that reduction of PtdIns(3,5)P_2 in mutant AP-1 complex components causes a defect in the trafficking of ubiquitinated GFP-CPS and GFP-Phm5p from the TGN via the PVC to the vacuole. We propose that the likely mechanism for this is that AP-1 recruits both Fab1p via binding to Apl2p and Vac14p via binding to Apl4p, thus activating Fab1p to direct ubiquitinated protein trafficking at the TGN. Thus we suggest that AP-1 is a regulator of Fab1p function.

6 DISCUSSION

6.1 Introduction

The production of PtdIns(3,5)P_2 by type III PIPkins now appears to be a pivotal mechanism in the execution of several diverse intracellular functions (Section 1.10). In *S. cerevisiae* it is clear that these processes are independently regulated by Fab1p and by its ability to functionally regulate distinct pools of PtdIns(3,5)P_2 within the cell (Cooke, 2002; Dove et al., 2004). How are these pools regulated? Vac14p is a global regulator of Fab1p and is involved in all Fab1p-related functions as described (Dove et al., 2002) (Section 1.7). Vac7p is also required for Fab1p activities in some strains, however with no obvious homologues in other organisms, the role of Vac7p in type III PIPkins remains equivocal (Gary et al., 2002). But, it is also likely that there are other unidentified proteins that help regulate Fab1p in order that PtdIns(3,5)P_2 is produced in the correct cellular environment. One consequence is that deletion of such regulators from the yeast genome would be expected to have compromised PtdIns(3,5)P_2 levels concomitant with one or more compromised PtdIns(3,5)P_2–related functions. In this study we have identified AP-1 complex component deletion mutants as having reduced PtdIns(3,5)P_2 levels with a simultaneous defect in trafficking therefore we propose AP-1 as a potential regulator of Fab1p function.

6.2 Yeast two-hybrid analysis

Using an extensive yeast two-hybrid screen we identified 338 potential regulators/effectors of Fab1p and after adjustment this tally fell to 306. This number appears high but when critically assessed, a high proportion of interactions are proteins of unknown function (32%) whereas proteins of unknown location account for 38% of the screen. Hence just over one third of proteins are completely unassigned in terms of function and location. This fact is indicative of the substantial numbers of ORFs identified from the yeast genome sequencing initiative that still require characterisation. Of the 306 ORFs identified,

approximately one quarter localise to the nucleus, which is surprising, as there is no evidence to suggest that Fab1p has any role in this compartment. It should be noted that yeast two-hybrid analysis requires that interacting proteins are imported into the nucleus and thus there remains the possibility that some of these nuclear reactions are spurious. Alternatively, it is also possible that Fab1p and its catalytic output PtdIns(3,5)P_2 have as yet unidentified nuclear functions so a physiological role for nuclear proteins found to interact with Fab1p should not be completely discounted. There are data that a pool of mammalian inositol lipids may exist in the nucleus of mammalian cells, so a nuclear role for PtdIns(3,5)P_2 should not be ignored (Irvine, 2002; Irvine, 2003). Furthermore, at the time of assessment of ORFs to investigate further (July 2002), potential interactors from the mitochondria (6%) were discounted based on the fact that there was no evidence in the literature to suggest that Fab1p had a role at this compartment. Recently a comprehensive proteome analysis of purified *S. cerevisiae* mitochondria localised Fab1p to this compartment (Sickmann et al., 2003). Hence there remains the possibility that Fab1p may be physiologically active in more compartments than previously thought.

Nonetheless, there still remained many ORFs that potentially bound to Fab1p, more than could practically be screened in the time available. It was anticipated that deletion mutants of authentic activators/effectors of Fab1p would display one or more of the phenotypes of a *fab1*Δ strain. To test this hypothesis, we carried out phenotypic analyses on deletion mutants of corresponding ORFs identified from our screen based on several criteria (Section 3.8) Consequently, we chose 17 ORFs that we predicted to be the most likely candidates as interactors with Fab1p (Table 3.9).

Phenotypic analyses (Chapter 4) identified 8 of the 17 deletion mutants as displaying similar phenotypes to *fab1*Δ cells (Table 6.2).

Deletion Mutant	Phenotypes observed
apl2Δ	GFP-Phm5p and GFP-CPS missorting and aberrant vacuole morphology
arp8Δ	no growth at 37 °C and poorly acidified vacuole
bsc5Δ	poorly acidified vacuole
inm1Δ	poorly acidified vacuole
sel1Δ	no growth at 37 °C and aberrant vacuole morphology
sif2Δ	poorly acidified vacuole
vma6Δ	no growth at 37 °C, poor vacuole acidification aberrant vacuole morphology
YNL123WΔ	poorly acidified vacuole

Table 6.2. Summary of deletion mutants displaying *fab1*Δ-like phenotypes. Deletion strains were subject to phenotypic analyses used to characterise *fab1*Δ cells (Section 1.10). 8 ORFs were found to demonstrate similar phenotypes to *fab1*Δ cells potentially suggesting a common mechanism of action.

The ORFs are:

Apl2p has been discussed in detail in Chapter 5 and later in this chapter.

Arp8p is an actin related protein involved in DNA binding and is a member of the *INO80* chromatin-remodelling complex. *arp8Δ* cells are auxotrophic for inositol on solid media (Shen et al., 2003). From our data Arp8p is essential for growth at 37 °C and appears to be play a role in vacuole acidification. These phenotypes have not been described for Arp8p before and are therefore novel findings.

Bsc5p (Bypass of Stop Codon 5) has not yet been characterised fully in terms of function (www.yeastgenome.org). In this study the deletion mutant exhibited poor acidification of the vacuole, a phenotype not described before.

Inm1p is involved in the *de novo* synthesis of inositol has been implicated in the phosphoinositide second messenger-signalling pathway (Murray and Greenberg, 2000). Phenotypes have been described for *inm1Δ* cells and include reduction in inositol monophosphatase activity and slight growth sensitivity to lithium or valproate (Murray and Greenberg, 2000). From our data Inm1p appears to be important in the maintenance of vacuole acidification, a role not described for Inm1p before.

The precise function of *S. cerevisiae* Sel1p (Ubx2p) is unknown, however it interacts with Cdc48p, an ubiquitin-selective AAA ATPase (ATPases associated with diverse cellular activities) and contains an ubiquitin-binding UBA domain at the N-terminus, an ubiquitin regulatory "X" UBX domain at the C-terminus and appears to interact with ubiquitinated proteins *in vivo* (Schuberth et al., 2004). Sel1p also contains an ubiquitin-interaction motif (UIM) and a novel motif of unknown function found in several UBX containing proteins (Hartmann-Petersen et al., 2004). A similar interaction with Cdc48 has also been observed in *S. pombe* (Hartmann-Petersen et al., 2004). Phenotypes of an *S. cerevisiae* deletion strain have recently been described and include sensitivity to various stresses, defects in the degradation of ubiquitinated substrates and sensitivity to growth at 37 °C (Schuberth et al.,

2004) as also demonstrated in this study. However the authors of these studies have not described aberrant vacuole morphology in *sel1*Δ cells, suggesting that Sel1p may be required to maintain wild-type vacuole morphology in yeast. However *sel1*Δ vacuoles are not swollen, therefore they do not fall into the Class II vacuole inheritance mutants as described by Weisman *et al* (Weisman, 2003). These data, along with the original yeast two-hybrid data showing that full-length Fab1p interacts with Sel1p suggests that Fab1p and Sel1p may be involved in an ubiquitination mechanism. Other workers have suggested the involvement of Fab1p in ubiquitination, (Katzmann et al., 2004; Reggiori and Pelham, 2002) therefore this interaction does warrant further investigation.

S. cerevisiae Sif2p is a WD40 containing protein that disrupts telomeric silencing when over-expressed (Neer et al., 1994). *sif2*Δ cells are hypersensitive to a range of stresses (Cockell et al., 1998) however a defect in vacuolar acidity is a novel observation in this strain.

Vma6p is a subunit of the vacuolar (H^+)-ATPase multi-subunit complex involved in the acidification of intracellular compartments in eukaryotic cells (Stevens and Forgac, 1997). The acidified vacuole phenotype in these cells has been described before (Bauerle et al., 1993) and has been observed in other deletion components of the complex, namely Vma4p (Odorizzi et al., 1998); therefore the acidified vacuole phenotype observed for *vma6*Δ cells was entirely expected. These cells also exhibited growth sensitivity at 37 °C and aberrant vacuole morphology thus they shared several phenotypes with *fab1*Δ cells. The mechanism by which Fab1p regulates vacuole acidification is undefined, and it may be that a physical interaction between Vma6p and Fab1p will prove to be of physiological relevance.

Deletion of the ORF YNL123WΔ caused a defect in vacuole acidification. According to the SGD website (www.yeastgenome.org) the YNL123W ORF shows protein sequence similarity to the mammalian Omi/HtrA2 family of serine proteases (Jones et al., 2003). No other information is known about this ORF hence the vacuolar acidification phenotype is a novel observation.

Thus nearly 50% of chosen ORFs yielded phenotypes coincident with *fab1*Δ cells and therefore, we believe this systematic approach of yeast two-hybrid analysis followed by a more in-depth phenotypic screen as being justified in our search for Fab1p effectors/regulators. Whether or not these deletion mutants turn out to be effectors/regulators remains to be seen but they will warrant further investigation. Due to time constraints only one ORF was chosen for further investigation, Apl2p.

6.3 Analysis of Apl2p

Apl2p, (the β-subunit of the AP-1 complex) was chosen for further investigation not only on the strength of these phenotypic analyses (Chapter 5) but also on other relevant data. In previous work, Apl4p (the γ-subunit of the AP-1 complex) interacts with Vac14p by yeast two-hybrid analysis (Dove et al., 2002). In light of our data suggesting that Apl2p interacts with Fab1p, it is likely that AP-1 has some role in Fab1p biology, possibly suggesting that AP-1 is acting as an effector/regulator of Fab1p. Secondly, the AP-1 complex has been relatively well characterised in terms of structure and function therefore some information was available in the literature.

6.3.1 AP-1 is required for Fab1p function

From our data all AP-1 complex component deletion mutants were found to have compromised PtdIns(3,5)P_2 production indicating a compromise in the functional output of Fab1p (Figure 5.5.2). It is also significant that PtdIns(3,5)P_2 is not completely ablated in AP-1 complex component deletion mutants. This suggests that AP-1, through activation of Fab1p, may be responsible for a small pool of PtdIns(3,5)P_2 production, and that AP-1 is not a universal activator of Fab1p. Had PtdIns(3,5)P_2 production in AP-1 complex component deletion mutants been completely abolished, we would have expected to observe all phenotypes associated with the loss of PtdIns(3,5)P_2. However with the potential loss of only a small pool of PtdIns(3,5)P_2 production in AP-1 mutants we might anticipate some but not all *fab1*Δ phenotypes to be manifest; and this was the case.

6.3.2 AP-1 is required for protein trafficking to the vacuole lumen

Our data reveal that AP-1 is required for the correct trafficking of GFP-CPS and GFP-Phm5p to the vacuole lumen. With respect to GFP-Phm5p, the trafficking defect is restored in *apl2*Δ, *apl4*Δ and *fab1*Δ cells by the attachment of an ubiquitin to GFP-Phm5p (Figure 5.5.5). Furthermore, these cells also traffic GFP-Sna3p in an ubiquitin-independent manner to the vacuole lumen suggesting that the TGN to vacuole trafficking mechanism is not compromised in these cells. Defects in GFP-CPS trafficking in *apl2*Δ and *apl4*Δ cells were similarly restored by the over-expression of *FAB1* (Figure 5.7). In other work, the over-expression of *FAB1* also restores wild-type vacuole morphology to *vac14*Δ cells (Dove et al., 2002); and thus our data are consistent with a loss of Vac14p mediated activation of Fab1p.

Genetic studies have suggested that AP-1 functions with clathrin to mediate protein retrieval from the secretory/endosomal pathway to the TGN (Cowles et al., 1997a; Phan et al., 1994; Rad et al., 1995; Stepp et al., 1995; Valdivia et al., 2002; Yeung et al., 1999). Thus, the association of Fab1p with Apl2p would implicate Fab1p in this process. In previous work, PtdIns(3,5)P_2 has been shown to be required for retrograde transport from the vacuole (Bryant et al., 1998; Dove et al., 2004). Transport to the vacuole requires PtdIns3*P* (Burd and Emr, 1998), which binds Fab1p via the FYVE domain (Section 1.6.1) but also acts as a substrate for the catalytic domain of Fab1p (Section 1.6.4). Thus Fab1p is ideally placed to regulate traffic in the opposite direction to PtdIns3*P* related traffic and this might be an important theme in Fab1p biology.

6.3.3 AP-1 function is not required for Fab1p-dependent vacuole morphology and acidification

Our data suggests that the vacuole morphology defects observed in *apl2*Δ and *apl4*Δ cells are independent of Fab1p function for the following reasons. Firstly, the vacuole morphology of *apl2*Δ and *apl4*Δ cells is not identical to that of *fab1*Δ cells. While these vacuoles are un-lobed, they are correctly acidified and they are not as large or as swollen as

*fab1*Δ cells. The vacuole phenotype observed in *apl2*Δ and *apl4*Δ cells is similar to the non-*vps* class II vacuole inheritance mutants (Weisman, 2003). It is therefore tempting to speculate that both *APL2* and *APL4* could be candidate genes for several as yet unidentified vacuolar mutants (*vac6, vac11* and *vac12*) (Weisman, 2003). Secondly, whilst all AP-1 complex component deletion mutants have reduced PtdIns(3,5)P_2 levels, only *apl2*Δ and *apl4*Δ cells display an aberrant vacuole morphology supporting the idea that AP-1 does not regulate Fab1p at the vacuole. Thirdly, it is possible that the defects observed in *apl2*Δ and *apl4*Δ cells are due to the disruption of clathrin binding; Apl2p and Apl4p unlike the other subunits of AP-1, both bind clathrin and thus the loss of these AP-1 subunits could result in aberrant vacuole morphology (Yeung and Payne, 2001) This hypothesis is supported by data using the non-clathrin binding mutants *apl2-1* and *apl4-1* (see below). And finally, over-expression of *FAB1* failed to restore the wild-type vacuole morphology in *apl2*Δ and *apl4*Δ cells even in cells where wild-type GFP-CPS trafficking was restored (Figure 5.7). Thus from these data it would appear that the vacuole defects observed in *apl2*Δ and *apl4*Δ cells are indeed independent of Fab1p.

In a previous study, mutation of the clathrin binding sites of Apl2p and Apl4p reduced the physical association of clathrin with AP-1 (Yeung and Payne, 2001). Therefore we investigated whether clathrin binding to Apl2p and Apl4p was required for protein trafficking and vacuole morphology in *apl2*Δ and *apl4*Δ cells. The non-clathrin binding *apl2-1* and *apl4-1* mutants, neither restored wild-type trafficking of GFP-CPS to the vacuole lumen nor vacuole morphology in their respective deletion mutants (Figures 5.6.1 and 5.6.2 respectively). As anticipated, the combination of these mutations in *apl2*Δ/*apl4*Δ revealed similar results (Figure 5.6.3). Thus these data suggest that binding of clathrin to both Apl2p and Apl4p is required for the trafficking of GFP-CPS to the vacuole and for the maintenance of wild-type vacuole morphology however the mechanism behind this remains unidentified.

Our data also indicate that the AP-1 complex is not involved in the acidification of the yeast vacuole and thus it is unlikely that Fab1p is activated by AP-1 to direct this process.

In conclusion, we propose that AP-1 activates Fab1p to generate PtdIns(3,5)P_2 in order to direct trafficking of ubiquitinated protein cargo to the vacuole. AP-1 complex component deletion mutants do not appear to be involved in other phenotypes displayed by *fab1*Δ cells implying that there are as yet unidentified proteins involved in activating Fab1p to direct these processes (Figure 6.3.3). Our observation that Fab1p and Apl2p are potential interactors and Apl4p interacts with Vac14p (Dove et al., 2002) suggest that AP-1 may recruit Vac14p and Fab1p to the TGN, thus activating Fab1p and PtdIns(3,5)P_2 production at this compartment. As previously mentioned AP-1 functions at the TGN in order to maintain the localisation of a number of proteins by retrieving them from the endosomal/secretory pathway back to the TGN; thus it is possible that retrieval of these proteins to the TGN is an AP-1 and Fab1p-dependent process.

The identification of Apl2p as a potential interactor to Fab1p and that Fab1p may be an effector of AP-1 has been mediated by the use of the yeast two-hybrid technique and the application of phenotypic analyses to characterise these interactions. As stated, several other ORFs identified by the yeast two-hybrid also remain to be characterised in greater detail with respect to Fab1p function. Thus, our approach of using the yeast two-hybrid in combination with phenotypic analyses deletion mutants has been validated; however, more work needs to be carried out in order to characterise the Apl2p/Fab1p and Apl4p/Vac14p interactions further.

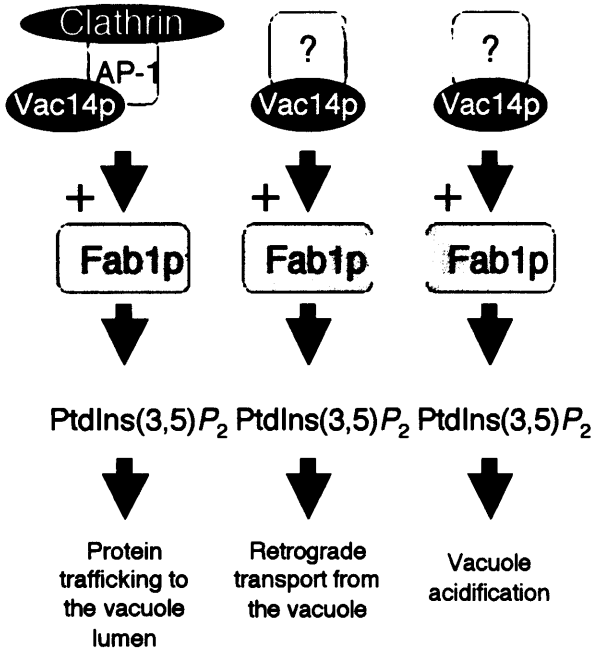

Figure 6.3.3. Proposed mechanism for AP-1 function in Fab1p-dependant protein trafficking to the vacuole. Retrograde transport from the lumen, and vacuole acidification mechanisms also require Vac14p and other as yet unidentified proteins.

6.4 Future Work

We would like to characterise the interaction between Fab1p, Vac14p and AP-1 to identify precisely where binding occurs between these proteins. This has been partially facilitated by the identification of an interaction between the trunk section of Apl4p and Vac14p (Dr. S. K Dove, personal communication) whereas from our yeast two-hybrid data, full-length Fab1p interacts with Apl2p. We aim to employ further yeast two-hybrid analysis, affinity chromatography and site directed mutagenesis to define the sites of interaction between these proteins and through mutagenesis disrupt potential areas of interaction thus elucidating more about the function of these proteins.

If Fab1p is an effector of AP-1, it is possible that other AP-1 dependant processes require Fab1p. Therefore we want to assay AP-1 function in *fab1*Δ and *vac14*Δ cells. Consequently we hope to develop and improve on existing assays whereby we can monitor AP-1 function in these cells. We aim to exploit an *in vivo* microscope assay and calcofluor growth assay to assess calcofluor binding and sensitivity in *fab1*Δ/*chs6*Δ and *vac14*Δ/*chs6*Δ cells thereby attempting to establish a role for Fab1p and Vac14p with respect to AP-1 function.

We also propose to fuse GFP to the C-terminus of Kex2p and analyse the location of this fusion protein in AP-1 complex component deletion mutants. Previous work has demonstrated that the combination of $chc1^{ts}$ with disruption of AP-1 subunit genes induces α-maturation defects with simultaneous missorting of Kex2p from the TGN (Phan et al., 1994; Rad et al., 1995; Yeung et al., 1999). Thus localisation of Kex2p requires clathrin and AP-1. To our knowledge, Kex2p-GFP localisation has not been assayed in single AP-1 complex component deletion mutants. Thus, if Kex2p-GFP is mislocalised to a compartment other than the TGN in AP-1 complex component deletion mutants, this assay will serve as a reference phenotype for these cells and a convenient *in vivo* assay for AP-1 function. However, this depends on an obvious mislocalisation of Kex2p-GFP. Therefore we aim to analyse the location of the large type I transmembrane protein Vps10p (Marcusson et al., 1994) in AP-1 complex component deletion mutants. Vps10p stabilisation and retention at the TGN is independent of AP-1 (Deloche et al., 2001). By

performing dual labelling experiments with Kex2p-GFP and Vps10p-RFP in *fab1*Δ, *vac14*Δ cells and AP-1 complex component deletion mutants, we hope to demonstrate a common mechanistic link between AP-1, Fab1p and Vac14p.

If AP-1 is interacting with Fab1p to generate a small localised pool of PtdIns(3,5)P_2, it is likely one or more PtdIns(3,5)P_2-specific binding proteins are recruited to this pool. Several PtdIns(3,5)P_2-binding proteins have recently been described; Ent3p, Ent5p, Svp1p and Vps24p (Dove et al., 2004; Eugster et al., 2004; Friant et al., 2003; Whitley et al., 2003) . Using the above assays to analyse AP-1 function in deletion mutants of these genes, may implicate AP-1 in a Fab1p dependant retrieval mechanism at the TGN. Other PtdIns(3,5)P_2-specific candidate proteins include Grd19p and Svp3p (Dove et al., 2004).

In conclusion, the yeast AP-1 adaptor complex regulates Fab1p to maintain wild-type levels of PtdIns(3,5)P_2 in *S. cerevisiae*. This regulation of PtdIns(3,5)P_2 is required for the trafficking of ubiquitinated cargos to the vacuole but does not appear to be required for other Fab1p-related functions. We propose that both Fab1p and AP-1 may be involved in regulating the retrieval of proteins to the TGN. Defining the mechanism of interaction between AP-1, Fab1p and Vac14p will be important, as it will help delineate the role of these proteins in trafficking pathways in yeast.

7 REFERENCES

Ahle, S., A. Mann, U. Eichelsbacher, and E. Ungewickell. 1988. Structural relationships between clathrin assembly proteins from the Golgi and the plasma membrane. *EMBO J.* 7:919-929.

Amerik, A.Y., J. Nowak, S. Swaminathan, and M. Hochstrasser. 2000. The Doa4 deubiquitinating enzyme is functionally linked to the vacuolar protein-sorting and endocytic pathways. *Mol. Biol. Cell.* 11:3365-3380.

Audhya, A., and S.D. Emr. 2002. Stt4 PI 4-kinase localizes to the plasma membrane and functions in the Pkc1-mediated MAP kinase cascade. *Dev. Cell.* 2:593-605.

Auger, K.R., C.L. Carpenter, L.C. Cantley, and L. Varticovski. 1989. Phosphatidylinositol 3-kinase and its novel product, phosphatidylinositol 3-phosphate, are present in *Saccharomyces cerevisiae*. *J. Biol. Chem.* 264:20181-20184.

Augsten, M., C. Hubner, M. Nguyen, W. Kunkel, A. Hartl, and R. Eck. 2002. Defective Hyphal induction of a Candida albicans phosphatidylinositol 3-phosphate 5-kinase null mutant on solid media does not lead to decreased virulence. *Infect. Immun.* 70:4462-4470.

Babst, M., D.J. Katzmann, E.J. Estepa-Sabal, T. Meerloo, and S.D. Emr. 2002. Escrt-III: an endosome-associated hetero-oligomeric protein complex required for mvb sorting. *Dev. Cell.* 3:271-282.

Baudin, A., O. Ozier-Kalogeropoulos, A. Denouel, F. Lacroute, and C. Cullin. 1993. A simple and efficient method for direct gene deletion in *Saccharomyces cerevisiae*. *Nucleic Acids Res.* 21:3329-3330.

Bauerle, C., M.N. Ho, M.A. Lindorfer, and T.H. Stevens. 1993. The *Saccharomyces cerevisiae VMA6* gene encodes the 36-kDa subunit of the vacuolar H(+)-ATPase membrane sector. *J. Biol. Chem.* 268:12749-12757.

Bidlingmaier, S., and M. Snyder. 2002. Large-scale identification of genes important for apical growth in *Saccharomyces cerevisiae* by directed allele replacement technology (DART) screening. *Funct. Integr. Genomics.* 1:345-356.

Blader, I.J., M.J. Cope, T.R. Jackson, A.A. Profit, A.F. Greenwood, D.G. Drubin, G.D. Prestwich, and A.B. Theibert. 1999. GCS1, an Arf guanosine triphosphatase-activating protein in *Saccharomyces cerevisiae*, is required for normal actin cytoskeletal organization in vivo and stimulates actin polymerization in vitro. *Mol. Biol. Cell.* 10:581-596.

Boehm, M., and J.S. Bonifacino. 2001. Adaptins: the final recount. *Mol. Biol. Cell.* 12:2907-2920.

Boehm, M., and J.S. Bonifacino. 2002. Genetic analyses of adaptin function from yeast to mammals. *Gene*. 286:175-186.

Bonangelino, C.J., N.L. Catlett, and L.S. Weisman. 1997. Vac7p, a novel vacuolar protein, is required for normal vacuole inheritance and morphology. *Mol. Cell Biol.* 17:6847-6858.

Bonangelino, C.J., J.J. Nau, J.E. Duex, M. Brinkman, A.E. Wurmser, J.D. Gary, S.D. Emr, and L.S. Weisman. 2002. Osmotic stress-induced increase of phosphatidylinositol 3,5-bisphosphate requires Vac14p, an activator of the lipid kinase Fab1p. *J. Cell Biol.* 156:1015-1028.

Bonifacino, J.S., and E.C. Dell'Angelica. 1999. Molecular bases for the recognition of tyrosine-based sorting signals. *J. Cell Biol.* 145:923-926.

Boronenkov, I.V., and R.A. Anderson. 1995. The sequence of phosphatidylinositol-4-phosphate 5-kinase defines a novel family of lipid kinases. *J. Biol. Chem.* 270:2881-2884.

Botstein, D., and G.R. Fink. 1988. Yeast: an experimental organism for modern biology. *Science*. 240:1439-1443.

Brickner, J.H., and R.S. Fuller. 1997. SOI1 encodes a novel, conserved protein that promotes TGN-endosomal cycling of Kex2p and other membrane proteins by modulating the function of two TGN localization signals. *J Cell Biol.* 139:23-36.

Bryant, N.J., R.C. Piper, L.S. Weisman, and T.H. Stevens. 1998. Retrograde traffic out of the yeast vacuole to the TGN occurs via the prevacuolar/endosomal compartment. *J. Cell Biol.* 142:651-663.

Bryant, N.J., and T.H. Stevens. 1997. Two separate signals act independently to localize a yeast late Golgi membrane protein through a combination of retrieval and retention. *J. Cell Biol.* 136:287-297.

Bryant, N.J., and T.H. Stevens. 1998. Vacuole biogenesis in *Saccharomyces cerevisiae*: protein transport pathways to the yeast vacuole. *Microbiol. Mol. Biol. Rev.* 62:230-247.

Burd, C.G., and S.D. Emr. 1998. Phosphatidylinositol (3)-phosphate signalling mediated by specific binding to RING FYVE domains. *Mol. Cell.* 2:157-162.

Cantley, L.C. 2002. The phosphoinositide 3-kinase pathway. *Science*. 296:1655-1657.

Cockell, M., H. Renauld, P. Watt, and S.M. Gasser. 1998. Sif2p interacts with Sir4p amino-terminal domain and antagonizes telomeric silencing in yeast. *Curr. Biol.* 8:787-790.

Coe, J.G., A.C. Lim, J. Xu, and W. Hong. 1999. A role for Tlg1p in the transport of proteins within the Golgi apparatus of *Saccharomyces cerevisiae*. *Mol. Biol. Cell.* 10:2407-2423.

Cooke, F.T. 2002. Phosphatidylinositol 3,5-bisphosphate: metabolism and function. *Arch. Biochem. Biophys.* 407:143-151.

Cooke, F.T. 2004. Phosphoinositides: older than we first thought? *Curr. Biol.* 14:R762-764.

Cooke, F.T., S.K. Dove, R.K. McEwen, G. Painter, A.B. Holmes, M.N. Hall, R.H. Michell, and P.J. Parker. 1998. The stress-activated phosphatidylinositol 3-phosphate 5-kinase Fab1p is essential for vacuole function in *S. cerevisiae*. *Curr. Biol.* 8:1219-1222.

Corvera, S., A. D'Arrigo, and H. Stenmark. 1999. Phosphoinositides in membrane traffic. *Curr. Opin. Cell Biol.* 11:460-465.

Cowles, C.R., G. Odorizzi, G.S. Payne, and S.D. Emr. 1997a. The AP-3 adaptor complex is essential for cargo-selective transport to the yeast vacuole. *Cell.* 91:109-118.

Cowles, C.R., W.B. Snyder, C.G. Burd, and S.D. Emr. 1997b. Novel Golgi to vacuole delivery pathway in yeast: identification of a sorting determinant and required transport component. *EMBO J.* 16:2769-2782.

Cozier, G.E., J. Carlton, A.H. McGregor, P.A. Gleeson, R.D. Teasdale, H. Mellor, and P.J. Cullen. 2002. The phox homology (PX) domain-dependent, 3-phosphoinositide-mediated association of sorting nexin-1 with an early sorting endosomal compartment is required for its ability to regulate epidermal growth factor receptor degradation. *J. Biol. Chem.* 277:48730-48736. Epub. 42002 Aug 48726.

Cullen, P.J., G.E. Cozier, G. Banting, and H. Mellor. 2001. Modular phosphoinositide-binding domains-their role in signalling and membrane trafficking. *Curr. Biol.* 11:R882-893.

De Camilli, P., H. Chen, J. Hyman, E. Panepucci, A. Bateman, and A.T. Brunger. 2002. The ENTH domain. *FEBS Lett.* 513:11-18.

Dell'Angelica, E.C., J. Klumperman, W. Stoorvogel, and J.S. Bonifacino. 1998. Association of the AP-3 adaptor complex with clathrin. *Science.* 280:431-434.

Dell'Angelica, E.C., C. Mullins, and J.S. Bonifacino. 1999. AP-4, a novel protein complex related to clathrin adaptors. *J. Biol. Chem.* 274:7278-7285.

Dell'Angelica, E.C., H. Ohno, C.E. Ooi, E. Rabinovich, K.W. Roche, and J.S. Bonifacino. 1997. AP-3: an adaptor-like protein complex with ubiquitous expression. *EMBO J.* 16:917-928.

Deloche, O., B.G. Yeung, G.S. Payne, and R. Schekman. 2001. Vps10p transport from the trans-Golgi network to the endosome is mediated by clathrin-coated vesicles. *Mol. Biol. Cell.* 12:475-485.

Desrivières, S., F.T. Cooke, P.J. Parker, and M.N. Hall. 1998. MSS4, a phosphatidylinositol-4-phosphate 5-kinase required for organization of the actin cytoskeleton in *Saccharomyces cerevisiae*. *J. Biol. Chem.* 273:15787-15793.

Doray, B., and S. Kornfeld. 2001. Gamma subunit of the AP-1 adaptor complex binds clathrin: implications for cooperative binding in coated vesicle assembly. *Mol. Biol. Cell.* 12:1925-1935.

Dove, S.K., F.T. Cooke, M.R. Douglas, L.G. Sayers, P.J. Parker, and R.H. Michell. 1997. Osmotic stress activates phosphatidylinositol-3,5-bisphosphate synthesis. *Nature (London).* 390:187-192.

Dove, S.K., R.K. McEwen, A. Mayes, D.C. Hughes, J.D. Beggs, and R.H. Michell. 2002. Vac14 Controls PtdIns(3,5)P(2) Synthesis and Fab1-Dependent Protein Trafficking to the Multivesicular Body. *Curr. Biol.* 12:885-893.

Dove, S.K., R.C. Piper, R.K. McEwen, J.W. Yu, M.C. King, D.C. Hughes, J. Thuring, A.B. Holmes, F.T. Cooke, R.H. Michell, P.J. Parker, and M.A. Lemmon. 2004. Svp1p defines a family of phosphatidylinositol 3,5-bisphosphate effectors. *EMBO J.* 23:1922-1933. Epub 2004 Apr 1922.

Duncan, M.C., G. Costaguta, and G.S. Payne. 2003. Yeast epsin-related proteins required for Golgi-endosome traffic define a gamma-adaptin ear-binding motif. *Nat. Cell Biol.* 5:77-81.

Epple, U.D., I. Suriapranata, E.L. Eskelinen, and M. Thumm. 2001. Aut5/Cvt17p, a putative lipase essential for disintegration of autophagic bodies inside the vacuole. *J. Bacteriol.* 183:5942-5955.

Erdman, S., L. Lin, M. Malczynski, and M. Snyder. 1998. Pheromone-regulated genes required for yeast mating differentiation. *J. Cell Biol.* 140:461-483.

Eugster, A., E.I. Pecheur, F. Michel, B. Winsor, F. Letourneur, and S. Friant. 2004. Ent5p is required with Ent3p and Vps27p for ubiquitin-dependent protein sorting into the multivesicular body. *Mol. Biol. Cell.* 23:23.

Fields, S., and O. Song. 1989. A novel genetic system to detect protein-protein interactions. *Nature.* 340:245-246.

Friant, S., E.I. Pecheur, A. Eugster, F. Michel, Y. Lefkir, D. Nourrisson, and F. Letourneur. 2003. Ent3p Is a PtdIns(3,5)*P2* effector required for protein sorting to the multivesicular body. *Dev. Cell.* 5:499-511.

Gallusser, A., and T. Kirchhausen. 1993. The beta 1 and beta 2 subunits of the AP complexes are the clathrin coat assembly components. *EMBO J.* 12:5237-5244.

Garcia-Bustos, J.F., F. Marini, I. Stevenson, C. Frei, and M.N. Hall. 1994. PIK1, an essential phosphatidylinositol 4-kinase associated with the yeast nucleus. *EMBO J.* 13:2352-2361.

Gary, J.D., T.K. Sato, C.J. Stefan, C.J. Bonangelino, L.S. Weisman, and S.D. Emr. 2002. Regulation of fab1 phosphatidylinositol 3-phosphate 5-kinase pathway by vac7 protein and fig4, a polyphosphoinositide phosphatase family member. *Mol. Biol. Cell.* 13:1238-1251.

Gary, J.D., A.E. Wurmser, C.J. Bonangelino, L.S. Weisman, and S.D. Emr. 1998. Fab1p is essential for PtdIns(3)*P* 5-kinase activity and the maintenance of vacuolar size and membrane homeostasis. *J. Cell. Biol.* 143:65-79.

Gaullier, J.M., E. Ronning, D.J. Gillooly, and H. Stenmark. 2000. Interaction of the EEA1 FYVE finger with phosphatidylinositol 3-phosphate and early endosomes. Role of conserved residues. *J. Biol. Chem.* 275:24595-24600.

Gaullier, J.M., A. Simonsen, A. D'Arrigo, B. Bremnes, H. Stenmark, and R. Aasland. 1998. FYVE fingers bind PtdIns(3)*P*. *Nature.* 394:432-433.

Gietz, R.D., and A. Sugino. 1988. New yeast-*Escherichia coli* shuttle vectors constructed with *in vitro* mutagenized yeast genes lacking six-base pair restriction sites. *Gene.* 74:527-534.

Gietz, R.D., and R.A. Woods. 2002. Transformation of yeast by lithium acetate/single-stranded carrier DNA/polyethylene glycol method. *Methods Enzymol.* 350:87-96.

Gillooly, D.J., A. Simonsen, and H. Stenmark. 2001. Cellular functions of phosphatidylinositol 3-phosphate and FYVE domain proteins. *Biochem. J.* 355:249-258.

Goffeau, A., B.G. Barrell, H Bussey, R.W. Davis, B. Dujon, H Feldmann, F. Galilbert, J.D. Hoheisel, C. Jacq, M. Johnston, E.J. Louis, H.W. Mewes, Y. Murakami, P. Philippsen, H. Tettelin and S.G. Oliver. 1996. Life with 6000 genes. *Science.* 275:1051-1052.

Gomes de Mesquita, D.S., H.B. van den Hazel, J. Bouwman, and C.L. Woldringh. 1996. Characterization of new vacuolar segregation mutants, isolated by screening for loss of proteinase B self-activation. *Eur. J. Cell Biol.* 71:237-247.

Graham, L.A., B. Powell, and T.H. Stevens. 2000. Composition and assembly of the yeast vacuolar H(+)-ATPase complex. *J. Exp. Biol.* 203 Pt 1:61-70.

Grant, B.D., W. Hemmer, I. Tsigelny, J.A. Adams, and S.S. Taylor. 1998. Kinetic analyses of mutations in the glycine-rich loop of cAMP-dependent protein kinase. *Biochemistry.* 37:7708-7715.

Greene, L.E., and E. Eisenberg. 1990. Dissociation of clathrin from coated vesicles by the uncoating ATPase. *J. Biol. Chem.* 265:6682-6687.

Guarente, L. 1983. Yeast promoters and lacZ fusions designed to study expression of cloned genes in yeast. *Methods Enzymol.* 101:181-191.

Guo, S., L.E. Stolz, S.M. Lemrow, and J.D. York. 1999. SAC1-like domains of yeast SAC1, INP52, and INP53 and of human synaptojanin encode polyphosphoinositide phosphatases. *J. Biol. Chem.* 274:12990-12995.

Han, G.S., A. Audhya, D.J. Markley, S.D. Emr, and G.M. Carman. 2002. The Saccharomyces cerevisiae LSB6 gene encodes phosphatidylinositol 4-kinase activity. *J. Biol. Chem.* 277:47709-47718. Epub 42002 Oct 47701.

Hanks, S.K., and T. Hunter. 1995. Protein kinases 6. The eukaryotic protein kinase superfamily: kinase (catalytic) domain structure and classification. *Faseb J.* 9:576-596.

Hartmann-Petersen, R., M. Wallace, K. Hofmann, G. Koch, A.H. Johnsen, K.B. Hendil, and C. Gordon. 2004. The Ubx2 and Ubx3 cofactors direct Cdc48 activity to proteolytic and nonproteolytic ubiquitin-dependent processes. *Curr. Biol.* 14:824-828.

Hemmer, W., M. McGlone, I. Tsigelny, and S.S. Taylor. 1997. Role of the glycine triad in the ATP-binding site of cAMP-dependent protein kinase. *J. Biol. Chem.* 272:16946-16954.

Herman, P.K., and S.D. Emr. 1990. Characterization of *VPS34*, a gene required for vacuolar protein sorting and vacuole segregation in *Saccharomyces cerevisiae*. *Mol. Cell. Biol.* 10:6742-6754.

Hettema, E.H., J. Valdez-Taubas, and H.R. Pelham. 2004. Bsd2 binds the ubiquitin ligase Rsp5 and mediates the ubiquitination of transmembrane proteins. *EMBO J.* 23:1279-1288. Epub 2004 Feb 1226.

Heuser, J.E., and J. Keen. 1988. Deep-etch visualization of proteins involved in clathrin assembly. *J. Cell Biol.* 107:877-886.

Hicke, L., and R. Dunn. 2003. Regulation of membrane protein transport by ubiquitin and ubiquitin-binding proteins. *Annu. Rev. Cell Dev. Biol.* 19:141-172.

Hinchliffe, K.A., A. Ciruela, and R.F. Irvine. 1998. PIPkins1, their substrates and their products: new functions for old enzymes. *Biochim. Biophys. Acta.* 1436:87-104.

Hirst, J., and M.S. Robinson. 1998. Clathrin and adaptors. *Biochim. Biophys. Acta.* 1404:173-193.

Holthuis, J.C., B.J. Nichols, and H.R. Pelham. 1998. The syntaxin Tlg1p mediates trafficking of chitin synthase III to polarized growth sites in yeast. *Mol. Biol. Cell.* 9:3383-3397.

Homma, K., S. Terui, M. Minemura, H. Qadota, Y. Anraku, Y. Kanaho, and Y. Ohya. 1998. Phosphatidylinositol-4-phosphate 5-kinase localized on the plasma membrane is essential for yeast cell morphogenesis. *J. Biol. Chem.* 273:15779-15786.

Hughes, W.E., M.J. Pocklington, E. Orr, and C.J. Paddon. 1999. Mutations in the *Saccharomyces cerevisiae* gene *SAC1* cause multiple drug sensitivity. *Yeast.* 15:1111-1124.

Hughes, W.E., R. Woscholski, Cooke F. T., R.S. Patrick, S.K. Dove, N.Q. McDonald, and P.J. Parker. 2000. *SAC1* encodes a regulated lipid phosphoinositide phosphatase, defects in which can be suppressed by the homologous Inp52p and Inp53p phosphatases. *J. Biol. Chem.* 275:801-808.

Hurley, J.H., and T. Meyer. 2001. Subcellular targeting by membrane lipids. *Curr. Opin. Cell Biol.* 13:146-152.

Ikonomov, O.C., D. Sbrissa, K. Mlak, M. Kanzaki, J. Pessin, and A. Shisheva. 2002. Functional dissection of lipid and protein kinase signals of PIKfyve reveals the role of PtdIns 3,5-*P2* production for endomembrane integrity. *J. Biol. Chem.* 277:9206-9211.

Ikonomov, O.C., D. Sbrissa, and A. Shisheva. 2001. Mammalian cell morphology and endocytic membrane homeostasis require enzymatically active phosphoinositide 5-kinase PIKfyve. *J. Biol. Chem.* 276:26141-26147.

Irvine, R.F. 2002. Nuclear lipid signalling. *Sci STKE.* 2002:RE13.

Irvine, R.F. 2003. Nuclear lipid signalling. *Nat. Rev. Mol. Cell Biol.* 4:349-360.

James, P., J. Halladay, and E.A. Craig. 1996. Genomic libraries and a host strain designed for highly efficient two-hybrid selection in yeast. *Genetics.* 144:1425-1436.

Jelen, F., A. Oleksy, K. Smietana, and J. Otlewski. 2003. PDZ domains - common players in the cell signaling. *Acta. Biochim. Pol.* 50:985-1017.

Jones, D.R., A. Gonzalez-Garcia, E. Diez, A.C. Martinez, A.C. Carrera, and I. Merida. 1999. The identification of phosphatidylinositol 3,5-bisphosphate in T- lymphocytes and its regulation by interleukin-2. *J. Biol. Chem.* 274:18407-18413.

Jones, J.M., P. Datta, S.M. Srinivasula, W. Ji, S. Gupta, Z. Zhang, E. Davies, G. Hajnoczky, T.L. Saunders, M.L. Van Keuren, T. Fernandes-Alnemri, M.H. Meisler, and E.S. Alnemri. 2003. Loss of Omi mitochondrial protease activity causes the neuromuscular disorder of mnd2 mutant mice. *Nature.* 425:721-727. Epub 2003 Oct 2008.

Katzmann, D.J., M. Babst, and S.D. Emr. 2001. Ubiquitin-dependent sorting into the multivesicular body pathway requires the function of a conserved endosomal protein sorting complex, ESCRT-I. *Cell.* 106:145-155.

Katzmann, D.J., S. Sarkar, T. Chu, A. Audhya, and S.D. Emr. 2004. Multivesicular body sorting: ubiquitin ligase Rsp5 is required for the modification and sorting of carboxypeptidase S. *Mol. Biol Cell.* 15:468-480. Epub 2003 Dec 2002.

Katzmann, D.J., C.J. Stefan, M. Babst, and S.D. Emr. 2003. Vps27 recruits ESCRT machinery to endosomes during MVB sorting. *J. Cell Biol.* 162:413-423.

Kay, B.K., M. Yamabhai, B. Wendland, and S.D. Emr. 1999. Identification of a novel domain shared by putative components of the endocytic and cytoskeletal machinery. *Protein Sci.* 8:435-438.

Kearns, M.A., D.E. Monks, M. Fang, M.P. Rivas, P.D. Courtney, J. Chen, G.D. Prestwich, A.B. Theibert, R.E. Dewey, and V.A. Bankaitis. 1998. Novel developmentally regulated phosphoinositide binding proteins from soybean whose expression bypasses the requirement for an essential phosphatidylinositol transfer protein in yeast. *EMBO J.* 17:4004-4017.

Keen, J.H. 1987. Clathrin assembly proteins: affinity purification and a model for coat assembly. *J. Cell Biol.* 105:1989-1998.

Kirchhausen, T. 1999. Adaptors for clathrin-mediated traffic. *Annu. Rev. Cell Dev. Biol.* 15:705-732.

Kirchhausen, T., K.L. Nathanson, W. Matsui, A. Vaisberg, E.P. Chow, C. Burne, J.H. Keen, and A.E. Davis. 1989. Structural and functional division into two domains of the large (100- to 115-kDa) chains of the clathrin-associated protein complex AP-2. *Proc. Natl. Acad. Sci. U S A.* 86:2612-2616.

Klionsky, D.J., P.K. Herman, and S.D. Emr. 1990. The fungal vacuole: composition, function, and biogenesis. *Microbiol. Rev.* 54:266-292.

Komada, M., R. Masaki, A. Yamamoto, and N. Kitamura. 1997. Hrs, a tyrosine kinase substrate with a conserved double zinc finger domain, is localized to the cytoplasmic surface of early endosomes. *J. Biol. Chem.* 272:20538-20544.

Kornfeld, S., and I. Mellman. 1989. The biogenesis of lysosomes. *Annu. Rev. Cell Biol.* 5:483-525.

Kunz, J., M.P. Wilson, M. Kisseleva, J.H. Hurley, P.W. Majerus, and R.A. Anderson. 2000. The activation loop of phosphatidylinositol phosphate kinases determines signaling specificity. *Mol. Cell.* 5:1-11.

Leevers, S.J., B. Vanhaesebroeck, and M.D. Waterfield. 1999. Signalling through phosphoinositide 3-kinases: the lipids take centre stage. *Curr. Opin. Cell Biol.* 11:219-225.

Lemmon, M.A. 2003. Phosphoinositide recognition domains. *Traffic.* 4:201-213.

Liu, X.F., and V.C. Culotta. 1999. Post-translation control of Nramp metal transport in yeast. Role of metal ions and the BSD2 gene. *J. Biol. Chem.* 274:4863-4868.

Liu, X.F., F. Supek, N. Nelson, and V.C. Culotta. 1997. Negative control of heavy metal uptake by the *Saccharomyces cerevisiae* BSD2 gene. *J. Biol. Chem.* 272:11763-11769.

Llorca, O., E.A. McCormack, G. Hynes, J. Grantham, J. Cordell, J.L. Carrascosa, K.R. Willison, J.J. Fernandez, and J.M. Valpuesta. 1999. Eukaryotic type II chaperonin CCT interacts with actin through specific subunits. *Nature.* 402:693-696.

Lohr, D., P. Venkov, and J. Zlatanova. 1995. Transcriptional regulation in the yeast GAL gene family: a complex genetic network. *Faseb J.* 9:777-787.

Lopez, F., M. Leube, R. Gil-Mascarell, J.P. Navarro-Avino, and R. Serrano. 1999. The yeast inositol monophosphatase is a lithium- and sodium-sensitive enzyme encoded by a non-essential gene pair. *Mol. Microbiol.* 31:1255-1264.

Marcusson, E.G., B.F. Horazdovsky, J.L. Cereghino, E. Gharakhanian, and S.D. Emr. 1994. The sorting receptor for yeast vacuolar carboxypeptidase Y is encoded by the *VPS10* gene. *Cell.* 77:579-586.

McEwen, R.K., S.K. Dove, F.T. Cooke, G.F. Painter, A.B. Holmes, A. Shisheva, Y. Ohya, P.J. Parker, and R.H. Michell. 1999. Complementation analysis in PtdInsP kinase-deficient yeast mutants demonstrates that *Schizosaccharomyces pombe* and murine Fab1p homologues are phosphatidylinositol 3-phosphate 5-kinases. *J. Biol. Chem.* 274:33905-33912.

Meijer, H.J., C.P. Berrie, C. Iurisci, N. Divecha, A. Musgrave, and T. Munnik. 2001. Identification of a new polyphosphoinositide in plants, phosphatidylinositol 5-monophosphate (PtdIns5*P*), and its accumulation upon osmotic stress. *Biochem. J.* 360:491-498.

Meijer, H.J.G., N. Divecha, H. Van den Ende, A. Musgrave, and T. Munnik. 1999. Hyperosmotic stress induces rapid synthesis of phosphatidyl-D-inositol 3,5-bisphosphate in plant cells. *Planta.* 208:294-298.

Mitra, P., Y. Zhang, L.E. Rameh, M.P. Ivshina, D. McCollum, J.J. Nunnari, G.M. Hendricks, M.L. Kerr, S.J. Field, L.C. Cantley, and A.H. Ross. 2004. A novel phosphatidylinositol(3,4,5)*P3* pathway in fission yeast. *J. Cell Biol.* 166:205-211. Epub 2004 Jul 2012.

Morishita, M., F. Morimoto, K. Kitamura, T. Koga, Y. Fukui, H. Maekawa, I. Yamashita, and C. Shimoda. 2002. Phosphatidylinositol 3-phosphate 5-kinase is required for the cellular response to nutritional starvation and mating pheromone signals in *Schizosaccharomyces pombe*. *Genes Cells.* 7:199-215.

Morvan, J., M. Froissard, R. Haguenauer-Tsapis, and D. Urban-Grimal. 2004. The ubiquitin ligase Rsp5p is required for modification and sorting of membrane proteins into multivesicular bodies. *Traffic.* 5:383-392.

Mu, F.T., J.M. Callaghan, O. Steele-Mortimer, H. Stenmark, R.G. Parton, P.L. Campbell, J. McCluskey, J.P. Yeo, E.P. Tock, and B.H. Toh. 1995. EEA1, an early endosome-associated protein. EEA1 is a conserved alpha-helical peripheral membrane protein flanked by cysteine "fingers" and contains a calmodulin-binding IQ motif. *J. Biol. Chem.* 270:13503-13511.

Munn, A.L. 2001. Molecular requirements for the internalisation step of endocytosis: insights from yeast. *Biochim. Biophys. Acta.* 1535:236-257.

Murray, M., and M.L. Greenberg. 2000. Expression of yeast *INM1* encoding inositol monophosphatase is regulated by inositol, carbon source and growth stage and is decreased by lithium and valproate. *Mol. Microbiol.* 36:651-661.

Neer, E.J., C.J. Schmidt, R. Nambudripad, and T.F. Smith. 1994. The ancient regulatory-protein family of WD-repeat proteins. *Nature.* 371:297-300.

Odorizzi, G., M. Babst, and S.D. Emr. 1998. Fab1p PtdIns(3)P 5-kinase function essential for protein sorting in the multivesicular body. *Cell.* 95:847-858.

Odorizzi, G., M. Babst, and S.D. Emr. 2000. Phosphoinositide signaling and the regulation of membrane trafficking in yeast. *Trends Biochem. Sci.* 25:229-235.

Ogawa, N., J. DeRisi, and P.O. Brown. 2000. New components of a system for phosphate accumulation and polyphosphate metabolism in *Saccharomyces cerevisiae* revealed by genomic expression analysis. *Mol. Biol. Cell.* 11:4309-4321.

Ohno, H., J. Stewart, M.C. Fournier, H. Bosshart, I. Rhee, S. Miyatake, T. Saito, A. Gallusser, T. Kirchhausen, and J.S. Bonifacino. 1995. Interaction of tyrosine-based sorting signals with clathrin-associated proteins. *Science.* 269:1872-1875.

Otte, S., W.J. Belden, M. Heidtman, J. Liu, O.N. Jensen, and C. Barlowe. 2001. Erv41p and Erv46p: new components of COPII vesicles involved in transport between the ER and Golgi complex. *J. Cell Biol.* 152:503-518.

Palmer, R.E., E. Hogan, and D. Koshland. 1990. Mitotic transmission of artificial chromosomes in cdc mutants of the yeast, *Saccharomyces cerevisiae. Genetics.* 125:763-774.

Patki, V., D.C. Lawe, S. Corvera, J.V. Virbasius, and A. Chawla. 1998. A functional PtdIns(3)*P*-binding motif. *Nature.* 394:433-434.

Patki, V., J. Virbasius, W.S. Lane, B.H. Toh, H.S. Shpetner, and S. Corvera. 1997. Identification of an early endosomal protein regulated by phosphatidylinositol 3-kinase. *Proc. Natl. Acad. Sci. U S A.* 94:7326-7330.

Payne, G.S., and R. Schekman. 1989. Clathrin: a role in the intracellular retention of a Golgi membrane protein. *Science.* 245:1358-1365.

Pearse, B.M. 1975. Coated vesicles from pig brain: purification and biochemical characterization. *J. Mol. Biol.* 97:93-98.

Pearse, B.M., and M.S. Robinson. 1984. Purification and properties of 100-kd proteins from coated vesicles and their reconstitution with clathrin. *EMBO J.* 3:1951-1957.

Phan, H.L., J.A. Finlay, D.S. Chu, P.K. Tan, T. Kirchhausen, and G.S. Payne. 1994. The *Saccharomyces cerevisiae* APS1 gene encodes a homolog of the small subunit of the mammalian clathrin AP-1 complex: evidence for functional interaction with clathrin at the Golgi complex. *EMBO J.* 13:1706-1717.

Ponting, C.P., and P. Bork. 1996. Pleckstrin's repeat performance: a novel domain in G-protein signaling? *Trends Biochem. Sci.* 21:245-246.

Preston, R.A., R.F. Murphy, and E.W. Jones. 1989. Assay of vacuolar pH in yeast and identification of acidification-defective mutants. *Proc. Natl. Acad. Sci. U S A.* 86:7027-7031.

Rad, M.R., H.L. Phan, L. Kirchrath, P.K. Tan, T. Kirchhausen, C.P. Hollenberg, and G.S. Payne. 1995. *Saccharomyces cerevisiae* Apl2p, a homologue of the mammalian clathrin AP beta subunit, plays a role in clathrin-dependent Golgi functions. *J. Cell Sci.* 108:1605-1615.

Rameh, L.E., and L.C. Cantley. 1999. The role of phosphoinositide 3-kinase lipid products in cell function. *J. Biol. Chem.* 274:8347-8350.

Rameh, L.E., K.F. Tolias, B.C. Duckworth, and L.C. Cantley. 1997. A new pathway for synthesis of phosphatidylinositol-4,5-bisphosphate. *Nature.* 390:192-196.

Rapoport, I., Y.C. Chen, P. Cupers, S.E. Shoelson, and T. Kirchhausen. 1998. Dileucine-based sorting signals bind to the beta chain of AP-1 at a site distinct and regulated differently from the tyrosine-based motif-binding site. *EMBO J.* 17:2148-2155.

Redding, K., C. Holcomb, and R.S. Fuller. 1991. Immunolocalization of Kex2 protease identifies a putative late Golgi compartment in the yeast *Saccharomyces cerevisiae. J. Cell. Biol.* 113:527-538.

Redding, K., M. Seeger, G.S. Payne, and R.S. Fuller. 1996. The effects of clathrin inactivation on localization of Kex2 protease are independent of the TGN localization signal in the cytosolic tail of Kex2p. *Mol. Biol. Cell.* 7:1667-1677.

Reggiori, F., and H.R. Pelham. 2001. Sorting of proteins into multivesicular bodies: ubiquitin-dependent and -independent targeting. *EMBO J.* 20:5176-5186.

Reggiori, F., and H.R. Pelham. 2002. A transmembrane ubiquitin ligase required to sort membrane proteins into multivesicular bodies. *Nat. Cell. Biol.* 4:117-123.

Robinson, M.S. 1987. 100-kD coated vesicle proteins: molecular heterogeneity and intracellular distribution studied with monoclonal antibodies. *J. Cell Biol.* 104:887-895.

Robinson, M.S. 2004. Adaptable adaptors for coated vesicles. *Trends Cell Biol.* 14:167-174.

Roth, M.G., and P.C. Sternweis. 1997. The role of lipid signaling in constitutive membrane traffic. *Curr. Opin. Cell Biol.* 9:519-526.

Rudge, S.A., D.M. Anderson, and S.D. Emr. 2004. Vacuole size control: regulation of PtdIns(3,5)P2 levels by the vacuole-associated Vac14-Fig4 complex, a PtdIns(3,5)*P2*-specific phosphatase. *Mol. Biol Cell.* 15:24-36. Epub 2003 Oct 2003.

Sbrissa, D., O. Ikonomov, and A. Shisheva. 2001. Selective insulin-induced activation of class I(A) phosphoinositide 3- kinase in PIKfyve immune complexes from 3T3-L1 adipocytes. *Mol. Cell Endocrinol.* 181:35-46.

Sbrissa, D., O.C. Ikonomov, and A. Shisheva. 1999. PIKfyve, a mammalian ortholog of yeast Fab1p lipid kinase, synthesizes 5-phosphoinositides. Effect of insulin. *J. Biol. Chem.* 274:21589-21597.

Sbrissa, D., O.C. Ikonomov, and A. Shisheva. 2000. PIKfyve lipid kinase is a protein kinase: downregulation of 5'-phosphoinositide product formation by autophosphorylation. *Biochem.* 39:15980-15989.

Sbrissa, D., O.C. Ikonomov, and A. Shisheva. 2002. Phosphatidylinositol 3-phosphate-interacting domains in PIKfyve. Binding specificity and role in PIKfyve. Endomenbrane localization. *J. Biol. Chem.* 277:6073-6079.

Sbrissa, D., O.C. Ikonomov, J. Strakova, R. Dondapati, K. Mlak, R. Deeb, R. Silver, and A. Shisheva. 2004. A mammalian ortholog of *Saccharomyces cerevisiae* Vac14 that associates with and up-regulates PIKfyve phosphoinositide 5-kinase activity. *Mol. Cell Biol.* 24:10437-10447.

Schmid, S.L. 1997. Clathrin-coated vesicle formation and protein sorting: an integrated process. *Annu. Rev. Biochem.* 66:511-548.

Schroder, S., and E. Ungewickell. 1991. Subunit interaction and function of clathrin-coated vesicle adaptors from the Golgi and the plasma membrane. *J. Biol. Chem.* 266:7910-7918.

Reggiori, F., and H.R. Pelham. 2002. A transmembrane ubiquitin ligase required to sort membrane proteins into multivesicular bodies. *Nat. Cell. Biol.* 4:117-123.

Robinson, M.S. 1987. 100-kD coated vesicle proteins: molecular heterogeneity and intracellular distribution studied with monoclonal antibodies. *J. Cell Biol.* 104:887-895.

Robinson, M.S. 2004. Adaptable adaptors for coated vesicles. *Trends Cell Biol.* 14:167-174.

Roth, M.G., and P.C. Sternweis. 1997. The role of lipid signaling in constitutive membrane traffic. *Curr. Opin. Cell Biol.* 9:519-526.

Rudge, S.A., D.M. Anderson, and S.D. Emr. 2004. Vacuole size control: regulation of PtdIns(3,5)P2 levels by the vacuole-associated Vac14-Fig4 complex, a PtdIns(3,5)*P2*-specific phosphatase. *Mol. Biol Cell.* 15:24-36. Epub 2003 Oct 2003.

Sbrissa, D., O. Ikonomov, and A. Shisheva. 2001. Selective insulin-induced activation of class I(A) phosphoinositide 3- kinase in PIKfyve immune complexes from 3T3-L1 adipocytes. *Mol. Cell Endocrinol.* 181:35-46.

Sbrissa, D., O.C. Ikonomov, and A. Shisheva. 1999. PIKfyve, a mammalian ortholog of yeast Fab1p lipid kinase, synthesizes 5-phosphoinositides. Effect of insulin. *J. Biol. Chem.* 274:21589-21597.

Sbrissa, D., O.C. Ikonomov, and A. Shisheva. 2000. PIKfyve lipid kinase is a protein kinase: downregulation of 5'-phosphoinositide product formation by autophosphorylation. *Biochem.* 39:15980-15989.

Sbrissa, D., O.C. Ikonomov, and A. Shisheva. 2002. Phosphatidylinositol 3-phosphate-interacting domains in PIKfyve. Binding specificity and role in PIKfyve. Endomenbrane localization. *J. Biol. Chem.* 277:6073-6079.

Sbrissa, D., O.C. Ikonomov, J. Strakova, R. Dondapati, K. Mlak, R. Deeb, R. Silver, and A. Shisheva. 2004. A mammalian ortholog of *Saccharomyces cerevisiae* Vac14 that associates with and up-regulates PIKfyve phosphoinositide 5-kinase activity. *Mol. Cell Biol.* 24:10437-10447.

Schmid, S.L. 1997. Clathrin-coated vesicle formation and protein sorting: an integrated process. *Annu. Rev. Biochem.* 66:511-548.

Schroder, S., and E. Ungewickell. 1991. Subunit interaction and function of clathrin-coated vesicle adaptors from the Golgi and the plasma membrane. *J. Biol. Chem.* 266:7910-7918.

Schu, P.V., K. Takegawa, M.J. Fry, J.H. Stack, M.D. Waterfield, and S.D. Emr. 1993. Phosphatidylinositol 3-kinase encoded by yeast *VPS34* gene essential for protein sorting. *Science*. 260:88-91.

Schuberth, C., H. Richly, S. Rumpf, and A. Buchberger. 2004. Shp1 and Ubx2 are adaptors of Cdc48 involved in ubiquitin-dependent protein degradation. *EMBO Rep.* 5:818-824. Epub 2004 Jul 2016.

Schuller, C., J.L. Brewster, M.R. Alexander, M.C. Gustin, and H. Ruis. 1994. The HOG pathway controls osmotic regulation of transcription via the stress response element (STRE) of the *Saccharomyces cerevisiae* CTT1 gene. *EMBO J.* 13:4382-4389.

Schultz, J., F. Milpetz, P. Bork, and C.P. Ponting. 1998. SMART, a simple modular architecture research tool: identification of signaling domains. *Proc. Natl. Acad. Sci. U S A.* 95:5857-5864.

Seeger, M., and G.S. Payne. 1992. A role for clathrin in the sorting of vacuolar proteins in the Golgi complex of yeast. *EMBO J.* 11:2811-2818.

Shaw, J.D., H. Hama, F. Sohrabi, D.B. DeWald, and B. Wendland. 2003. PtdIns(3,5)*P2* is required for delivery of endocytic cargo into the multivesicular body. *Traffic.* 4:479-490.

Shen, X., R. Ranallo, E. Choi, and C. Wu. 2003. Involvement of actin-related proteins in ATP-dependent chromatin remodeling. *Mol. Cell.* 12:147-155.

Shih, W., A. Gallusser, and T. Kirchhausen. 1995. A clathrin-binding site in the hinge of the beta 2 chain of mammalian AP-2 complexes. *J. Biol. Chem.* 270:31083-31090.

Shisheva, A. 2001. PIKfyve: the road to PtdIns 5-P and PtdIns 3,5-P(2). *Cell. Biol. Int.* 25:1201-1206.

Shisheva, A., D. Sbrissa, and O. Ikonomov. 1999. Cloning, characterization, and expression of a novel Zn2+-binding FYVE finger-containing phosphoinositide kinase in insulin-sensitive cells. *Mol. Cell Biol.* 19:623-634.

Shoemaker, D.D., D.A. Lashkari, D. Morris, M. Mittmann, and R.W. Davis. 1996. Quantitative phenotypic analysis of yeast deletion mutants using a highly parallel molecular bar-coding strategy. *Nat. Genet.* 14:450-456.

Sickmann, A., J. Reinders, Y. Wagner, C. Joppich, R. Zahedi, H.E. Meyer, B. Schonfisch, I. Perschil, A. Chacinska, B. Guiard, P. Rehling, N. Pfanner, and C. Meisinger. 2003. The proteome of *Saccharomyces cerevisiae* mitochondria. *Proc. Natl. Acad. Sci. U S A.* 100:13207-13212. Epub 12003 Oct 13223.

Sikorski, R.S., and P. Hieter. 1989. A system of shuttle vectors and yeast host strains designed for efficient manipulation of DNA in *Saccharomyces cerevisiae*. *Genetics*. 122:19-27.

Simonsen, A., A.E. Wurmser, S.D. Emr, and H. Stenmark. 2001. The role of phosphoinositides in membrane transport. *Curr. Opin. Cell Biol.* 13:485-492.

Siniossoglou, S., E.C. Hurt, and H.R. Pelham. 2000. Psr1p/Psr2p, two plasma membrane phosphatases with an essential DXDX(T/V) motif required for sodium stress response in yeast. *J. Biol. Chem.* 275:19352-19360.

Spormann, D.O., J. Heim, and D.H. Wolf. 1992. Biogenesis of the yeast vacuole (lysosome). The precursor forms of the soluble hydrolase carboxypeptidase yscS are associated with the vacuolar membrane. *J. Biol. Chem.* 267:8021-8029.

Srinivasan, S., M. Seaman, Y. Nemoto, L. Daniell, S.F. Suchy, S. Emr, P. DeCamilli, and R. Nussbaum. 1997. Disruption of three phosphatidylinositol polyphosphate 5-phosphatase genes from *S. cerevisiae* results in pleiotropic abnormalities of vacuole morphology, cell shape and osmohomeostasis. *Eur. J. Cell Biol.* 74:350-360.

Stack, J.H., D.B. DeWald, K. Takegawa, and S.D. Emr. 1995. Vesicle-mediated protein transport: regulatory interactions between the Vps15 protein kinase and the Vps34 PtdIns 3-kinase essential for protein sorting to the vacuole in yeast. *J. Cell Biol.* 129:321-334.

Stenmark, H., and R. Aasland. 1999. FYVE-finger proteins--effectors of an inositol lipid. *J. Cell Sci.* 112:4175-4183.

Stenmark, H., R. Aasland, B.H. Toh, and A. D'Arrigo. 1996. Endosomal localization of the autoantigen EEA1 is mediated by a zinc- binding FYVE finger. *J. Biol. Chem.* 271:24048-24054.

Stephens, L.R., K.T. Hughes, and R.F. Irvine. 1991. Pathway of phosphatidylinositol(3,4,5)-trisphosphate synthesis in activated neutrophils. *Nature*. 351:33-39.

Stepp, J.D., K. Huang, and S.K. Lemmon. 1997. The yeast adaptor protein complex, AP-3, is essential for the efficient delivery of alkaline phosphatase by the alternate pathway to the vacuole. *J. Cell Biol.* 139:1761-1774.

Stepp, J.D., A. Pellicena-Palle, S. Hamilton, T. Kirchhausen, and S.K. Lemmon. 1995. A late Golgi sorting function for *Saccharomyces cerevisiae* Apm1p, but not for Apm2p, a second yeast clathrin AP medium chain-related protein. *Mol. Biol. Cell.* 6:41-58.

Stevens, T., B. Esmon, and R. Schekman. 1982. Early stages in the yeast secretory pathway are required for transport of carboxypeptidase Y to the vacuole. *Cell.* 30:439-448.

Stevens, T.H., and M. Forgac. 1997. Structure, function and regulation of the vacuolar (H+)-ATPase. *Annu. Rev. Cell. Dev. Biol.* 13:779-808.

Stolz, L.E., C.V. Huynh, J. Thorner, and J.D. York. 1998a. Identification and characterisation of an essential family of inositol polyphosphate 5-phosphatases (*INP51, INP52* and *INP53* gene products) in the yeast *Saccharomyces cerevisiae. Genetics.* 148:1715-1729.

Stolz, L.E., W.J. Kuo, J. Longchamps, M.K. Sekhon, and J.D. York. 1998b. *INP51,* a yeast inositol polyphosphate 5-phosphatase required for phosphatidylinositol-4,5-bisphosphate homeostasis and whose absence confers a cold-resistant phenotype. *J. Biol. Chem.* 273:11852-11861.

Sudol, M. 1996. Structure and function of the WW domain. *Prog. Biophys. Mol. Biol.* 65:113-132.

Swaminathan, S., A.Y. Amerik, and M. Hochstrasser. 1999. The Doa4 deubiquitinating enzyme is required for ubiquitin homeostasis in yeast. *Mol. Biol. Cell.* 10:2583-2594.

Takegawa, K., D.B. DeWald, and S.D. Emr. 1995. *Schizosaccharomyces pombe* Vps34p, a phosphatidylinositol-specific PI 3-kinase essential for normal cell growth and vacuole morphology. *J. Cell Sci.* 108:3745-3756.

Toker, A., and L.C. Cantley. 1997. Signalling through the lipid products of phosphoinositide-3-OH kinase. *Nature.* 387:673-676.

Uetz, P., L. Giot, G. Cagney, T.A. Mansfield, R.S. Judson, J.R. Knight, D. Lockshon, V. Narayan, M. Srinivasan, P. Pochart, A. Qureshi-Emili, Y. Li, B. Godwin, D. Conover, T. Kalbfleisch, G. Vijayadamodar, M. Yang, M. Johnston, S. Fields, and J.M. Rothberg. 2000. A comprehensive analysis of protein-protein interactions in *Saccharomyces cerevisiae. Nature.* 403:623-627.

Urech, K., M. Durr, T. Boller, A. Wiemken, and J. Schwencke. 1978. Localization of polyphosphate in vacuoles of *Saccharomyces cerevisiae. Arch. Microbiol.* 116:275-278.

Valdivia, R.H., D. Baggott, J.S. Chuang, and R.W. Schekman. 2002. The yeast clathrin adaptor protein complex 1 is required for the efficient retention of a subset of late Golgi membrane proteins. *Dev. Cell.* 2:283-294.

Valdivieso, M.H., P.C. Mol, J.A. Shaw, E. Cabib, and A. Duran. 1991. CAL1, a gene required for activity of chitin synthase 3 in *Saccharomyces cerevisiae. J. Cell Biol.* 114:101-109.

Vanhaesebroeck, B., and D.R. Alessi. 2000. The PI3K-PDK1 connection: more than just a road to PKB. *Biochem. J.* 346 Pt 3:561-576.

Vida, T.A., and S.D. Emr. 1995. A new vital stain for visualizing vacuolar membrane dynamics and endocytosis in yeast. *J. Cell Biol.* 128:779-792.

Vida, T.A., G. Huyer, and S.D. Emr. 1993. Yeast vacuolar proenzymes are sorted in the late Golgi complex and transported to the vacuole via a prevacuolar endosome-like compartment. *J. Cell Biol.* 121:1245-1256.

Vinh, D.B., and D.G. Drubin. 1994. A yeast TCP-1-like protein is required for actin function in vivo. *Proc. Natl. Acad. Sci. U S A.* 91:9116-9120.

Wach, A., A. Brachat, R. Pohlmann, and P. Philippsen. 1994. New heterologous modules for classical or PCR-based gene disruptions in *Saccharomyces cerevisiae*. *Yeast.* 10:1793-1808.

Wang, Y.X., N.L. Catlett, and L.S. Weisman. 1998. Vac8p, a vacuolar protein with armadillo repeats, functions in both vacuole inheritance and protein targeting from the cytoplasm to vacuole. *J. Cell Biol.* 140:1063-1074.

Wang, Y.X., H. Zhao, T.M. Harding, D.S. Gomes de Mesquita, C.L. Woldringh, D.J. Klionsky, A.L. Munn, and L.S. Weisman. 1996. Multiple classes of yeast mutants are defective in vacuole partitioning yet target vacuole proteins correctly. *Mol. Biol. Cell.* 7:1375-1389.

Weisman, L.S. 2003. Yeast vacuole inheritance and dynamics. *Annu. Rev. Genet.* 37:435-460.

Weisman, L.S., R. Bacallao, and W. Wickner. 1987. Multiple methods of visualizing the yeast vacuole permit evaluation of its morphology and inheritance during the cell cycle. *J Cell Biol.* 105:1539-1547.

Whiteford, C.C., C.A. Brearley, and E.T. Ulug. 1997. Phosphatidylinositol 3,5-bisphosphate defines a novel PI 3-kinase pathway in resting mouse fibroblasts. *Biochem. J.* 323:597-601.

Whitley, P., B.J. Reaves, M. Hashimoto, A.M. Riley, B.V. Potter, and G.D. Holman. 2003. Identification of mammalian Vps24p as an effector of phosphatidylinositol 3,5-bisphosphate-dependent endosome compartmentalization. *J. Biol. Chem.* 278:38786-38795. Epub 32003 Jul 38723.

Wilcox, C.A., K. Redding, R. Wright, and R.S. Fuller. 1992. Mutation of a tyrosine localization signal in the cytosolic tail of yeast Kex2 protease disrupts Golgi retention and results in default transport to the vacuole. *Mol. Biol. Cell.* 3:1353-1371.

Winzeler, E.A., D.D. Shoemaker, A. Astromoff, H. Liang, K. Anderson, B. Andre, R. Bangham, R. Benito, J.D. Boeke, H. Bussey, A.M. Chu, C. Connelly, K. Davis, F. Dietrich, S.W. Dow, M. El Bakkoury, F. Foury, S.H. Friend, E. Gentalen, G. Giaever, J.H.

Hegemann, T. Jones, M. Laub, H. Liao, and R.W. Davis. 1999. Functional characterization of the *S. cerevisiae* genome by gene deletion and parallel analysis. *Science.* 285:901-906.

Wurgler-Murphy, S.M., T. Maeda, E.A. Witten, and H. Saito. 1997. Regulation of the *Saccharomyces cerevisiae HOG1* mitogen-activated protein kinase by the PTP2 and PTP3 protein tyrosine phosphatases. *Mol. Cell Biol.* 17:1289-1297.

Wurmser, A.E., and S.D. Emr. 1998. Phosphoinositide signaling and turnover: PtdIns(3)P, a regulator of membrane traffic, is transported to the vacuole and degraded by a process that requires lumenal vacuolar hydrolase activities. *EMBO J.* 17:4930-4942.

Xu, J., D. Liu, G. Gill, and Z. Songyang. 2001. Regulation of cytokine-independent survival kinase (CISK) by the Phox homology domain and phosphoinositides. *J. Cell Biol.* 154:699-705.

Xu, W., S.C. Harrison, and M.J. Eck. 1997. Three-dimensional structure of the tyrosine kinase c-Src. *Nature.* 385:595-602.

Yaffe, M.B., and S.J. Smerdon. 2004. The use of in vitro peptide-library screens in the analysis of phosphoserine/threonine-binding domain structure and function. *Annu. Rev. Biophys. Biomol. Struct.* 33:225-244.

Yamamoto, A., D.B. DeWald, I.V. Boronenkov, R.A. Anderson, S.D. Emr, and D. Koshland. 1995. Novel PI(4)*P* 5-kinase homologue, Fab1p, essential for normal vacuole function and morphology in yeast. *Mol. Biol. Cell.* 6:525-539.

Yeung, B.G., and G.S. Payne. 2001. Clathrin interactions with C-terminal regions of the yeast AP-1 beta and gamma subunits are important for AP-1 association with clathrin coats. *Traffic.* 2:565-576.

Yeung, B.G., H.L. Phan, and G.S. Payne. 1999. Adaptor complex-independent clathrin function in yeast. *Mol. Biol. Cell.* 10:3643-3659.

Zaremba, S., and J.H. Keen. 1983. Assembly polypeptides from coated vesicles mediate reassembly of unique clathrin coats. *J. Cell Biol.* 97:1339-1347.

Zhang, Y., R. Sugiura, Y. Lu, M. Asami, T. Maeda, T. Itoh, T. Takenawa, H. Shuntoh, and T. Kuno. 2000. Phosphatidylinositol 4-phosphate 5-kinase Its3 and calcineurin Ppb1 coordinately regulate cytokinesis in fission yeast. *J. Biol. Chem.* 275:35600-35606.

Zheng, B., J.N. Wu, W. Schober, D.E. Lewis, and T. Vida. 1998. Isolation of yeast mutants defective for localization of vacuolar vital dyes. *Proc. Natl. Acad. Sci. U S A.* 95:11721-11726.

Ziman, M., J.S. Chuang, M. Tsung, S. Hamamoto, and R. Schekman. 1998. Chs6p-dependent anterograde transport of Chs3p from the chitosome to the plasma membrane in *Saccharomyces cerevisiae*. *Mol. Biol. Cell.* 9:1565-1576.